AD-A258 926

AFIT/GSE/ENY/92D-1

A Two-Stage Intercontinental Ballistic Missile (ICBM)

Design Optimization Study and

Life Cycle Cost Analysis

THESIS

GSE-92D-1

AFIT/GSE/ENY/92D-1

DTIC
ELECTE
JAN 0 7 1993
S
B
D

93-00032

93   1 04 037

AFIT/GSE/ENY/92D-1

A Two-Stage Intercontinental Ballistic Missile (ICBM)

Design Optimization Study and

Life Cycle Cost Analysis

THESIS

Presented to the Faculty of the School of Engineering

of the Air Force Institute of Technology

Air University

In Partial Fulfillment of the

Requirements for the Degree of

Master of Science in Systems Engineering   DTIC QUALITY INSPECTED 1

David P. Blanks, M.B.A., B.S.   Douglas M. Bruce, B.S.
Captain, USAF   Captain, USAF

Anthony M. Logue, B.A.E.   Ralph A. Sandfry, B.S.
Captain, USAF   First Lieutenant, USAF

Stephen J. Skotte, B.S.   Michael L. Zywien, B.S., B.A.
Captain, USAF   Captain, USAF

December, 1992

Acknowledgements

i

Table of Contents

List of Figures

List of Tables

Abstract

Realities of recent changes in the fiscal environment and the international domestic security structure have caused the strategic community to make some difficult decisions to preserve the capability of the current ICBM force. One of these decisions is to view Minuteman III as the centerpiece of the strategic force well into the next century. Extending the life of the 24-year-old Minuteman III system requires system solutions that provide required performance at an affordable life cycle cost.

The intent of this study is to demonstrate the feasibility of designing a 2-stage ICBM to perform the Minuteman III mission. The main area of research is to take advantage of recent developments in missile technology and materials, including "Integrated Stage Concept" and more conventional technologies. It is believed that such a system could prove more affordable to build, maintain and support while providing the required system performance.

Five final missile designs are developed and presented. A recommendation is made to pursue an Integrated Stage second stage design based on mission performance, system readiness and cost decision criteria.

A TWO-STAGE INTERCONTINENTAL BALLISTIC MISSILE (ICBM) DESIGN OPTIMIZATION STUDY AND LIFE CYCLE COST ANALYSIS

I. Introduction

Realities of the recent changes in this nation's fiscal environment and the international and domestic security structure have caused the strategic community to make some difficult decisions to preserve the capability of the current Intercontinental Ballistic Missile (ICBM) force. One of these decisions is to view Minuteman III (MM III) as the centerpiece of the force well into the next century. Extending the life of the 24-year-old system requires system solutions that provide required performance at an affordable life cycle cost.

This systems engineering design study demonstrates the feasibility of a 2-stage ICBM to perform the Minuteman mission. Both conventional and *integrated stage* technologies are investigated as potential design approaches. The research takes advantage of recent developments in missile technology and materials, and the end result is a system that should prove more affordable to build, maintain, and support while providing the required system performance.

Chapter 1 provides necessary background and a basis to claim that the project is feasible. Chapter 2 describes the systems engineering methodology that is used to formulate, organize, plan and solve the problem. Chapters 3 through 6 describe the preliminary design of the system's second stage, resulting in five candidate designs. Chapter 7 presents the conclusions from the study and makes recommendations for future work. Detailed Appendices are included to fully describe the work of individual design groups in the areas of trajectory and performance analysis (A), propulsion system design (B), structures and materials (C), and system readiness (D).

1.1 Background

In recent years, the United States military establishment has been shifting its priorities in systems development. A past emphasis on operational performance has now been broadened to include higher levels of equipment reliability and supportability (5:p1) and reduced system life cycle cost (LCC). Evidence of a growing concensus that reliability and cost merit increased attention and resources is abundant, starting at the top levels of Department of Defense (DoD) policy, working down into specifications for new systems and even being reflected in the attention given by publications such as *Aviation Week and Space Technology* (35).

The *Reliability and Maintainability Action Plan R&M 2000* defines the Air Force policy that reliability and maintainability (R&M) will be considered coequal with cost, schedule and performance during acquisition (or major modification) of new systems(94:p3).

The *SAC Perspective on ICBM Programs* (11) brings system development guidance into the context of the changes in the international and domestic environment that have been witnessed in the last few years. Mounting budget deficits and perceptions of a declining strategic threat have led to a decision to view MM III as the centerpiece of the ICBM force (11:p2). Key factors that led to this decision include the following:

- high costs to maintain Peacekeeper (for example, guidance repair on Peacekeeper is considerably more expensive and manpower intensive than for other ICBMs)

- the need to replace Peacekeeper-unique support equipment by the year 2003

- upgrades to MM III have the potential to reduce maintenance, security and manpower costs (11:p2,3).

The primary objective of the operating command is to preserve the capability of the current Minuteman force while extending its useful service life beyond the year 2010 (67). The Air Force's operating, development and procurement commands have outlined the requirements for Minuteman

1-2

life extension in the Minuteman Long Range Plan (MLRP) (94). The MLRP identifies "necessary projects" to be addressed in the immediate future, including guidance system improvements and stage washout/remanufacture. Fiscal conditions call for innovative and creative solutions that will reduce total system life cycle costs while preserving required system alert readiness and in-flight performance.

SAC 001-92, *Draft Mission Need Statement for Prompt Strategic Strike Capability For 2010* (52), dated 10 January 1992, says

> "Prompt, highly accurate intercontinental strategic weapon delivery will remain a key element of the TRIAD beyond [the year] 2010. Defense planners should attempt to identify changes to current operations concepts, doctrine, tactics and organization to allow our strategic forces to meet future demands. Several possible solutions [should be considered] for this need including Minuteman ICBM life extension and the design [and production] of a new system."

The Mission Need Statement lists the following relevant constraints:

- affordability

- basing mode complementary to existing systems

- robust and enduring C^3 (command/control/communication)

- world-wide targeting capability with time to target comparable to or better than existing baseline systems

- low operations and support costs

- high alert rate

It is clear that this guidance reflects an interest in more than performance alone. It opens the door to exploring system solutions that provide adequate performance while at the same time improving alert rates and reducing life cycle cost.

One such solution that has been proposed (78) is the replacement of the second and third stages of a traditional ICBM with a single stage. An optimized two-stage missile design, taking advantage of recent advances in propulsion and materials science, integrated stage technologies, and manufacturing techniques could prove more affordable to build, maintain and support while providing the required system performance. Air Force policy (as defined by the goals of the *R&M 2000 Action Plan*) and the operating command's view of the importance of R&M and cost (as reflected in the *SAC Perspective* memo) provide a clear framework to propose a major modification to the Minuteman III weapon system. Since each missile is located in an unmanned, remote silo and must be maintained continuously on alert, the missile and its support equipment must remain highly reliable, maintainable, supportable and affordable. Therefore, these factors become critical in the weapon system design.

The need to maintain MM III as a key element of the strategic TRIAD into the next century seems clear from the guidance discussed so far. What is not clear yet is whether the Air Force should continue to remanufacture and improve the existing system, or whether a more radical two-stage approach should be tried in the interest of life cycle cost savings. The latter approach is the basic focus of this design project. The rest of this chapter is aimed at establishing the basis and feasibility of this research by addressing the following questions:

- What is the baseline MM III system's mission, operational capability and physical description?

- What is the basis for advocating a two-stage alternative to the current system?

- What technologies should be investigated in designing a two-stage ICBM?

- Is a two-stage design feasible from a mission performance point of view?

1.2 What is a Minuteman III ICBM?

1.2.1 System Overview. The mission of the Minuteman III weapon system is the defense of the United States through the deterrence of an enemy attack. If, however, this deterrence should

fail, MM III would deliver retaliatory, thermonuclear warheads to preselected enemy targets. The "weapon system" includes all of the related equipment, materiel, services, and personnel required to keep the instrument of combat, the missile itself, a self-sufficient unit of striking power in its operational environment. It should be noted here that this design project deals only with a small portion of the total weapon system, but a total system approach must be taken even if only a portion of the system is impacted by the advocated design change.

There are two versions of the Minuteman missile currently in operational status:

- Minuteman II (LGM-30F) (MM II)

- Minuteman III (LGM-30G) (MM III)

The LGM-30G evolved from the older F version, and it is the newer MM III which will serve as the baseline for this design study.

The MM III LGM-30G missile (Figure 1.1) consists of a three stage, solid propellant booster, a liquid propellant post-boost propulsion system (called the propulsion system rocket engine, PSRE), an inertial guidance system, a reentry system and structural interstages.

The 78,000 pound (Table 1.1) assembled missile rests upright in the launch silo (Figure 1.2) during the ground phase of operation. The missile computer runs automatic (periodic) and commanded status checks and tests, responds to interrogations and commands received through the ground electronic system, and maintains spatial orientation and gravity update while emplaced in the launcher. When launched, the missile is boosted for approximately three minutes by the three solid propellant motors burning in sequence. Each stage is separated from the missile after motor burnout. Boost flight can be terminated before third stage burnout as mission requirements dictate (shorter range mission). Thrust termination, and mechanical and electrical disconnect of the third stage from the PSRE, are sequenced by the guidance set. Post-boost maneuvering thrust

payload shroud

4.3 ft

guidance set
psre

stage 3 motor

interstage

raceway

stage 2 motor

59.9 ft

interstage

stage 1 motor

5.5 ft
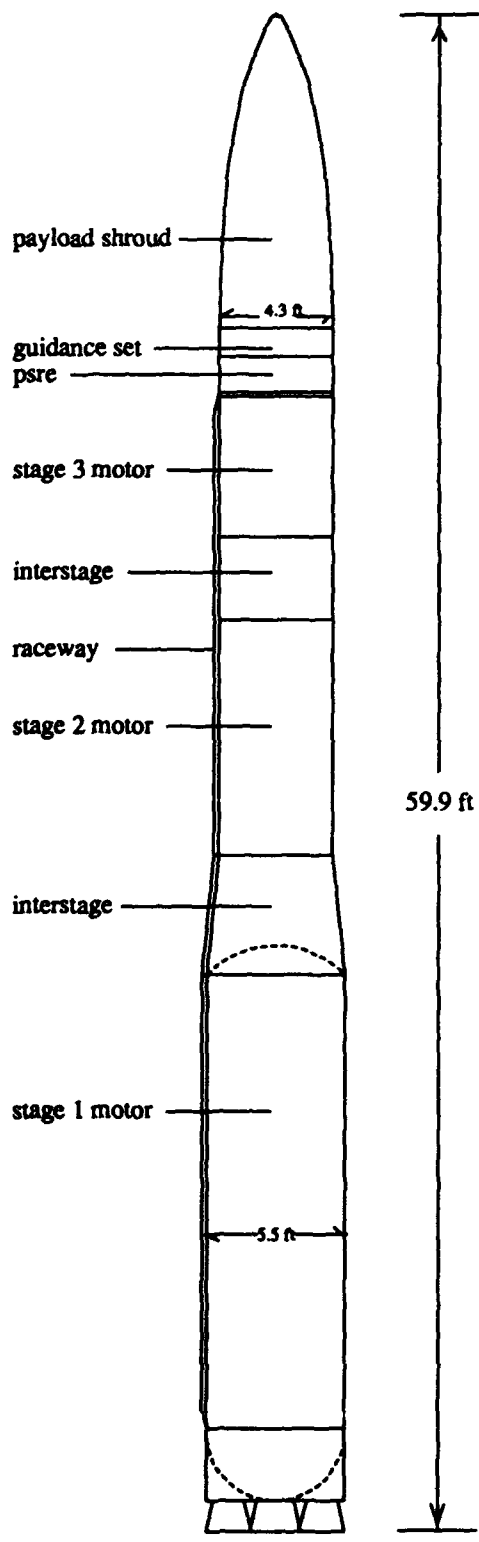
Figure 1.1. Minuteman III Missile

MINUTEMAN III PHYSICAL DIMENSIONS			
Component	Length (in)	Diam (in)	Weight (lbs)
Nozzles	15.794		
Skirt	36.000	66	
Stage 1	222.640	66	50252
Interstage 1/2	57.900	66-52	431
Stage 2	108.700	52	15,518
Interstage 2/3	38.120	52	152
Stage 3	63.513	52	
Separation Joint	1.680	52	
PSRE	17.195	52	598
MGS	13.250	52	
Shroud/Payload	142.850	52	1700
Totals	717.642	66-52	77,426

Table 1.1. Minuteman III Dimensions

is provided by the PSRE, control by the guidance set. The reentry system deploys the warheads according to a pre-flight loaded software program.

Additional missile structure consists of a skirt and two interstages. These structural items support the missile in the launch position, join the three motor stages aerodynamically and structurally, provide stage separation, and contribute to flight stability for each stage during powered flight. The exterior of the missile is insulated with a layer of cork for structural protection against plume, aerodynamic heating and weather environmental effects during boost. The raceway, located on the outer surface of the missile, contains and supports the guidance control cable as it runs from the missile skirt to the missile guidance system (MGS). Pull-away connectors at the stage separation joints permit cable separation during missile staging. The cable is supported, over the length of the motors and interstages, between layers of resilient foam covered by a fiberglass cover.

1.2.2 Physical Description of System Components. Since parts of the system will be referred to constantly throughout this document, some additional detail about each missile component is provided here as a reference for later discussion.
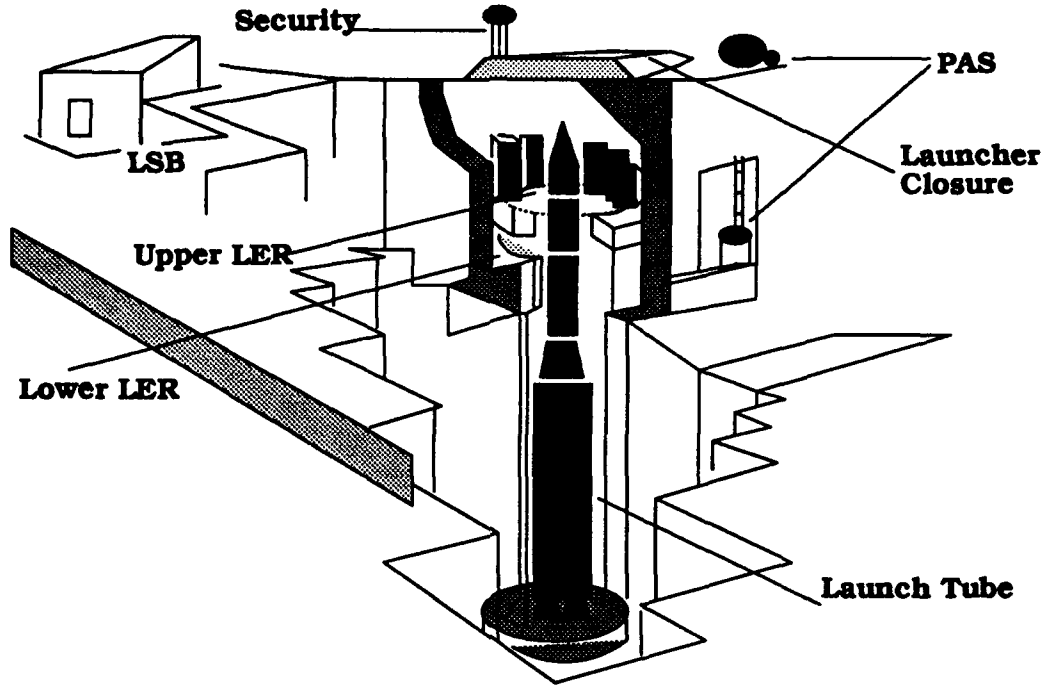
Figure 1.2. Minuteman Launch Facility

1.2.2.1 The Launch Facility and Launch Control Facility. Refer to Figure 1.2. The function of the launch facility (LF) is to provide the ground support and physical protection necessary to keep a missile ready to launch at all times. The LF is an unmanned, hardened and underground facility that consists of a launcher (launcher closure, upper and lower level equipment rooms, launch tube), a launcher support building, security system, personnel access door, and a service area. The missile and all its supporting equipment (called operational ground equipment - OGE) are enclosed in the launcher or "silo". The missile occupies a central tube called the launch tube. Associated OGE is arranged in a two-level equipment room surrounding the top of the tube. The missile and all OGE are shock isolated for protection against nuclear blast effects.

The launch control facility (LCF) serves as a manned control and monitoring station for the LFs. In addition, the LCF provides physical protection for the men and equipment required for missile launch.

1-8

1.2.2.2 First Stage Motor. The first stage motor (Figure 1.3) consists of a steel motor case and an aft closure with four movable, nozzles and a nozzle control unit. The motor case serves as the missile skin with the interstage attached at the forward end of the case. The motor case, aft closure areas, and nozzles are insulated from exhaust gases by molded plastic, Buna-N rubber insulation and high density graphite parts. A low-temperature ablative insulation protects the motor case exterior from aerodynamic heating. The large movable nozzles on the first stage are
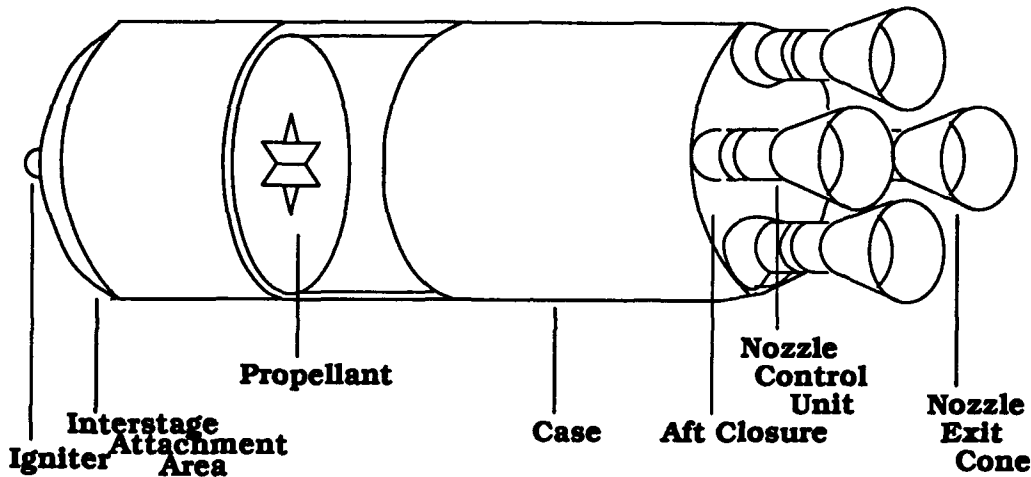
Figure 1.3. MM III First Stage Motor

necessary for programmed roll and pitch maneuvers and for attitude corrections during first stage operation. Also, the size and weight of the missile at this time is greatest, requiring maximum force for control. Thus, large nozzle gimballing forces are needed for first stage control.

Into the motor case, a one-piece casting or "grain" with a six-point star hollow core is cast of high-performance solid propellant. This grain shape maintains constant thrust by keeping a constant surface area (as the propellant burns away). The composite propellant consists of ammonium perchlorate (oxidizer) and aluminum powder (fuel), bound together by a rubbery polybutadiene acrylic binder and an epoxy-resin curing agent (105).

1.2.2.3 Second Stage Motor. The second stage motor (Figure 1.4) consists of a tita-

Interstage Att'ch Area

Injector Control Unit

TVC Gas Generator
Case

Igniter

Propellant

Interstage Att'ch

Injector Ports (4 groups)
Nozzle Exit Cone

Nozzle Throat

Roll Control Nozzle (4)

Roll Control Gas Generator
Injector Control Unit

Injectant Tank
Aft Closure
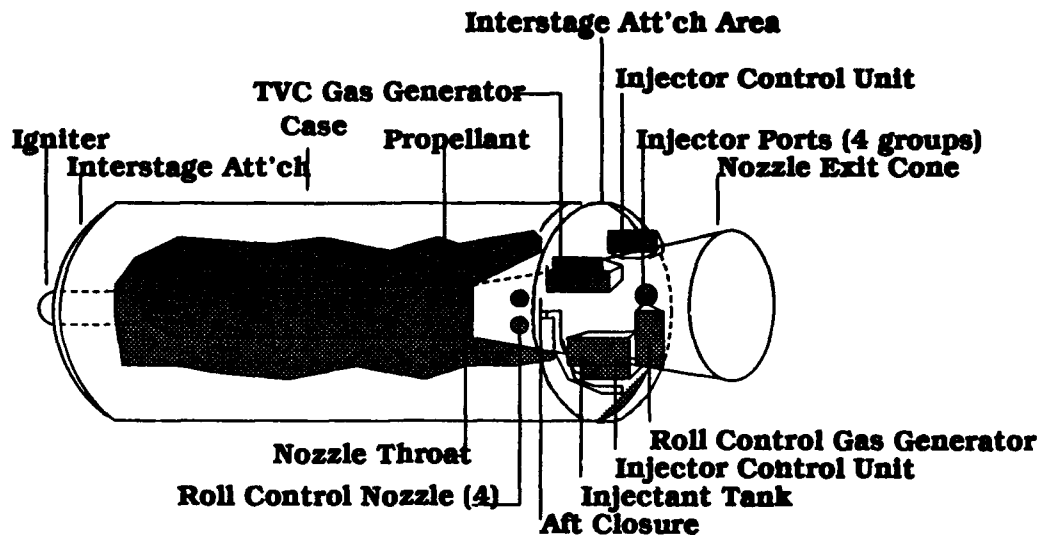
Figure 1.4. MM III Second Stage Motor

nium alloy motor case, solid composite propellant, an igniter, an aft closure with a single, fixed, submerged nozzle, a thrust vector control system (TVC), and a roll control system.

The propellant is aluminum powder and ammonium perchlorate bound by a carboxy-terminated polybutadiene polymer. The propellant is cast into a hollow circular bore configuration with fins in the forward end to provide a relatively constant burning-surface/time relationship (105).

During second stage flight, the liquid injection TVC (LITVC) controls missile attitude on the pitch and yaw axes in response to commands from the D-37 guidance computer. Freon from a toroidal storage tank is selectively injected into the nozzle at four points 90^0 apart. This produces shock waves in the flow which shifts pressure distributions inside the nozzle. This provides a thrust offset vector that causes the missile to correct its pitch attitude. The D-37 controls the quantity of freon injected and the time required to correct missile attitude. The missile carries enough freon to control a flight involving maximum activity due to severe disturbances, and a "dumping" capability

is provided to get rid of any extra freon (weight) above a desired amount at various points during flight.

Roll control is accomplished by releasing warm gas through two pairs of roll control nozzles on opposite sides of the missile. Warm gas for roll control is provided by a gas generator separate from the gas generator used for pressurizing the freon.

1.2.2.4   Third Stage Motor.   The third stage motor (Figure 1.5) consists of a fiberglass (s-glass) motor case, solid (aluminum based) propellant, an igniter, a single fixed submerged nozzle, a liquid injection TVC system (similar to that used on the second stage motor) and a thrust termination system.
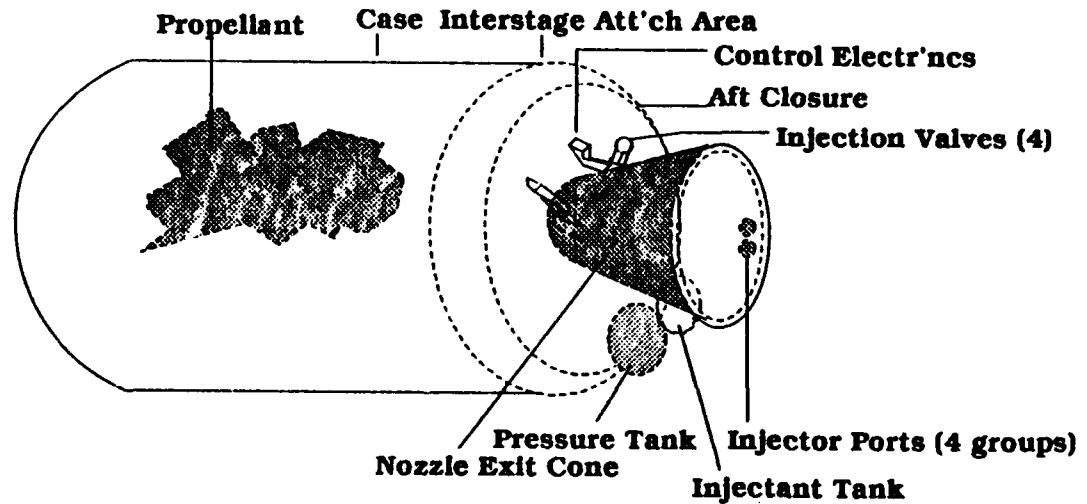
Figure 1.5. MM III Third Stage Motor

One way in which the Stage 3 yaw and pitch control system differs from Stage 2 is in the method of pressurizing the injectant. In Stage 2, a gas generator uses the exhaust gases generated from burning solid propellant to provide the necessary pressure for the injectant. In Stage 3, a pressurized helium tank is used to pressurize the injectant. A command from the D-37 opens an

isolation valve which lets pressurized helium pass through a regulator to the injectant tank. The injectant tank has a steel outer case and a collapsible inner tank bladder (like a bellows). As the helium pressurizes one side of the bladder, the injectant (strontium perchlorate) is forced out.

Roll control is accomplished with a gas generator and a roll control valve at the forward end of the motor. Upon command from the D-37, the gas generator is ignited with an explosive squib device. A valve vents generated gas through two nozzles which extend through the motor skirt.

The thrust termination system consists of six thrust termination ports at 60^0 spacing around the front of the motor case. Shaped charges blow the ports open on command from the D-37 computer. This allows the chamber pressure to vent forward which momentarily creates a negative (opposing) thrust causing the third stage to drop away from the PSRE.

1.2.2.5 Propulsion System Rocket Engine (PSRE). This portion of the LGM-30G can be thought of as a "fourth stage". The PSRE provides the thrust required for post-boost vehicle maneuvering. It includes separate pressurant, fuel, and oxidizer storage tanks (liquid propellant). It also contains 11 rocket engines and associated valves and manifolds. The "fourth stage" adds a portion of controlled flight that is nearly equal in time to the combined first three stages.

1.2.2.6 Missile Guidance Set (MGS) . The MGS is an integral part of the missile. It is referred to as the NS20A1 for the MM III system. The NS20A1 is contained in a cylindrical shaped unit mounted on the PSRE. The MGS is made up of five major subunits: a gyrostabilized platform, missile guidance set control, P92 amplifier assembly, D-37 computer and a dual battery (two batteries in one case) for power.

1.2.2.7 Reentry Vehicle (REEV) . For the purpose of this study, the "reentry vehicle" consists of everything above the MGS. This equipment includes an aerodynamic titanium heat shield (shroud), chaff and chaff dispensers, payload support structure and bulkhead, and the actual payload which is really the reentry vehicle.

1.2.2.8 Stage Separation . To accomplish stage separation, the missile interstages are equipped with an arm-disarm mechanism, a detonator assembly, and a linear charge. The linear charge is installed in an enclosed cavity around the circumference of the interstage separation joint. The detonators are fired electrically by a programmed signal from the MGS concurrent with ignition of the succeeding stage. The skirt of the succeeding stage is blown off in four sections by longitudinal charges. Ignition of these charges occurs after stage separation.

1.3 Three Stages Versus Two Stages

Classical long range missiles such as the Minuteman I, II, and III and Peacekeeper ICBM systems have all been designed and built using three stages. The reason: a priority on system performance with lesser emphasis on cost and supportability. Strictly from a performance point of view, more stages give better system performance in terms of range and/or weight of payload delivered. However, the marginal increase in performance with each additional stage becomes increasingly smaller; in fact the most dramatic performance increase comes with the jump from one stage to two (103, 107). Two-stage designs have traditionally lost out to three-stage designs because of the fact that the three-stage design was the only one capable, within the technology limits present in the 1960's, 70's and 80's, of delivering a multiple warhead (heavy) payload to the required operating ranges.

Since one of the key elements of this project is to demonstrate that delivery of a Minuteman III post-boost vehicle to a required point in space can be accomplished with two stages instead of the traditional three, some discussion of the basic rocket equations of motion for staged systems is a necessary first step in such a presentation.

1.3.1 Basic Rocket Equation . The basic "rocket equation" (any vehicle producing thrust by ejecting mass is considered (103:p185) to be a rocket) is well known (87, 103, 107) and is given

here as

$$\Delta V = V_e[ln(m_0/m)]$$

where ΔV (in the case of an ICBM) is the change in velocity from launch to burnout of the booster, V_e is the axial exit velocity of the differential fuel mass elements from the motor nozzle, m_0 is the initial mass of the system, and m is the final system mass after all propellant is burned. Therefore, the burnout or final velocity of the vehicle depends only on the exhaust velocity of the engine and how much of the total vehicle is fuel. Performance is enhanced, then, by a vehicle designed with minimum structural mass.

1.3.2 Staging . As a solid rocket engine burns up all its usable propellant, the structure associated with that engine becomes useless mass and therefore a detriment to system performance. If this "dead weight" can be disposed of as its utility disappears, performance can be enhanced. The common way to do this is to *stage* the vehicle, shedding used up engines and empty fuel tanks as the vehicle accelerates on its flight path. In this way, a smaller vehicle proceeds from the point of staging with considerably less dead mass (103:p191).

From this discussion, it is clear that more performance (higher terminal velocity) is obtained as the amount of dead weight *dropped* increases. In the extreme, as the number of stages increases to infinity, higher velocities can be obtained for a given "payload". While this is technically true, it is most informative to look at the *incremental* benefit gained from adding stages to an ideal single stage system.

Figure 1.6 (103:p192) shows a 2-stage rocket, with each stage broken down into its structure and propellant masses. The initial mass of the kth stage (m_{0k}) is the mass of everything above the separation plane for that stage. The final mass of stage k (m_{fk}) is the structural mass of that stage plus the total mass of the remaining stages. The final ($n + 1$) stage has the payload mass (m_*).
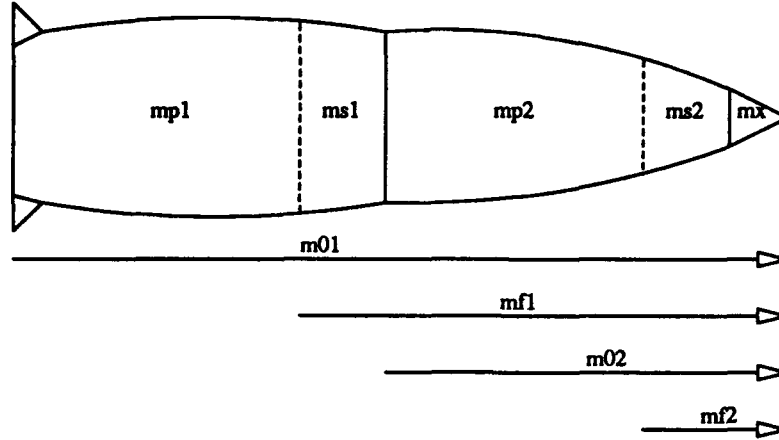
Figure 1.6. Staging

If the vehicle's *overall payload ratio* is defined as the fraction of the total vehicle which is payload,

$$\pi_* = \frac{m_*}{m_{01}}$$

, the rocket equation shows that if π_* is small (m_{01}/m_* is large), ΔV is large. To see the advantage conferred by staging, the overall payload ratio is expanded:

$$
\begin{aligned}
\pi_* &= \frac{m_*}{m_{01}} \\
&= \left(\frac{m_*}{m_{0n}}\right)\left(\frac{m_{0n}}{m_{0,n-1}}\right)...\left(\frac{m_{02}}{m_{01}}\right) \\
&= \prod_{k=1}^{n} \pi_k
\end{aligned}
$$

and a small overall payload ratio can be obtained from the product of individual stage payload ratios, each of which is kept small by the exclusion of the dead weight of the previous stage. The overall payload ratio, π_*, is plotted in Figure 1.7 (103:p193) as a function of $\Delta V/V_e$ (assuming $V_{ek} = V_e$ for each stage and identical stage payload ratios, π_k) for different multistage vehicle configurations. This figure clearly shows significant improvement in burnout velocity for a 2-stage system over a single stage system, some additional improvement for a 3-stage system, and some

1-15

additional improvement as the number of stages goes to infinity. It is most interesting, for this
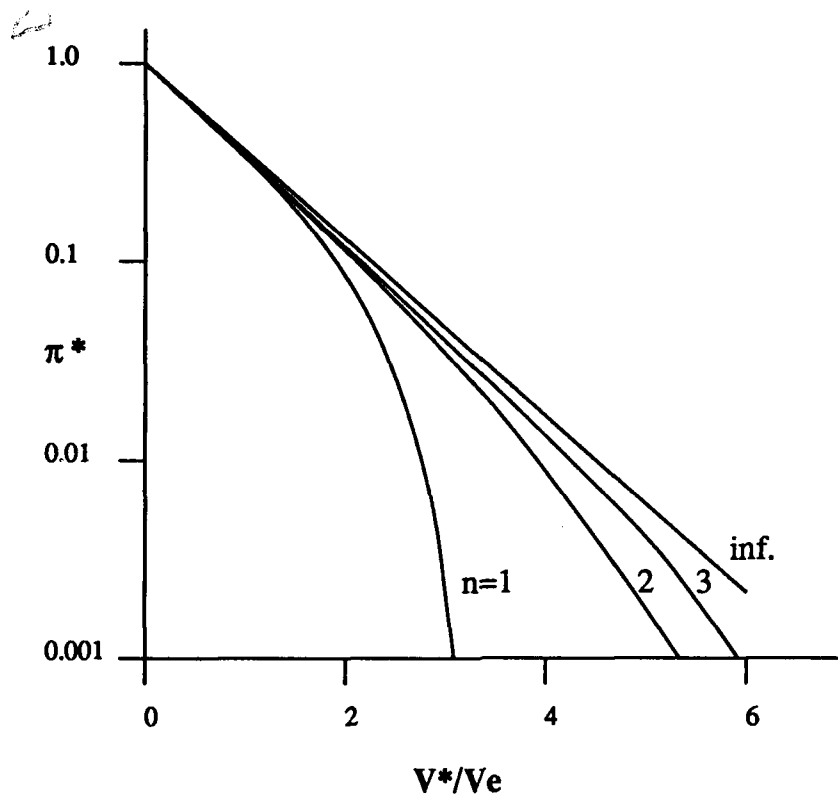
Figure 1.7. Incremental Burnout Speed Gains With Added Stages

project, to note that the additional gain in going from two to three stages is much smaller than

that gained in going from one to two stages. Strictly in terms of performance, then, three stages

is better than two. However, if other considerations (e.g. cost, reliability) become as important as

performance, a two stage configuration can be considered as a potential alternative.

1.4 Statement of Approach

The main thrust of the research in this document, then, is to investigate the technical mission

performance feasibility, alert availability, in-flight reliability, supportability, producibility, and life

cycle cost of a 2-stage ICBM to replace the current 3-stage Minuteman III missile. This can

be done either by looking at conventional technologies that have been used in Minuteman and

Peacekeeper developments in the past, or by looking at the use of technology upgrades that have been investigated recently for Small ICBM, the Army's MIST program (72), and other applications.

The most current operational ICBM systems (MM III and Peacekeeper) use solid propellant motors, whose technology is driven by requirements for

- 24 hour readiness

- large payloads

- minimizing maintenance

The production of these motors is really an art form, and the keys are in the propellant's mechanical properties, stored chemical energy, ballistic properties, the durability of the propellant/liner/insulation chemical bond, grain design, and the repeatability of the burn performance. The MM III system has been in the field for over twenty years, and there are several issues related to the current state of technology that must be addressed now:

- Stage 3 is nearing its second remanufacture cycle due to ageout (cracking) of propellants and to "debonding" of the propellant/liner/insulation interface

- Stage 2 is undergoing its third remanufacture for the same reasons

- Environmental concerns mandate changes in current

    - primers, solvents and cleaners,

    - liquids (freon) used in LITVC, and

    - propellant burn characteristics (environmentally "cleaner" exhaust products),

- Some materials currently used (s-glass for the third stage motor case, for example) are no longer available.

Therefore, with the goals of extending useful service life, enhancing environmental compliance and assuring material/supplier availability well into the next century, the question of whether current technology should be transferred directly or whether new technologies should be explored is very relevant to this work.

Much work has been done over the last several years (56, 85) on advanced concepts and technologies for ICBM applications. These concepts and technologies include

- Integrated Stage,

- Continuous batch processing for propellants,

- Advanced motor liner materials,

- New motor case materials,

- Guidance System upgrades and improvement.

The Integrated Stage Concept (ISC) entails the integration of the rocket motor nozzle into the motor case, thus removing the need for a heavy interstage structure (and its accompanying system performance penalty). The Integrated Stage concept involves application of the following technologies:

- *aft reverse dome forced-deflection nozzle* (which is shorter than conventional nozzles) is integrated into the motor case (rather than extending out beyond the case as in a traditional motor design),

- *composite case with full open end* to accomodate the completely submerged nozzle and for ease and cost savings in manufacture,

- *hot gas valves for thrust vector control* removing the need for environmentally unacceptable liquids such as freon, and

- *boron based solid propellants* to provide particle-free exhaust necessary for hot gas valve operation.

The complete details of the integrated stage concept are presented in Chapter 4, Appendix B, and Appendix C. Continuous batch processing of propellants addresses the propellant aging issue, and this, too, will be discussed in more depth in Chapter 4 and Appendix B. Advanced liners with an estimated service life of up to 35 years (94) are being investigated now for the current MM III remanufacture cycle (see Appendix D). Guidance System improvements will not be investigated specifically in this study, but since the MGS is one of the chief maintenance drivers in the current system, any future system upgrades must address this issue as well (see Chapter 7).

The following approach will be taken in this study:

1. Investigate the use of both conventional and integrated stage technologies in optimized designs for a two-stage ICBM booster that meet the performance requirements of the current MM III ICBM system.

2. Assess the alert availability and in-flight reliability of all candidate designs.

3. Combine the availability/reliability assessments with an assessment of other Integrated Logistic Support factors to characterize the overall supportability of each candidate design.

4. Assure that the candidate designs are producible within today's manufacturing capability.

5. Estimate the overall Life Cycle Cost of each candidate second stage design.

This project is challenging, and involves planning, research, modeling and analysis. The chapters that follow outline a systems engineering approach to complete the project. However, prior to undertaking such a difficult task, there is one important question to be answered. Since a two-stage booster has never been built to meet the MM III application, there is no certainty that a two-stage design is even feasible. Therefore, a preliminary feasibility analysis is performed

1-19

to quantify what is possible within the constraints of this study. The next section details the preliminary "feasibility study."

1.5   Feasibility of a Two-Stage Booster

1.5.1   Philosophy .   For preliminary analysis, the current MM III performance is determined using the equations of motion for an ideal rocket under a uniform gravitational field and in purely vertical flight. These equations are used to calculate the total change in velocity, ΔV, imparted to the payload between launch (from rest) and burnout of the third stage booster. This analysis establishes the initial MM III baseline performance (benchmark), which is then compared with a similar analysis for a two-stage design. The equations provide a means for determining a first-order estimate of the structural ratio required for the second stage of a two-stage design. A brief discussion of the ideal rocket equations and the results of this analysis follow.

1.5.2   The Ideal Rocket Equation.   Before a discussion of the ideal rocket equation can be made, some rocket design parameters must be defined. The first, and most important, parameter is the stage structural ratio, ϵ. The stage structural ratio is defined as the structural mass of the booster stage divided by the sum of the structural mass and propellant mass of the stage. In this analysis it is simply the percentage of the total stage that is not propellant.

Another important parameter requiring definition is the payload ratio, π. It is defined to be the payload mass for the stage under consideration, divided by the total stage mass. For a multi-stage missile, the payload ratio for the first stage, for example, would be the mass of all of the missile components above the first stage, divided by the first stage mass.

A third important parameter to be defined is the specific impulse, or I_{sp}, for the booster. It is defined as the impulse per unit mass of the propellant divided by earth's gravitational constant, g. Dividing by g is arbitrary in this case, and is done to allow the I_{sp} to be expressed in units of seconds (50:p322).

The total change in velocity, in *ft/sec*, for a single stage ideal rocket can be expressed as:

$$\Delta V = -g I_{sp} ln[\epsilon + (1 - \epsilon)\pi]$$

where g is $32.2 ft/sec^2$. This equation is extended to the n-stage rocket by simply summing the individual stage ΔV contributions to obtain the total missile ΔV. In equation form, this is expressed as:

$$\Delta V_{total} = \sum_{i=1}^{n} -g I_{sp_i} ln[\epsilon_i + (1 - \epsilon_i)\pi_i]$$

where the summation index i represents the ith stage. The simplicity of this equation allows calculation of a first estimate of ΔV with very limited data, although some loss of accuracy does occur. Implicit in the equation are several assumptions which need to be addressed. First, the equation is independent of the burn time of the booster. The equation is only a function of the initial and final masses of each stage. As a result, an impulsive burn is assumed. With an impulsive burn, gravity does not have a chance to act upon the missile and slow it down, whereas for a real missile, the gravitational effects "build up" with time. This force is not accounted for in the ideal rocket equation. Another force absent from the equation is aerodynamic drag, which also slows the missile. Both of these assumptions result in an overestimation of the missile's performance. However, despite the fact that this equation does not accurately predict the missile performance, it can still be used to compare missile designs, as long as these assumptions are uniformly used for all of the designs being examined, including the benchmark. This is the approach taken for the preliminary feasibility analysis for the two-stage design.

1.5.3 MMIII Analysis. Using the ideal rocket equation, the MM III total ΔV for a 2300 pound payload is calculated to be 25,194 ft/sec. This establishes the performance baseline against which the two-stage design was to be compared. A stage-by-stage breakdown of the ΔV for the MM III is presented in Table 1.2.

Stage	ϵ	π	I_{sp}(sec)	ΔV(ft/sec)
1	0.09954	0.33691	237	6937
2	0.11363	0.39995	287.5	7026
3	0.09233	0.22252	285.15	11231
			Total	25194

Table 1.2. MM III Stage Parameters and ΔV

1.5.4 Two-Stage Design Analysis . In applying the ideal rocket equations to the MM III, the structural and payload ratios and I_{sp}'s for each stage are well-defined. However, for the two-stage missile, only the first stage data (MM III stage 1) is available and estimates of the design parameters for the second stage are needed. In the absence of any data for a new second stage, the second stage weight is left as a variable ranging from 20,000 lbm to 50,000 lbm. However, the *distribution* of the second stage weight is not yet accounted for. Thus the structural ratio for the second stage is also left as a variable. Further, an estimate of the second stage I_{sp} is required. Based upon current boron and aluminum-based propellant data, and information obtained from the Phillips Lab, an I_{sp} of 300 seconds is used for the analysis.

Structural ratios varying from 0.065 to 0.085 (in increments of 0.005) are examined (with the stage 2 weights varying as described above) and plots of stage 2 propellant weight versus ΔV for each structural ratio are generated. The 2300 lb payload case is presented in Figure 1.8.

The horizontal line represents the MM III ΔV requirement. As can be seen, the curves corresponding to structural ratios of 0.080 and above cannot meet the ΔV requirement regardless of propellant weight, and the $\epsilon = 0.075$ case can only meet the requirement with approximately 35,000 lbm of propellant. Since the total MM III weight above stage 1 (stages 2 and 3 combined with payload) is 26,000 lbm, the two-stage design second stage plus payload is limited to a weight equal to or less than 26,000 lbs for structural integrity considerations. Therefore, even a 0.075 structural ratio is inadequate to meet the ΔV requirement.
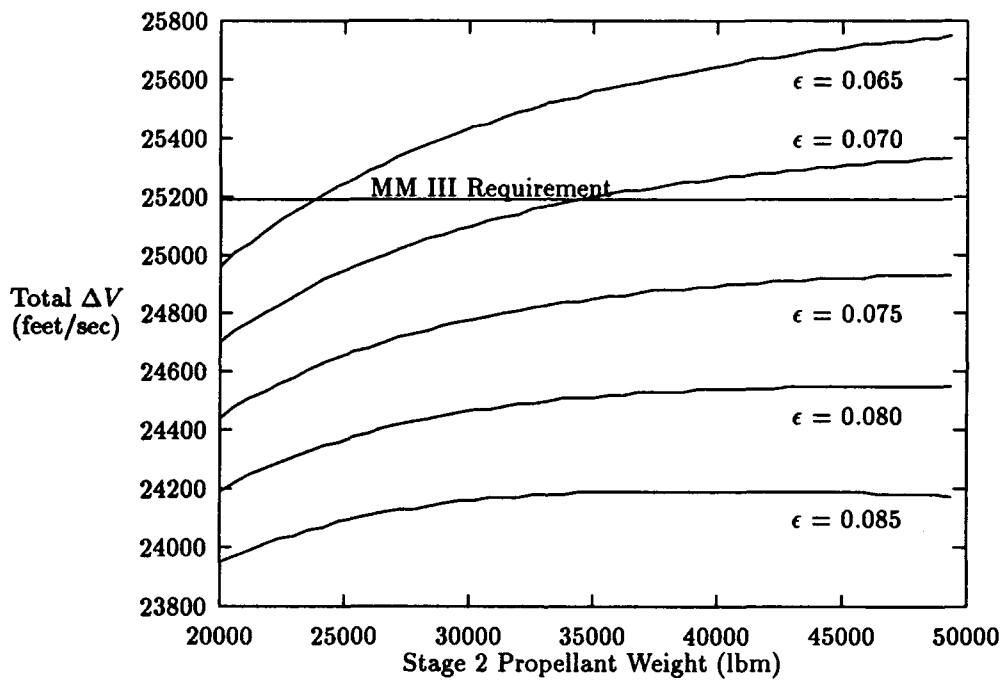
Figure 1.8. Stage 2 Propellant Weight Vs. ΔV For Variable ϵ - 2300 Pound Payload

In order to determine the *exact* maximum structural ratio and still meet the ΔV requirement, the ideal rocket equation is modified by setting ΔV equal to 25,194 ft/sec (the MM III ΔV_{total}) and solving for the second stage structural ratio, thus obtaining the following equation:

$$\epsilon_2 = \frac{\exp\left\{\frac{25,194 + g I_{sp_1} ln[\epsilon_1 + (1-\epsilon_1)\pi_1]}{-g I_{sp_2}}\right\} - \pi_2}{1 - \pi_2}$$

Substituting the appropriate values for the variables based upon a payload weight of 2300 lbm and a stage 2 weight of 23700 lbm (26000 lbm - 2300 lbm payload) yields a structural ratio of 0.06881. A similar analysis based upon a payload weight of 1500 lbm yields a maximum structural ratio of 0.10108 for the MM III required ΔV. Thus, based upon the ideal rocket equation, for the two-stage design to be feasible, a second stage structural ratio between 0.10108 and 0.06881 must be acheived for the 1500 - 2300 lbm payload range. A literature review (Appendix C) reveals that structural ratios within this range can be attained using both conventional and integrated stage technologies.

1.6 Summary

This chapter introduces the need for an engineering design study to address the problem of designing a two-stage ICBM to meet the Minuteman III mission. Subsequent chapters detail the program planning, research, modeling, analysis, optimization and decision making involved with the actual booster design. The two-stage system design is hereafter referred to as *NEMESIS*, for *NExt Minuteman Enhancement Systems Integration Study.*

II. The Systems Engineering Process - A Program Plan

2.1 Introduction

The transformation of an operational need into a description of system performance parameters and a preferred system configuration comes about through a process called "Systems Engineering". Blanchard and Fabrycky (17:p24) define systems engineering as the application of efforts necessary to

1. transform the need into a preferred configuration through the use of an iterative process of functional analysis, synthesis, optimization, definition, design, test and evaluation.

2. integrate related technical parameters and insure compatibility of all physical, functional and program interfaces, in a manner that optimizes the total system definition and design.

3. integrate performance, producibility, reliability, maintainability, supportability and other specialties into the total engineering effort.

Chase (24) says that systems engineering is the

> "process of selecting and synthesizing the application of the appropriate scientific and technical knowledge in order to translate system requirements into a system design, and, subsequently, to produce the composite of equipment, skills, and techniques and to demonstrate that they can be effectively employed as a coherent whole to achieve some stated goal or purpose".

Hall (43) gave a structure and a methodology to these definitions that, in effect, provides a model of systems engineering that can be used to generate a set of alternatives to meet the needs of a particular project. His paper about a three dimensional *morphology* (Figure 2.1) investigates and describes three fundamental dimensions of systems engineering:

1. A time dimension segmented by major milestone decisions. The intervals between milestones are *phases* which define a coarse structure of activities in the life of a project.

2. A problem solving procedure or series of logical steps that must be performed in each phase of the life of a project.

3. The body of facts, models and procedures (knowledge) needed to get a problem solved.

Program Planning
Project Planning
Development
Production
Distribution
Operation
Retirement

World Events
Political Environment
Engineering

Problem Definition | Value System Design | System Synthesis | System Analysis | Optimization | Decision Making | Planning for Action
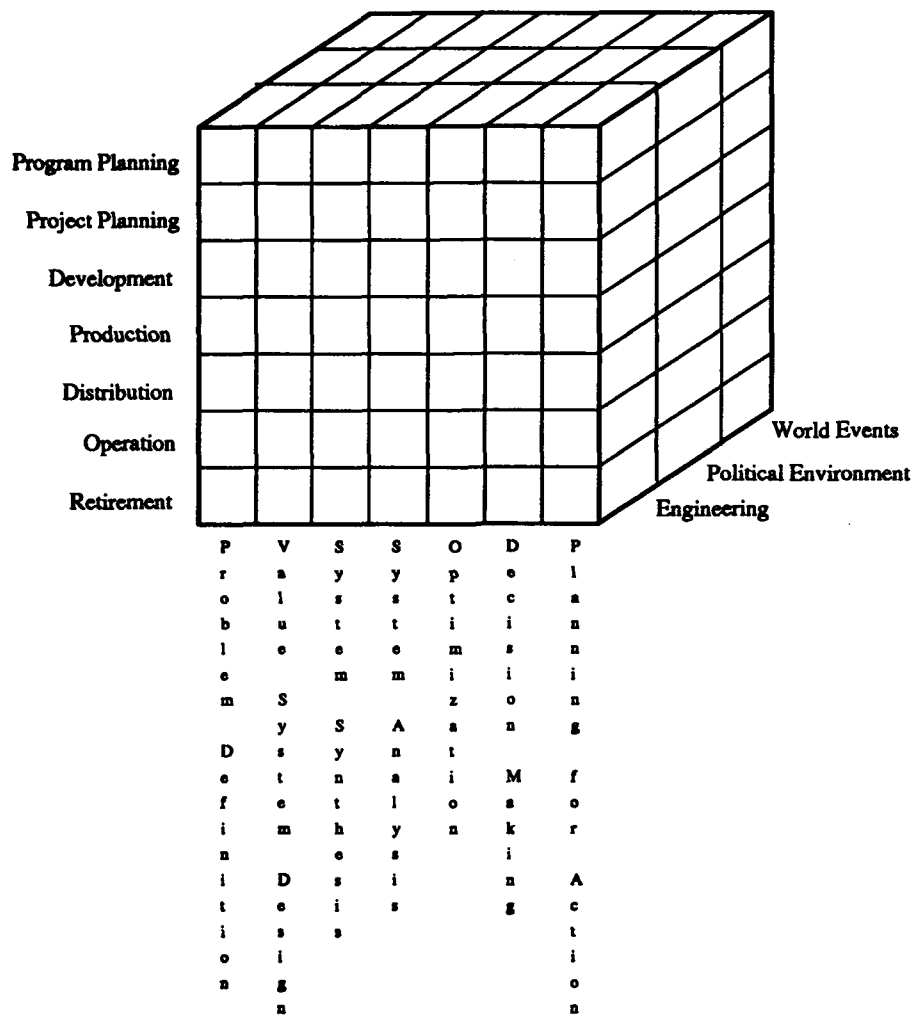
Figure 2.1. Hall's Morphological Box

Hall combined the first two dimensions in what he referred to as an "activity matrix" because each element in the matrix is defined by a unique "activity" at the intersection of a time phase and a logical step of that phase.

2-2

The structure of this matrix and the implied sequence of activities provides a framework within which the systems engineer can operate.

The design project described in this volume involves only the first two phases of the Hall Activity Matrix:

- Program Planning - defining the kinds of activities and projects that should be pursued into more detailed levels of planning (88:p499).

- Project Planning - distinguished from program planning by interest focused on just one project (or set of projects) that leads to a terminal milestone decision to develop the "best" of the alternative systems disclosed during planning (43:p150).

The object of the remainder of this study, then, is to apply Hall's systems engineering methodology to develop

- a "Unified Program Plan" for the design project

- a quantifiable set of alternative *optimized* designs for a 2-stage ICBM that meets the current Minuteman III requirements

- a measurable set of criteria upon which to base a judgement of the design alternatives with the ultimate aim of recommending one (or more) designs for further development.

The remainder of this chapter focuses on the overall program plan.

2.2   Unified Program Plan

The program planning phase of Hall's morphological box is further defined and developed in Hill and Warfield's paper on Unified Program Planning (UPP) (49). The form specified in the activity matrix, specifically the seven logical steps, is used as the basic format for the UPP. Hill and Warfield point out that the form of the plan is determined iteratively with the content. The resulting format for this design study is as follows:

1. *Problem Definition* - required for value system design and subsequent steps: defining program scope, needs, constraints, and alterables

2. *Value System Design* - defining and ranking objectives in a hierarchical structure; relating objectives to needs, constraints, and alterables; and defining a set of objective attainment measures

3. *System Synthesis* - defining alternative solutions and forming a plan for evaluating them

4. *System Analysis* - determining consequences of alternvatives

5. *Optimization* - making each alternative the "best" possible within the constraints and objectives of the program

6. *Decision Making* - selecting and implementing decision-making criteria.

Each of these areas is considered in more detail in the following sections.

2.3 Problem Definition

The main thrust of the design study is to design and estimate the performance, readiness, and cost of a two-stage version of the MM III. Because a two-stage ICBM that will meet the system requirements has not previously been built and tested, the basic feasibility of the concept must first be investigated. Two basic design alternatives are possible:

1. Design using the existing MM III first stage and a new second stage - in effect, replacing the MM III second and third stage with a new second stage.

2. Design a completely new missile replacement.

The project sponsor, Phillips Laboratory's Advanced Ballistic Missiles Applications Branch at Edwards AFB, California, directed the first alternative for this design study, because of the proven excellent performance of MM III Stage 1 during its operational life.

The following, then, is a specific statement of the problem to be addressed in this design study:

"Design a new second stage to replace current Minuteman III stages two and three. Integrate this new second stage design with the existing Minuteman III stage 1 and post-boost vehicle. Estimate the ballistic performance, alert availability, in-flight reliability, and life-cycle cost of the complete system. Meet current Minuteman III range, payload, and silo envelope requirements. Address maintainability, producability, and supportability impacts of the new design".

2.3.1 Assessment of Scope. Initially, an outscoping is done to encompass all pertinent factors of the problem. Once the problem is sufficiently bounded, it is focused on the key factors of the specific problem. The study is limited to the following specific areas:

- investigate the feasibility of of a two-stage design

- evaluate performance

- evaluate availability/reliability

- determine life cycle cost

- use existing technologies or those with significant existing development

- use material and propellant properties representative of the state of the art

- use existing silos for basing the new missile

2.3.2 System Needs. A *need* of the system is an attribute, condition, or parameter which is necessary for a successful solution to the problem statement. The system-level needs are high-level needs which tie directly to solving the stated problem: a feasibility assessment of a two-stage design alternative to meet the current system's requirements. The needs for this design study (as defined by the project sponsor and refined by the design group) are as follows:

1. Meet all mission performance requirements of MM III

2. Operate in the MM III environment

3. Meet baseline availability/reliability

4. Supportability assessment

5. Producibility assessment

6. Life cycle cost analysis

These needs are tied to specific project *objectives* later in this chapter.

2.3.3 System Constraints. There are many constraints inherent to individual technologies and their applications. System-level constraints are high level limits on the possible design alternatives. As possible solutions are analyzed in later steps, lower-level constraints become evident and play a major role in shaping alternatives. At the system level, however, there are three key constraints:

1. The missile must fit into an existing MM III silo.

2. Use existing MM III first stage and post-boost vehicle.

3. Investigate only solid propellant motor designs.

These constraints are further defined in terms of project objectives and specification requirements during the *system synthesis* planning step.

2.3.4 System Alterables. In every design there are variable parameters and decisions which interact to form the differences between alternative designs. These are defined as the "alterables" of the system. The system-level alterables are made up of various technology choices, subsystem design options, and physical characteristics that are permitted within the system constraints. The alterables for this study are:

1. Physical Characteristics

- case size and shape

- nozzle size and shape

- subsystem weights

2. Structural design/materials

3. Nozzle type and design

4. Propellant chemistry

5. Propellant grain design (burn time, operating pressure)

The system needs, constraints and alterables form a set of criteria which bound the design space of possible alternatives that are available to solve the problem. Determining the *objectives* for a successful solution to the problem is part of *value system design*, the next step in the planning process.

2.4 Value System Design

In the previous section, the basic research problem was defined in terms of specific needs, constraints and design variables. The next step in a logical systems engineering approach is to postulate and clarify specific "objectives" that will help resolve the problem, and to come up with ways to measure attainment of those objectives. This logical step is referred to in the literature as *value system design* (88, 49, 43).

Hill and Warfield (49) define three aspects of *value system design*:

- defining objectives and ordering them in a hierarchical structure

- relating the objectives to needs, constraints and design variables (alterables)

- defining a set of measures on the objectives by which to determine the successful attainment of those objectives.

The focus of this section is to continue the planning phase of the systems engineering process by translating the problem definition into a measurable hierarchy of *objectives* which have "value" towards the attainment of the ultimate goal: an optimized solution to the overall design problem.

2.4.1 Value, Objectives and the Objective "Tree". The degree to which a particular alternative is "preferred" over another alternative is a measure of its "value" (89:p69). A "value system" provides the basis for making decisions about the relative value of a set of alternatives. *Value System Design*, therefore, will be defined to be *the transformation of the properties (needs, constraints and variables) of the design problem into a set of interacting elements which will ultimately provide the basis for decision making.*

Webster (32) defines an *objective* as *an end sought.* Hill and Warfield further define a specific syntax for the form of an objective: *infinitive verb + object word or phrase + constraints.* Selection of objectives to be pursued represents a claim (by the group devising the objectives) that the objectives have a possible value in the context of the overall problem (89:p70). The overall idea, then, is to give some precision and structure to program planning by treating a *subjective* problem (in terms of *subjective* needs, alterables and constraints) using *objective* methodologies.

Using Hill and Warfield's procedure for value system design as a guide, the products of the problem definition step (needs, alterables, constraints and the interactions among them) are used as the basis for defining program objectives and an objective hierarchy or "tree". The starting point is simply to define an objective that is clearly contributory toward the solution of the basic problem:

- Design a new second stage to replace Minuteman III stages 2 and 3.

As soon as one objective is defined, the process continues by considering lower and higher level objectives related to it. A lower level objective is one that is contributory to the one that is stated first. Higher level objectives will have to be such that the one stated first is contributory to it.

If this process is continued until all aspects of the problem are accounted for, the result is a kind of "tree" structure with the highest level objectives at the top and the contributory objectives branching successively to the lowest level of the tree (Figure 2.2).
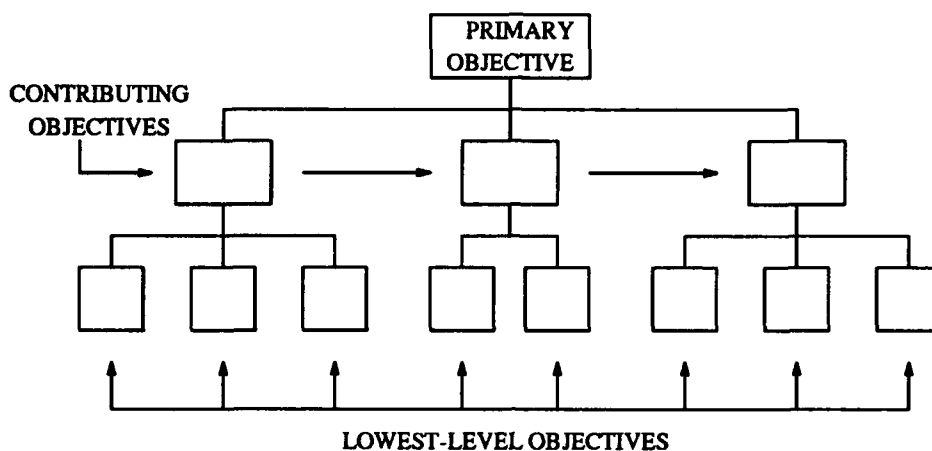
Figure 2.2. Generic Objectives Tree

At the lowest level, the objectives should be directly measurable in some sense, so that the attainment of the objectives can be stated quantitatively in terms relevant to the overall project goal. In this way, some assessment can be made as to whether "progress" (in terms of the value system) is being made. Using the procedure described above, a manageable set of objectives is defined for this study.

2.4.1.1 Program Objectives. Thirteen program *objectives* were identified after careful review and discussion of the program scope, needs, alterables and constraints. In no particular order of priority, the objectives are:

1. To design an optimized second stage to replace Minuteman III stages 2 and 3.

2. To meet the mission performance requirements of the current system.

3. To analyze the Life Cycle Cost of the optimized design(s).

4. To meet or improve current baseline performance in the areas of system supportability, reliability and availability.

5. To define a system performance baseline.

6. To define a modeling benchmark for performance simulation.

7. To design, code and build a trajectory model (for mission performance evaluation of the baseline and all candidate designs).

8. To accurately model the Minuteman III powered-flight trajectory as validation for the design trajectory model.

9. To define a cost model that is appropriate for analyzing the cost of an ICBM system.

10. To identify cost drivers and all design parameters needed as inputs to the cost model.

11. To design all candidate alternatives with priority consideration given to cost, performance and supportability.

12. To define Minuteman III availability, reliability and supportability baselines.

13. To model 2-stage design availability/reliability/supportability and to assess design performance with respect to the baseline.

Each of these objectives was carefully stated in terms of the syntax advocated by Hill and Warfield. Each objective was further tested to insure that it met a specific program need or fit within a constraint. Each was evaluated to see that it either contributed to the attainment of a higher level objective or served as an axiological statement of the top-level program "values". A final check was made to insure that the entire scope of the program was covered by the stated objectives. Having satisfied these considerations, the next step was to form a logical "tree" to order and organize the objectives into a framework that could form a measurable basis for the remaining program planning steps in the systems engineering "morphology".

2.4.1.2   The Objectives Tree. The objectives tree (Figure 2.3) is formed from the list

provided in the previous section. Notice that at the top level, the objectives are more general and

related to the value system defined for the project, and at the lowest level, the objectives are more

specific and measurable.
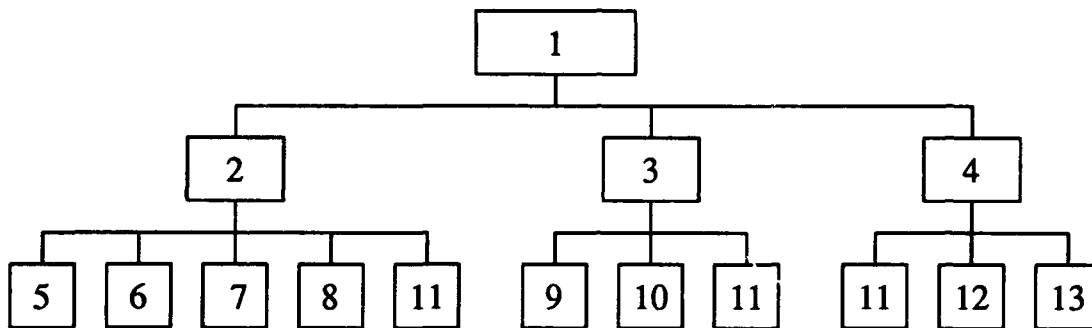
Figure 2.3. Project Objectives Tree

The top level objective covers the general problem statement for the project. The second-tier

objectives (2-4) break the needs into three general categories for evaluation purposes: performance,

cost and supportability or readiness. These second-tier objectives are further broken down to third-

tier tasks, and this breakdown could conceivably continue to even more levels until all project-

related activities were specifically defined. Stopping at the third-tier level is appropriate here

because specific measures of attainment can be identified at this level. A further breakdown, while

appropriate for the execution of various activities associated with the third-tier objectives, is not

required for an understanding of program planning. What is required now is a set of measures on

the objectives by which to determine their attainment.

2.4.2   Objective Measures. Defining a set of objective measures is a key concern in program

planning. Too often, objectives are defined without thought as to how their accomplishment will

be measured. As previously stated, axiological objectives usually can be found at the top of the

objective tree. These top-level objectives serve a directing or "inspirational" purpose, but are not

very useful for planning. The lowest-level objectives are more useful for planning, because they are readily converted into planned, measurable activities.

An examination of Figure 2.3 provides insight into which objectives are measurable and how they may be measured. The top-level objective is measurable only in terms of its contributory objectives, and so the logical place to start is at the bottom.

2.4.2.1 Measures of System Performance Objectives. Objectives 5-8 and 11 all contribute to the attainment of Objective 2. In order to "meet the mission performance requirements," then, the following must be done:

- define a baseline of "performance"

- define a modeling scenario as a basis for an equitable comparison of the baseline with the designed systems

- model the system dynamics and validate the model

- evaluate the performance of all designs (using the model)

- design all alternatives with cost, performance and supportability in mind.

Baseline performance was established through discussions with Phillips Lab personnel. For this study, baseline performance is defined with respect to a specific scenario generated with "POST" (Program to Optimize Simulated Trajectories), a FORTRAN program used by Phillips Lab systems personnel (see Appendix A)(79). The final measure of baseline performance is a specification, presented in Chapter 3.

A system model is generated using the CAD package $Matrix_x$. The basic equations of motion are implemented in a routine that numerically evaluates the basic equations over the booster burn time and predicts position, velocity, acceleration, and flight path angle at the end of each stage. The model is validated against comparable output from POST.

2-12

The specific measure of system performance is an *energy ratio* which relates *NEMESIS* design performance to the baseline and gives a maximum payload capability associated with a particular design.

Design to cost, design to producibility, design for availability and design for performance are evaluated independently and a final design matrix is used to assess the combined effect of all these factors in the design for a particular candidate.

2.4.2.2   Measures of Cost Objectives. Objectives 9-11 all contribute to the attainment of Objective 3. To "assess cost", the following are required:

- define an appropriate cost model

- identify all design cost drivers and design parameter inputs

- consider cost in basic design decisions.

The cost model chosen for this project is really two models: STACEM (for R& D and production costs) and STRAMICE (for operations and support costs). Details are presented in later chapters.

Cost drivers and required model inputs were identified during detailed discussions with Phillips Lab personnel and by a review of documentation available with the models (18). Design drivers in the form of weights and complexity factors are required as inputs.

2.4.2.3   Measures of Readiness Objectives. Objectives 11-13 are contributory to Objective 4. To "maintain or improve performance in terms of the "ilities", the following are needed:

- a supportability baseline

- a model or set of criteria to judge *NEMESIS* performance with respect to the baseline

- consider the "ilities" during preliminary design

The supportability baseline was determined from extensive research (67, 74, 75, 94) and interviews with system experts. Baseline models of system availability and in-flight reliability are developed and used as a basis to judge the performance of *NEMESIS* design configurations.

The overall objective tree and the related objective measures are the key outcomes from the value system design step of the program planning phase. A framework for the design process is now in place, and planning proceeds to the next step in Hall's morphology: *system synthesis*.

2.5 System Synthesis

System synthesis activities are aimed at answering the following questions:

- What are the alternative approaches for attaining each objective?

- How is each alternative approach described? (49:p)

The answers to these questions are usually in the form of a series of activities which form a plan to evaluate alternative approaches for attaining the program objectives. Three major "linkages" must be given visibility:

1. the relationship between planned activities and program objectives

2. the interaction between planned activities and program constraints

3. a measurement system relating progress on activities to the attainment of objectives.

Various techniques are available to accomplish these linkages. Hill and Warfield (49) use cross-interaction matrices to relate attainment of objectives to accomplishment of activities. The resulting program planning linkages give an overall view of a program, relating needs, alterables, constraints, societal sectors, agencies, objectives, objective measures, activities, and activity measures. One figure is used to portray the overall program as planned at the end of system synthesis.

For this project, the design team started with a synthesized program chart. However, because of several changes in program direction and changes in sponsor personnel that occurred fairly late in the project, the original plan underwent several significant revisions, and all the charts and interaction matrices were not re-generated with each change in the overall plan. Instead:

- program scope and problem definition were frozen during a teleconference with the new sponsor management

- measurable objectives were identified (as previously presented) to cover all program needs/constraints

- activities associated with the objectives were identified and an exhaustive list was compiled by each responsible design group

- the design team, in conjunction with the sponsor and faculty advisors, tied activities to objectives and scheduled all activities to meet the overall program plan

With this integrated set of objectives, activities, and measures linked with a detailed schedule of all key program events, the logic step of *analyzing alternatives* could be undertaken.

2.6 System Analysis

The system analysis step considers all possible alternatives and evaluates the various consequences. With this information, the list of all possible design solutions is reduced. The resulting options are optimized to make their characteristics as favorable as possible before proceeding to the decision-making step. Chapter 4 describes the various methodologies and rationale for generating specific design options.

The scope of this study includes a description of which technologies are valid for consideration. Within this area, the use of Integrated Stage Concept (ISC) technologies has been emphasized by the sponsor. Therefore, the class of all possible design solutions includes ISC missile stages as well as conventional technology stages. Within each of these categories many possibilities exist for

further segmentation and classification. For this study, missile designs are broken into one of two categories: ISC and conventional.

Both ISC and conventional missile categories have attractive characteristics which makes it necessary to consider both approaches. Both conventional and ISC two-stage missile designs are capable of satisfying the requirements of the "corporate" or "agency" policy. Here, the "agency" is the sponsor, but in a larger sense, the "agency" is the operating command and the National Command Authority. The sponsor is naturally interested in application of new technologies, but the use of ISC technology must fit within the guidelines established by the Users (see Chapter 1). These guidelines encourage any affordable solution, including more conventional approaches. Furthermore, the higher inherent risk of relatively undemonstrated technology may outweigh any performance, cost, or reliability advantage in the User's decision-making process.

A preliminary analysis of both the conventional and ISC two-stage design feasibility is presented in Chapter 1. Since a structural ratio of between 0.0683-0.10058. is shown to be feasible with either approach, and since the relative costs, performance, reliability, and supportability risks and benefits are not clear without additional analysis, both approaches are investigated in the preliminary design phase (Chapters 3-6) of the study. The costs, risks, and benefits of each design approach are evaluated and the results are presented in terms of the decision criteria. The specific criteria used in this design study are presented later in this chapter.

2.7 System Optimization

Each design alternative which survives the analysis phase of the study is improved as much as possible prior to decision making. Life cycle cost, availability, reliability, producability, and supportability are all characteristics which are desirable to improve. However, maximizing the utility of each of these areas is done with qualitative rather than quantitative techniques. Only system performance can be described as a continuous, although implicit, function of design vari-

ables. Non-linear optimization techniques are used in Chapter 5 to maximize system performance for each design alternative.

The "best" design solution involves more than just system performance. An overall comparison of each design is done in terms of performance, life cycle cost, reliability/availability, and other supportability factors. A final matrix of designs and their respective characteristics is created in Chapter 6. The decision-making criteria developed in the following section are applied to each design alternative to develop the conclusions and recommendations of Chapter 7.

2.8   Decision Making in Program Planning

2.8.1   Decision Making Factors. During the previous steps in program planning, measures were defined for determining the attainment of program objectives, a set of activities and a schedule was defined, and alternative approaches to meet the program objectives were identified and examined. What remains to be done is to decide on the criteria which will be used to select projects or alternatives for further systems development.

Four major factors concern the decision maker in evaluating alternative projects:

1. Are the scopes of the projects consistent with "corporate" or "agency" policy?

2. What are the comparative project costs (in terms of life-cycle cost)?

3. What are the risks associated with the proposed projects?

4. What is the "worth" or benefit associated with each project?

These factors are looked at implicitly as the basic approaches to problem solution are considered in the previous section. Now, attention is turned to the specific criteria used to guide decisions about the value of a particular design or design approach.

2.8.2   Decision Criteria. Many ways to compare projects are discussed in the literature. Many of these methods, however, are more appropriate to program phases where a single, scalar-

valued criterion function can be established to combine all the major evaluation factors. Alternatively, weighting criteria can be assigned to multiple factors if a clear preference for one factor over another can be established. In this project, the sponsor is not driving a decision in terms of either a single factor or of a weighted combination of factors. What is desired is a comparison of any and all feasible design alternatives in terms of the three main objective criteria: mission performance, cost and readiness.

The complex nature of decision analysis in large-scale systems projects can be attacked in this case by taking advantage of the basic structure in the problem. An objective hierarchy has been established which, in effect, decomposes the main problem into three coupled subproblems. It should be possible to solve each of these problems independently and then coordinate the independent solutions to provide a single solution or set of solutions to the overall problem. The advantages of this approach are:

- the problem is reduced to a more manageable level

- a division of labor is facilitated and individuals can be assigned to work on pieces of the problem most suited to their abilities

- weighting or importance factors can still be assigned late in the project if the relative importance of the factors changes due to some influence currently outside the controllable boundaries of the project.

Therefore, the decision criteria are defined in the three main areas of evaluation as follows:

1. Mission Performance Criteria (MPC)

- What is the maximum payload that the *NEMESIS* design alternative can carry and still obtain an energy ratio equal to 1.0 (as determined by the output of the trajectory model)?

- Implication - more payload indicates a better design from a mission performance stand-point.

2. Cost Analysis Criteria (CAC)

- What is the Life Cycle Cost of the *NEMESIS* design alternative as determined by the STACEM and STRAMICE cost models?

- Implication - lower cost is better.

3. Readiness Criteria (RC)

- What is the availability ratio associated with a particular *NEMESIS* design alternative, as determined by the availability analysis?

- Implication - higher availability ratio is better.

For each optimized NEMESIS design alternative, the MPC, CAC, and RC are computed, and the results are summarized in Chapter 6. Results are presented, without prejudice, to the sponsor. If a single *NEMESIS* design stands out as clearly superior in all three areas of evaluation, it is recommended (Chapter 7) as the preferred approach. If the decision is not as clear-cut, the sponsor's input will be sought, and a weighting approach could be considered in making a final decision regarding the "best" alternative design(s).

2.9 Summary and a Look Ahead

This chapter presents an overall program plan to solve the main design problem. First, the problem is defined in terms of a clear and unambiguous problem statement, a set of needs, alterables and constraints, and a clearly bounded scope. Next, a value system design approach to defining objectives and objective measures gives a framework to the plan. This framework is synthesized in a set of activities, activity measures and a schedule designed to make and measure progress

toward the attainment of the objectives. Analysis and optimization of potential design alternatives highlights two fundamental approaches to solve the problem: conventional and integrated stage technologies. Both approaches are deemed worthy to continue into the next program phase. Finally, an overall approach to decision making is discussed, and criteria are established for picking the "best" design(s).

In the chapters that follow, the logic steps of the program planning phase are repeated in the *project* or *preliminary design* phase of the program (recall Figure 2.1). Chapter 3 presents a definition of the problem in terms of specification requirements, as well as a value system design methodology in terms of a set of integrated project models. Chapter 4 presents a design synthesis and analysis methodology leading to the generation of 33 unique *NEMESIS* design alternatives. Chapter 5 presents the approach to system performance optimization, and highlights the iterative, interactive nature of the design process. Chapter 6 presents the results in terms of five optimized design alternatives. Chapter 7 discusses conclusions, recommendations and possible follow-on work as planning for the next (prototype development) program phase.

III. System Requirements and Methodology

3.1 Introduction

This chapter establishes the design and performance requirements for the *NEMESIS* system. It also describes the design and integration of the various computer models that are used as tools to quantify and evaluate all system design options.

The previous chapters have presented some background and a program plan in terms of needs, alterables, constraints and specific objectives that must be met to insure that a complete systems approach is taken to solve this design problem. The main objective is to design a second stage booster that, when integrated with the current MM III first stage

- meets MM III mission performance requirements for payload delivery

- is reliable, available, supportable and producible

- is affordable in terms of life cycle cost

In order to transition from a *program planning* phase into a *project planning* and preliminary design phase of the systems engineering process, the objectives must be focused into design *requirements* that are clear and measureable in terms of system design variables and quantifiable performance measures.

In the previous chapter, the top level objectives were further broken down into lower level objectives. "Meet mission performance requirements" broke down into

- define baseline requirements

- determine feasibility of a two-stage booster

- model system performance

- assess performance of each candidate design

"Evaluate life cycle cost" was further refined to

- develop and implement a cost model

- generate all system design variables needed as cost model inputs

- estimate the life cycle cost of all optimized candidate designs

And finally, "design a reliable, available, supportable and producible system" becomes

- define baseline requirements

- model system reliability and availability

- establish weighting criteria for producibility and supportability assessment

- assess performance of each candidate design

Notice that the following common themes are evident as the objectives get closer to the bottom level:

1. A baseline must be established.

2. A model must be developed and validated against the baseline.

3. Alternatives must be generated and evaluated with the validated models.

4. The "best" alternative(s) must be identified and decisions made.

This chapter details the work that was done to address the first two "themes" listed above: to establish a system baseline "specification" and to develop and validate the models needed to quantitatively evaluate candidate designs against the baseline. Subsequent chapters discuss the generation, analysis and optimization of these design alternatives.

3.2 Problem Definition - A System Baseline

In the previous chapter, an overall program plan was established that details the various needs, alterables, constraints and objectives for the design work and gives a clear description of the problem to be addressed. Now, the task is to transform these needs, alterables, constraints, and objectives into a working specification for the two-stage design. This specification is needed to give a set of measurable baseline criteria upon which to make judgements about the "goodness" of a particular design. Since the MM III system is the baseline for the proposed 2-stage *NEMESIS* design, all requirements are derived from the requirements on MM III. In the sections that follow, each of the overall program needs and constraints developed in Chapter 2 is used as a basis for a *system* requirement.

3.2.1 Program Need/Constraint: Fit Into Existing Silo.

Since the *NEMESIS* must fit an existing Minuteman III silo and interface with current ground support equipment (GSE), the following physical characteristics and interface requirements apply:

1. Physical Characteristics (78)

    - Maximum diameter of air vehicle - less than 12 feet

    - Maximum height of air vehicle - less than 90 feet

    - Maximum system weight - 78,000 pounds

2. Functional Interfaces

    - Vehicle - GSE communication through existing D37-D Guidance Computer

    - Existing vehicle battery power and ground power will be used

    - Ground coolant as currently provided

    - Telemetry and self-test as currently provided

    - Startup/initialization sequence unchanged

- Safe/arm and calibration/alignment systems unchanged

3.2.2 Program Need/Constraint: Use Existing MM III Stage 1 and Post-Boost Vehicle. The success of the current MM III first stage (never remanufactured in 24 years of fielded service) led to sponsor direction to design a system with the current MM III first stage as a "given". In addition, the entire MM III "fourth stage", including the PSRE and MGS, is a "given" for this project. In between the current Stage 1 and the current post-boost vehicle (PBV), a single stage replacement for the current stages 2 and 3 is desired. Therefore, the following requirements apply:

1. Physical Characteristics

   - Stage 2 maximum diameter - 66 inches (to mate with current Stage 1)

   - Stage 2 minimum diameter - 52 inches (to mate with current PBV)

   - Max weight of Stage 2 and PBV - 27000 pounds ≡ max capability of Stage 1

   - Booster system will be two stages (including current Stage 1)

2. Functional Characteristics

   - Use existing MM III MGS for guidance and control

   - Flight control modifications above Stage 2 are assumed to be exclusively software modifications

   - Staging sequence modifications above Stage 2 are assumed to be software modifications

3.2.3 Program Need/Constraint: Meet Mission Performance Requirements of MM III. The 2-stage booster design must perform the mission of the current 3-stage MM III system. Therefore, in terms of payload (PBV) delivery requirements, the system must have

1. 8000 mile range

2. MM III accuracy (not addressed in this study)

3. A throw-weight capability of between 1500-2300 pounds

Since the PBV is not a candidate for design change in this project, and since the PBV follows (basically) a ballistic trajectory after the boost phase of powered flight, the real specifications for the design project need to focus on the desired PBV dynamics at the end of boosted flight. To know the end position of a ballistic projectile, the following are needed:

- altitude at completion of second stage boost

- velocity at completion of second stage boost

- flight path angle at end of boost

- downrange position at end of boost

- PBV mass

Therefore, the system mission performance requirements can be appropriately re-stated in terms of altitude, velocity, flight path angle and mass at end of Stage 2 burn. It was desireable to obtain a measure of system performance that is not dependent on the mass of the PBV. For this purpose, the PBV altitude and velocity can be combined into a specific energy measure where the system's total energy at the end of boost is the sum of the system's kinetic energy and the system potential energy:

$$E_{total} = m(\frac{1}{2}V^2 + gh)$$

If both sides are divided by the mass, m, the total energy per unit mass or *specific energy* can be defined as

$$E_{specific} = \frac{1}{2}V^2 + gh$$

and the performance measure is no longer dependent on the mass of the vehicle above stage two. The specific energy for the current 3-stage baseline is taken from the output of Phillips Lab's POST

simulation for a given scenario (details in Appendix A). If an energy ratio is formed as

$$E_{ratio} = \frac{E_{specific,NEMESIS}}{E_{specific,MMIII}}$$

then the final specification for *mission performance* reduces to the following measures:

1. Energy ratio must be ≥ 1.0

2. Payload capability for energy ratio ≥ 1.0 must be greater than 1500 pounds

These measures are subject to the constraint that the flight path angle at end of Stage 2 boost must match output of the POST simulation of the 3-stage MM III for a given payload.

3.2.4   Program Need/Constraint - Operating Environment is Similar to MM III .   There are really two distinct operating environments for an ICBM: the alert environment and the in-flight environment.

In the alert environment, the key design drivers are the temperature, pressure and humidity within the silo. Each bears some impact on the aging characteristics of the system (see Appendix D for details). The design specifications for alert-status operation are (12):

1. Pressure — 16 psia (max)

2. Temperature — $45^0 F - 110^0 F$ (70^0 nominal used)

3. Humidity — 3-100% for temperatures $\leq 44^0 F$; dewpoint of $44^0 F$ used for temperatures above $44^0 F$

In the flight performance environment, internal propellant burn temperatures, burn pressures and burn times, as well as external aerodynamic heating, accelerations and vibrations drive the system design. Parameters such as motor case size and thickness, insulation thickness and the operation of guidance, flight control and staging electronics are all dependent on the expected in-flight environment. In addition, the requirement to fly through and survive post-nuclear blast debris

drives the design of case external protective materials.. For this project, the following characteristics bound the primary internal and external environment parameters:

1. Max internal burn pressure - 1800 psi

2. Aerodynamic heating - $260^0 F$ maximum

3. Max longitudinal accelleration - 18 g's (12)

4. Nuclear debris - see Table C.9, Appendix C

3.2.5 Need/Constraint: Meet Baseline Reliability/Availability. The baseline system has maintained a very impressive alert availability and in-flight reliability record over its system life (see Appendix D for details). The goal in the current research is to maintain that record and, if possible, to identify areas for potential improvement. Therefore, in terms of specification goals:

1. Use solid propellants to meet 24-hour, no-notice alert availability

2. Meet the baseline 3-stage alert availability model prediction

3. Meet the baseline 3-stage in-flight reliability model prediction

4. Meet or exceed the baseline 17-year motor design life

5. Use current Minuteman maintenance concept

3.2.6 Need/Constraint: Assess Impact of Design on Other Supportability Elements . An overall system design must address other Integrated Logistics Support (ILS) program elements such as field support and test equipment requirements, maintenance manhours, number of parts, number of spares required, etc. Though a full-blown ILS analysis is beyond the scope of this project (Chapter 2), a qualitative assessment of each candidate design will be made as to whether the design is supportable in comparison to the baseline.

3.2.7 Need/Constraint: Producibility Assessment. One of the key features of a design that contributes to its attractiveness and affordability is whether or not the design can be built within the current state of the art in manufacturing and materials. For this project, technologies and manufacturing techniques will be considered only if the development schedules for the candidates would make them available now or within a time frame that would support the next MM III remanufacture cycle.

3.2.8 Need/Constraint: Life Cycle Cost Analysis. Each design will be examined with cost reduction as a primary concern. Reducing weight by judicious design and/or elimination of parts, improving supportability by reducing maintenance manhours, and streamlining manufacture of system components are a few examples of areas that can lead to an overall life cycle cost savings. A life-cycle cost analysis will be made on each candidate design, and the cost will be considered with mission performance, availability, supportability and producability in identifying the "best" system option(s).

With the baseline requirements identified, attention can now be given to the design methodology to be used to synthesize and analyze design alternatives.

3.3 Design Synthesis and Assessment — An Overview of the Modeling Process

All the attention to this point has been aimed at understanding the background and motivation for the current work, and at clearly defining and scoping the problem in terms of objectives and specification requirements. Now, the focus turns to the methodology to be used to synthesize and evaluate design alternatives.

System "synthesis" is primarily concerned with the answers to three questions (89:p73):

1. What are the alternative approaches for attaining each objective?

2. How is each alternative described?

3. How is the attainment of objectives measured?

Synthesis, then, implies a linkage between the design objectives and the design alternatives. Linking the objectives, activities to accomplish the objectives, objective measures and activity measures to design alternatives is accomplished by the development, use and analysis of information obtained from a series of integrated project element models. It is the goal of this section to give an overview of the modeling process, and to show how each model is used (singly and in a systems sense) to generate and synthesize system design alternatives that can be tested against the baseline requirements.

In previous sections, the design performance criteria were presented. These criteria can be summarized in the following questions:

- Does the design meet performance requirements for specific energy and payload carrying capability while functioning in the required dynamic environment?

- Does the design meet baseline requirements for alert availability and in-flight reliability?

- Is the design supportable and producible?

- What is the life cycle cost of the design alternative?

In order to answer these questions, the integration team designed, coded, and tested several integrated computer models. These models are created from scratch in some cases. In other cases, existing code is exploited for this application. Each of these models is discussed in detail in the appropriate appendix. It is the intent here to discuss the goals and purposes of each model, to show how the models interact, and to show how, in total, they contribute to the overall system design process and help answer the questions posed above.

3.3.1 The Propulsion Model . The propulsion performance model is the starting point for estimating the performance of the given stage configuration. The choice of propellant, propulsion technologies, and physical characteristics for the propulsion model yield chamber pressure, chamber

temperature, and stage component weight estimates for the structural model. Some of the weight estimates are provided by the AIDE-II program provided by Aerojet. Thrust and mass flow time histories are generated for use by the trajectory simulation.

The propulsion model is shown schematically in Figure 3.1. The choice of propulsion technology is a key factor in determining the performance of a missile (stage). Recent developments in Integrated Stage Concept (ISC) technologies make an ISC stage possible. More conventional missile technologies are also considered. The propellant to be used is an important design parameter, and it is linked to the choice of ISC or conventional technologies. Boron-based propellant is necessary for ISC stages while an aluminum-based propellant is suitable for conventional missile stages. Other inputs may include the nozzle throat and exit areas, chamber pressure, mass of propellant, and key grain design parameters. Which of these parameters are necessarily chosen is dependent on the choice of grain design. The generation of a viable grain design becomes a primary issue in designing a stage to meet the given mission.
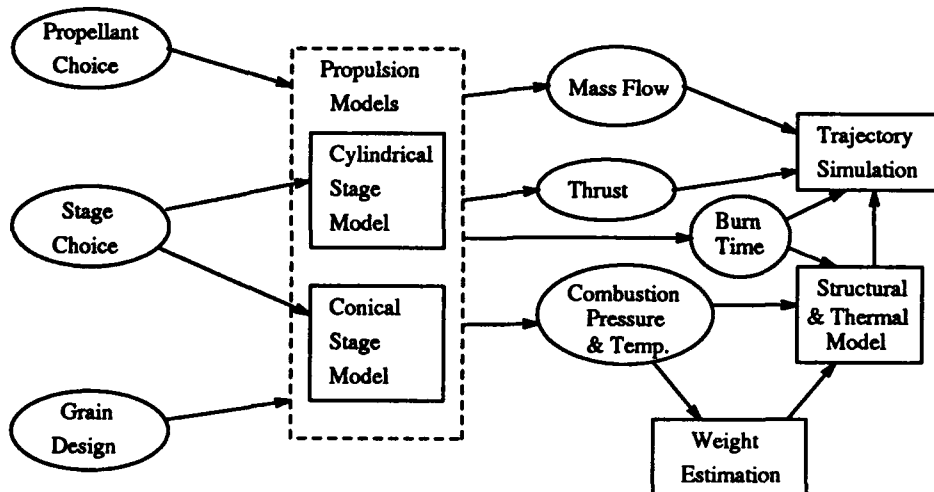
Figure 3.1. Propulsion Performance Model

Outputs of the model include the physical dimensions of the grain size and the grain design. The chamber pressure may be an output, again depending on the grain design chosen. In either case, the outputs are provided to the structural model.

3.3.2 The Structures, Thermal and Materials (STM) Models

3.3.2.1 The Case Structural Model.

The Structures, Thermal and Materials (STM) group had the responsibility to design a solid booster case, an internal case insulation and liner, and an external protective material (EPM) to shield the case in its expected operating environment.

Filament-wound composite materials are chosen for second stage motor case design (see Appendix C). The method used to determine composite thickness for the integrated second stage is called *netting analysis*, which is a simplified procedure used mainly to estimate fiber stress in a cylindrical vessel subject to internal pressures (directly applicable for cylindrical ICBM case design). The netting analysis procedure adapted for this study

- determines a minimum thickness to withstand the internal pressure loads determined in the propulsion model for a particular motor grain design,

- examines the buckling criteria and other principal normal stresses to ensure that the pressure vessel does not collapse under a given load,

- calculates case volume based on the geometric properties of the design generated in the first two steps.

Similar calculations are used to design a conical-shape case, except that the filament wind-angle is optimized for each of the three sections of the conical body: aft dome (conventional design only), barrel and forward dome. Again, minimum thickness, buckling criteria and case volume are the outputs used in the other system element models.

3.3.2.2 Insulation/Protection Design - The Thermal Model.

Internal insulation must protect the case from the high temperature of combustion that develops during missile flight. The location of the insulation (between the case and the propellant) allows it to act as a heat sink. The insulation must absorb enough heat such that the case wall temperature stays below a specified limit (135^0C) that is a function of the case material properties. Two very different propellants are considered in this project:

- boron propellants for integrated stage designs which burn at 2895^0C

- aluminum propellants for conventional stage designs which burn at 3264^0C

The thickness of the insulation depends on both the burn temperature and the *exposure time* or *burn time* of the propellant in the motor. The burn time varies with a particular grain design.

External Protective Material (EPM) is needed for two reasons:

1. The ICBM is required to fly (at very high velocities) through and survive post-nuclear blast debris.

2. Aerodynamic heating effects raise the external skin temperature to a maximum of 260^0C (and, again, 135^0C is the permissible limit for the case material).

In order to determine the required thickness of the internal case insulation and the external protective material for a variety of motor grain designs, a computer model is needed. Using a finite difference approximation of the general heat diffusion equations, a FORTRAN model is developed. The model inputs are thermal conductivity, specific heat, density and thickness for the EPM, case and internal insulation materials. The outputs are the temperatures at several points within each of the three (EPM, case, insulation) materials, and the temperatures at each interface as functions of time. EPM and insulation thicknesses are adjusted iteratively until the temperature at the inner and outer case walls stays below 135^0C through second stage burnout.

Note that the motor liner, which primarily provides a bonding surface between the solid propellant and the insulation, is not included in the thermal calculations. Therefore, any potential thermal benefit that the liner might provide is not accounted for in this model.

3.3.2.3 Weight Estimation . A model to estimate the weights of the EPM, case, liner and internal insulation is needed to supply information to the trajectory and cost models. Using material thicknesses and densities, propellant grain burn properties, and bounded missile dimensions as inputs, the weight model provides case, EPM, liner and internal insulation weights. The weights are used in the trajectory model to calculate structural ratios, and in the cost model as a primary cost driver.

Figure 3.2 is a schematic representation of the entire structural model.

3.3.3 The Trajectory Model . The Trajectory/Performance Simulation (TPS) is developed as a tool for defining the MM III performance requirements and for evaluating the flight vehicle performance of the various 2-stage designs. Simplifying assumptions are incorporated into the TPS to attain reasonably accurate results while maintaining an appropriate level of complexity relative to the other models used in this design study. The TPS (Figure reftpsfig) is composed of 4 main sections: an atmosphere and gravity model, a drag model, a thrust model, and a fourth-order Runge-Kutta differential equation integration algorithm for solution of the gravity turn equations of motion.

3.3.3.1 The Atmosphere, Gravity and Drag Models. The atmospheric model used for the TPS is the ARDC Model Atmosphere developed in 1959 (10). The parameters used in the model are the speed of sound, atmospheric pressure, and atmospheric density, all functions of altitude. The atmosphere model was used solely for the purpose of calculating drag (a function of Mach number and density) and MM III stage 1 thrust (a function of ambient pressure). No wind or air turbulence was included.
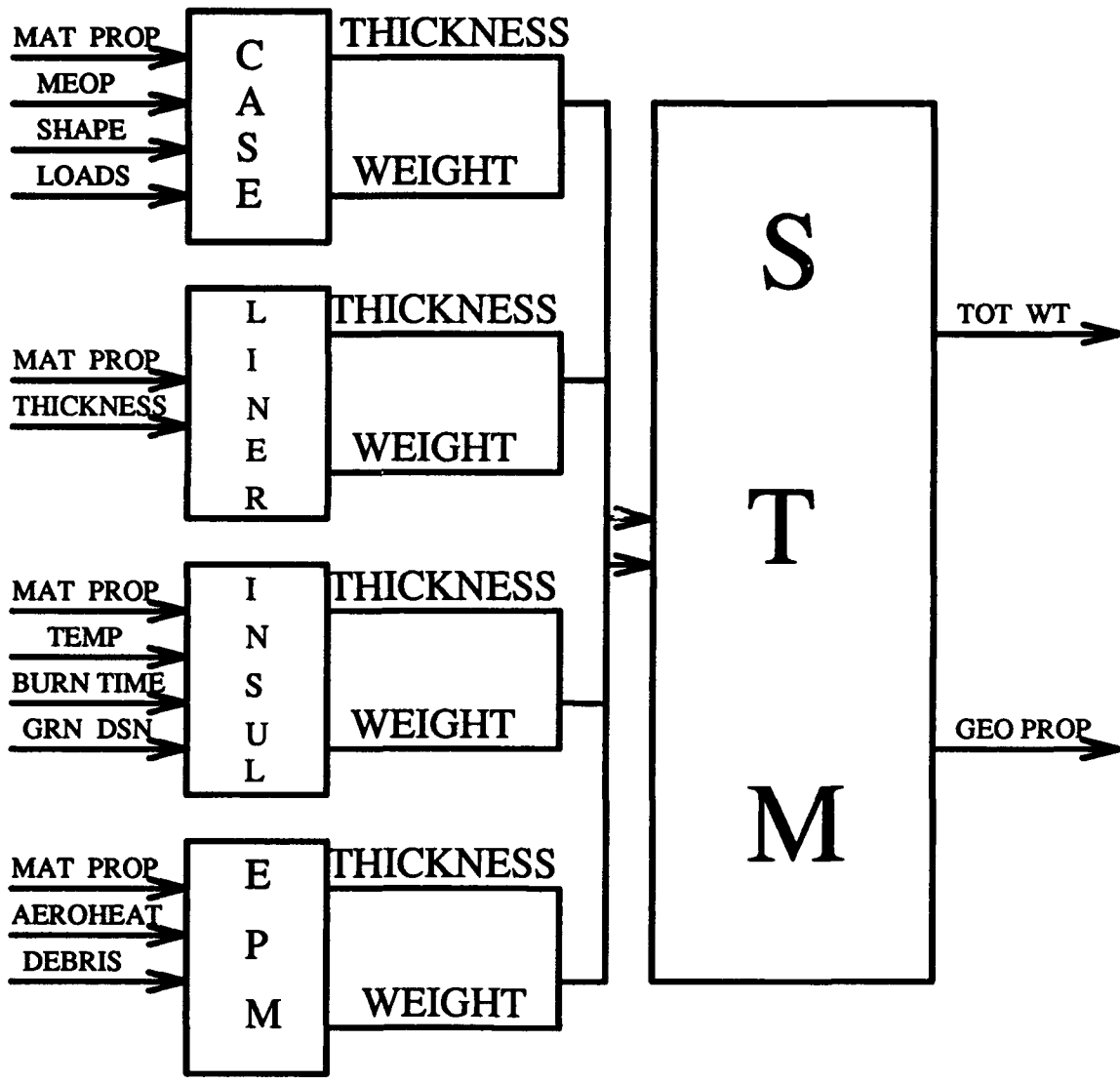
Figure 3.2. Structural Model Inputs and Outputs
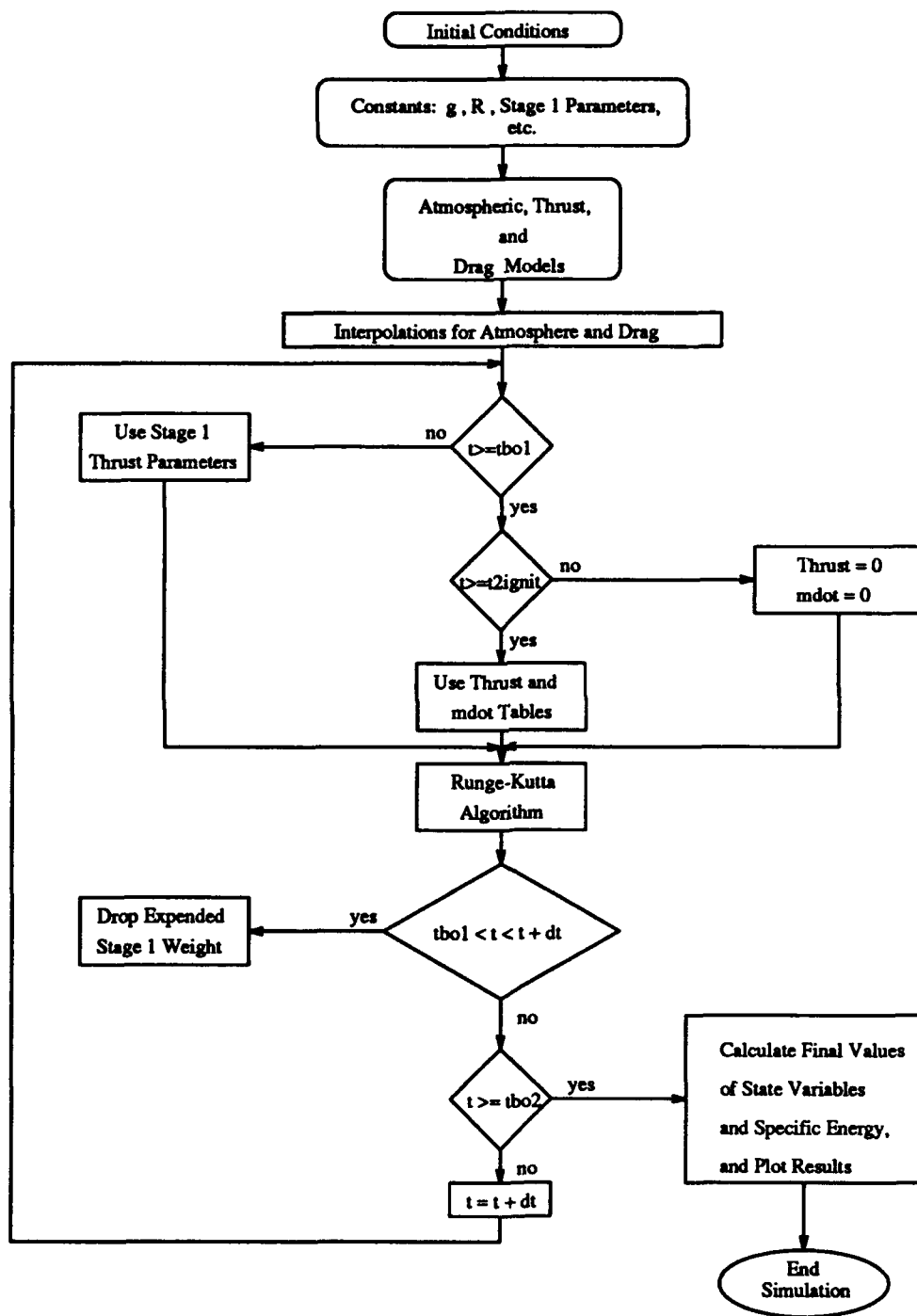
Figure 3.3. TPS Flowchart

The earth's gravitational attraction was modeled with the following equation:

$$g(H) = g_e \left(\frac{R_e}{R_e + H} \right)^2$$

No oblate earth effects are included in the gravity model.

The drag model is based upon a simplified version of the drag model used by the Phillips Lab simulation. Since a gravity turn trajectory is being simulated, zero angle of attack is maintained throughout the flight, thus modeling drag due to lift is unnecessary. The drag coefficient, C_{D0}, as a function of Mach number, is obtained directly from the POST (Appendix A) simulation.

3.3.3.2 The Thrust Model .   Missile thrust calculation is handled in two different ways. First, for the MMIII and Stage 1 of the 2-stage design, the thrust is calculated using the assumptions of constant mass flow rate, exit pressure, and specific impulse. Appendix A shows that these assumptions are appropriate. For the 2nd stage of the 2-stage design, a more accurate method for modeling thrust and mass flow rate is used. Actual time histories of the thrust and mass flow rates are generated for a particular grain design and input directly into the simulation as thrust and mass flow rate tables.

3.3.3.3 Numerical Integration .   A fourth order *Runge-Kutta* numerical integration algorithm is implemented to integrate the time derivatives of velocity, flight path angle, altitude, downrange position, and missile mass. Initial conditions are obtained from the program VERT (discussed in Appendix A) for each of the state variables (except for flight path angle). The initial value for the flight path angle is iterated until the target flight path angle is obtained. Data from the drag, atmosphere, and thrust (where appropriate) tables are then read into memory along with the values for all system weights and simulation constants.

3.3.3.4 Performance Measures .   In order to determine whether the 2- stage design meets the MM III max range requirement, an appropriate quantitative performance measure must be defined. Also, since the TPS is restricted to simulate the powered flight phase alone, the performance measure must be defined within that flight phase. Various approaches were considered in defining a proper performance measure. Of these approaches, matching the burnout state provides the best measure of performance. The total energy of the payload at MM III stage 3 burnout for the maximum range trajectory was adopted as the performance measure for the 2-stage design. This parameter is adequate as long as the PBV weights remain equal for the MM III and the 2-stage design. In order to compare performance with different PBV masses, the *specific energy* is used. Note that the specific energy of the MM III is assumed to be the same for all PBV weights. This means that the energy ratio figure is mission dependent. However if only small differences in payload are assumed, this measure should be a solid measure for the purposes of this study.

3.3.4 System Readiness Model .   In the system design or development environment, information regarding the reliability and maintainability of various alternatives is likely to be imperfect. Therefore, a simulation model is needed so that different values can be included without difficulty, and sensitivity analysis can be performed to determine how parameter changes impact simulated system performance.

There are really two types of "readiness" to evaluate with an ICBM:

- strategic alert availability

- in-flight reliability

As a missile stands alert in a silo for years at a time, there are certain components that fail due to stress or environmental conditions (guidance electronics, flight control electronics, batteries, payload components, case coatings), while other components fail due simply to aging (propellants, ordnance, liners). On the other hand, when the system is called upon to perform its mission,

3-17

the stresses it must withstand and the environment in which it operates are totally different. In addition, there is no way to repair an ICBM once it is launched. Therefore, an "availability" model must capture and evaluate performance under alert conditions, while an "in-flight reliability" model must capture mission reliability.

The system readiness "model" for this project, then, is really four distinct models:

- a 3-stage baseline alert availability model

- a 3-stage baseline in-flight reliability model

- a 2-stage alert availability model

- a 2-stage in-flight reliability model

Each model treats the system measure of merit (availability or reliability) as a series combination cf subsystems. A series configuration was chosen because all equipment must function for the system to be considered available (alert status) or for the system to adequately perform its mission (in-flight reliability). Each design group supplies failure rates and associated uncertainty as inputs to the model.

The failure and repair mechanisms associated with each model element are modeled mathematically using appropriate probability distributions. Age-related failure phenomena are modeled using Weibull distributions. Random field or flight failures are handled with exponential models. Repair times are modeled as a constant 100 hours for guidance and 75 hours for reentry system elements and as a constant 7 days for all downstage equipment, based on past MM III experience (77, 26).

Markov processes (see Appendix D) are used to model the availability of each subsystem element. The system "availability" is then calculated as the product of all individual element availabilities (series model). In-flight reliability is calculated by determining a system reliability baseline and allocating reliabilities to untested new technologies (such as liners, boron propellants and hot

3-18

gas valves) such that the system requirement (as determined by the baseline) is met. The reliability and availability assessments, together with a qualitative assessment of other Integrated Logistic Support (ILS) factors, are then given consideration with system cost and mission performance to pick the best overall system design.

3.3.5 Cost Model . Life-cycle costs (LCC) are total estimated expenditures for a system, from "cradle to grave". In life-cycle costing (LCC), *major factors* are predictable factors that influence program costs. These could be process oriented (capital, labor, material, management), product oriented (the product itself, performance characteristics, operational use, support) and environmental/programmatic (competition, funding, type of contract, schedule) (71). *Cost drivers* are a means of quantifying major factors. They capture the influence of one or more factors on program costs. *Cost modeling* is a method for deriving life-cycle costs through quantitative or qualitative means, or some combination of the two.

A *cost model* is the end result of cost modeling. The purpose is to provide cost estimates over a relevant range, given established constraints and underlying assumptions. Generally, these models take the form of a dependent variable (cost) and one or more independent variables (cost drivers).

No existing model completely characterizes solid rocket booster cost in terms of the total life cycle, therefore two models are chosen for this projet. One model, called STACEM, to evaluate DDT&E and production costs, and another, STRAMICE, to cover O&S costs.

3.3.5.1 STACEM . The *(Solid Technology Assessment and Cost Evaluation Model)* (STACEM) is a cost model software package developed by Booz-Allen & Hamilton Incorporated, under government contract. It is a general purpose cost model designed to provide the solid propulsion (as opposed to liquid fuel motors) industry and Government organizations with a reliable tool which can conduct a broad range of life-cycle cost analyses for solid rocket boosters (SRBs)

(18:Vol 1). Its purpose is to provide the user with " . . a tool for quickly evaluating diverse solid propulsion systems, configurations, and life cycle scenarios" (18:Vol 1).

Structure. The model divides the missile life-cycle into five phases, providing a detailed work breakdown structure for each of these phases. The five phases are (1) solid rocket booster production, (2) launch and support, (3) post-launch recovery, (4) refurbishment, and (5) design, development, test and evaluation (DDT&E). Based on these descriptions, the first and fifth phases are the only ones relevant to the *NEMESIS* project. Cost drivers are supplied to the model in the form of weights and complexity factors. A complete listing of the required weights and factors is presented in Chapter 4.

3.3.5.2 STRAMICE. A review of STACEM documentation, reveals that the model is not useful for estimating the operating and support (O&S) costs of the alternative booster designs. Specifically, with respect to the O&S portion of the booster life-cycle, the STACEM database included only space launch vehicle cost figures. Since support facilities and operations for space boosters greatly differ from those of silo-based ICBMs, the reliability of a STACEM generated ICBM O&S cost estimate is questionable for this study.

The search to find a suitable approach to the O&S portion of the estimate led to the Strategic Missile Cost Estimating (STRAMICE) model in AFR 173-13, *Cost Analysis* (31:pp128-131). Since the last printing of STRAMICE, only one new ICBM program has been introduced and seriously considered for acquisition by the Air Force: Small ICBM, or "Midgetman." The June 1991 O&S cost report for that program discussed a STRAMICE derivative as the basis for the resulting estimate (33). The STRAMICE shell can be quite useful in estimating Minuteman-related O&S costs, provided the cost factors are updated to reflect current conditions.

To make the original STRAMICE model useful for this O&S estimating purpose, three types of adjustments were needed. The first type of adjustment involved updating cost factor inputs for inflation and current pay scales. The second type of alteration addressed the model inputs

for manpower requirements. Specifically, in the example that accompanied the original model, the recommended manning inputs were based on a force of fifty Minuteman ICBMs (31:p130). Therefore, the STRAMICE model was updated for manning inputs for a 500 missile fleet. The third and final type of change incorporated in the model were adjustments to the original STRAMICE algorithms where it was believed estimating accuracy could be improved. Through review of the Small ICBM O&S estimate, some approaches were identified and adopted that were simple, yet more representative of current conditions. Since the original STRAMICE factors are outdated and the source cannot be identified, the estimates from the updated model should be more accurate and credible.

For all practical purposes, the 2nd stage booster designs may be considered Minuteman III upgrades, or modifications. One can expect to find many similarities between the current Minuteman III program and the proposed designs with respect to operations and support. In fact, outside of minor changes, most support equipment, facilities, and manpower requirements should remain constant. As such, analogous system estimating techniques are justified. Since the example that accompanied STRAMICE indicates the model was developed around the Minuteman program, this model should support analogous estimating procedures (31:pp128-131).

3.4   Model Integration

The models discussed in the previous sections are all designed with a systems approach so that each modeled facet of the design (propulsion, structures, trajectory, readiness and cost) benefits from information provided by the other models. In the same way, each model contributes something to the other models in terms of required inputs or feedback. This total system integration of all the element models signals the culmination of the *system synthesis* step in the systems' engineering "project design" phase. With this system model as a tool, a large number of potential designs can be generated, analyzed and optimized.

Figure 3.4 is a schematic representation of the integrated "system model". To understand how this model is actually implemented, a sample scenario and flow of a typical design is presented here.

3.4.1 Design Process Flow

1. Candidate technologies and materials are chosen by the propulsion, structures, and thermal designers. Candidates are chosen based on expected performance, cost, supportability, and producability criteria established within each area of expertise in the context of the overall system requirements.

2. The propulsion motor design provides

   - thrust and mass flow profiles and burn times for the trajectory model,

   - grain length, burn time, burn pressure, and grain pattern burn history data for the case/structure and thermal models,

   - weights, I_{sp}, average thrust, propellant mass and propellant density for the cost model, and

   - service life estimates and variance of estimated parameters for the readiness model.

3. Using inputs from the propulsion model, the structures/materials model generates case, liner, EPM and insulation designs, and these are provided as

   - weights to the trajectory and cost models, and

   - service life estimates and variances for the readiness model.

4. A trajectory analysis is done and max payload, energy ratio and max acceleration are fed, through an optimization routine (see Chapter V), back to the propulsion group for refinement, and the process starts again at step 1.
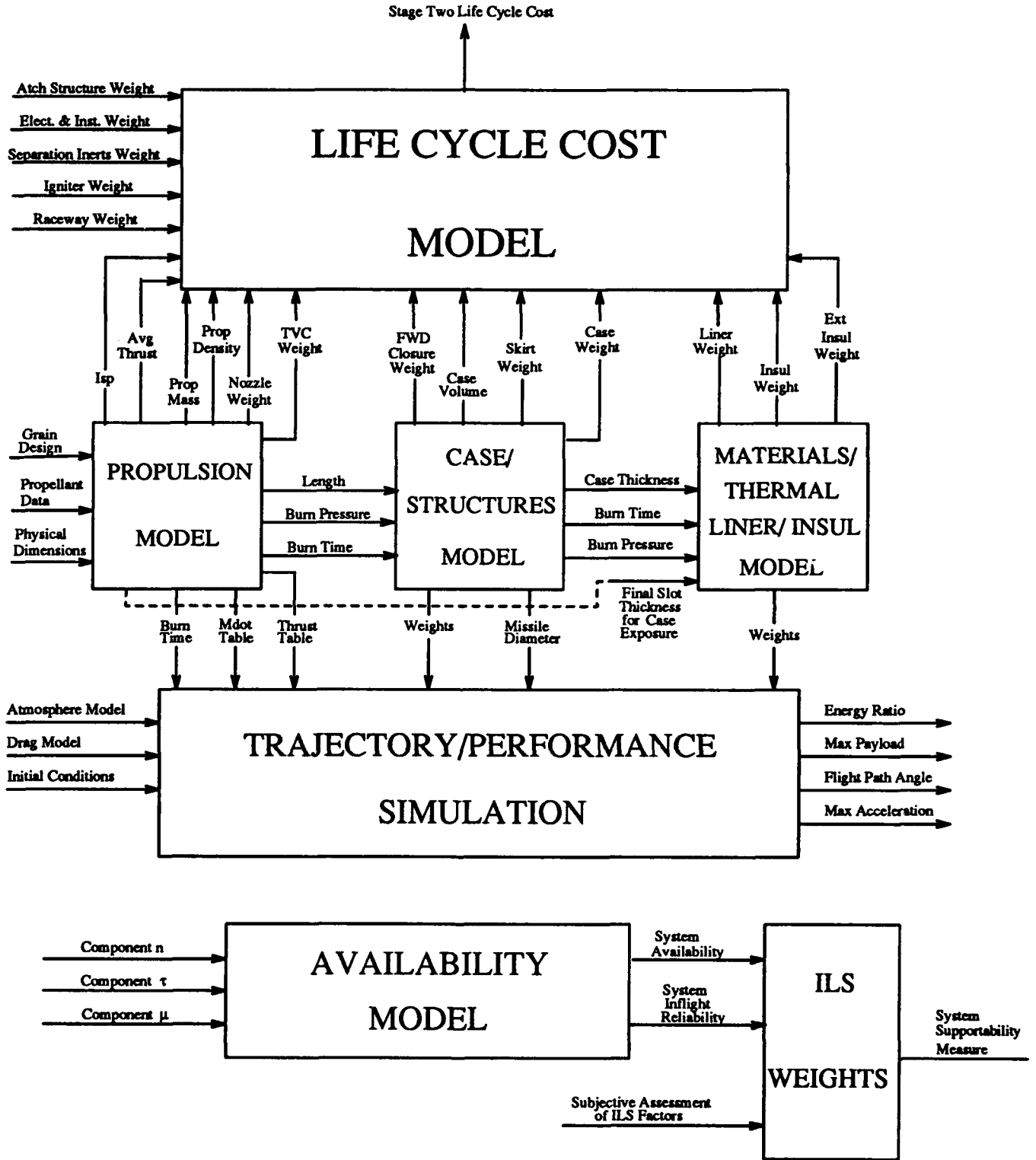
Figure 3.4. Integrated System Design Model

5. An availability/in-flight reliability analysis is done for each model element and for the entire system, and this information is fed back to each design group to incorporate in subsequent iterations.

6. A cost analysis of the candidate designs is done only after each main configuration has been optimized in terms of performance. Non-performing designs are not costed.

This process is applied to all design configurations, and the results are presented in the next chapter which discusses the iterative *DESIGN-ANALYSIS-SYNTHESIS* process that forms the core of systems engineering.

IV. Generation of Design Options

4.1 Introduction

The design study involves the replacement of the 2nd and 3rd stages of the current Minuteman III ICBM with a new 2nd stage. This new stage is required to provide as much performance as the two existing stages, within the constraints placed on the project. Through discussions with the project sponsor, Phillips Laboratory, it was determined that significant development work in the laboratories and the major missile contractors involves the Integrated Stage Concept (ISC). Various studies have been performed that analyze the performance and cost benefits of integrated stage technologies (56, 7). Since the lab advocates an integrated stage approach to the problem, the project work initially focused on this approach. However, although the integrated stage concept showed promise as a potential solution to the problem, it was decided that more conventional technologies should also be evaluated.

4.2 Booster Technology

4.2.1 Integrated Stage Concept (ISC).
The integrated stage concept is a "new" look at how boosters for ICBM's are designed. ISC has been pursued in the solid rocket industry for the last 15 to 20 years (95), however only recently have advances in materials and techniques allowed the concept to be considered feasible for incorporation into a system design. There are four technologies that make up the integrated stage concept:

1. Full Diameter Joint and Reverse Dome – Consists of nested reverse dome closure that must withstand buckling pressure and operate as a nozzle exit cone and attach at the full diameter of the chamber. Significantly reduces the interstage requirements since the nozzle does not extend to the lower stage. The nozzle exit area is maximized to the outside diameter of the stage.

2. Hot Gas Valve (HGV) – A gas bleed valve (used to provide thrust vector control) that opens to bleed exhaust from the burning propellant and inject it into the nozzle cone to effectively deflect

the exhaust, providing control of the vehicle. The HGV requires no additional liquid propellant to be carried for the TVC, but instead uses the hot gas generated by the burning propellant from the motor chamber. The valves are a simplified, lightweight design that are commanded by the guidance computer.

3. Forced Deflection Nozzle – A multi-discrete throat nozzle used to efficiently turn and expand chamber gases in a relatively short distance. Propellant chamber gases are radially directed into the exit cone contour, which facilitates turning the flow back to a condition parallel to the nozzle exit. Keeping the flow parallel at the nozzle exit maintains high thrust efficiencies. A short nozzle is highly desirable to keep the overall stage length to a minimum and to maximize the amount of propellant carried in the stage.

4. Clean Low Oxidizing Fuel (CLO) – A propellant, using boron as a fuel, that eliminates solid exhaust particles in the chamber and throat. The clean exhaust is required to keep the HGV from being clogged as they open and close. Boron propellants, although they have a slightly lower I_{sp} than standard aluminum propellants, provide for reduced two-phase losses (see Appendix B). Thus, the use of boron propellants results in improved motor *delivered I_{sp}* when compared to the use of aluminum propellants (7).

The design options that are possible with the technologies associated with the integrated stage concept were investigated first. The basic design of the booster stage is established by the use of the integrated stage, the full open case with a forced-deflection nozzle using boron as the propellant and hot gas valves for thrust vector control. The use of ISC is a "total package": all the components are required for the stage design. Substituting aluminum propellant for the boron is ruled out because of the lower performance, erosion, and impact on the hot gas valve design. Aluminum is a much "dirtier" fuel (more solid exhaust particles) and would tend to clog the hot gas valves and erode the forced-deflection nozzle throats. A conventional gimballed nozzle cannot be fully submerged into a case, and a submerged forced-deflection nozzle cannot be gimballed.

The only structural option within this design approach was the choice of a *conical* stage versus a constant diameter *cylindrical* stage. The conical stage basically eliminates the interstage and the weight associated at each end, but a penalty is incurred with a longer case. The constant diameter case is easier to manufacture and is shorter (in comparison), but requires a fairly heavy interstage to connect to the post boost vehicle. The throat size and grain design parameters are the design variables which determine a motor design's performance characteristics. Different combinations of these variables are evaluated (8 for each design choice: conical ISC and cylindrical ISC) to model their effect on performance and to completely explore the design space.

4.2.2 Conventional Technology. It was also determined that a conventional stage design (utilizing technologies developed for the Small ICBM and Peacekeeper programs) will be evaluated. The more "proven" technology would lower the development risk and could lower cost. An initial determination was made that the nozzle should be a "flexseal design" with an actuator to gimbal the nozzle for thrust vectoring. This represents the "state of the art" technology applied within the SICBM program and carries a "reasonable" weight penalty. The latest maximum performance aluminum propellant available was chosen for the conventional stage design.

Again, the preliminary decisions narrowed the basic conventional design configuration choices to two: *conical* versus *cylindrical*. Preliminary analysis indicated that the overall design for either choice was feasible, although only at payload options that are lighter than the current MM III multiple warhead payload. The throat size and grain design parameters are the design variables which determine a motor design's performance characteristics. Different combinations of these variables are evaluated (8 for each design choice: conical and cylindrical) to model their effect on performance and to explore the design space. An additional configuration analyzed is a small diameter (52 inch) booster with only one throat size and grain design. The smaller diameter will reduce the interstage requirements at the PBV, while keeping the interstage requirements to the MM III first stage constant.

4.2.3 Grain Design. A major area of the total system design that needs to be carefully and extensively investigated is the design of the propellant grain. Since the propellant choices are known (boron or aluminum), the burn rate and specific impulse associated with each type of propellant are known values from previous testing (6) (see Appendix B). The problem reduces to determining a grain design that provides the necessary specific impulse within the system constraints on burn time, combustion pressure, and dynamics. The use of hot gas valves for ISC designs restricts the burn time to less than 80 seconds (to keep the development risk low for the valves) (14, 80). The initial design approach was to use a star pattern design for a neutral burn with constant thrust (13). This approach simplifies the trajectory model and is common in booster design. The case is then designed to withstand the maximum burn pressure (constant for a neutral grain design), and makes best use of the structural weight. Unfortunately, with such a relatively light payload, the maximum constant thrust is limited to approximately 55,000 pounds (to keep the maximum g's that the payload would encounter within specification). This requires that the burn time be long (at least 115 seconds) in order to deliver the necessary total specific impulse at the thrust level allowed. Additionally, the physical constraint of a 66 inch diameter case limits the burn rate to an unacceptably low rate that could not provide adequate thrust (see Appendix B for details). To summarize, neutral star patterns are unable to meet mission requirements and constraints.

Another possible approach is an end-burning grain that provides long burn times at low thrust levels and a neutral thrust profile. An end burner allows for nearly complete burning of the propellant carried by the booster. Such a design was limited to a burn area of 3200 square inches (64 inch inside case diameter). This type of design proved impractical since the resulting burn times are over 2 minutes. In addition to exceeding the burn time constraint for the HGV's, long burn times are undesirable for other reasons. In the end burner, longer burn times mean much more internal insulation is required, increasing weight and decreasing volume available for propellant. Also, the longer the stage burns, the more gravity acts to decrease performance.

A modification of the end burner was attempted with the initial surface area increased substantially, resulting in a regressive burn profile. The thrust level started high and then decreased as the burn progressed (see Appendix B). This approach showed initial promise because the large mass results in low g's initially and the lower thrust at the end does not impart high accelerations on the payload. Analysis proved that the burn area decreases substantially early in the flight and quickly levels off at a very low thrust level. The resulting burn time again exceeded 2 minutes.

A slotted grain design, similar to the MM III 2nd stage six-slot design, is considered which can produce a regressive burn. Configurations with 3 to 8 slots are also evaluated, however, modeling of this pattern shows their thrust drops off quickly (see Appendix B). The total impulse delivered is not sufficient to meet mission requirements.

In an attempt to improve on the multi-slot design another grain design is evaluated that can best be described as a long slot with a central circle, or slotted tube. It is essentially the same as the other slotted designs but with only two, colinear slots (Figure B.7). This design is regressive, but starts at a high thrust level and the thrust does not decrease as rapidly as with the end-burner or multi-slot designs. This design also provides flexibility in the dimensions of slot length and width, which are used to effectively tailor the burn profile to match desired performance. This approach proved to be very successful in providing the required specific impulse. An additional benefit of this approach is that virtually all fuel is burned. The slotted grain design, then, is the design of choice with both the boron and aluminum propellants, as well as for the conical and cylindrical-shaped stage options.

4.3 Design For Costs

With the basic design for the second stage bounded by the grain design considerations discussed in the previous section, an important issue is the life cycle cost associated with each design. Because defense funding is limited and today's weapons system programs span many years at bil-

lions of dollars, estimates of life cycle costs are necessary to determine the amount and type of equipment the Air Force can procure to fill a given mission need. The Department of Defense has shifted the focus for costing a system away from just considering the design, development and procurement costs to the entire costs for a program during its lifetime, the "cradle to grave" expenses. These costs include

> ". . . all expenses for [system] research and development, production, modification, transportation, introduction of the item into the inventory, new facilities, operation, support, maintenance, disposal, and any other costs of ownership, less any salvage revenue at the end of its lifetime" (92).

For cost analysis purposes, the bulk of these costs are generally grouped into three broader categories: research and development, investment, and operations and support.

By themselves, life-cycle cost estimates do not identify the optimal solutions. They are certainly a driving force in the defense acquisition process. To produce a complete research package that facilitates comparison of alternate designs and assessment of program cost feasibility, Phillips Laboratory requires life-cycle cost estimates for the second stage booster designs under review (59).

4.3.1 Design Considerations - DDT&E and Production. Major factors that traditionally affect total expendable booster program cost (in decreasing order of impact) include characteristics of the booster case, the thrust vector control system, the nozzle, the propellant, and the insulation (23, 81). Several cost drivers are generally used to quantitatively address these major factors. Those identified in the *Low Cost Solid Propulsion Study* (23) are listed below:

The cost drivers noted above are relevant to the designs being considered (23, 18). The design process is geared to minimizing the weight in each area in the attempt to keep the cost to a minimum. From a literature review and other qualitative assessment (e.g. phone survey with Ballistic Missile Organization cost experts), it was determined that no "new technologies" are incorporated in the designs (23, 18). The concepts used in the designs are not revolutionary; they

Factor	Cost Drivers
Booster Case	Method of Manufacture MEOP or PV/W
Thrust Vector Control	Nozzle Design Horsepower (movable nozzle) Total side impulse (fixed nozzle)
Nozzle	Submergence Manufacturability
Propellant	Specific Impulse Burn Rate Processing Method
Insulation	Thickness requirement Method of fabrication Method of assembly

Table 4.1. Cost Drivers

are extensions of existing technologies. As such, complexity factors would adequately capture the effects of the technologies employed. No additional cost drivers are necessary to capture the effects of technology on cost.

4.3.1.1 STACEM Input Variables. STACEM (see Chapter 3) documentation was reviewed and it was determined that the cost drivers for the 2-stage booster design are adequately addressed by the model. Values for the STACEM input variables are obtained from a variety of sources. The solid rocket booster (SRB) specific inputs are from the 2-stage design configurations.

4.3.1.2 Component Weights. Weight values for the following items are required by STACEM and are provided for each design:

- Electrical and Instrumentation
- Separation Systems
- Structures
- Flight Recovery
- Ignition
- Liner
- Nozzle
- Propellant
- Thrust Vector Control/Thrust Vector Actuator
- Insulation
- Case

- Booster Recovery (inert)

Some of the weight inputs are assumed constant between all of the designs. They incorporate some existing MM III components and actual MM III data is used for the weights. The specific booster components assumed constant are electrical & instrumentation, separation systems, and "structures" weights (which includes stage connecting rings, fasteners, raceway cover, etc.) and ignition. Since ICBMs are expendable, a value of zero is assigned to the flight recovery and booster recovery variables. The remaining components are design dependent, and are determined through trade-off analysis and optimization techniques.

Nozzle. The forced-deflection nozzle is a complex design due to the loading and temperature requirements it must withstand. It represents a high risk, large development cost impact to the ISC designs. The benefit of the complete submergence of the nozzle into the case is the elimination of the interstage weight and the associated costs. The conventional bell shaped nozzle is well proven, efficient design. The large area which extends beyond the case must be covered by an interstage and is a weight penalty.

Propellant. Using boron propellant represents a trade-off in higher initial acquisition costs versus increased performance of aluminum propellants. The weights associated with each are the same since the designs maximized the amount of propellant carried, by weight.

TVC/TVA. With the emerging technology of the hot gas valves, the weight required to vector the thrust can be significantly reduced. The valves are relatively lightweight and simple in operation versus the gimballed nozzle for the same vectoring requirements . The overall simplicity of the valves provides higher reliability and fewer maintenance requirements. The actuated gimballed nozzle is also considered for its lower development risk and proven capability.

Insulation. Design work attempted to minimize the insulation weight for each design alternative. The higher operating temperature of the boron propellants does require a thicker layer of insulation than the conventional designs.

Case Design. The case design considers materials that meet the required performance in the operating envelope of the missile and that give the lightest case. The case is designed to withstand the maximum expected operating pressure (MEOP) with the lightest case possible. Composite materials are not new to booster design (SICBM, Peacekeeper), and provide a significant

weight reduction over the metal cases used in the current MM III 1st stage. Minimizing the motor operating pressure has a direct impact on the case thickness and resulting case weight. Highly exotic materials that could prove even lighter are not considered due to their high performance risk and correspondingly high acquisition costs.

4.3.2 Complexity Factors. Complexity factors ara a means of differentiating among design alternatives and the development required of the technology involved. A review of the designs determined the necessary inputs for the complexity factors. The values assigned are based on surveys of contractors experienced in developing solid rocket motor design technologies and the documentation available for review. A limit was placed on the choice of complexity factors to the following definitions: 0.6 corresponds to follow-on, existing (off-the-shelf) technologies, 0.9 equates to "related" or "similar" technologies, and a value of 1.0 represents entirely new programs or technologies. The preliminary nature of the designs did not warrant a finer breakdown of the complexity factors, although the cost models accept a range of values from 0.4 to 1.0.

Case Design. The complexity factor is a 0.6 for all the designs. The use of composite materials is considered common in booster design (for example MM III, SICBM and Peacekeeper all use composites). The integrated stage requires the full open case, which is easier to manufacture since there is no aft dome to wind (65).

TVC/TVA. Significant development is expected in all the designs for this factor. The hot gas valves for integrated stage are entirely new, and a complexity factor of 1.0 is required. Development work to date has only been performed in the labs and on smaller systems (40). The conventional stage designs use an actuator and flexseal which must be developed for this application, justifiying a 0.9 complexity factor. Actuators are used on the upper stages of the Peacekeper and SICBM, but the stages are smaller than the proposed designs (6).

Nozzle. The nozzle for the integrated stage is a new technology that requires considerable additional development, and a factor of 1.0 is used. The conventional nozzle and its flexseal will have to be uniquely designed for this stage, but can build on existing nozzle programs, justifying a factor of 0.9.

Propellant. The boron propellants have not been used in a booster design of this size and complexity. A final propellant mix needs to be tested for performance and aging properties. The

boron propellant is a new development that carries a complexity factor of 1.0. The propellant for the conventional stage is an aluminum-based composite that has been used before, and so a factor of 0.6 is assigned.

Insulation. The unique grain design incorporated in the boosters will require some development of the insulation to maintain the required case wall temperature for both conventional and integrated stage design approaches. The complexity involved is equal between the designs since the material choice (Kevlar/EPDM) is the same for all the designs considered. A factor of 0.9 is used in all designs.

Liner. The program is geared towards developing a 35-year liner, a much longer life than current MM III 17-year liners. Compatibility with either propellant choice is a design issue. A factor of 0.9 is chosen for all the designs.

The remaining complexity factors (see Table 4.2) for all the design choices are 0.6. With these factors, there is nothing technically unique to the booster designs considered in this study. These components use technology that is simply a follow-on to the current MM III program.

Electical & Instrum	Ship & Logistics	Range Spares
Seperation	Booster Prog Spt	Facilities/Ground Spt
Structures	Addtl Booster	Rec Land Veh/Eq
Ignition	System Support	Rec Sea Veh/Eq
Pre-Ship Assembly	Range Ops	DDT&E
Addtl Motor	Fac Supt Rng Ops	

Table 4.2. Complexity Factors

4.3.3 Design Considerations - Operations and Support Costs. All the designs are generated under the assumption that the second stage booster design will replace the Minuteman III 2nd and 3rd stages without any required structural changes to the remaining missile components (first stage, post-boost vehicle and payload) (81). In other words, the new booster will be a perfect fit. However, an upgrade to the aging NS-20 guidance system will most likely accompany any Minuteman life-extension program. In fact, independent research is already underway for a replacement system, the Advanced Inertial Measurement System (AIMS) guidance package (81). It is assumed that this guidance system will be fitted to the modified missiles during the new booster phase-in period. However, because the guidance system design is not addressed through this research, associated

4-10

DDT&E and production costs are not addressed in the estimate. Estimated changes in O&S costs attributable to the change in guidance systems will be highlighted accordingly.

This early in the design development phase it should be noted that differences in the proposed booster designs are not significant enough to merit separate O&S estimating assumptions, conditions and constraints. As such, one O&S cost estimate addresses all potential design configurations. The designs must all meet a 20 year life span (59).

4.4 Design For Availability

The alert rate of the current MM III system is very high (75) and to improve upon it will be difficult. Any of the new design candidates could improve the reliability in one subsystem, but may not be advantageous in another system. A complicating factor is that many of the failures that occur in an ICBM are not detectable at time of failure. A failure may not be found until a missile returns to the depot for some other reason. For the current system, only the NS-20 Guidance System and the payload are continuously monitored. Other checks done on a monthly basis include tests of the flight control equipment, command signal decoder, and raceway electrical continuity. Only failures in the guidance set and payload can be repaired in the silo. All others require the missile to be returned to the depot. The goal in the design process is to maintain or slightly improve the high alert rate of the MM III system.

AFOTEC breaks availability into categories of "real" and "apparent" availability (51). This distinction is important to this study because ICBM's are in a storage or dormant state for most of their useful life. Failures may not be detected for a long period of time or until a firing is attempted. These situations where an item is failed (and unavailable), but undetected, give rise to the definitions of "apparent" and "real" availability.

A series system is chosen for the availabity model (see Appendix D) since all equipment must function for the system to be considered available. Failure in the system can result due to stress or environmental conditions (guidance electronics, flight control electronics, batteries, payload components, case coatings) or due to simple aging (propellants, ordnance, liners). In considering the design options, attention has to be given to whether a proposed component or design would be more apt to fail under the conditions. For each stage design option, the interstage ordnance, flight control ordnance, and stage igniter elements are not candidates for change. The elements

4-11

that do change from the current design are the liner aging properties, propellant aging properties, and flight control system equipment, depending on the design option chosen.

4.4.1 Liner Properties. The liner provides the bonding surface for the propellant (on one side) and the insulation (on the other side). A secondary function is to prevent chemical migration between propellant and insulation. As the motor ages, the liner is critical in preserving the tight interface bond needed for reliable motor performance. For the boron propellant, Aerojet has developed a suitable liner, but it has not been fully characterized or age tested with the propellant (2). Although system experts feel that a 35 year liner is technically feasible (84), there is a risk in the design associated with this approach that could negatively impact the availability analysis. The lack of good data requires using more uncertainty in the model. Since the integrated stage concept involves several technologies, the impact of one can not be separated from the impact of all the technology. The use of aluminum propellant in the conventional design provides much less risk, although the same development effort is required for a 35-year liner life. There is much less uncertainty to be reflected in the model paramaters for this design choice.

4.4.2 Propellant Properties. The aging of solid propellants often causes cracks to form. This can be catastrophic to motor performance if the cracks are very large and seriously change the burn surface area. The complex chemistry of propellants makes precise prediction of aging effects very difficult. The probability of significant cracking in solid propellants is a function of the time that the missile is in the silo. The aluminum propellants have been extensively tested and have a large historical data base to support their use and to estimate the expected lifetime of the propellant. Therefore, there is relatively low risk in the use of aluminum propellant in the designs.

There is very little aging data available for boron propellants. Small scale testing and accelerated aging tests have been performed by contractors (72), but an exact propellant formulation has to be age tested before usable data can be obtained. This places the boron propellant design at higher risk in development and increases the uncertainty in the design life. The model parameters must reflect the uncertainty in the actual aging properties of the boron propellant, which in turn reduces the overall system availability.

4.4.3 Thrust Vector Control. The integrated stage concept requires that hot gas valves provide the necessary thrust vectoring of the nozzle. The valves are a relatively new development

item that are only possible due to recent advances in materials that allow operation in a high temperature, high flow rate environment. Although a known risk from a development standpoint, the design is relatively simple in operation and makes use of inert ceramics that don't corrode or suffer from aging. This is very important to the availability of the missile, and benefits could be expected in the overall availability rate for this subsystem with this design approach. The conventional approach of gimballing the nozzle involves a much more complex electrical/hydraulic actuator and movable nozzle. The conventional approach is much more technically proven, however, so the technical complexity may be partially offset by the lower risks associated with this approach.

4.5 Design For Producibility

The overall concept behind designing for producibility varies with each missile configuration. The overiding consideration, however, is always to consider technology and processes that are currently available or in development. No design is to be considered if it involves a process or technology that could not be proven within the next 10 years to support production.

Filament Winding. In the case of structures, the use of filament winding is a proven technology already used by several missile systems (93). Regardless of the overall configuration, the production of EPM, case, and insulation uses the base concept of filament winding. Filament winding for conventional designs allows for production of only a single case, whereas an ISC design presents opportunities to produce two cases simultaneously due to the lack of the aft dome being wound integrally. The integrated stage allows for producibility gains that should manifest as lower production costs. Several manufacturers build filament winding equipment capable of producing cases with diameters proposed in the *NEMESIS* designs. Generally, the suitability of computer controlled, filament winding production for a particular application varies depending on complexity of design shape, amount of material being applied simultaneously, and the relative degrees of freedom for material application. In this application, filament winding (discussed in detail in Appendix C) is clearly the manufacturing technology of choice for producing all potential booster case designs.

External Protective Material (EPM). EPM provides protection for the missile against a variety of environments. In particular, protection against *pebbling* from atmospheric debris is crucial to maintaining case integrity. Production of EPM also takes advantage of filament winding in manufacture. After the insulation and case are wound onto the mandrel, EPM is wound directly

onto the case. In the conventional case designs, EPM is wound one case at a time. Two cases can be wound at once in an ISC application. EPM, however, does not cover the case domes. Rather, the protective material is either wound or laid integrally with the skirt and interstage attachments. EPM technology is directly associated with composite technology. Therefore, as advances are made in composites, EPM producibility improves in direct proportion. A current design that incorporates EPM filament winding is the SICBM.

Liner/Insulation. Within the rocket motor case are two interfaces that require attention with regards to producibility: insulation and liner. Insulation is used to ensure the composite case materials maintain their strength during boost (while exposed to the extreme temperatures of propellant combustion). The insulation material is typically a rubber-based substance combined with composite fibers to ease producibility. Filament wound first onto the mandrel, insulation realizes the same benefits as other structural portions of the design in terms of shape. After removal of the mandrel, an application of liner is placed within the rocket motor case. The liner provides the propellant to insulation bond. Applied in a variety of techniques, liner technology continues to improve and should be a low risk approach for this application.

Thrust Vector Control. For thrust vector control, the ISC designs use hot gas valves for maneuvering. The hot gas valves are relatively simple in design and, although requiring expensive materials, should be easy to produce (9). In the conventional designs, well established mechanical actuators for a gimballed nozzle form the base technology of the propulsion design. The actuator for the conventional design is well proven technology that is used for other booster programs.

Propellant Processing. One possible producibility improvement is continuous processing, where the propellant is mixed and poured in a continuous "assembly line" fashion rather than in multiple batches. This method is faster, safer, and allows for greater system control over propellant properties (99). Contractors already utilize continuous processing for aluminum propellants, and boron-based designs should also be able to take advantage of advances in this process. The full-open case in the ISC designs also allows for simpler loading of the propellant and the grain shape.

Booster Shape. Varying the design based on shape, whether cylindrical or conical, only affected the overall producability to a small extent. Although cylindrical designs required the use of interstaging, conical designs mandated using precise tapers to match up with existing stages.

Cylindrical designs are used on several programs (SICBM, Peacekeeper) and have well established manufacturing techniques. The conical shape provides gains in performance and weight savings, but there is little experience building the large diamter booster for this application in a conical shape (38).

Nozzle. The integrated stage designs require the nozzle to be completely submerged into the case. The forced-deflection nozzle is a complex piece to design and build, and it requires a heavy attachment ring and reinforcement. The conventional nozzle is a less complex, proven technology that is easier to build.

4.6 Design For Performance

Two approaches are considered to evaluate *NEMESIS* designs in terms of mission performance. The first approach is to design the two-stage missile so that it is capable of delivering a set payload to a given "point-in-the-sky". This approach involves choosing a representative payload weight within the specified range (1500 - 2300 pounds), then designing the second stage to maximize performance. Design factors in the form of structural weights, mass flow rate profiles and thrust profiles are inputs to the trajectory model. Numerical output is then produced in the form of an *energy ratio*. This ratio relates the performance of a particular *NEMESIS* design to the required MM III performance using the same payload weight. An energy ratio greater than or equal to 1.0 indicates successful delivery of the payload to the required "point-in-the-sky" with sufficient energy to match or exceed the total baseline energy. A ratio less than 1.0 indicates failure to achieve the required performance with the given payload.

The second approach also uses energy ratio for performance evaluation. If the payload is treated as a variable, the specific energy of a *NEMESIS* design is adjusted (by adjusting the payload weight) until an energy ratio of at least 1.0 is achieved. If the payload-carrying capability is greater than the specified minimum (1500 pounds), the design is viable. Otherwise, the design is rejected.

In terms of performance, the designed second stage must produce a thrust profile that provides enough energy to the system at stage two burnout, while at the same time keeping system acceleration below the 18g limit. The overall missile design is evaluated in the TPM simulation.

Four second stage design configurations are selected for consideration. As mentioned previously in this chapter, integrated stage and conventional technologies are considered as the two distinct technologies considered for *NEMESIS*. A further division within each configuration is the geometric shape of the second stage. Because the diameter of the MM III first stage and post-boost vehicle are different, different second stage shapes and diameters are considered. The diameter of the MM III first stage is 66 inches and the diameter of the post-boost vehicle is 52 inches. The advantage of having the second stage upper and/or lower diameter(s) the same as that of the MM III interfaces is that interstage weights are significantly reduced. First, a conical second stage is considered. With both technologies, the conical second stage upper and lower diameters, 52 and 66 inches respectively, match the MM III interfaces. Second, a cylindrical second stage is considered. With both technologies, the cylindrical second stage is 66 inches in diameter over the entire length. Thus, the cylindrical design requires a substantial interstage at the post-boost vehicle interface to transition from 66 to 52 inches (the one exception is a cylindrical conventional design with a diameter of 52 inches over the entire length). The small diameter cylindrical option is not considered for the integrated stage because the lower diameter must be 66 inches for proper "nesting" with the MM III 1st stage. The advantage of integrated stage is in the "nesting" of the lower stage into the upper stage's nozzle, thus eliminating wasted space.

4.6.1 Weight Estimation. A vital area of performance prediction involves weight estimation of the vehicle components. Weight is a driver for both performance and cost and, as such, is a critical aspect of all designs. Since the constraints of this study include a given first stage, post-boost vehicle and payload, the weights in the estimation are only for the new 2nd stage that is being designed. The design solutions attempt to minimize the weight where possible, while still maintaining the required performance.

An important constraint is that *the new 2nd stage can not weigh any more than the combined weights of the existing 2nd and 3rd stage of the Minuteman III*. This allows for a total stage weight of 24,000 lbs, which is divided among the stage components. The major areas of detailed weight estimation are: case, nozzle, internal insulation, liner, igniter, thrust vector control (TVC)/thrust vector actuation(TVA), external protective material, interstage, propellant, and "miscellaneous". The propulsion, structural, and thermal models are used to determine the weights where possible, but it was not possible to create models for all the weight categories (see Table 4.3 below).

4-16

CATEGORIES	ISC	CONVENTIONAL
Case	Structures Model	Structures Model
Nozzle	Aerojet Program	Regression Model
Int Insulation	Thermal Model	Thermal Model
Liner	Structures Model	Structures Model
Propellant	Propulsion Model	Propulsion Model
External Insulation	Thermal Model	Thermal Model
TVC/TVA	Aerojet Program	Regression Model
Igniter	Data Search	Data Search
Interstage:		
1st to 2nd	Aerojet Program	Data Search
2nd to PBV	Data Search	Data Search
Miscellaneous	Data Search	Data Search

Table 4.3. Source of Weight Estimation

A data search of current programs and literature are utilized in several weight estimating areas. Table 4.4 presents the data gathered to support the estimates.

Category	MRBM	AICBM	MX	SICBM
Nozzle	16.7	80	453	395.8
Igniter	3	10	19.1	18.3
TVC/TVA	7.4	29	72.5	119.9
Interstage	14.2	79	394	26.5
Misc	13.3	39	199	84.9
Inert Weight, lbm	147.8	764	1999	2122
Stage Weight, lbm	940	6277	17686	25501
Stage Diameter, in	26	46	92	44.5

Table 4.4. Conventional Booster Weights

4.6.1.1 Case, Liner, and Insulation. The structural and thermal models provide weight estimates for the case, liner, internal insulation, and external protective material. The programs take the output from the propulsion program, specifically the operating pressure and burn time, to determine the detailed weights. Each of the designs are evaluated with the programs to provide estimates that are included in the overall stage weight. Appendix C contains detailed information on the material choice and properties. The insulation weight reflects the grain design. Different grain patterns expose different amounts of the case to the hot exhaust gases for different lengths of time. Properties for the insulation are chosen that are representative of current insulation design practices.

4.6.1.2 Propellant. As previously discussed, the total allowable propellant weight is determined from the payload weight and the maximum load-bearing capability of the first stage. The initial feasibility study in Chapter 1 determined that the structural ratio needs to be in the range of .0683-.10058. Since the single stage needs to provide as much or more performance than the current 2 stages, the maximum propellant that can be carried is a necessary condition to achieve the required total specific impulse. Assuming a structural ratio of 0.07 and a maximum payload weight of 2300 lbs, the remaining available weight of 22,100 lbs of propellant is used for each design. The propulsion model uses this amount of propellant along with the other inputs to determine the stage performance.

4.6.1.3 Igniter, Interstage, and Miscellaneous. The igniter, interstage, and any miscellaneous weights are estimated using data available on similar missile components. The use of comparable systems and discussions with current designers provide confidence that the weights proposed are conservative (6). The igniter weight is chosen as 20 lbs for all the designs since the data indicate the igniter weight becomes relatively constant as the stage weight approaches 20,000 lbs. The interstage weight is determined dependent on whether it is an ISC or conventional design. For the ISC designs, the Aerojet program provides weights for the connection to the lower stage. The connection to the PBV is an approximation using a scaling of the current interstage weight of the MM III. The conventional design interstage weights come from the same MM III approximation and an output from the structural model for the structure weight of the interstage. The category of "miscellaneous" is used to include the weights of the cabling, raceway, fasteners, and other weights not specifically included in the other categories.

4.6.1.4 ISC Design (Nozzle, TVC). For the integrated stage technology design options, a program called AIDE II (41) is used to estimate the total weight of the nozzle assembly. The program is Aerojet proprietary and used by the company for their preliminary design analysis. Special permission was obtained to use the program and to include the output in the final design analyses. The input file for the program is modified to represent the particular case materials and stage operating parameters for each stage design. The program calculates the total weight of the nozzle assembly (case, liner, insulation, throat, etc) and this is used for the weight of the bottom 43 inches of the stage. This length is an output of the AIDE II program and is roughly constant for all ISC designs.

4.6.1.5 Conventional Stage (Nozzle, TVC/TVA). In the absence of a model that can estimate the weight of the nozzle and thrust vector control/actuation system for the conventional stage design, a linear regression model is used to estimate these component weights. A data search for nozzle and TVC/TVA weights on comparable systems, either fielded (Peacekeeper), in development (SICBM), or studied by various contractors (MRBM, AICBM), provide the component weight data base. A relationship between nozzle weight and inert stage weight (the linear regression equation) provides a means of relating the two variables, as shown in Table 4.4 and Figure 4.1. A similar approach is used for the TVC/TVA system, relating TVC/TVA weight to a total stage weight (see Table 4.4 and Figure 4.2). With this approach, there is no variability between designs since overall stage weight is assumed relatively constant at 23,900 lbs with inert weight of 1800 lbs. A large part of the conservativism in these estimates comes from the fact that materials available today provide weight savings over those used in older programs.
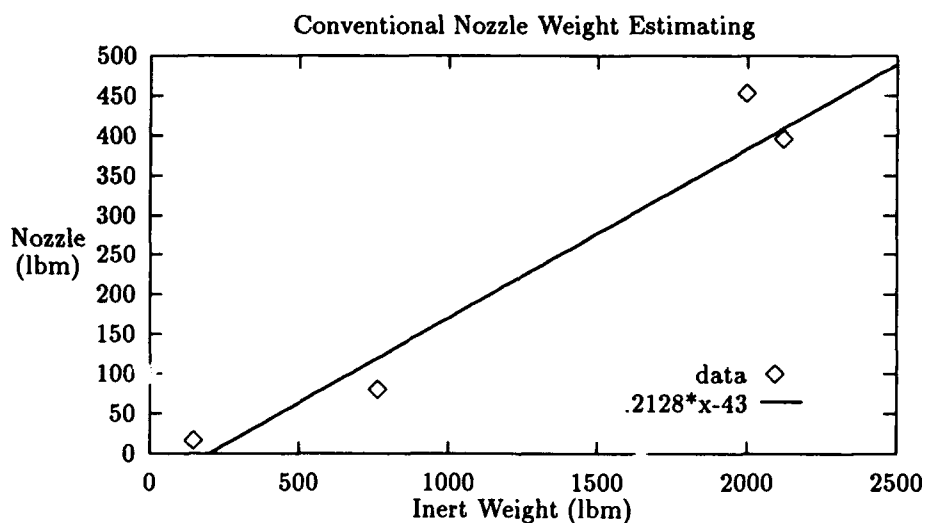
Figure 4.1. Conventional Nozzle Weight Estimation

4.6.1.6 Weight Estimation Conclusions. Integrated stage technology is still a new development area and represents a high degree of risk in weight estimation. The conventional technologies require the least development, but a lack of better models increases the uncertainty
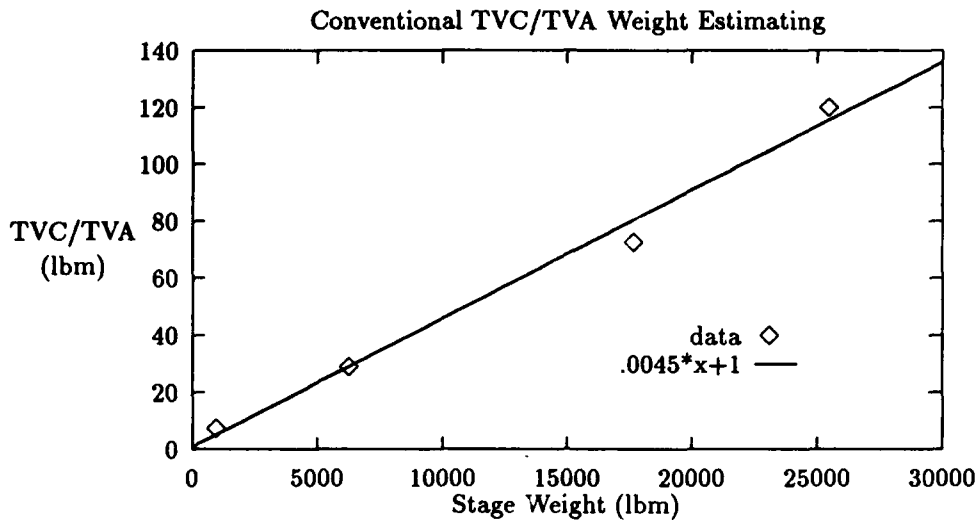
Figure 4.2. Conventional TVC/TVA Weight Estimation

in the weight estimates associated with these designs. Generally an attempt is made to keep each weight conservative (large) so that the overall stage weight estimate errs on the heavy side.

4.6.2 Mission Profile. Regardless of the particular combination of design parameters (motor design, payload weight, etc.), all *NEMESIS* designs are required to follow the same basic mission profile. Figure 4.3 presents the events of a typical *NEMESIS* mission starting from launch, continuing through stage two burnout, and into the ballistic flight phase. At 3.15 seconds into the mission, the flight path angle is instantaneously changed from 90 degrees and the gravity turn is initiated. The gravity turn trajectory continues through stage 1 burnout, the 1 second coast period before stage 2 ignition, and throughout the remainder of the powered flight portion of the trajectory. The only variables between *NEMESIS* designs are the initial flight path angle deflection at 3.15 seconds, and the time of stage two burnout. All other events and their associated times are common to all the designs.

4.6.3 Design Iterations. Tables 4.5–4.9 show the subsystem weights (pounds), total *NEME-SIS* weights (pounds), combustion chamber pressures (pounds per square inch), burn times (seconds) and energy ratios (unitless) for the 33 "designs" generated. Each "design" is a different combination of design variables: nozzle and grain design parameters. The combinations are de-
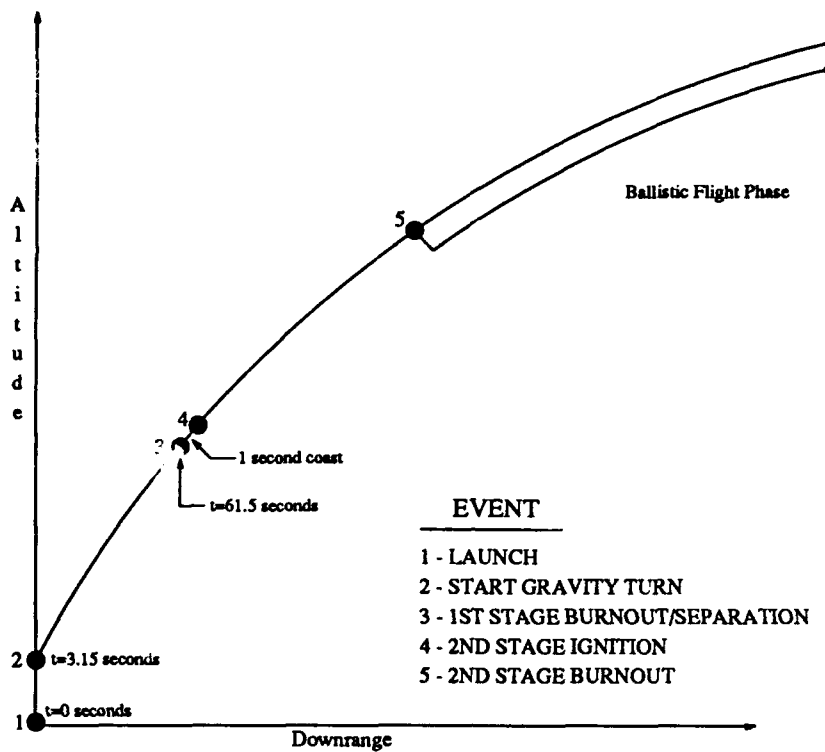
Figure 4.3. Typical *NEMESIS* Mission Profile

rived such that the *NEMESIS* design space is completely explored. Designs 1-8, shown in Table 4.5, represent cylindrical ISC stages with an 1800 pound payload. Designs 9-16, shown in Table 4.6, represent conical ISC stages with an 1800 pound payload. Designs 17-24, shown in Table 4.7, represent cylindrical conventional stages with a 66 inch diameter and 1600 pound payload. Designs 25-32, shown in Table 4.8, represent conical conventional stages with a 1600 pound payload. Design 33, shown in Table 4.9, is the small diameter (52 i. ·h) cylindrical conventional stage concept with an 1800 pound payload. These configurations are used in Chapter 5 to optimize the effect of the design variables on energy ratio, burn time, maximum combustion temperature, and maximum vehicle acceleration.

DESIGN CHARACTERISTICS	DESIGN OPTION							
SUBSYSTEM WEIGHTS	1	2	3	4	5	6	7	8
CASE	289.5	196.9	370.3	244.1	452.9	290.5	533.2	332.1
LINER	74.2	74.2	87.2	87.2	84.1	84.3	95.9	96.1
NOZZLE/TVC	479	421.7	514.1	438.5	578.1	482.3	574.8	489.9
INSULATION	213.7	232.1	325.6	360.8	155.7	163.9	202.6	203.8
EPM	191.4	246.8	215.8	285.1	135.2	180.4	149.2	196.0
IGNITER	20	20	20	20	20	20	20	20
MISC	65	65	65	65	65	65	65	65
INTERSTAGE	341.8	310	367.1	318.4	583.3	346.5	553.1	350.6
SKIRT	10	10	10	10	10	10	10	10
TOTAL WT	1684.5	1576.7	1974.9	1829.2	2084.2	1642.6	2203.9	1763.5
PRESSURE	1319.9	817.1	1536.1	951.0	1939.9	1201.0	2051.0	1269.8
BURN TIME	82.4	99.8	89.2	108.0	49.2	59.6	49.4	59.8
ENERGY RATIO	1.003	0.995	0.955	0.956	0.930	0.991	0.918	0.973
MAX G's	9.116	7.55	8.025	6.604	23.211	21.361	19.028	17.441

Table 4.5. Integrated Stage/Cylindrical Design Matrix

DESIGN CHARACTERISTICS	DESIGN OPTION							
SUBSYSTEM WEIGHTS	9	10	11	12	13	14	15	16
CASE	327.1	185.4	448.5	226.7	444.2	222.1	561.5	269.2
LINER	91.8	91.0	107.1	107.1	98.5	98.6	115.5	115.7
NOZZLE/TVC	507	459.1	543.9	477.3	550.6	482.44	568.8	497.6
INSULATION	220.4	272.9	302.6	371.3	195	218.7	258.6	294.6
EPM	168.9	240.5	199.5	278.9	156.6	245.6	169.4	253.8
IGNITER	20	20	20	20	20	20	20	20
MISC	65	65	65	65	65	65	65	65
INTERSTAGE	279.8	192.2	313.8	197.2	382.6	199.25	468.2	203.7
SKIRT	10	10	10	10	10	10	10	10
TOTAL WT	1689.9	1536.0	2010.4	1753.5	2021.5	1561.7	2237.0	1729.5
PRESSURE	1547.2	706.9	1780.4	813.4	1861.0	850.2	2077.8	949.3
BURN TIME	62.6	85.8	65.0	88.4	48.6	66.6	49.0	67.0
ENERGY RATIO	0.996	0.994	0.961	0.964	0.941	0.993	0.926	0.966
MAX G's	12.532	9.316	10.33	7.57	20.31	16.455	13.7	10.65

Table 4.6. Integrated Stage/Concial Design Matrix

DESIGN CHARACTERISTICS	DESIGN OPTION							
SUBSYSTEM WEIGHTS	17	18	19	20	21	22	23	24
CASE	368.8	200.5	479.6	260.5	464.9	252.8	555.8	302.2
LINER	91.4	91.5	104.6	104.7	95.8	96.0	107.9	108.2
NOZZLE/TVA	455	455	455	455	455	455	455	455
INSULATION	194.2	240.1	299.3	360.5	145.3	176.5	187.4	228.7
EPM	135.0	174.2	154.1	218.1	105.9	158.6	118.9	171.6
IGNITER	20	20	20	20	20	20	20	20
MISC	65	65	65	65	65	65	65	65
INTERSTAGE	445	445	445	445	445	445	445	445
SKIRT	10	10	10	10	10	10	10	10
TOTAL WT	1784.5	1701.3	2032.6	1938.8	1806.9	1678.9	1965.0	1805.7
PRESSURE	1744.4	945.1	2030.3	1100.0	2124.2	1150.9	2301.1	1246.7
BURN TIME	62.6	80.0	67.8	86.6	47.4	60.6	47.8	61.2
ENERGY RATIO	1.017	1.008	0.976	0.95	1.015	1.007	1.037	0.986
MAX G's	12.285	9.67	10.75	8.28	22.25	18.74	17.16	12.68

Table 4.7. Conventional/Cylindrical Design Matrix

DESIGN CHARACTERISTICS	DESIGN OPTION							
SUBSYSTEM WEIGHTS	25	26	27	28	29	30	31	32
CASE	325.4	201.7	419.9	260.4	411.5	255.2	518.1	321.5
LINER	108.5	108.5	123.9	124.0	115.3	115.4	132.4	132.6
NOZZLE/TVA	455	455	455	455	455	455	455	455
INSULATION	212.2	239.1	291.4	332.3	172.4	201.4	227.4	267.3
EPM	151.4	203.8	172.7	228.6	125.7	167.4	144.1	191.9
IGNITER	20	20	20	20	20	20	20	20
MISC	65	65	65	65	65	65	65	65
INTERSTAGE	335	335	335	335	335	335	335	335
SKIRT	10	10	10	10	10	10	10	10
TOTAL WT	1682.4	1638.0	1892.9	1830.3	1709.8	1624.4	1907.0	1798.3
PRESSURE	1509.1	934.3	1736.5	1075.1	1815.0	1123.7	2026.5	1254.6
BURN TIME	53.8	65.2	55.8	67.6	41.8	50.6	42.2	51.0
ENERGY RATIO	1.015	0.994	0.988	0.97	1.01	0.997	0.987	0.984
MAX G's	15.24	12.43	12.37	10.04	26.6	22.09	17.468	14.45

Table 4.8. Conventional/Conical Design Matrix

DESIGN CHARACTERISTICS	DESIGN OPTION
SUBSYSTEM WEIGHTS	33
CASE	351.3
LINER	119.1
NOZZLE/TVA	455
INSULATION	198.6
EPM	132.7
IGNITER	20
MISC	65
INTERSTAGE	325
SKIRT	10
TOTAL WT	1676.7
PRESSURE	1882.6
BURN TIME	47.0
ENERGY RATIO	0.9945
MAX G's	18.268

Table 4.9. "Skinny" Conventional/Cylindrical Design Matrix

V. Performance Optimization

5.1 Introduction

Before comparing the performance of the missile configurations, each option should have the best performance possible. Within the scope of this project, this essentially means the "best" grain design and nozzle for optimal propulsion performance; delivering the most payload possible to the same state as Minuteman III. Optimizing the stage's performance also means determining reasonable limits on the variable propulsion parameters. Incorporting other constraints into the optimization is also included, such as dynamic limits of the guidance system and burn time limits on thrust vector control systems.

5.2 Background

5.2.1 Optimization Concepts. There are many references which detail methods for optimizing an objective function (8). This overview covers the basic concepts used for this chapter in finding a maximum value of an objective function. Parameter optimization involves finding the maximum or minimum value of an objective function subject to certain constraints. The objective function is a function of certain parameters, called design variables. The constraints may be either equality or inequality constraints of the design variables themselves or of functions of the variables.

A non-linear optimization problem can be solved by either direct or indirect methods. An example of a direct method is finding a function's extrema by setting the first derivative equal to zero and solving the ensuing equation. The possible extreme points are checked with the function's second derivative to detect maximas and minimas. Indirect methods, often called search methods, start with a valid combination of design variables and use gradient information to move up the objective function in the direction of increasing values. This method of "hill-climbing" is often used with complex functions which are difficult to differentiate. A direct method is used in this project; however, the presence of more than one design variable as well as constraints complicate the process. The optimal points may be local instead of global maxima.

Similar to the one-variable first derivative method of finding maxima, Lagrange multipliers and slack variables are used to find maxima of constrained multivariable functions. Lagrange multipliers are used to augment the objective function with constraints equations. Also, slack

variables are introduced for inequality constraints. The resulting Lagrange function is partially differentiated with respect to each design variable, Lagrange multiplier, and slack variable. Similar to setting the first derivative equal to zero, the set of conditions known as *Kuhn-Tucker Conditions* must be satisfied in order to have an optimal point (8). The problem can be considered in n-space as finding the highest point of an objective function of $n-1$ design variables in the n-space topography within the region bounded by the inequality constraints. The point must also lie on the surface of any equality constraints. If the optimal point lies on an inequality constraint line or surface, then the slack variable associated with that variable is zero. This feature will be important later in interpreting the limitations each constraint places on the optimal solution.

5.2.2 Implicit Function Optimization. The optimization routine outlined above assumes that an explicit objective function exists. Unfortunately, the optimization of propulsion performance involves a more difficult objective function. The performance measure to be maximized can be calculated, but there does not exist an explicit function in terms of propulsion system parameters. Therefore, non-linear regression analysis is used to approximate the actual objective function. Analysis Of Variance methods (ANOVA) are used to determine which regression model factors are statistically significant. This enables the regression model approximation to the actual function to be as simple as possible.

5.2.2.1 ANOVA. ANOVA is an enumerative method of exploring the design space. Factorial designs are used to efficiently sample the objective function within a region. For this project, only two levels are sampled for each variable: high and low. For k, variables this leads to 2^k factorial designs, or "experiments". The ANOVA method takes the 2^k objective function values and partitions the variance into parts due to differences between the designs and due to differences within each design. The sum of the squares of the differences is the key statistic used in the analysis. By using contrasts (47:p114), the effect of each design variable and combinations of design variables is calculated. An F-statistic test is used to determine which factors of the single variables and combinations of them are statistically significant in affecting the objective function results. Those factors found insignificant will be removed from the proposed regression model, assuming that removal of a particular factor does not violate good engineering judgement. Reference (47) contains much more information regarding ANOVA and related topics on design of experiments.

5.3 Methodology

The optimization of the propulsion system to provide maximum performance requires a decision on an objective function. Then, this implicit function is approximated by a first-order regression model. ANOVA is used to eliminate unnecessary terms in the model. Non-linear optimization of the resulting regression equation, subject to limits on variables and regression models of constraint functions, provides the maximum value of the objective function. This is the desired optimal combination of propulsion variables.

5.3.1 Objective Function. Maximizing performance means finding the missile stage which delivers the most payload possible to the same state as third stage burnout of Minuteman III. This state is defined as the combination of velocity, altitude, and attitude. The analysis in Chapter 1 illustrates that it is unlikely the new second stage will be able to exceed the current system's performance. Therefore, performance is measured by the comparison of the total energy at final stage burnout. The ratio of the new system's energy to Minuteman III's energy is the parameter to be maximized and is defined in Chapter 1. This objective function is used to find the optimal performance stage. If the energy ratio is greater than unity then an increase in payload is possible, but the optimal design is still the same.

The energy ratio, which should be at least unity for a successful design, is primarily a function of the total impulse of the propulsion system. Since the system is still operating in a gravity field during second stage burn, longer burn times are detrimental. However, for similar burn times the maximum energy ratio corresponds to maximum total impulse. Also, heavier structural weight will decrease the amount of payload that the missile can deliver to the proper energy state. All these factors influence the optimal design.

5.3.2 Design Variables. The propulsion performance is a function of the propellant's properties, the grain design, and the nozzle characteristics. For this study, the propellant is either an aluminum or boron based solid propellant. The specific impulse, I_{sp}, delivered is largely dependent on the propellant. The amount the nozzle expands the exhaust also affects the I_{sp}. For a given propellant and nozzle, the grain design determines much of the propulsion system's characteristics, including the thrust curve, the combustion pressure curve, and the burn time. See Appendix B for additional details on these topics. Considering these effects, the variables which affect performance

are the grain design parameters and the nozzle throat and exit areas. However, for this study the nozzle exit area is assumed to be constant: for an ISC stage the first stage diameter determines the exit area, and for the conventional nozzle a reasonable maximum size is chosen. Nozzle throat area, A_{th}, represents the nozzle's effect in the optimization.

For the slotted tube grain design described in Appendix B, there are only two independent grain design variables. The design variables for the optimization are therefore:

- A_{th} - nozzle throat area

- F - grain pattern slot half thickness

- R_1 - grain pattern central tube radius

The energy ratio as a function of these variables is approximated by a regression model. Performance constraints as a function of these variables are also modeled with regression models.

5.3.3 Constraints. The primary constraints on the system are maximum burn time, maximum acceleration, and possibly maximum pressure. The burn time is particularly important for the ISC systems. Hot gas valves have been successfully tested with burn times as long as 40 seconds (82). Experts believe that somewhere over one minute of burn time is a current practical limit for hot gas valve operation (68). Therefore, a maximum burn time of 80 seconds is used for this study.

The guidance system is limited dynamically to no more than 18 times the standard acceleration of gravity. This 18 g limit is the most restrictive dynamic constraint on the system. Therefore, 18 g's is the dynamic constraint on the system used in this study.

Combustion pressure in the case has a large impact on propulsion performance as well as structural weight. Higher pressure improves propulsion efficiency by reducing dissociation in the exhaust gases (50:p368). The thrust is also a function of combustion pressure as shown in Appendix B. The burn time, however, is *inversely* proportional to combustion pressure (50:p386). With respect to just propulsion performance, higher combustion pressure is desirable. However, higher pressures require more structural weight. The case must be made thicker for the higher pressure, and the nozzle may also be heavier. The reverse-dome of the forced-deflection nozzle works best in tension. Since the back of the nozzle is in the high pressure combustion chamber, the nozzle's dome is under compression and must be strengthened. Also, the curvature discontinuity

where the reverse dome meets the case creates a stress concentration. This increases the local stress considerably higher than that experienced by a conventional case. This joint must be stronger, and therefore heavier, than its conventional counterpart.

With the complexity of combustion pressure's effect on performance, a specific limit on maximum pressure is difficult to determine. Most recent solid rocket designs, using the latest material advances, have used pressures over 1500 psia (76). Therefore, a reasonable maximum of 1800 psia is used for the design operating combustion pressure. A minimum of 300 psia is also used.

Parameter	Min	Max
Pressure, psia	300	1800
Acceleration, g's	0	18
Burn Time, sec.	0	80

Table 5.1. Summary of Constraints

5.3.4 Regression Model. The model uses first order effects and interactions of the three design variables. The resulting model, with all possible elements, is as follows:

$$Y = \beta_0 + \beta_1 A + \beta_2 B + \beta_3 A \cdot B + \beta_4 C + \beta_5 A \cdot C + \beta_6 B \cdot C + \beta_7 A \cdot B \cdot C \qquad (5.1)$$

where:

$$A = \text{Linear effect of } A_{th}$$

$$B = \text{Linear effect of } F$$

$$C = \text{Linear effect of } R_1$$

$$A \cdot B = \text{Effect of } A_{th} \cdot F \text{ interaction}$$

$$A \cdot C = \text{Effect of } A_{th} \cdot R_1 \text{ interaction}$$

$$B \cdot C = \text{Effect of } F \cdot R_1 \text{ interaction}$$

$$A \cdot B \cdot C = \text{Effect of } A_{th} \cdot F \cdot R_1 \text{interaction}$$

This model is used to approximate the following implicit functions as a function of the design variables: energy ratio, maximum acceleration, burn time, and maximum combustion pressure.

5.4 Example: Integrated Stage Concept - Cylindrical Stage

Each of the four primary design options generated are optimized:

- ISC - Cylindrical

- ISC - Conical

- Conventional - Cylindrical

- Conventional - Conical

This section details the optimization of the energy ratio for the ISC - Cylindrical stage case.

5.4.1 ANOVA. For the first order regression model with three design variables, 2^3, or 8 factorial "designs" are required. A high and low value for each variable is selected. These values are selected to capture as much of the design space as possible and still have reasonable pressures, dynamics, and total impulse. These 8 points represent a rectangular region in the design space, with the optimal point somewhere inside (see Figure 5.1).
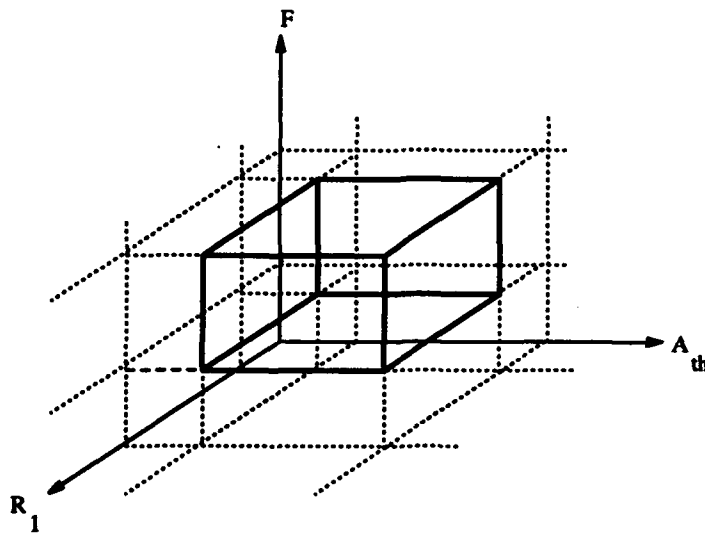
Figure 5.1. Factorial Design Space

Some of these factorial designs exceed system constraints for pressure, dynamics, and burn time. However, they are relatively close to the limits and are necessary to bound the "reasonable"

region in the design space. These designs are selected to determine the effects of design variables on performance in the region, not to have every one of them meet every constraint.

5.4.1.1   High-Low Values. To select the design variable high and low values, some estimation of reasonable limits is required for the grain design parameters. A lower limit is selected for both F and R_1. The thinnest slot deemed reasonable, for manufacturing and structural purposes, is 2 inches. This makes 1 inch the minimum for half the slot thickness, F. For the central radius, R_1, 5 inches is selected as minimum. This should allow enough volume for the igniter to start the entire surface with hot, high pressure gases. The high-low values used for the ISC-Cylindrical case are shown in Table 5.2.

Design	A_{th}	F	R_1
1	45	1	5
2	60	1	5
3	45	5	5
4	60	5	5
5	45	1	12
6	60	1	12
7	45	5	12
8	60	5	12

Table 5.2. ISC-Cylinder Factorial High-Low Values

5.4.1.2   Performance Predictions. Running the propulsion performance model, structural model, and the trajectory simulation provides the performance data for each of the 8 factorial designs. The matrix of the factorial designs is shown in Table 5.3, where:

Design	A_{th}	F	R_1	P_{max}	A_{max}	T_{burn}	E_{ratio}
1	-	-	-	1319.86	9.116	82.4	1.0030
2	+	-	-	817.14	7.550	99.8	0.9954
3	-	+	-	1536.14	8.025	89.2	0.9554
4	+	+	-	951.04	6.604	108.0	0.9557
5	-	-	+	1939.88	23.211	49.2	0.9304
6	+	-	+	1201.00	21.361	59.6	0.9911
7	-	+	+	2051.02	19.028	49.4	0.9175
8	+	+	+	1269.81	17.441	59.8	0.9730

Table 5.3. ISC-Cylinder Factorial Designs

+   =   high value of variable

$$- \quad = \quad \text{low value of variable}$$

$$P_{max} \quad = \quad \text{maximum combustion pressure during burn}$$

$$A_{max} \quad = \quad \text{maximum acceleration during burn}$$

$$T_{burn} \quad = \quad \text{burn time}$$

$$E_{ratio} \quad = \quad \text{ratio of final energy states}$$

A payload weight of 1800 pounds is used for each factorial design.

5.4.1.3 Pertinent Factors. Concentrating on the energy ratio regression equation, the vector of the 8 E_{ratio} values may be used to calculate the regression equation coefficients. However, ANOVA is first used to determine which of the 8 factors are statistically significant. Using contrasts, the average effect of each factor is measured. These effects are represented by the sum of squared differences attributed to that effect. By dividing by the respective degree of freedom, the mean square is calculated for each factor. Within the assumptions of ANOVA, the ratio of each mean square with the mean square for error in the data produces an F-statistic. This value is compared against an F-distribution value for some α level of significance. In this manner, each of the 8 factors are checked for statistical significance (47:pp98-104).

Since each "experiment" is a run of the computer models, there is only one data point per design. Therefore, there is not any error between replications of the same design. This means that there is no actual sum or mean square for error. This problem is solved by assuming that the error measured by the most complex interaction, the A-B-C factor, represents the sum square for error. This solution to the single replication problem is called "confounding with error" (86). For the energy ratio data, an ANOVA table is constructed which summarizes the results (see Table 5.4).

The F-distribution value for two α values are:

$$F_{1,1,\alpha=0.05} = 161.4$$

$$F_{1,1,\alpha=0.10} = 39.86$$

Source of Variation	Degree of Freedom	Sum of Squares (SS)	Mean Square (MS)	$\frac{MS}{MSE}$
A	1	0.001482	0.001482	69.11
B	1	0.001749	0.001749	81.55
AB	1	9.11×10^{-7}	9.11×10^{-7}	0.043
C	1	0.001188	0.001188	55.39
AC	1	0.001907	0.001907	88.87
BC	1	3.962×10^{-4}	3.962×10^{-4}	18.47
Error = ABC	1	2.145×10^{-5}	2.145×10^{-5}	NA

Table 5.4. ANOVA for Energy Ratio, ISC-Cylinder Stage

The $\alpha = 0.05$ value is primarily used, but the 10% value helps determine the lower limit of significance. Comparing the final column of Table 5.4 to the F-distribution values, the following factors are included in the regression model:

- A - effect of nozzle throat area, A_{th}

- B - effect of slot half thickness, F

- C - effect of central radius, R_1

- $A \cdot C$ - effect of $A_{th} \cdot R_1$ interaction

- $B \cdot C$ - effect of $F \cdot R_1$ interaction

In this case, the only insignificant factor is the $A \cdot B$ interaction.

The process is easily repeated for the vectors of data corresponding to P_{max}, A_{max}, and T_{burn}. The same F-distribution values are used for determining significant factors. ANOVA Tables for each output vector are calculated.

Maximum Pressure:

The ANOVA for maximum pressure is shown in Table 5.5.

Significant factors include:

- A - effect of nozzle throat area, A_{th}

- B - effect of slot half thickness, F

Source of Variation	Degree of Freedom	Sum of Squares (SS)	Mean Square (MS)	$\frac{MS}{MSE}$
A	1	850147	850147	4240
B	1	35130	35130	175.2
AB	1	1944	1944	9.70
C	1	42206	42206	2105
AC	1	23358	23358	116.5
BC	1	3622	3622	18.07
Error = ABC	1	200.5	200.5	NA

Table 5.5. ANOVA for Maximum Pressure, ISC-Cylinder Stage

- C - effect of central radius, R_1

- $A \cdot C$ - effect of $A_{th} \cdot R_1$ interaction

Maximum Acceleration:

The ANOVA for maximum acceleration is shown in Table 5.6.

Source of Variation	Degree of Freedom	Sum of Squares (SS)	Mean Square (MS)	$\frac{MS}{MSE}$
A	1	5.158	5.158	2964
B	1	12.852	12.852	7384
AB	1	0.0208	0.0208	11.96
C	1	309.33	309.33	177727
AC	1	0.0253	0.0253	14.54
BC	1	4.600	4.600	2643
Error = ABC	1	0.00174	0.00174	NA

Table 5.6. ANOVA for Maximum Acceleration, ISC-Cylinder Stage

Significant factors include:

- A - effect of nozzle throat area, A_{th}

- B - effect of slot half thickness, F

- C - effect of central radius, R_1

- $B \cdot C$ - effect of $F \cdot R_1$ interaction

Burn Time:

Source of Variation	Degree of Freedom	Sum of Squares (SS)	Mean Square (MS)	$\frac{MS}{MSE}$
A	1	406.1	406.1	1678
B	1	29.65	29.65	121.0
AB	1	0.245	0.245	1.0
C	1	3256	3256	1329
AC	1	29.65	29.65	121.0
BC	1	26.65	26.65	108.8
Error = ABC	1	0.245	0.245	NA

Table 5.7. ANOVA for Burn Time, ISC-Cylinder Stage

The ANOVA for burn time is shown in Table 5.7.

Significant factors include:

- A - effect of nozzle throat area, A_{th}

- B - effect of slot half thickness, F

- C - effect of central radius, R_1

- $A \cdot C$ - effect of $A_{th} \cdot R_1$ interaction

- $B \cdot C$ - effect of $F \cdot R_1$ interaction

5.4.2 Regression Models. Once the insignificant factors have been eliminated from the regression equations, the regression coefficients are calculated from Equation 5.2

$$\beta = \left[\mathbf{X}^T \cdot \mathbf{X} \right]^{-1} \cdot \mathbf{X}^T \cdot \mathbf{Y} \tag{5.2}$$

where $\mathbf{Y}$ is the data vector of either E_{ratio}, P_{max}, or T_{burn}, and $\mathbf{X}$ is a matrix corresponding to high and low design variable values. The variables are "coded" by

$$x_{coded} = \frac{x - \mu_x}{\sigma_x} \tag{5.3}$$

where μ_x is the average of the high and low variable values, and σ_x is half the different between the high and low value. The columns of the $\mathbf{X}$-matrix correspond to each of the possible factors: single variables and their interactions. The coded value for the interaction columns is calculated by the

5-11

product of the coded value of each of the interacting variables. The coding of these variables does not affect the results and makes the calculations easier.

The following is a full **X**-matrix including all factors. For those with fewer significant factors, the insignificant columns are eliminated.

$$
\mathbf{X} =
\begin{bmatrix}
A & B & AB & C & AC & BC \\
- & - & + & - & + & + \\
+ & - & - & - & - & + \\
- & + & - & - & + & - \\
+ & + & + & - & - & - \\
- & - & + & + & - & - \\
+ & - & - & + & + & - \\
- & + & - & + & - & + \\
+ & + & + & + & + & +
\end{bmatrix}
$$

Using Equation 5.2, the regression coefficients are calculated for each of the four regression models corresponding to an ISC-cylindrical stage. However, these regression coefficients are in terms of the coded variables. Substituting for the coded variables with Equation 5.3 yields the regression equations in terms of the design variables.

The regression equations for each of the models are as follows:

Energy Ratio:

$$
\begin{aligned}
E_{ratio} = {} & 1.20975 - 0.003184 A_{th} - 0.01594 F - 0.037373 R_1 + \\
& 5.8810 \times 10^{-4} A_{th} \cdot R_1 + 0.001005 F \cdot R_1
\end{aligned}
\tag{5.4}
$$

Maximum Pressure:

$$
P_{max} = 2091.85 - 25.968 A_{th} + 33.133 F + 173.69 R_1 -
$$

$$2.0585 A_{th} \cdot R_1 \tag{5.5}$$

Maximum Acceleration:

$$A_{max} = 3.7006 - 0.10707 A_{th} + 0.28698 F + 2.10161 R_1 -$$
$$0.10832 F \cdot R_1 \tag{5.6}$$

Burn Time:

$$T_{burn} = 31.5357 + 1.5733 A_{th} + 3.1786 F - 1.1321 R_1 -$$
$$0.073333 A_{th} \cdot R_1 - 0.260714 F \cdot R_1 \tag{5.7}$$

5.4.2.1 Modeling Error. A measure of how much of the total variance in the data is captured by each model is the correlation coefficient, R^2. For each regression model, the significant factors' sum of squares from the ANOVA are used to calculate R^2 (47:p135):

$$SS_{regression} = \sum SS_{significant}$$
$$SS_{total} = \sum_{i=1}^{8} SS$$
$$R^2 = \frac{SS_{regression}}{SS_{total}}$$

The correlation coefficients for the four regression models are shown in Table 5.8. These are all very good correlation coefficients - all are very close to unity. Therefore, the models adequately capture the variability of the data.

Model	R^2
E_{ratio}	0.996685
P_{max}	0.995685
A_{max}	0.999856
T_{burn}	0.991961

Table 5.8. Correlation Coefficients, ISC-Cylinder

5.4.3 Parameter Optimization. The regression equations approximate the actual, although implicit, functions of energy ratio, maximum pressure, maximum acceleration, and burn time. With these relationships, non-linear parameter optimization is applied to maximize the energy ratio subject to several constraints. A computer program called GINO (General Interactive Nonlinear Optimization) (62), is used for the optimization. The objective function, which is the E_{ratio} regression equation, is maximized subject to the following constraints:

$$
\begin{array}{llll}
P_{max} & \equiv & f_1(A_{th}, F, R_1) & \leq & 1800 \text{ psia} \\
A_{max} & \equiv & f_2(A_{th}, F, R_1) & \leq & 18 \text{ g's} \\
T_{burn} & \equiv & f_3(A_{th}, F, R_1) & \leq & 80 \text{ sec.} \\
45 \text{ in.}^2 & \leq & A_{th} & \leq & 60 \text{ in.}^2 \\
1 \text{ in.} & \leq & F & \leq & 5 \text{ in.} \\
5 \text{ in.} & \leq & R_1 & \leq & 12 \text{ in.}
\end{array}
$$

The ranges on the design variables correspond to the high and low values used to determine the regression equation coefficients.

5.4.3.1 Optimal Solution: ISC-Cylinder. The results from GINO are as follows:

$$
E_{ratio_{max}} = 0.997
$$

where the optimal design variable values are

$$
\begin{array}{rcl}
A_{th}^* & = & 45 \text{ in.}^2 \\
F^* & = & 1 \text{ in.} \\
R_1^* & = & 5.437 \text{ in.}
\end{array}
$$

GINO also gives values for the slack variables for the constraints. Slack variables for the burn time constraint, minimum F, and minimum A_{th} are all zero. This means that the optimal solution in the 3-dimensional design space lies on these constraint surfaces, and not the others. This illustrates how the choice of constraints affects the optimal solution. The degree which each of these three constraints affects the solution is measured by the magnitude of their corresponding Lagrange multiplier. GINO provides these "Price" values which correspond to their respective Lagrange multipliers: The constraint for minimum R_1 also has a very low slack variable, indicating

Constraint	Price
$T_{burn_{max}}$	-0.00211
F_{min}	-0.014192
A_{th}	-0.002466

that the optimal-performing motor design is very much related to minimizing the initial port volume.

Further discussion of these results and others are discussed in later sections.

5.4.3.2 Optimal ISC-Cylindrical Stage Grain/Nozzle Design. The optimal point of design variables is evaluated by the performance models. Table 5.9 shows good correlation between the results of the regression equation optimization and the performance model results. The limit on burn time is very effective, and the pressure, acceleration, and energy ratio all fall within expected limits. The "optimal" combination of design variables found by GINO produces a motor design which, when evaluated by the performance models, outperforms the original eight ISC-Cylindrical designs.

E_{ratio}	1.004
T_{burn}	80.0 sec.
P_{max}	1344 psia
A_{max}	9.786 g's
Total Impulse	6.3691×10^6 lbf·sec
Thrust$_{avg}$	79,613 lbf

Table 5.9. ISC-Cylinder Optimal Design Parameters

5.5 Additional Results

The three remaining design options are optimized in the same fashion as the ISC-Cylindrical stage. The results presented include the factorial designs, the regression models, and optimization results.

5.5.1 ISC-Conical Stage.

5.5.1.1 Factorial Designs. The high-low values for this design vary somewhat from the cylindrical stage case. Grain design variables F and R_1 are selected in the Propulsion Model for the base of the conical grain. The parameters get smaller as the port area tapers up to the top

of the conical grain. In order for the grain to have a significant opening at the top, the minimum grain parameters are:

$$F \geq 4 \text{ in.}$$

$$R_1 \geq 10 \text{ in.}$$

The remaining high-low values are determined by experimenting to find the largest feasible region of the design space.

Design	A_{th}	F	R_1
9	50	4	10
10	80	4	10
11	50	9	10
12	80	9	10
13	50	4	13
14	80	4	13
15	50	9	13
16	80	9	13

Table 5.10. ISC-Conical Factorial High-Low Values

Running the performance models provides the data for each of the 8 factorial designs. A payload weight of 1800 pounds is used for each design. The matrix of the factorial designs is shown in Table 5.11.

Design	A_{th}	F	R_1	P_{max}	A_{max}	T_{burn}	E_{ratio}
9	-	-	-	1547.23	12.53	62.6	0.9964
10	+	-	-	706.90	9.32	85.8	0.9938
11	-	+	-	1780.39	10.33	65.0	0.9613
12	+	+	-	813.42	7.57	88.4	0.9638
13	-	-	+	1860.95	20.31	48.6	0.9407
14	+	-	+	850.23	16.46	66.6	0.9930
15	-	+	+	2077.75	13.70	49.0	0.9261
16	+	+	+	949.28	10.65	67.0	0.9663

Table 5.11. ISC-Conical Factorial Designs

5.5.1.2 Regression Models. The insignificant factors are eliminated from the regression equations and the resulting equations are:

Energy Ratio:

$$E_{ratio} = 1.48154 - 0.005146A_{th} - 0.014443F - 0.046029R_1 +$$

$$0.0005144A_{th} \cdot R_1 + 0.0007933F \cdot R_1 \qquad (5.8)$$

Maximum Pressure:

$$P_{max} = 672.28 - 6.3884A_{th} + 85.727F - 0.81462A_{th} \cdot F +$$

$$194.039R_1 - 1.84384A_{th} \cdot R_1 \qquad (5.9)$$

Maximum Acceleration:

$$A_{max} = -16.6706 - 0.10734A_{th} + 2.42753F + 3.6151R_1 -$$

$$0.28223F \cdot R_1 \qquad (5.10)$$

Burn Time:

$$T_{burn} = 33.1722 + 1.36556A_{th} + 1.900F - 1.14556R_1 -$$

$$0.05889A_{th} \cdot R_1 - 0.1400F \cdot R_1 \qquad (5.11)$$

The regression coefficients for the four regression models are shown in Table 5.12

Model	R^2
E_{ratio}	0.990755
P_{max}	0.999962
A_{max}	0.997330
T_{burn}	0.999993

Table 5.12. Correlation Coefficients, ISC-Conical

5.5.1.3 Optimization Results. The results of the optimization from GINO are as follows:

$$E_{ratio_{max}} = .995123$$

where the payload is 1800 pounds. The optimal design variables are:

$$A_{th}^* = 54.9 \text{ in.}^2$$

$$F^* = 4 \text{ in.}$$

$$R_1^* = 10 \text{ in.}$$

However, inspection of the factorial designs shows that in this case the regression-based optimization is close, but slightly off. The optimal solution actually corresponds to the first factorial design, which is only slightly different in the throat area value. This difference is probably due to a "bump" in the regression equation. As in the ISC-Cylindrical case, the optimal grain design corresponds to minimal port area. In this case, there is no problem with a burn time constraint. This is due to the thinner average burn distance for the conical versus cylindrical stages.

The optimal point of design variables is evaluated by the performance models. Table 5.13 shows the resulting performance values. Again, there is good agreement between the values and the constraints of the optimization.

E_{ratio}	0.9964
T_{burn}	62.6 sec.
P_{max}	1547 psia
A_{max}	12.53 g's
Total Impulse	6.31122×10^6 lbf · sec
$Thrust_{avg}$	100,818 lbf

Table 5.13. ISC-Conical Optimal Design Parameters

5.5.2   Conventional-Cylindrical Stage.

5.5.2.1   Factorial Designs. The high-low values for this design are similar to those for the ISC-Cylindrical stage. The high-low values of the design space region are shown in Table 5.14.

Running the performance models provides the data for each or the 8 factorial designs. A payload weight of 1600 pounds is used for each design. This lighter payload is necessary for the conventional designs in order to make the E_{ratio} close to unity. The matrix of the factorial designs is shown in Table 5.15.

Design	A_{th}	F	R_1
17	45	1	5
18	65	1	5
19	45	5	5
20	65	5	5
21	45	1	9
22	65	1	9
23	45	5	9
24	65	5	9

Table 5.14. Conventional-Cylindrical Factorial High-Low Values

Design	A_{th}	F	R_1	P_{max}	A_{max}	T_{burn}	E_{ratio}
17	-	-	-	1744.40	12.28	62.6	1.017
18	+	-	-	945.10	9.67	80.0	1.008
19	-	+	-	2030.25	10.75	67.8	0.976
20	+	+	-	1099.97	8.28	86.6	0.950
21	-	-	+	2124.23	23.50	47.4	1.015
22	+	-	+	1150.89	18.74	60.6	1.007
23	-	+	+	2301.06	17.16	47.8	1.037
24	+	+	+	1246.69	12.68	61.2	0.986

Table 5.15. Conventional-Cylindrical Factorial Designs

5.5.2.2   Regression Models. The insignificant factors are eliminated from the regression equations and the resulting equations are:

Energy Ratio:

$$E_{ratio} = 1.04513 - 0.00005A_{th} - 0.007375F - 0.0035R_1 -$$

$$0.000375A_{th} \cdot F - 0.003125F \cdot R_1 \tag{5.12}$$

Maximum Pressure:

$$P_{max} = 2873.45 - 33.923A_{th} + 44.584F + 165.180R_1 -$$

$$1.8633A_{th} \cdot R_1 \tag{5.13}$$

Maximum Acceleration:

$$A_{max} = -2.9875 + 0.0030A_{th} + 1.1163F + 4.2625R_1 -$$

$$0.0260A_{th} \cdot R_1 - 0.29625F \cdot R_1 \qquad (5.14)$$

Burn Time:

$$T_{burn} = 23.488 + 1.205A_{th} + 3.1625F - 0.6875R_1 -$$

$$0.060A_{th} \cdot R_1 - 0.3375F \cdot R_1 \qquad (5.15)$$

The correlation coefficients for the four regression models are shown in Table 5.16

Model	R^2
E_{ratio}	0.970281
P_{max}	0.995208
A_{max}	0.999871
T_{burn}	0.999627

Table 5.16. Correlation Coefficients, Conventional-Cylindrical

5.5.2.3 Optimization Results. The results of the optimization from GINO are as follows:

$$E_{ratio_{max}} = 1.0168$$

$$A_{th}^* = 45 \text{ in.}^2$$

$$F = 1 \text{ in.}$$

$$R_1 = 5 \text{ in.}$$

As in previous cases, the optimal performance corresponds to the minimum allowable port area design. The burn time constraint is not active in the aluminum-based propellant stage due to the higher burn rate of the aluminum versus boron-based propellant.

The optimal point of design variables is evaluated by the performance models. Table 5.17 shows the resulting performance values.

5.5.3 Conventional-Conical Stage.

E_{ratio}	1.017
T_{burn}	62.6 sec.
P_{max}	1744.40 psia
A_{max}	12.28 g's
Total Impulse	6.33264×10^6 lbf · sec
$Thrust_{avg}$	101,160 lbf

Table 5.17. Conventional-Cylindrical Optimal Design Parameters

5.5.3.1 Factorial Designs. The high-low values for this design are similar to those for the ISC-Conical stage. The high-low values of the design space region are shown in Table 5.18.

Design	A_{th}	F	R_1
25	60	4	10
26	80	4	10
27	60	9	10
28	80	9	10
29	60	4	13
30	80	4	13
31	60	9	13
32	80	9	13

Table 5.18. Conventional-Conical Factorial High-Low Values

Running the performance models provides the data for each or the 8 factorial designs. Again, for the conventional technology stage, a payload weight of 1600 pounds is used for each design. The matrix of the factorial designs is shown in Table 5.19.

Design	A_{th}	F	R_1	P_{max}	A_{max}	T_{burn}	E_{ratio}
25	-	-	-	1509.06	15.24	53.8	1.015
26	+	-	-	934.27	12.43	65.2	0.994
27	-	+	-	1736.46	12.37	55.8	0.988
28	+	+	-	1075.06	10.04	67.6	0.970
29	-	-	+	1815.03	26.60	41.8	1.010
30	+	-	+	1123.70	22.09	50.6	0.997
31	-	+	+	2026.48	17.47	42.2	0.987
32	+	+	+	1254.61	14.45	51.0	0.984

Table 5.19. Conventional-Conical Factorial Designs

5.5.3.2 Regression Models. The insignificant factors are eliminated from the regression equations and the resulting equations are:

Energy Ratio:

$$E_{ratio} = 1.25142 - 0.002925A_{th} - 0.009833F - 0.01583R_1 +$$

$$0.000195A_{th} \cdot R_1 + 0.0004733F \cdot R_1 \qquad (5.16)$$

Maximum Pressure:

$$P_{max} = 737.48 - 6.5549A_{th} + 94.030F - 0.83575A_{th} \cdot F +$$

$$212.84R_1 - 1.8918A_{th} \cdot R_1 \qquad (5.17)$$

Maximum Acceleration:

$$A_{max} = -23.3548 - 0.1584A_{th} + 3.3107F + 5.0380R_1 -$$

$$0.38367F \cdot R_1 \qquad (5.18)$$

Burn Time:

$$T_{burn} = 24.007 + 1.0467A_{th} + 1.6400F - 0.68667R_1 -$$

$$0.04667A_{th} \cdot R_1 - 0.1200F \cdot R_1 \qquad (5.19)$$

The correlation coefficients for the four regression models are shown in Table 5.20

Model	R^2
E_{ratio}	0.982145
P_{max}	0.999920
A_{max}	0.993833
T_{burn}	0.999936

Table 5.20. Correlation Coefficients, Conventional-Conical

5.5.3.3 Optimization Results. The results of the optimization from GINO are as follows:

$$E_{ratio_{max}} = 1.0142$$

$$A_{th}^* = 60 \text{ in.}^2$$

$$F = 4 \text{ in.}$$

$$R_1 = 10 \text{ in.}$$

As in previous cases, the optimal performance corresponds to the minimum allowable port area design. The burn time constraint is not active which is due to the higher burn rate of the aluminum versus boron-based propellant. Also, as in the ISC-conical stage, the shorter web thickness leads to a shorter burn time. These effects make the burn time for this design the shortest of those analyzed.

The optimal point of design variables is evaluated by the performance models. Table 5.21 shows the resulting performance values.

E_{ratio}	1.015
T_{burn}	53.8 sec.
P_{max}	1509 psia
A_{max}	15.24 g's
Total Impulse	6.22272×10^6 lbf · sec
$Thrust_{avg}$	115,664 lbf

Table 5.21. Conventional-Conical Optimal Design Parameters

5.6 Optimization Conclusions

The four optimized designs point out several key trends in the various effects on stage performance of a slotted tube grain design.

1. The optimal performance grain in most cases corresponds to the grain design with the minimum initial port area. The lower limits of the grain design parameters are active constraints in each optimization. These lower limits have the most significant effect on stage performance of all the system constraints. Therefore, detailed design of the grain should include an examination of methods to effectively lower these limits. Methods could include adding more igniters in order to decrease the initial port area required for adequate ignition of the burn surface.

2. The lower weight of ISC stages, due to the elimination of interstage weight, improves ISC performance over conventional technology stages.

3. The burn time is lower for conical stages compared to cylindrical stages, given equal bottom diameters. The taller, more slender conical stages have a thinner average propellant web thickness.

4. The only active constraints other than grain design parameters is the maximum burn time and minimum throat size in the ISC-Cylindrical stage.

VI. Results

6.1 Introduction

This chapter summarizes the results of the *NEMESIS* design study in terms of mission performance, cost and availability of the four optimized design configurations presented in Chapter 5:

- ISC Cylindrical Stage

- ISC Conical Stage

- Conventional Cylindrical Stage

- Conventional Conical Stage.

Performance analysis is done using the trajectory performance model (TPM). Total stage weight from the output of the structures/thermal/materials (STM), AIDE II, and other weight estimation models, together with the mass flow and thrust time histories are inputs to the TPM. The TPM is then iterated (by varying payload and the initial flight path angle) until an energy ratio of 1.0 (or very close to 1.0) at the correct burnout flight path angle is achieved. The payload-carrying capability for the desired burnout condition is then used as the measure of mission performance.

Cost analysis is accomplished using the STACEM and STRAMICE models presented in Chapters 3 and 4. Inputs to the models are system component weights and "complexity factors" for each optimized design configuration.

Availability analysis uses the Markov Process models presented in Appendix D. ISC and conventional *NEMESIS* design approaches are compared to a 3-stage system baseline availability. An availability ratio is formed by dividing the calculated *NEMESIS* design availability at year 10 by the comparable baseline availability. In this way, a single number is used to capture the essence of the model results and to compare the performance of the design alternatives.

6.2 Mission Performance Results

6.2.1 Overview . The optimized motor design parameters (throat area, grain pattern slot half- thickness and grain pattern central tube radius) presented in Chapter 5 are used in the

propulsion model to simulate optimal motor performance for a particular design configuration. The chamber burn characteristics (time, pressure, thrust, mass flow, and temperature) are then used as inputs to the other (STM, AIDE II, etc.) system models, and an overall optimized system design is developed.

To evaluate the mission performance of a candidate design, the TPM needs the following parameters:

- total weight of stage 2

- motor thrust time history

- mass flow time history

- payload weight

- initial flight path angle

The total weight of a second stage design comes from summing the individual component weights. The STM model provides weights for the motor case, liner, external protective material (EPM) and internal insulation. Propellant weight is 22,100 pounds for all designs (Chapter 4). Nozzle and thrust vector control (TVC) weights are calculated with either the Aerojet AIDE II package (for ISC) or by using a linear interpolation model (for conventional) based on the weights of some existing systems (see Chapter 4). The weight of additional structure (igniters, raceway cover and cabling, all electrical components, stage separation components and interstage structure, skirts, and other (miscellaneous) components is added as required for a particular design configuration. All these weights are added to determine the total design stage weight.

The total stage weight and the mass flow and thrust histories are input into the TPM. This model is iterated (by varying payload and the initial flight path angle) until an energy ratio of close to 1.0 is achieved at the desired burnout flight path angle (differs slightly depending on the payload - Appendix A). The maximum payload is then used as the measure of mission performance capability.

6.2.2 Design Option I: ISC Cylindrical Stage .

From Chapter 5, the optimal motor design variables for this design configuration (Figure 6.1) are $A_{th}^* = 45in.^2$, $F^* = 1in.$, and $R_1^* = 5.437in.$ When these parameters are used in the propulsion model, the results are shown in Table 6.1. Note

Parameter	Value
T_{burn}	80.0 sec.
P_{max}	1344.89 psia
$Thrust_{avg}$	79613 lbf

Table 6.1. ISC Cylindrical Stage Motor Design Parameters

that average thrust is given in Table 6.1, but the actual thrust and mass flow histories as a function of time are input to the TPM. Using these design variables and parameters, the design weights for case, liner, skirt, ISC components, insulation, and EPM were determined with the STM and AIDE II models. Weights for igniter and "miscellaneous" (electrical and instrumentation, separation system, raceway) were taken directly from estimates for the MM III system . As can be seen in Figure 6.1, an interstage structure is required to connect stage 2 with the post-boost vehicle. An estimate for this interstage weight is calculated using a scaling of the actual MM III Stage1-Stage2 interstage weight.

A complete summary of the design characteristics and weights for the ISC Cylindrical Stage *NEMESIS* design is presented in Table 6.2.

This design was evaluated with the TPM to determine mission performance. Results are presented in Table 6.3.

6.2.3 Design Option 2: ISC Conical Stage . The optimal motor design variables for this design configuration (Figure 6.2) are: $A_{th}^* = 54.9in.^2$, $F^* = 4in.$, $R_1^* = 10in.$ Using the same procedure described in the previous section, design characteristics and weights are presented in Table 6.4. Note that since the stage tapers to the aft diameter of the post- boost vehicle, no heavy interstage structure is required with this design. However, the longer case (a direct result of tapering) together with the additional case and insulation thicknesses (required for the increased burn pressure associated with this design) results in a net increase (4.6 pounds) in overall structural weight, with a corresponding dip in performance (Table 6.5).

6.2.4 Design Options 3A and 3B: Conventional Cylindrical Stage . Two designs are investigated within the basic configuration of a conventional cylindrical stage:
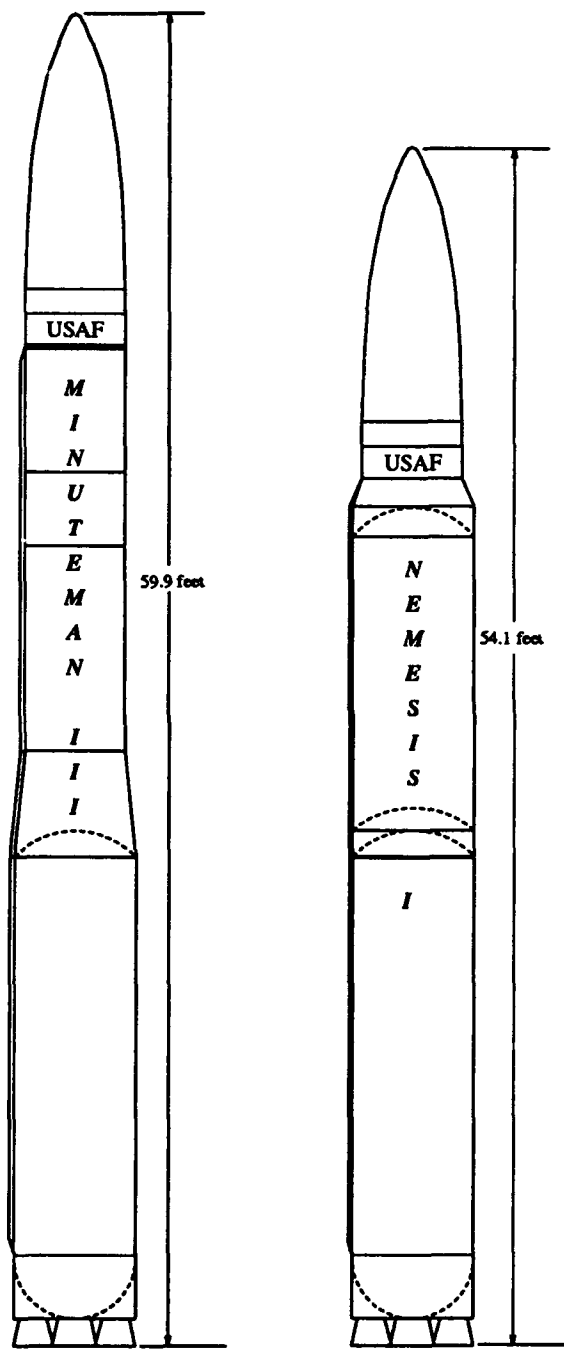
Figure 6.1. Opt 1 - ISC Cylindrical *NEMESIS* Design
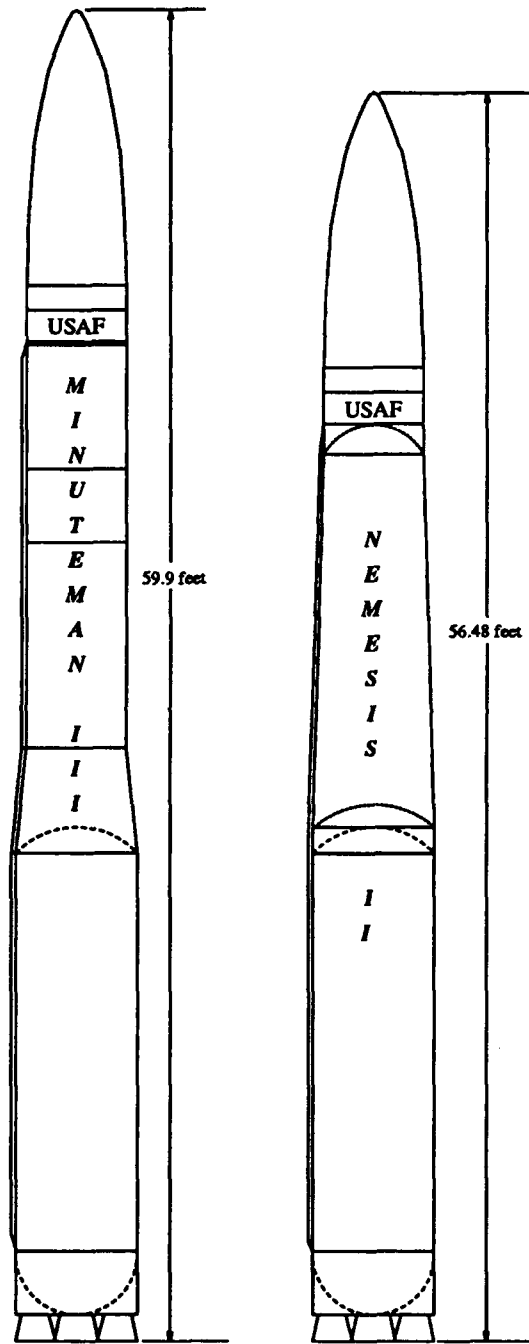
Figure 6.2. Opt 2 - ISC Conical *NEMESIS* Design

Design Characteristics	Value
Case Outer Diameter	66 *inches*
Stage Length	15.5 *ft*
Case Volume	225.3 *ft³*
Propellant Density	0.0624326 *lbm/in³*
Average Thrust	79,613 *lbf*
Total Impulse	6,369,050 *lbf · sec*
Burn Time	80.0 *seconds*
Burn Pressure (max)	1344.89 *psi*
$I_{s}p$	288.77 *lbf · sec/lbm*
Structural Ratio	0.07064
Component Weight Estimate	**Pounds**
Electrical and Instrumentation	40
Separation System	15
Structures	
Forward Closure	23.9
Attachment Structure	343
Skirts	10
Raceway	10
Igniter	20
Liner	74.5
Nozzle	423
TVC	56.3
Insulation	206.5
Case	270.9
External Insulation	185.9
Total Structural Weight	1679
Propellant	22100

Table 6.2. ISC-Cylindrical Stage Design

1. A large (66 inch) diameter stage that matches the Stage 1 diameter and requires additional interstage structure to mate with the post-boost vehicle (Figure 6.3).

2. A small (52 inch) diameter stage that requires interstage between Stage 1 and Stage 2, but no significant structure between Stage 2 and the post boost vehicle (Figure 6.4).

Since Chapter 5 shows that optimal performance of a conventional cylindrical design corresponds to minimum allowable port area design, the results of the optimization of the large-diameter cylinder

Specific Energy Ratio	Max Payload	Max g's	Initial Flt Pth Ang	Final Flt Pth Ang
0.9997	1820	9.234	77.9^0	23.19^0

Table 6.3. Mission Performance of ISC Cylindrical Stage - Option 1

Design Characteristics	Value
Case Outer Diameter	
bottom	66 *inches*
top	52 *inches*
Stage Length	17.88 *ft*
Case Volume	247.98 *ft²*
Propellant Density	0.0624326 *lbm/in³*
Average Thrust	101,468 *lbf*
Total Impulse	6,331,610 *lbf · sec*
Burn Time	62.4 *seconds*
Burn Pressure (max)	1547.0 *psi*
I_{sp}	287.4 *lbf · sec/lbm*
Structural Ratio	0.07280

Component Weight Estimate	Pounds
Electrical and Instrumentation	40
Separation System	15
Structures	
Forward Closure	19.2
Attachment Structure	280
Skirts	10
Raceway	10
Igniter	20
Liner	97.6
Nozzle	440.6
TVC	66.4
Insulation	220.4
Case	332.8
External Insulation	183.6
Total Structural Weight	1735.6
Propellant	22100

Table 6.4. ISC-Conical Stage Design

were applied directly for the smaller diameter case (i.e. minimum port area was assumed to provide the optimum performance). Two cylindrical designs are therefore presented in Table 6.6 (66 inch case) and Table 6.7 (52 inch case). The associated performance is given in Table 6.8.

6.2.5 Design Option 4: Conventional Conical Stage . The optimal motor design parameters for this configuration (Figure 6.5) are: $A_{th}^* = 60in.^2$, $F^* = 4in.$, $R_1^* = 10in.$ When these parameters are used to generate motor design characteristics and corresponding stage weights, the results are as given in Table 6.9. Associated performance is given in Table 6.10.

6.2.6 Summary of Mission Performance Results . The results of the mission performance analysis of the five design configurations presented in the preceeding sections is given in summary
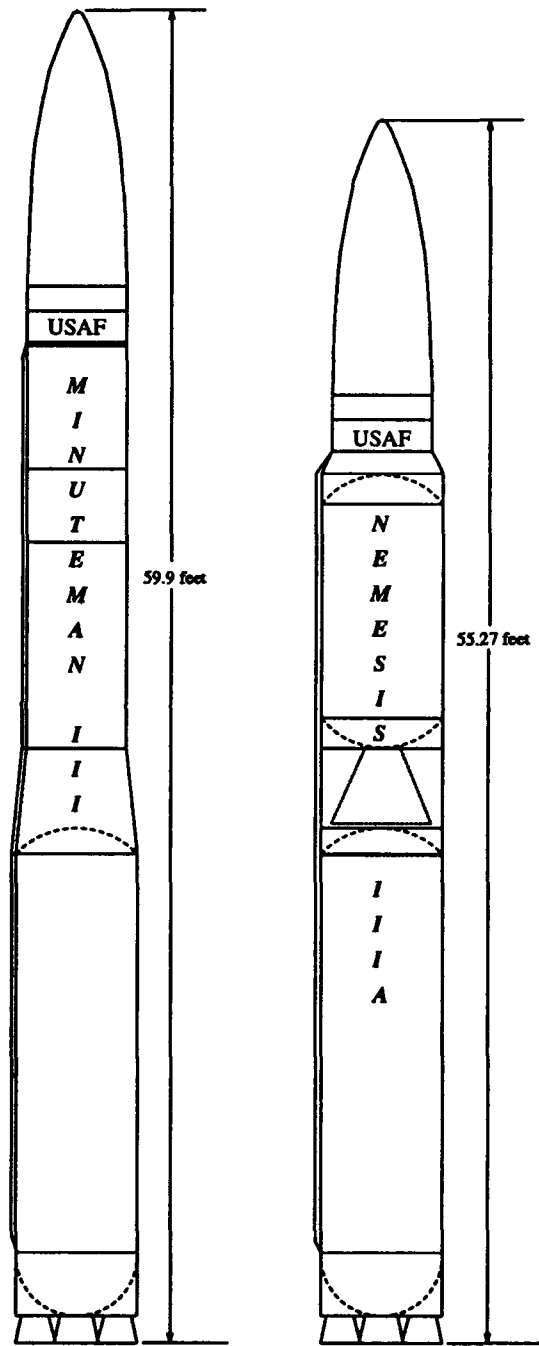
Figure 6.3. Opt 3A - 66 Inch Conventional Cylindrical *NEMESIS* Design
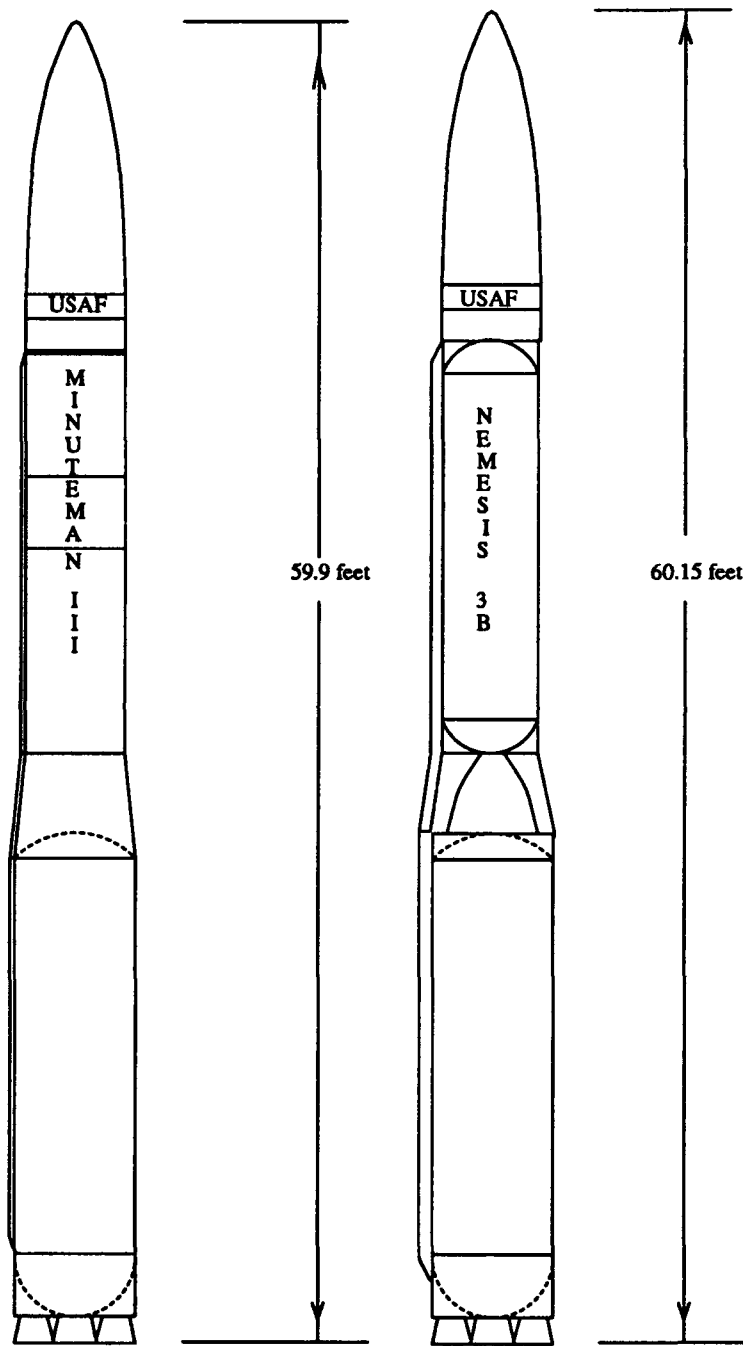
Figure 6.4. Opt 3B - 52 Inch Conventional Cylindrical *NEMESIS* Design
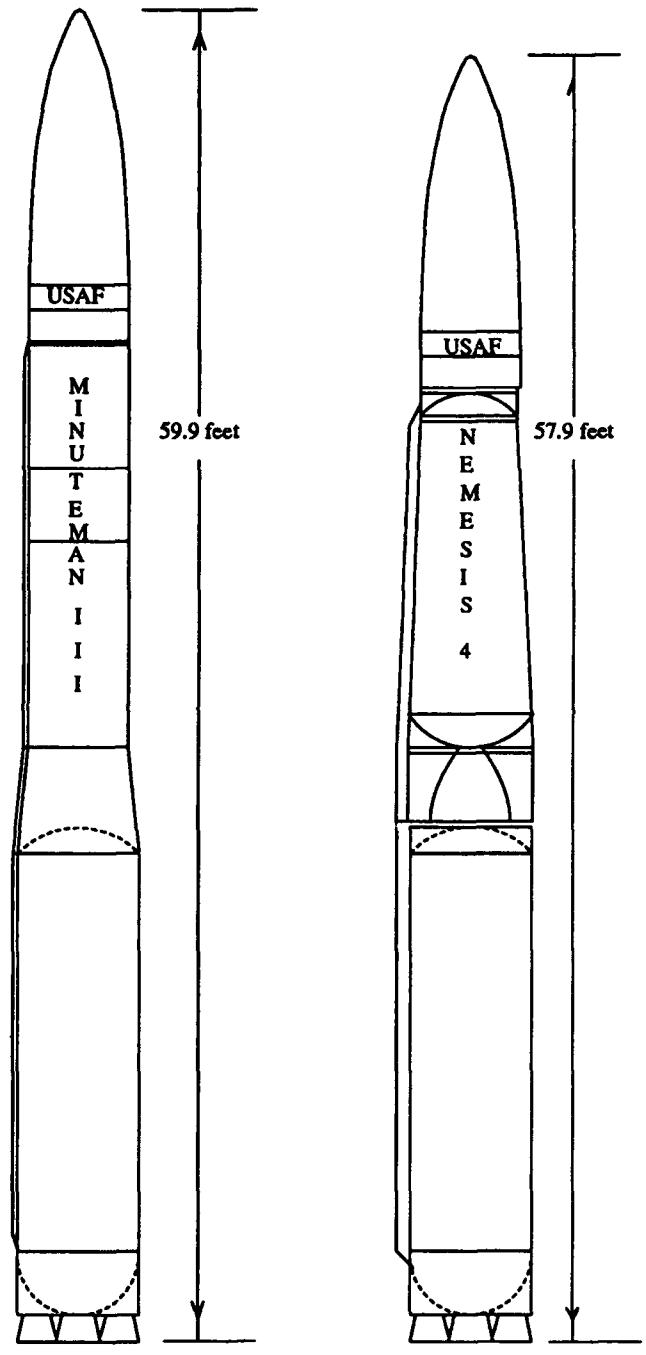
Figure 6.5. Opt 4 - Conventional Conical *NEMESIS* Design

Specific Energy Ratio	Max Payload	Max g's	Initial Flt Pth Ang	Final Flt Pth Ang
1.0000	1730	11.8	77.55^0	23.38^0

Table 6.5. Mission Performance of ISC Conical Stage - Option 2

form in Table 6.11. The mission performance criteria of payload capability associated with an energy ratio ≈ 1.0 shows that the ISC designs outperform all of the conventional designs. All five designs are within specification constraints for maximum allowable acceleration, burnout flight path angle and total system weight, and each can carry a payload heavier than 1500 pounds. Therefore, all five designs are feasible according to the mission performance criteria.

6.3 Readiness Results

6.3.1 Overview . This section summarizes the results of the Readiness Analysis, which is presented in detail in Appendix D. The decision criteria for this aspect of the overall system design uses only the results of the *availability* analysis presented in Appendix D. Reliability results are presented only in terms of a required allocation, and a subjective analysis was done of "other" logistics support factors, so only the availability analysis provides a truly *objective* criteria upon which to base a comparison of the designs. Availability is defined, the failure modes of an ICBM are discussed, the procedure used to model ICBM availability is summarized, and results are presented for a 3-stage baseline, a 2-stage ISC design, and a 2-stage conventional design. The availability decision criteria is presented in terms of an availability ratio comparing 2-stage alternatives to the baseline.

6.3.2 Availability Definition. The definition of availability is taken from Kapur and Lamberson's (60) definition of "intrinsic availability":

- *intrinsic availability* - the probability that a system is operating in a satisfactory manner at any point in time when used under stated conditions. It is a more restrictive measure than *availability* in that administrative and logistics time connected with the repair cycle (included in the *availability* measure) are left out. For example, unavailability of spare parts decreases the availability of a system, but does not impact the *intrinsic availability*.

6-11

Design Characteristics	Value
Case Outer Diameter	66 inches
Stage Length	16.68 ft
Case Volume	225.15 ft^2
Propellant Density	0.064131 lbm/in^3
Average Thrust	101,160 lbf
Total Impulse	6,332,640 lbf·sec
Burn Time	62.6 seconds
Burn Pressure (max)	1744.4 psi
I$_s$p	287.4 lbf · sec/lbm
Structural Ratio	0.07532
Component Weight Estimate	**Pounds**
Electrical and Instrumentation	40
Separation System	15
Structures	
Forward Closure	58.3
Attachment Structure	445
Skirts	10
Raceway	10
Igniter	20
Liner	106.3
Nozzle	350
TVC	105
Insulation	193
Case	309.9
External Insulation	135
Total Structural Weight	1798
Propellant	22100

Table 6.6. Conventional-Cylindrical Stage Design (66 in. diameter)

Mathematically, this can be expressed as

$$A_i = \frac{OperatingTime}{OperatingTime + ActiveRepairTime}$$

This definition is consistent with the concept development or preliminary design phase into which this project fits, and it focuses only on those areas that are within the controllable scope of the project.

6.3.3 Failure Modes and the Basic Model . Over the years, the following ICBM failure modes have been identified:

Design Characteristics	Value
Case Outer Diameter	52 inches
Stage Length	22 ft
Case Volume	240.86 ft^2
Propellant Density	0.064131 lbm/in^3
Average Thrust	129,582 lbf
Total Impulse	6,194,000 lbf·sec
Burn Time	47.8 seconds
Burn Pressure (max)	1565 psi
$I_s p$	281.3 lbf · sec/lbm
Structural Ratio	0.0705

Component Weight Estimate	Pounds
Electrical and Instrumentation	40
Separation System	15
Structures	
Forward Closure	40.7
Attachment Structure	325
Skirts	10
Raceway	10
Igniter	20
Liner	119.1
Nozzle	350
TVC	105
Insulation	198.6
Case	310.6
External Insulation	132.7
Total Structural Weight	1676.7
Propellant	22100

Table 6.7. Conventional-Cylindrical Stage Design (52 in. diameter)

- age-related service life limitations of liners, propellant, igniter ordnance, nozzle entrance caps, o-ring seals, batteries, flight control ordnance, stage separation and skirt jettison ordnance, and post-boost vehicle liquid propellants

- guidance system and payload failures on fielded systems (maintenance driver on current system)

Option	Specific Energy Ratio	Max Payload	Max g's	Initial Flt Pth Ang	Final Flt Pth Ang
3A (66 in.)	1.0000	1690	12.02	77.45^0	23.50^0
3B (52 in.)	0.9945	1675	18.27	76.90^0	23.13^0

Table 6.8. Mission Performance of Conventional Cylindrical Stage - Options 3A, 3B

Design Characteristics	Value
Case Outer Diameter	
bottom	66 inches
top	52 inches
Stage Length	19.32 ft
Case Volume	269.24 ft^2
Propellant Density	0.064131 lbm·in^3
Average Thrust	115,664 lbf
Total Impulse	6,331,610 lbf·sec
Burn Time	53.8 seconds
Burn Pressure (max)	1509.1 psi
I_{sp}	282.4 lbf · sec/lbm
Structural Ratio	0.07120

Component Weight Estimate	Pounds
Electrical and Instrumentation	40
Separation System	15
Structures	
Forward Closure	41.7
Attachment Structure	335
Skirts	10
Raceway	10
Igniter	20
Liner	120.31
Nozzle	350
TVC	105
Insulation	212.2
Case	283.5
External Insulation	151.4
Total Structural Weight	1694.1
Propellant	22100

Table 6.9. Conventional-Conical Stage Design

- field downstage failures in flight control equipment, command signal decoder and raceway cables

- random flight or static fire failures of motors, flight control equipment, ordnance, guidance set, post-boost vehicle and reentry systems

- random personnel-induced handling failures

The scope of this design project is focused on a single stage motor replacement for the current Minuteman stages 2 and 3. Therefore, no re-design is intended in Stage 1, the missile guidance set or the post-boost vehicle. For modeling purposes, any failure and repair of these components will be the same for both the baseline and the 2-stage design. In the case of the stage igniters and ordnance and the interstage ordnance, no design change is planned other than to remove the need

Specific Energy Ratio	Max Payload	Max g's	Initial Flt Pth Ang	Final Flt Pth Ang
0.9990	1675	14.92	77.15^0	23.44^0

Table 6.10. Mission Performance of Conventional Conical Stage - Option 4

Opt	Eng Ratio	Payload	Max g	γ_i	γ_f	Sys Wt (lbs)
1	0.9997	1820	9.234	77.9^0	23.19^0	75,830
2	1.0000	1730	11.8	77.55^0	23.38^0	75,887
3A (66 in.)	1.0000	1690	12.02	77.45^0	23.50^0	75,849
3B (52 in.)	0.9945	1675	18.27	76.90^0	23.13^0	75,828
4	0.9990	1675	14.92	77.15^0	23.44^0	75,745

Table 6.11. Mission Performance of All *NEMESIS* Design Options

for an entire set of this equipment (no stage 3 ingnition needed and no stage 2-stage 3 separation required). The differences between the predicted reliability or availability, then, will come from

- removal of potential failure mechanisms due to reduction in number of stages

- any specific reliability improvements in the project's stage 2 motor design (conventional or integrated stage)

To account for differences due to both stage reduction and fundamental design change, these elements are included in the series system models:

- Stage 1

- Post-Boost Vehicle and Payload

- Missile Guidance Set

- Command Signal Decoder

- Upper stage - PBV Separation Ordnance

- *Stage$_i$* Flight Control Subsystem

- *Stage$_i$* Propulsion Subsystem (propellant, propellant-liner bonding, nozzle components)

- *Stage$_i$* Igniter Ordnance

- *Stage$_i$* Flight Control Subsystem Ordnance

- Stage 1-2 Separation Ordnance

- Stage 2-3 Separation Ordnance (3-stage model only)

The first four elements listed are constant (unchanged) for all designs. Differences due to ordnance are due only to reduction in numbers of stages, not to any fundamental changes in the design of these elements. Differences due to flight control and propulsion subsystems are impacted by both reduction in number of stages and fundamental changes in design, so fidelity is required in these two components, but nowhere else.

6.3.4 Model Elements . The failure and repair mechanisms associated with each model element presented in the previous section are modeled mathematically using appropriate stochastic distributions (see Appendix D). Discussion of the expected design changes associated with new liners, propellants, and flight control equipment is presented in Chapter 4. The corresponding Markov element models are derived in Appendix D.

For the 3-stage baseline, system availability is the product of 17 element availabilities:

- reentry system

- stage separation systems (3 needed)

- missile guidance set

- stage 3 liner, propellant, flight control equipment, igniter and TVC ordnance

- stage 2 liner, propellant, flight control equipment, igniter and TVC ordnance

- command signal decoder

- stage 1

For the 2-stage design, the number of system elements is reduced to 11 (for a conventional design) or to 10 (for an integrated stage design). A summary of two-stage system elements is now presented. For the integrated stage design:

- reentry system, missile guidance, command signal decoder and stage 1 same as above

- two sets of stage separation equipment

- second stage liner, boron propellant, igniter, and hot gas valves

6-16

and for the conventional design:

- reentry system, missile guidance, command signal decoder, stage 1

- two sets of stage separation equipment

- liner, aluminum propellant, igniter, actuators, flight control equipment

6.3.5 Results of Availability Analysis. The calculated system "real" availabilities are now presented for the 3-stage baseline, one Integrated Stage *NEMESIS* design option, and one conventional option. It is again important to note that though the parameters for the 3-stage design were based on Minuteman III data, the model of availability used in this report was not intended to match reported System Availability in the Weapon System Effectiveness Reports. Rather, the intent was to baseline an availability yardstick for 2-stage design evaluation. Therefore, these model numbers, which do not account for all logistics elements involved in a true system availability analysis, should not be construed as reflecting the actual reported Minuteman Availability. In fact, a true comparison would need to be classified, and that problem was intentionally avoided for this study.

The calculated system "real" availabilities over a period of twenty years are given below. Recall that "real" system availability was defined in Section 3 as *the percentage of time that an asset would actually operate as intended if the user began a mission execution.* The fact that a missile could sit failed and therefore "unavailable" in the silo for a period of time before the failure is detected is accounted for in these calculations.

```
3-STAGE "REAL" AVAILABILITY
(USING M1 = SLE FOR ELEMENT CALCULATIONS)

   YEAR       SYSTEM AVAILABILITY

  0.50000     0.98076643779529
  1.00000     0.97595973106006
  2.00000     0.96658887461609
  3.00000     0.95753150396677
  4.00000     0.94877620415692
  5.00000     0.94031275947876
  6.00000     0.93212316954753
  7.00000     0.92415610480403
  8.00000     0.91620720942807
  9.00000     0.90741715621602
 10.00000     0.89460360984377
 11.0000      0.86853779207278
 12.0000      0.81007298715534
```

```
13.0000      0.69517707988211
14.0000      0.51838739732669
15.0000      0.31691701860479
16.0000      0.15201077072682
17.0000      5.6206251992312D-02
18.0000      1.6342271926321D-02
19.0000      4.0175482736661D-03
20.0000      9.6104333067406D-04
```

2-STAGE (INTEGRATED STAGE)
"REAL" AVAILABILITY
(USING WEIBULL PARAMETERS AND M1 = SLE
AS APPROPRIATE)

```
        YEAR          SYSTEM AVAILABILITY

        0.50000       0.98197049887035
        1.00000       0.97716045534430
        2.00000       0.96777806991798
        3.00000       0.95870955574999
        4.00000       0.94994349764175
        5.00000       0.94146992770754
        6.00000       0.93327200805903
        7.00000       0.92529903319264
        8.00000       0.91735961955578
        9.00000       0.90885708120251
       10.00000       0.89834735205013
       11.0000        0.88304899097819
       12.0000        0.85858919467338
       13.0000        0.81931820161137
       14.0000        0.75953227726334
       15.0000        0.67578778382137
       16.0000        0.56974298095295
       17.0000        0.44978303648227
       18.0000        0.32949343356189
       19.0000        0.22295734208270
       20.0000        0.13955675058805
```

2-STAGE (CONVENTIONAL STAGE)
"REAL AVAILABILITY"
(USING WEIBULL PARAMETERS AND M1 = SLE
 AS APPROPRIATE)

```
        0.500000      0.98136828367189
        1.00000       0.97655990865375
        2.00000       0.96718328553644
        3.00000       0.95812018592779
        4.00000       0.94935763216118
        5.00000       0.94087806707175
        6.00000       0.93264393724348
        7.00000       0.92457832166004
        8.00000       0.91652568507258
        9.00000       0.90811840958917
       10.00000       0.89822423724963
       11.0000        0.88331204640022
       12.0000        0.85476190145032
       13.0000        0.79805088336619
```

```
14.0000      0.69907623621054
15.0000      0.55748982267722
16.0000      0.39495143781742
17.0000      0.24553434291005
18.0000      0.13470007392556
19.0000      6.7251769785559D-02
20.0000      3.2583529688547D-02
```

As can be seen in the results, the two-stage alternative designs track the high availability of the baseline very well for the first ten years of operation. The risk associated with the boron propellants, the new liners and the hot gas valves (in the integrated stage designs) appears to be offset by the gains due to the reduction of an entire set of equipment associated with the extra stage. After year 10, a fairly dramatic improvement can be seen in the availability of the two-stage design. Fewer failures can be expected as the years go on with this design, hence availability falls at a much slower rate than is seen with the 3-stage vehicle. These observations should be tempered by the fact that several design life improvements are already on contract for MM III, and gains made by these potential improvements are not reflected in the baseline calculations presented here.

The availability ratio can now be calculated from the simulation results. Year 10 is picked as a baseline for comparison for two reasons:

1. It is long enough into the expected life of the system so that even some age-related failures could start to show up.

2. It is not so far into the expected life that unfair comparisons of the 17 year baseline liner and the 35 year design liner will predominate.

The *availability ratio* is calculated using

$$AV_{ratio} = \frac{AV_{NEMESIS}(10)}{AV_{baseline}(10)}$$

For the ISC designs,

$$AV_{ratio} = \frac{0.89834735205013}{0.89460360984377} = 1.004184805$$

For the conventional designs,

$$AV_{ratio} = \frac{0.89822423724963}{0.89460360984377} = 1.004047186$$

These results are essentially equivalent, so there really does not seem to be any significant difference between the ISC and conventional approaches. Technical risk associated with the ISC designs seems to be somewhat offset by the design simplicity of the hot gas valve thrust vector control system. Both approaches at least match the baseline availability requirement.

6.4 Life Cycle Cost Analysis Results

6.4.1 Overview .   This section focuses on the results of the cost estimating efforts. Specifically, it presents the program design, development, test and evaluation (DDT&E) and production estimates for the alternative booster designs, as determined by the STACEM cost model. The one-time costs of booster integration (refitting) are also identified. Because of the similarity in designs from an operations and support perspective, one O&S estimate is presented for all designs. The Strategic Missile Cost Estimating (STRAMICE) model was chosen for the operations and support cost estimate. Finally, for comparative purposes, a status quo Minuteman III baseline estimate is contrasted with total O&S figures under a conversion program where a constant force of 500 missiles is maintained. Years cited in this chapter are fiscal years (FY) and all cost figures presented are expressed in FY 1992 dollars.

The first section of this chapter gives a detailed weight breakdown for the components that make up each alternative design. While this was sufficient to estimate system performance, the complexity factors (see Chapter 4) associated with the technologies included in each design choice must be included as an additional input to STACEM.

With system component weights and associated complexity factors determined, a total life cycle cost for each design can be estimated. The life cycle cost for each optimal design (integrated stage conical vs constant diameter, conventional conical vs constant diameter) is evaluated. The conventional cylindrical design with the 52 inch diameter is priced as a fifth design alternative. The optimal designs provide for maximum performance within the program constraints and "reasonable" risks (reflected in the complexity factors) for the technologies involved. Since life cycle costs are a

critical aspect of any program today, the tradeoffs between performance and cost must be seriously considered. The integrated stage approach represents higher risk due to the state of development of the technologies, but performance (payload capability and availability), as shown in the previous sections, is better. The conventional approach involves less development initially, but the reduced performance must be considered in the determination of the "best" system design.

6.4.2 DDT&E and Production Costs . DDT&E and production cost schedules and estimates for the five proposed booster designs are now presented. These estimates are generated by STACEM.

```
              OPTION 1 - ISC CYLINDRICAL
           DDT&E and Production Cost Breakdown Totals
                    FY 1992, $Thousands
```

CBS number	Cost Category	Amount $Thousand	Percent of Total
0	Total DDT&E and Production Cost:	733,002	100.00
1.	Solid Rocket Booster Production:	636,874	86.89
1.01	.Electrical & instrumentation	41,650	5.68
1.02	.Separation system	8,631	1.18
1.03	.Structures	15,032	2.05
1.04	.Solid rocket motor	335,077	45.71
1.04.1	..Case	60,843	8.30
1.04.2	..Insulation	12,992	1.77
1.04.3	..Liner	1,296	.18
1.04.4	..Solid fuel	109,190	14.90
1.04.5	..Nozzle	75,978	10.37
1.04.6	..Thrust vector control	54,112	7.38
1.04.7	..Ignition system	3,113	.42
1.04.8	..Preship-assembly & checkout	7,106	.97
1.04.9	..Additional motor-level items	10,448	1.43
1.05	.Flight recovery equipment	0.	.00
1.06	.Shipping and logistics	1,345	.18
1.07	.Booster program support	35,392	4.83
1.08	.Additional booster-level items	49,288	6.72
1.09	.Overall systems support	25,954	3.54
1.10	.Additional G&A and fees	124,506	16.99
1.10.1	..General & Administrative	51,237	6.99
1.10.2	..Fees	73,269	10.00
5.	DDT&E	96,128	13.11
5.01	.Stage engineering	7,852	1.07
5.02	.Propulsion	11,198	1.53
5.03	.Training	351	.05
5.04	.Test hardware	8,306	1.13
5.05	.Test operations	41,429	5.65
5.06	.Facilities	23,928	3.26
5.07	.Ground support equipment	457	.06

5.08	.System integration	2,244	.31
5.09	.Tooling	268	.04
5.10	.Additional G&A and fees	95	.01
5.10.1	..General & Administrative	54	.01
5.10.2	..Fees	42	.01

OPTION 2 - ISC CONICAL
DDT&E and Production Cost Breakdown Totals
FY 1992, $Thousands

CBS number	Cost Category	Amount $Thousand	Percent of Total
0	Total DDT&E and Production Cost:	747,236	100.00
1.	Solid Rocket Booster Production:	651,029	87.12
1.01	.Electrical & instrumentation	41,650	5.57
1.02	.Separation system	8,631	1.15
1.03	.Structures	11,824	1.58
1.04	.Solid rocket motor	347,528	46.51
1.04.1	..Case	62,689	8.39
1.04.2	..Insulation	13,315	1.78
1.04.3	..Liner	1,347	.18
1.04.4	..Solid fuel	109,190	14.61
1.04.5	..Nozzle	82,556	11.05
1.04.6	..Thrust vector control	57,777	7.73
1.04.7	..Ignition system	3,113	.42
1.04.8	..Preship-assembly & checkout	7,134	.95
1.04.9	..Additional motor-level items	10,407	1.39
1.05	.Flight recovery equipment	0.	.00
1.06	.Shipping and logistics	1,347	.18
1.07	.Booster program support	36,627	4.90
1.08	.Additional booster-level items	49,290	6.60
1.09	.Overall systems support	28,860	3.59
1.10	.Additional G&A and fees	127,273	17.03
1.10.1	..General & Administrative	52,376	7.01
1.10.2	..Fees	74,897	10.02
5.	DDT&E	96,207	12.88
5.01	.Stage engineering	7,633	1.02
5.02	.Propulsion	11,216	1.50
5.03	.Training	351	.05
5.04	.Test hardware	8,577	1.15
5.05	.Test operations	41,429	5.54
5.06	.Facilities	23,928	3.20
5.07	.Ground support equipment	452	.06
5.08	.System integration	2,246	.30
5.09	.Tooling	277	.04
5.10	.Additional G&A and fees	99	.01
5.10.1	..General & Administrative	55	.01
5.10.2	..Fees	43	.01

OPTION 3A – CONVENTIONAL 66in.CYLINDRICAL
DDT&E and Production Cost Breakdown Totals
FY 1992, $Thousands

CBS number	Cost Category	Amount $Thousand	Percent of Total
0	Total DDT&E and Production Cost:	1,040,800	100.00
1.	Solid Rocket Booster Production:	952,776	88.95
1.01	.Electrical & instrumentation	41,650	4.00
1.02	.Separation system	8,631	.83
1.03	.Structures	19,390	1.86
1.04	.Solid rocket motor	541,042	50.06
1.04.1	..Case	61,143	5.87
1.04.2	..Insulation	12,697	1.22
1.04.3	..Liner	1,376	.13
1.04.4	..Solid fuel	65,434	6.29
1.04.5	..Nozzle	178,951	17.19
1.04.6	..Thrust vector control	180,828	17.37
1.04.7	..Ignition system	3,113	.30
1.04.8	..Preship-assembly & checkout	7,090	.68
1.04.9	..Additional motor-level items	10,408	1.00
1.05	.Flight recovery equipment	0.	.00
1.06	.Shipping and logistics	1,343	.13
1.07	.Booster program support	59,665	5.73
1.08	.Additional booster-level items	49,317	4.74
1.09	.Overall systems support	43,754	4.20
1.10	.Additional G&A and fees	180,984	17.39
1.10.1	..General & Administrative	74,479	7.16
1.10.2	..Fees	106,505	10.23
5.	DDT&E	115,024	11.05
5.01	.Stage engineering	8,091	.78
5.02	.Propulsion	25,508	2.45
5.03	.Training	351	.03
5.04	.Test hardware	11,616	1.12
5.05	.Test operations	41,429	3.98
5.06	.Facilities	23,928	2.30
5.07	.Ground support equipment	806	.08
5.08	.System integration	2,682	.26
5.09	.Tooling	452	.04
5.10	.Additional G&A and fees	161	.02
5.10.1	..General & Administrative	90	.01
5.10.2	..Fees	71	.01

OPTION 3B – CONVENTIONAL 52in. CYLINDRICAL
DDT&E and Production Cost Breakdown Totals
FY 1992, $Thousands

CBS number	Cost Category	Amount $Thousand	Percent of Total

CBS number	Cost Category	Amount $Thousand	Percent of Total
0	Total DDT&E and Production Cost:	1,047,118	100.00
1.	Solid Rocket Booster Production:	932,095	89.02
1.01	.Electrical & instrumentation	41,650	3.98
1.02	.Separation system	8,631	.82
1.03	.Structures	14,285	1.36
1.04	.Solid rocket motor	529,703	50.59
1.04.1	..Case	62,101	5.93
1.04.2	..Insulation	12,891	1.23
1.04.3	..Liner	1,416	.14
1.04.4	..Solid fuel	65,434	6.25
1.04.5	..Nozzle	186,487	17.81
1.04.6	..Thrust vector control	180,828	17.27
1.04.7	..Ignition system	3,113	.30
1.04.8	..Preship-assembly & checkout	7,095	.68
1.04.9	..Additional motor-level items	10,337	.99
1.05	.Flight recovery equipment	0.	.00
1.06	.Shipping and logistics	1,344	.13
1.07	.Booster program support	60,576	5.79
1.08	.Additional booster-level items	49,265	4.70
1.09	.Overall systems support	44,422	4.24
1.10	.Additional G&A and fees	182,220	17.40
1.10.1	..General & Administrative	74,988	7.16
1.10.2	..Fees	107,232	10.24
5.	DDT&E	115,023	10.98
5.01	.Stage engineering	7,805	.75
5.02	.Propulsion	25,515	2.44
5.03	.Training	351	.03
5.04	.Test hardware	11,891	1.14
5.05	.Test operations	41,429	3.96
5.06	.Facilities	23,928	2.29
5.07	.Ground support equipment	800	.08
5.08	.System integration	2,681	.26
5.09	.Tooling	459	.04
5.10	.Additional G&A and fees	163	.02
5.10.1	..General & Administrative	92	.01
5.10.2	..Fees	72	.01

OPTION 4 - CONVENTIONAL CONICAL
DDT&E and Production Cost Breakdown Totals
FY 1992, $Thousands

CBS number	Cost Category	Amount $Thousand	Percent of Total
0	Total DDT&E and Production Cost:	1,044,598	100.00
1.	Solid Rocket Booster Production:	929,590	88.99
1.01	.Electrical & instrumentation	41,650	3.99
1.02	.Separation system	8,631	.83
1.03	.Structures	14,692	1.41

1.04	.Solid rocket motor	527,524	50.50
1.04.1	..Case	63,577	6.09
1.04.2	..Insulation	13,365	1.28
1.04.3	..Liner	1,420	.14
1.04.4	..Solid fuel	65,434	6.26
1.04.5	..Nozzle	182,380	17.46
1.04.6	..Thrust vector control	180,828	17.31
1.04.7	..Ignition system	3,113	.30
1.04.8	..Preship-assembly & checkout	7,097	.68
1.04.9	..Additional motor-level items	10,310	.99
1.05	.Flight recovery equipment	0.	.00
1.06	.Shipping and logistics	1,344	.13
1.07	.Booster program support	60,431	5.79
1.08	.Additional booster-level items	49,272	4.72
1.09	.Overall systems support	44,316	4.24
1.10	.Additional G&A and fees	181,730	17.40
1.10.1	..General & Administrative	74,786	7.16
1.10.2	..Fees	106,944	10.24
5.	DDT&E	115,088	11.01
5.01	.Stage engineering	7,831	.75
5.02	.Propulsion	25,518	2.44
5.03	.Training	351	.03
5.04	.Test hardware	11,849	1.13
5.05	.Test operations	41,429	3.97
5.06	.Facilities	23,928	2.29
5.07	.Ground support equipment	800	.08
5.08	.System integration	2,681	.26
5.09	.Tooling	458	.04
5.10	.Additional G&A and fees	163	.02
5.10.1	..General & Administrative	92	.01
5.10.2	..Fees	71	.01

As evidenced by the estimates presented on the preceding pages, costs for booster DDT&E and production vary significantly between the integrated stage and conventional designs. Some explanation is needed to justify this difference.

Looking at the total stage structural weights, design 3A is the heaviest, and the other two conventional designs are the lightest. DDT&E and production costs for these three options, however, are comparable. This might seem surprising unless the model is well understood. The first important point to understand is that there is no simple linear relationship between total stage weight and total stage cost. Rather, the relationship is a complex interaction among the model cost estimating relationships (CERs) for all the elements of the work breakdown structure. The variables of complexity, component weights, and stage volume show up in all levels of the CERs. Therefore, the most important cost consideration, particularly in the production estimate, is the *distribution* of weight among all the stage elements. The second thing to grasp is that some of

the stage elements are used as variables in many more CERs than are other elements. Therefore, a small change in a component of the stage motor, for example, could show up in many levels of CERs, and therefore contribute to a significant difference in total system cost.

The significant difference between ISC and conventional stage costs, then, is explained only by a careful inspection of the complex interactions among complexity factors, individual component weights and total case volume as implemented in the CERs of the STACEM model. These interactions are explained in some detail in the users manual (18) and in the Joyce/Poppert thesis (59).

6.4.2.1 *Design, Development, Test, and Evaluation.* The complexity factor assigned to research, development, and testing is 0.6. For the first three sub- categories (stage engineering, propulsion, and training), and the test operations and facilities sub-categories, complexity factors did not change among designs.

Differences in individual booster component weights accounted for some of the differences in estimated costs under the test hardware and tooling sub-categories. Key components were the motor case, insulation, and propellant. Between these three components, the difference in design weights amounted to ≈ 50 pounds between the lightest integrated stage and heaviest conventional. Because the integrated stage design components tended to be lighter, this difference in weights partially explains the cost divergence.

Since the cost of ground support equipment, system integration, fees, and general and administration charges are based on percentages of the costs discussed above, these categories further contributed to the differences in estimates.

For the two categories of design, the largest cost categories in the DDT&E phase of the life-cycle are the test operations and facilities. In both cases, costs associated with test operations accounted 40-43 percent of the total DDT&E cost, while the facilities category account for approximately twenty-five percent of the cost.

6.4.2.2 *Production.* As stated earlier, the complexity factors, component weights, and total case volume of the different categories plays a key role in the divergence of costs. The integrated stage designs are consistently rated more complex in terms of cost risk; however, their

overall estimated costs are lower due to the distribution of weight and total volume of the ISC designs compared with the conventional designs.

The first two production cost sub-categories (electrical and instrumentation, separation system) are the same among all designs because all assumed current MM III values for the related variables. As such, the complexity factors and component weights are identical for the five boosters.

The next set of production cost categories addresses the solid rocket motor and individual components of the motor. Differences in individual component weights, and complexity factor ratings contributed to a variations in cost here also.

In the production phase, shipping and logistics costs are a function of total motor weight. Total booster weight, total impulse, and average thrust are factors in the cost of the booster program support and overall system support cost categories. The "additional booster level items" cost category is a function of the total booster weight, the number of motors produced, and the learning rate. Estimates for general and administration (G&A) charges are determined by taking a percentage of the sum of all production costs calculated to this point. Finally, fees (contractor profit) are calculated as a percentage of all these costs including the general and administrative costs. It should be noted that STACEM estimates figures for G&A and fees in this manner, based on historical patterns. In reality, fees are generally negotiated at some fixed amount since they cannot be cost dependent under DoD guidelines.

It is not surprising that the largest cost categories under the production phase are administrative costs and solid rocket motors. Administrative costs account for approximately seventeen percent of all costs for this phase. The solid rocket motor cost category accounts for between forty-five and fifty percent of the total costs. A review of the costs reveals some substantial differences between the ISC (first number) and the conventional designs (second number). Major cost sub-categories for the solid rocket motor are the case (approximately 18 versus 11 percent), the propellant (approximately 33 versus 12 percent), the nozzle (approximately 23 versus 35 percent), and the TVC/TVA (approximately 17 versus 34 percent). All percentages are of the *motor* production costs. The gimballed nozzle is a major cost penalty in the conventional designs, driving substantially higher production costs in both the nozzle and TVA. Over $200 million of the difference between production costs of the ISC designs versus the conventional designs can be attributed to these two areas.

As noted previously, total DDT&E and production costs for the designs range from approximately $733.002 million to $1,047.118 million. Average unit cost of each of the 674 solid rocket motors is roughly $1.1 million for the integrated stage and $1.5 million for the conventional . Because unit costs include a fixed overhead component, these costs are expected to increase if fewer than 674 motors are produced. In this case, fewer motors are available to absorb the fairly fixed DDT&E and production set-up costs.

6.4.2.3 Booster Integration Costs. Integration of the proposed booster with MM III components is assumed to occur at the Ogden Logistics Center. Costs associated with this one-time effort include missile breakdown, buildup and roundtrip transportation. The estimated cost of breakdown and buildup was $50,000 per missile. This recycling cost is based on the expert opinion of a MM III production manager (59). The roundtrip transportation figures used are the actual rates charged for MM III. These rates are station dependent and are listed below (59):

```
Minot AFB, ND - Hill AFB, UT:          $27,616
Grand Forks AFB, ND - Hill AFB, UT:    $27,616
F.E. Warren AFB, WY - Hill AFB, UT:    $ 8,253
Malstrom AFB, MT - Hill AFB, UT:       $24,172
```

To arrive at the booster integration costs, the number of missiles at each base are multiplied with the sum of the recycling and roundtrip transportation costs. These costs would be incurred during the program phase-in period (2000 - 2010), according to the missile wing conversion schedule (unknown at the time of the review). Calculations for the total estimated integration costs follow:

```
Minot AFB:       150 x ($50,000 + $27,616) = $11,642,400
Grand Forks AFB:150 x ($50,000 + $27,616) = $11,642,400
F.E. Warren AFB:150 x ($50,000 + $ 8,253) = $ 8,737,950
Malstrom AFB:     50 x ($50,000 + $24,172) = $ 3,708,600

    Total Estimated Integration Costs:    $35,731,350
```

6.4.3 Operations and Support Costs. The O&S cost model STRAMICE is used to generate the estimate. The results are summarized below. The same O&S estimate for a two-stage *NEMESIS* applies to all booster designs.

MM III Steady-State O\&S Estimate

	Cost Element	Annual O&S Dollars in Millions
1	Unit Mission Personnel	$213.545
2	Unit Level Consumption	$10.518
3	Depot Maintenance	$79.016
4	Sustaining Investment	$26.027
5	Other Direct Costs	$82.380
6	Installation Sup. Personnel	$26.578
7	Indirect Personnel Support	$58.724
8	Acquisition & Training	$8.155
	TOTAL:	$504.943

Two-Stage NEMESIS Steady-State O&S Estimate

	Cost Element	Annual O&S Dollars in Millions
1	Unit Mission Personnel	$213.545
2	Unit Level Consumption	$10.518
3	Depot Maintenance	$74.416
4	Sustaining Investment	$26.027
5	Other Direct Costs	$82.380
6	Installation Sup. Personnel	$26.578
7	Indirect Personnel Support	$58.724
8	Acquisition & Training	$8.155
	TOTAL:	$500.344

Based on the deployment schedule, O&S costs for each year of the program's assumed twenty year service life are computed. Design specific O&S costs for a particular year are calculated as a fraction of the steady-state rate above, in proportion to the cumulative number of two-stage missiles activated. The calculations and resulting O&S schedule are presented below. These figures do not include O&S costs related to the MM III ICBMs maintained during phase-in to keep a constant force of 500.

20 Year Operations and Support Costs
Two-Stage NEMESIS ICBM Fleet

Year	Boosters Activated	Cum. Force	Weighted-Average Operating and Support Cost
2000	20	20	20/500 x 500.344 = $ 20.014
2001	53	73	73/500 x 500.344 = $ 73.050
2002	53	126	26/500 x 500.344 = $ 26.087
2003	53	179	179/500 x 500.344 = $179.123
2004	53	232	232/500 x 500.344 = $232.160
2005	53	285	285/500 x 500.344 = $285.196
2006	53	338	338/500 x 500.344 = $338.233
2007	53	391	391/500 x 500.344 = $391.269
2008	53	444	444/500 x 500.344 = $444.305
2009	53	497	497/500 x 500.344 = $497.342
2010	3	500	500/500 x 500.344 = $500.344

```
2011                500        500/500 x 500.344 = $500.344
2012                500        500/500 x 500.344 = $500.344
2013                500        500/500 x 500.344 = $500.344
2014                500        500/500 x 500.344 = $500.344
2015                500        500/500 x 500.344 = $500.344
2016                500        500/500 x 500.344 = $500.344
2017                500        500/500 x 500.344 = $500.344
2018                500        500/500 x 500.344 = $500.344
2019                500        500/500 x 500.344 = $500.344
        Total Estimated
          Program O&S Costs ($millions):          $7,590.219
```

6.4.4 Comparison of Status Quo and Mixed Force O&S. For the designs under review, the status quo alternative is an unchanged MM III fleet of 500 missiles, maintained through the year 2019. To form a basis of comparison between O&S costs under the status quo and those for the two-stage designs, the proposed modifications are viewed as a continuation of the MM III program. In that respect, annual O&S costs during the twenty year life require a component for two-stage missiles and one for the remaining Minuteman IIIs, until conversion of all 500 missiles is complete. Up to that point, annual O&S costs address a mixed force of 500 missiles.

Operations and support costs under the mixed force concept are determined by summing the weighted-averages of the annual steady-state O&S estimates previously noted. For example, in the second year of operations (2001), a total of 73 two-stage missiles will be in service. To maintain a constant force of 500 missiles, 427 MM IIIs will remain deployed. The O&S costs associated with this mixed force are determined as follows:

```
Two-stage missiles:     (73/500) x $500.344 million
Minuteman IIIs:       + (427/500) x $504.943 million

Total O&S, FY 2001:            $504.272 million
```

The resulting twenty year operations and support cost schedule for the mixed Minuteman fleet is now presented. In the scenario presented, the constant outlays associated with steady-state operations begin with the year 2010 and continue through the end of fiscal year 2019.

```
            20 Year Operations and Support Costs
               Mixed Minuteman ICBM Fleet

      2-Stage   2-Stage   MM III                   Mixed
      Missiles  Missile   Missiles       MM III     Force
Year  Deployed  O&S Cost  Deployed  O&S Cost  O&S Cost
```

2000	20	$ 20.014	480	$484.745	$504.759
2001	73	$ 73.050	427	$431.221	$504.272
2002	126	$126.087	374	$377.697	$503.784
2003	179	$179.123	321	$324.173	$503.297
2004	232	$232.160	268	$270.649	$502.809
2005	285	$285.196	215	$217.125	$502.322
2006	338	$338.233	162	$163.602	$501.834
2007	391	$391.269	106	$110.078	$501.347
2008	444	$444.305	56	$ 56.554	$500.859
2009	497	$497.342	3	$ 3.030	$500.372
2010	500	$500.344	0	$ 0.000	$500.344
2011	500	$500.344	0	$ 0.000	$500.344
2012	500	$500.344	0	$ 0.000	$500.344
2013	500	$500.344	0	$ 0.000	$500.344
2014	500	$500.344	0	$ 0.000	$500.344
2015	500	$500.344	0	$ 0.000	$500.344
2016	500	$500.344	0	$ 0.000	$500.344
2017	500	$500.344	0	$ 0.000	$500.344
2018	500	$500.344	0	$ 0.000	$500.344
2019	500	$500.344	0	$ 0.000	$500.344

Total Estimated
Mixed Fleet O&S Costs ($millions): $10,029.093

Based on the Minuteman III steady-state estimate of annual O&S expenditures, the cost of the status quo alternative is $10,098.86 million (20 years x $504.943 million per year). This assumes no dramatic life extension measures are undertaken. The total estimated O&S savings of adopting one of the proposed two-stage booster designs is $69.767 million ($10,098.860 million - $10,029.093 million).

To determine where specific cost savings would be realized, cost elements 3.1 and 3.2 (missile and guidance depot maintenance) are analyzed with the related cost factors for the revised STRAM-ICE cost model. The review shows that 88.6 percent of the annual steady-state O&S savings is attributable to the AIMS guidance assumption noted on page 4-12. Reductions in depot missile repair workload for a two- stage system account for the remaining 11.4 percent of the savings. These percentages hold constant for the twenty year O&S comparison as well. Consequently, of the estimated $69.767 million in savings over the proposed missile's operational life, $61.824 million is related to the AIMS guidance and $7.943 million is due to the two- stage design.

6.4.5 *Costs Summary.* This section highlights the results of the cost estimating efforts. It presents program design, development, test and evaluation (DDT&E) and production estimates for the alternative booster designs, as determined by the STACEM cost model. The one-time costs of booster integration (refitting) are then identified. Using a revised STRAMICE model and simple

weight-average techniques, one O&S cost schedule for all 2-stage approaches is produced. Finally, a status quo MM III baseline estimate is contrasted with total O&S figures under a conversion program scenario where a constant force of 500 missiles is maintained over the program life. Years cited in this chapter are fiscal years and all cost figures presented are expressed in FY 1992 dollars.

6.5   Summary of Results - The System Performance Matrix

The results of the *NEMESIS* systems engineering study are summarized in Table 6.12. Note that only the DDT&E and Production costs (STACEM outputs) are presented in Table 6.12. The *booster integration* costs and the *O&S* costs are the same for all design alternatives and therefore add nothing to the comparative analysis of the five designs. The results are discussed, and some recommendations are made in the next chapter.

DESIGN OPTION	MISSION PERF. (PAYLOAD) (pounds)	COST (STACEM) $M	AVAILABILITY (RATIO)
1	1820	733.002	1.0042
2	1730	747.236	1.0042
3A	1690	1,040.800	1.0040
3B	1675	1,047.118	1.0040
4	1675	1,044.598	1.0040

Table 6.12. The System Performance Matrix

VII. Conclusions and Recommendations

7.1 Introduction

In Chapter 6, the results of this systems engineering design/integration study are presented in terms of the three key evaluation criteria: mission performance, life cycle cost, and system readiness. The presentation in this chapter examines the results in the context of the decision criteria discussed in Chapter 2:

- Mission Performance Criteria (MPC)

- Cost Analysis Criteria (CAC)

- Readiness Criteria (RC)

Each of the five *NEMESIS* designs is shown to be feasible in terms of both mission performance and system readiness. In terms of cost, the ISC approach is clearly the best. The five designs are now compared to see if a particular design stands out as "best" and the conclusions are presented in the next section.

The design study would be incomplete, however, without a thorough discussion of the conclusions in terms of the study limitations and recommendations for further research. These recommendations complete the preliminary design study and establish the groundwork for a potential prototype development phase in the systems engineering process.

7.2 Conclusions

Table 6.12 in Chapter 6 presents the performance of the five *NEMESIS* design options. The results are presented again in Table 7.1, except that the overall ranking (1 for "best", 5 for "worst") replaces the actual performance assessment criteria.

Option 1, the ISC Cylindrical design, rates as the best in all performance criteria. Option 2 (ISC Conical) rates just below Option 1 in mission performance and cost, and it outperforms all the conventional options. Clearly, then, the ISC approach rates "best" overall in terms of the results of this design study.

The performance differences, in terms of the payload-carrying capability, among the designs are not very great: one hundred and fifty pounds difference from the best to the worst designs. In

APPROACH	OPTION	MSN PERF RANK	COST RANK	READINESS RANK
ISC	1	1	1	1
ISC	2	2	2	1
CONV	3A	3	3	2
CONV	3B	4	5	2
CONV	4	4	4	2

Table 7.1. Ranking of Designs With Respect to Evaluation Criteria

light of the uncertainty associated with the models in the overall estimate of system weights, this difference cannot be considered to be significant, and therefore, no design should be ruled out on the basis of performance criteria alone.

In the area of cost, the conventional design costs are significantly higher than the costs associated with the ISC designs. This is somewhat surprising, considering that the weights of options 3B and 4 are lower, and complexity factors are lower for conventional technology in all cases. However, as highlighted in Chapter 6, the production costs associated with the gimballed nozzle technology and the associated distribution of system weight show up in many of the cost estimating relationships, and this difference translates into significantly higher costs.

The difference in terms of system availabilitiy does not distinguish very well between the ISC and conventional approaches. A much more sophisticated model is required to really highlight these differences. Based on the results of this study, both ISC and conventional 2-stage designs should be able to match or even exceed the excellent performance of the baseline.

To summarize the conclusions of the study:

1. All five designs presented in Chapter 6 are feasible. Each design can put a payload greater than 1500 pounds to the right point in space with sufficient total energy to meet the Minuteman III mission requirements. However, none of the designed systems can carry the current (multiple warhead, 2300 lb) payload with sufficient energy. Therefore, the two-stage approach (using either ISC or conventional technology) is a viable alternative to the current system only for single warhead and/or reduced range missions.

2. Each 2-stage design has the potential to meet or exceed the reliability and availability requirements of the baseline. Meeting the system reliability requirement is dependent upon

designing the motor chamber, thrust vector control and guidance subsystems with an in-flight reliability of at least 0.97 (Appendix D). The ability to meet availability requirements is facilitated by liner, guidance, and other system improvements that are already planned for the next MM III remanufacture. These improvements would also have to be included in a 2-stage replacement.

3. The ISC approach is superior to the conventional approach in terms of cost. Performance and readiness of the two approaches, given the direction, constraints and limitations of this study, is roughly the same.

4. Within the ISC approach, both a large diameter cylindrical stage and a conical stage should be studied further before one is selected over the other. The study results, in terms of both performance and cost, are too close to be considered significantly different.

5. If a conventional approach is selected, the large diameter cylindrical design gives better performance at lower cost.

Some discussion of the study constraints and limitations, along with some recommendations for further study, are presented in the next section.

7.3 System Level Recommendations

If the two-stage approach is chosen for future MM III upgrades, one more system design study is recommended. The new study would look at a *true* 2-stage replacement for the current system, removing two key constraints of this study: using the existing first stage and the current post-boost vehicle. No matter how good Stage 1 performance has been and is now, nothing lasts forever, and a remanufacture will eventually have to be considered. An alternative to remanufacture could be total replacement of MM III with a new 2-stage system that truly optimizes the vehicle to meet all aspects of the required mission.

The *NEMESIS* designs presented in this study all have weight margin. The driving constraint is the 27000 pound limit on the weight above Stage 1. *NEMESIS* stage 2 designs (with their associated maximum payload) all weigh close to 25,600 pounds. If the propellant weight used in the study (22,100 pounds) is allowed to increase, the models could be run and some additional

performance could conceivably be achieved. This would be a minimum-effort extension of the work already presented in this document.

The qualitative level of analysis done in this study for the Logistics Support factors of field and depot support equipment, shipping containers, training equipment, test equipment, and maintenance/support/training manpower levels and skills needs to be quantified before the prototype development phase begins. These factors can significantly impact overall life cycle cost, and so the assumptions and simplifications used in this study should be tested and quantified.

7.4 Structural/Thermal Design & Modeling Recommendations

Several STM areas have been identified that require further study if *NEMESIS* is considered for prototype development. First, charring of the insulation at the propellant/insulation boundary was not taken into account. Charring occurs when Kevlar undergoes decomposition at approximately $450^{\circ}C$ and forms a char layer. The char layer resists erosion much better than the virgin material, but has different thermal and structural properties. Second, the thermal properties of the EPM, case and insulation vary with temperature. Since, in the *NEMESIS* design, worst case values are used in the thermal model, accounting for varying thermal properties will decrease EPM and insulation thicknesses, and therefore decrease weight. Third, insulation erosion occurs when the propellant is expelled at high enough velocities to shear off the insulation (Mach ¿ 0.09). The internal flow characteristics must be analyzed to determine the extent of this effect. Fourth, the parameter driving insulation thickness is the case's ability to withstand heat and maintain its structural properties. The *NEMESIS* design does not allow the case temperature to exceed $135^{\circ}C$. Although the composite fibers can withstand a temperature well above $135^{\circ}C$, the requirement is derived from the glass transition temperature of the composite resin. Morton Thiokol performed a study on high temperature composites. Several commercially available fibers are used along with high temperature resin to filament wind pressure vessels. Test results showed that high temperature composites are structurally effective up to $315^{\circ}C$, a significant improvement over the *NEMESIS* design. (70) Based on results from the thermal and weight models, internal insulation weight would be reduced by approximately one-third for each design (a savings of up to 70 pounds). Fifth, as mentioned previously, the particle impact requirement drives EPM design. If this requirement becomes unnecessary and high temperature composite materials are used for the case wall, than

the EPM system can be deleted altogether. High temperature composites can withstand $315^\circ C$, which is more than sufficient for the $260^\circ C$ aeroheating requirement. The resulting weight savings (up to 185 pounds) translates directly to increased payload capability. Sixth, the benefits of filament winding need to be more accurately quantified. Due to the selection of fibers in the EPM, case and internal insulation in the *NEMESIS* design, all three systems can be manufactured using the filament winding process. The use of one manufacturing process results in significant cost savings because less manufacturing equipment, process paperwork and learning will be required. In addition, the filament winding process can be automated, which results in reduced manpower requirements. Finally, integrated stage technology drastically reduces the cost of manufacturing the case (i.e. two cases for the price of one).

With regards to the structural analysis of the design, several areas lend themselves to greater study. Netting analysis is a well established and proven *top level* view of pressure vessel integrity, however, finite element analysis (FEA) would provide a more accurate representation of stress/strain relationships. For example, localized buckling versus columar buckling would tend to present a more accurate loading scheme for the design. Also, examining the necessity of maintaining constant stress on the fibers while winding deserves greater analysis. In this light, examining residual stresses, particularly thermal, on the fibers and the vessel itself after curing requires study. Further, rather than analyzing based on typical fiber and resin properties, a need exists to identify and produce test data on specific materials for missile usage. Finally, subscale testing of specific filament wound designs of pressure vessels could provide substantial data to help compare various designs. Overall, most STM recommendations and potential benefits lie in a greater *in depth* analysis than time or resources allowed in this study.

7.5 Propulsion System Design & Modeling

7.5.1 Conventional Technology Review. The conventional designs investigated for this study use a gimballed, flexseal nozzle with an electro-hydraulic actuator. This represents the technology in the SICBM program. There are other design options available by incorporating new technologies. Using hot gas valves with a conventional nozzle, which is not submerged into the case, is an approach which could be exploited in a new design. The weight advantage and simplicity of the valve design would be available, although the propellant would have to be piped from the aft dome to the valves.

Also, the boron propellant would be required, or some other cleaner-burning propellant would have to be developed. Partial submergence of the nozzle into the case would decrease the piping required and save additional weight by decreasing the interstage which must cover the extended part of the nozzle. Blow-down thrust vector actuation systems, which act much like the hot gas valves but with their own source of gas, are another option within the conventional design. Although a fairly heavy system, the nozzle can be fixed, which is simpler and lighter than a movable nozzle. The SICBM uses this approach for their stage 2 booster, so it is well proven technology.

7.5.2 Weight Estimation. The weight estimating relationships developed within the study are largely an extrapolation of data from existing systems. All estimations are intended to be conservative, so the total may reflect a conservative estimation. Since weight is a strong driver in the models used to estimate the life cycle costs, more realistic estimations may mean a change in the LCC estimate for any single design. A more detailed analysis of the weights for the components that make up a stage should be completed as part of a follow-on study.

7.5.3 Grain Design. The optimization results of Chapter 5 show that the optimal performance grain design has several active constraints. Most consistent of these is the lower limits placed on slot thickness and tube inner radius. Post-optimality analysis indicates that relaxing these constraints provides additional payload-carrying capability. To explore possible performance improvements, additional research is needed to justify relaxing any of these constraints. In particular, the volume requirement for proper ignition is a driver in determining the grain design parameter lower limits. Better modeling of the igniter gas flow characteristics within the slotted tube as well as a better understanding of the requirements for proper propellant ignition are required. A smaller slot and/or tube may be possible, or perhaps a larger igniter is necessary to decrease the initial port volume. Several igniters placed at the top and bottom of the grain, instead of just at the top, may also enable a decrease in initial port volume and an increase in motor performance. Further attention may also be focused on the mechanical properties and loading conditions of the grain during the burn. While not currently considered the driving constraint, changing the lower limits of the grain design parameters may make structural concerns more critical. Overall, the slotted tube grain design provides satisfactory performance, but it may be possible to improve the "optimal" results.

The slotted tube grain design provided the required regressive thrust profile. However, there is certainly the possibility of better performing grain designs. The slotted tube design is relatively simple (geometrically). This is necessary to allow for reasonable calculation of volume and burn surface area as a function of burn distance. More "complex" grain designs may provide improved performance, but require much more detailed modeling of port volume and burn surface area functions. These more complicated designs may include more intricate geometric shapes, such as a double-anchor grain design or other patterns which produce a regressive thrust profile. Also, the modeling in this study assumed either constant or zero taper of the grain pattern along the length of the motor. Many operational rocket motors have grain designs which employ highly tapered ports near the ends of the grain. These inconsistencies in the length-wise port shape are used to help control the burn surface area time history. These and other "tricks of the trade," such as using inhibitor to control the thrust profile, make the modeling of the burning characteristics unreasonably complicated for the scope of this preliminary design study. The slotted tube grain design demonstrates the feasibility of the single stage replacement of the 2nd and 3rd stages of MM III, but no claim is made that it is the "best" design possible.

7.6 Trajectory/Performance Simulation Recommendations

The trajectory/performance simulation used in this study incorporates several simplifying assumptions commensurate with the level of detail required for a *preliminary* design analysis. These assumptions include a non-rotating, spherical earth, restriction of the trajectory to a pure gravity turn, and examining only the powered flight phase of the *NEMESIS* mission profile. In order to proceed to the *detailed* design process, a more accurate, higher fidelity analysis tool is required. Some recommendations for changes to upgrade the current simulation for the detailed design phase follow. The most significant improvement to the current simulation can be acheived by modeling the *entire* mission profile, not just the powered flight phase. However, incorporating this change within the context of the current simulation would result in an extremely heavy computational burden on the computer presently in use. A new approach is to use a trajectory optimizer routine such as the POST simulation used by the Phillips Lab (see Appendix A). Using POST provides the advantages of accounting for rotating, oblate earth effects, non-zero angles of attack and their associated drag penalties, and includes provisions for analyzing the entire trajectory from launch until warhead impact. With POST, the actual *range* of the missile, not an indirect predictor of the

range such as the specific energy, is calculated. Furthermore, POST is already developed, validated, and verified to produce accurate reults, thus eliminating those steps in the modeling process. Finally, direct, parameter-by-parameter comparisons between the MM III POST simulation and a *NEMESIS* POST simulation can be made. Further trajectory analysis within the framework of a POST simulation for the *NEMESIS* includes the variation of the initial time of transition to non-vertical flight. This was not investigated using the current simulation in the interest of simplifying the analysis. Instead, the MM III transition time of 3.15 seconds was used for all proposed designs.

Another possible area for investigation is the time and sequence of events associated with the staging process. Again, the MM III staging sequence was assumed for the *NEMESIS* designs for simplicity, but possible performance gains may be realized with a different coasting time or stage separation event sequence. In summary, adoption of the POST simulation or a similar event-oriented trajectory optimization program and investigation of the areas addressed above are recommended if *NEMESIS* is to proceed to the detailed design phase.

7.7 *Cost Model Recommendations*

A major limitation of the majority of cost models is their reliance on previous program data. This does not always incorporate the major technology advances that often show up as lighter hardware, but higher material costs. The link between weight and costs is complicated as more lightweight composite structures are developed which are very expensive to manufacture. Existing cost models are based on "bending metal", and don't recognize that lighter items can be even more expensive to produce due to the processes involved. STACEM was developed based on data available on historical booster programs that generally used metal cases or early development composites and gimballed nozzles. The development and production costs of the hot gas valves and the forced-deflection nozzle may not be adequately estimated by STACEM. Neither approach has been used historically and therefore no data to support the cost estimate from STACEM is available. The validity of the cost estimating relationships in the model in these areas needs furthur investigation to assure the estimates are reasonable.

The STRAMICE model was the best tool found to support the O&S cost of the LCC analysis. Unfortunately, the model did not have the fidelity to show a manpower savings of a 2 stage booster over 3 stages. The 2 stage designs investigated in this study showed higher availability that should

result in less work for the depots and an opportunity to reduce manpower for maintenance. Higher availability should allow for less spare requirements and lower overall parts storage. Since O&S costs are a considerable portion of life-cycle costs, a much more detailed analysis of the O&S costs must be part of any follow-on study.

7.8 Reliability/Availability Recommendations

All documents reviewed for this study identify the missile guidance system as the reliability and alert availability driver in the MM III system. Significant upgrades have been proposed for the near term (Advanced Inertial Measurement System - AIMS) and for the long term (Guidance Upgrade Program) (94). Any future system upgrade, whether two stages or three, must include a guidance upgrade if significant improvement in reliability and availability is expected.

In this study, in-flight reliability of the 2-stage systems is analyzed, and allocations of motor and thrust vector control reliability are made such that the system meets the baseline requirement. No other approach made sense at this time, because usable data on the burn performance of boron propellants and hot gas valve technology is insufficient or not available. Boron propellants have not been tested in sufficient batch size to reasonably extrapolate results to a prediction of ICBM motor reliability. Hot gas valves have been tested (40) for burn times of 40 seconds. Again, extrapolating to burn times of 60-80 seconds cannot be made without significant risk. Therefore, recommend further testing of boron propellants and hot gas valve technology before proceeding with an ISC ICBM development.

Development of a 35-year liner should proceed even if the *NEMESIS* 2-stage option is rejected and MM III stages are remanufactured. Propellant/liner/insulation debonding drives current estimates of motor service life, and an increase in liner performance translates directly to better overall system alert availability.

7.9 Summary

This study has demonstrated the feasibility of a two-stage replacement for the MM III. Analysis included the factors of performance, life-cycle cost, and readiness. The systems engineering process described in Chapter 2 provided the methodology for conducting this study. The logical

steps in the process and the recommendations made in this chapter provide the framework for planning the next phase, prototype development.

Appendix A. *Performance Measurement and Trajectory Model*

A.1 *Introduction and Purpose*

The overall design of the *NEMESIS* system will be judged from a systems perspective. That is, the overall "worth" of the system must be such that some baseline performance is achieved in the evaluated areas of

- cost

- readiness, supportability, producability

- technical feasibility and mission performance.

Evaluation of the cost, readiness, supportability and producability of the system are discussed in the main body of this document and in other appendices. The purpose of this appendix is to discuss the details of the method used in this design project to evaluate the technical (mission) performance of the designed system.

The basic measure of system "performance" for the *NEMESIS* booster is that it must deliver a given payload to a "basket" in the sky such that the payload has sufficient energy to continue (with some minor post-boost corrections) on a ballistic trajectory to a given target impact point. It is not the intent of this project to fully evaluate and design a complicated guidance program for the booster and the post-boost vehicle to meet a particular accuracy requirement for payload delivery. Rather, the concern is with designing a second stage booster to integrate with the existing Minuteman III first stage such that the energy imparted to the post-boost vehicle is identical to the total energy delivered by the current 3-stage Minuteman III system for a given targeting scenario.

In order to evaluate the system energy at the end of the last (second) boost phase and to judge the performance of any given second stage booster design, four things are needed:

1. A good understand' of the overall system dynamics

2. A baseline set of criteria to use as a standard against which to evaluate system design options

3. A way to predict the overall performance of the various booster design options with respect to the various baseline criteria

4. A final yardstick or measure of "system performance" that can be used to make clear and unambiguous decisions about the "goodness" of a particular design.

This appendix discusses all of these areas in detail. First, the basic ballistic missile trajectory equations of motion are derived and explained. Next, the baseline is established using results from Phillips Laboratories *POST* simulation of Minuteman III performance. All assumptions and starting conditions are covered to set the framework for verification and validation of an AFIT trajectory model, which is the tool used to predict overall system performance for a given second stage booster design. Finally, the concept of the system's *specific energy* at the end of stage two burn is presented as the measure of system performance that will be used for decision making.

A.2 Basic System Dynamics

The trajectory of an Intercontinental Ballistic Missile (ICBM) has three parts:

- powered flight

- "free" flight of the post-boost vehicle and payload

- re-entry of the payload into earth atmosphere.

The focus of this design project is on the "powered" portion of the flight, and so only that segment will be discussed here.

A rocket powered missile gains velocity by burning propellant. A ground based missile like an ICBM needs to carry enough propellant to overcome inertia, gravity and also to overcome the drag forces in the densest part of the atmosphere near the earth's surface. Because the powered flight trajectory of a long-range ICBM must involve this atmospheric portion of flight, aerodynamic forces (lift, drag) and physical forces (thrust and gravity) produce bending moments which impact vehicle design. Since the ultimate range of an ICBM is a function of the amount of fuel it carries and its total weight, a premium is placed on reducing the structural mass of the vehicle to minimize total missile weight and to maximize the amount of propellant it can carry.

A way to minimize structural mass is to sacrifice structural strength and rigidity in the transverse (radial) axis of the missile, since transverse loads can be made minimal through choice of the proper trajectory. By contrast, axial loading is significant throughout a flight, no matter what

A-2

trajectory is chosen. Thus, most of the structural weight is distributed to provide axial strength. This tradeoff between propulsion mass, structural mass and overall missile strength is a driver in missile design and has an important result. Most large missiles are not capable of flying through the atmosphere at an angle of attack except at relatively low velocities, and so nozzle steering is not an option except for very minor corrections. Turning at high velocities in the atmosphere must instead be handled by the dynamics of what is referred to in the literature (87, 27, 103, 107) as a *gravity turn*.

The aerodynamic loads generated by trying to fly a large missile through the atmosphere at an angle of attack at several times the speed of sound could result in a catastrophic missile booster structural failure. Culler and Freied (27) first discussed a "sensible and simple" trajectory that can be used during atmospheric flight. They called it a "gravity turn" and also referred to it as a "zero angle of attack" or "no lift" trajectory. The basic principle is to keep the boosters's thrust vector always aligned with the vehicle's velocity vector starting from some non-zero, non-vertical initial velocity. Figure A.1 shows the forces acting on a simplified, single stage rocket in flight over the earth. Thrust and drag act along the vehicle's axis, while gravity acts as shown. As can be seen from the figure, the aerodynamic moments are minimized and the force of gravity provides the turning force for the required trajectory path.

In order to understand and apply the gravity turn concept to a "performance" evaluation of an ICBM, a basic analysis of the kinematics (position, velocity and acceleration) and kinetics (relationships between forces and motion) associated with the scenario of Figure A.1 is present. The development given here follows lecture notes (44), but similar derivations can be found in Wiesel (103), Zarchan (107) and Hill and Peterson (50). The goal of this analysis is to come up with some basic relationships among the key variables that describe missile performance. These variables would include the following:

- Thrust - the force reaction to the velocity of burning propellant mass exiting the booster motor nozzle (a function of the booster motor grain design).

- Drag - an aerodynamic force associated with assymetry of pressure distributed on the surface of the vehicle travelling through the atmosphere. For an ICBM, this acts in a direction opposing the velocity vector (a retarding force). The drag on a vehicle is a function of air density (altitude), vehicle speed, vehicle cross-sectional area and vehicle shape.
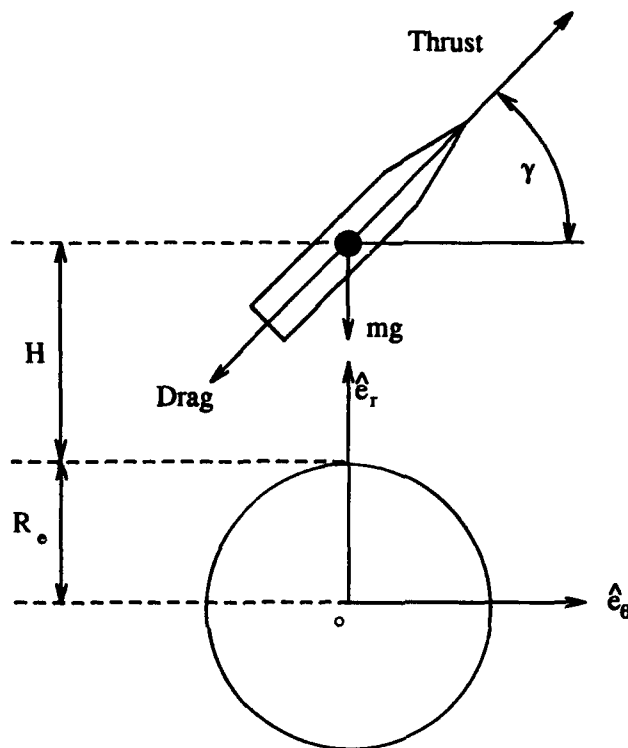
Figure A.1. Basic Forces Acting on a Single Stage ICBM

- Velocity

- Weight - a function of mass and gravity, both of which change as a function of time as the
  missile burns propellant mass and as it reaches higher altitudes (with corresponding reduction
  in gravitational force).

- Earth radius - 20,925,672.57 feet

- Altitude

- Vehicle flight path angle - the angle between the missile velocity vector and the local horizon,
  measured in the counter-clockwise sense.

A basic ballistic path (beginning and end points at the same elevation) is completely deter-
mined if the initial velocity and launch angle are known. In the case of an extremely long-range
system like an ICBM, two additional requirements for payload "launch" to a particular impact
point are to have an initial altitude and down-range position . Therefore, the initial task is to

derive the equations of motion for a gravity turn trajectory such that the resulting equations can be solved for booster/payload position (downrange and altitude), velocity and flight path angle as functions of time.

Referring again to Figure A.1, the kinematic descriptions of the vehicle's motion (position, velocity, and acceleration) will be derived first. These equations are for a single stage vehicle near a spherical earth assuming that the thrust vector and velocity vector are aligned (gravity turn or zero angle of attack). The equations would apply equally well in the case of a multistage vehicle, except that the initial conditions at the start of each stage would change to reflect the path traveled in the previous stage.

First, the position vector in the (spherical) earth frame can be written (in cylindrical coordinates) as

$$\vec{r} = (R + H)\epsilon_r$$

where R is the earth's radius and H is the altitude above the earth's surface of the vehicle's center of mass. Since the vehicle is not traveling "straight up" ($\gamma = 90^0$), the angular velocity component in the ϵ_θ direction due to the curvature of the earth with respect to a fixed (inertial) frame must be described. The magnitude of this angular velocity is a function of the vehicle's speed with respect to the earth and it's position, and is given by

$$\omega = \frac{V}{r}$$

Since only the component of $\vec{V}$ in the direction of ϵ_θ is a factor, this magintude can be re-written as

$$\omega = \frac{V \cos\gamma}{R + H}$$

and if ϵ_z is defined as

$$\epsilon_z = \epsilon_r \times \epsilon_\theta$$

this results in a final expression for the angular velocity vector describing rotation with respect to an intertial frame:

$$\vec{\omega} = \frac{V \cos\gamma}{R + H}\epsilon_z.$$

Differentiating the position vector, $\vec{r}$, to get the velocity:

$$\dot{\mathbf{r}} = \dot{\mathbf{r}}_{rel} + \vec{\omega} \times \vec{r}$$

$$= (\dot{R} + \dot{H})\vec{e}_r + \frac{V\cos\gamma}{R+H}\vec{e}_z \times (R+H)\vec{e}_r$$

$$= \dot{H}\vec{e}_r + V\cos\gamma\vec{e}_\theta$$

But $\dot{H} = V\sin\gamma$, so

$$\dot{\mathbf{r}} = V\sin\gamma\vec{e}_r + V\cos\gamma\vec{e}_\theta$$

This differential equation can be expressed in terms of the components as

$$\dot{\mathbf{r}} = \dot{H}\vec{e}_r + \dot{X}\vec{e}_\theta$$

and therefore,

$$\dot{H} = V\sin\gamma \qquad\qquad (A.1)$$

and

$$\dot{X} = V\cos\gamma \qquad\qquad (A.2)$$

These are the first two equations needed to describe the gravity turn trajectory. They describe the vehicle's down range position and altitude as a function of time, vehicle velocity and flight path angle. Most importantly, these equations can be used to get downrange position and altitude at the time of stage (1,2 or 3) burnout, which is critical information needed to help assess whether the vehicle hits the required "basket in the sky".

The vehicle acceleration can be found by differentiating the velocity vector. Applying the Coriolis theorem and the chain rule from differential calculus:

$$\ddot{\mathbf{r}} = \ddot{\mathbf{r}}_{rel} + \omega \times \dot{\mathbf{r}}$$

$$= (\dot{V}\sin\gamma + V\dot{\gamma}\cos\gamma)\vec{e}_r +$$

$$(\dot{V}\cos\gamma - V\dot{\gamma}\sin\gamma)\vec{e}_\theta +$$

$$\frac{V^2 sin\gamma cos\gamma}{R+H}\epsilon_\theta -$$
$$\frac{V^2 cos^2\gamma}{R+H}\epsilon_r$$

Now the kinematic description is complete and it is time to include the external forces acting on the vehicle. The basic equation is Newton's law

$$\sum \vec{F} = m\vec{a}$$

In the ϵ_r direction, the forces are

$$T sin\gamma$$

$$-D sin\gamma$$

$$-mg$$

Summing the forces gives $(T - D)sin\gamma - mg$. Equating these forces to mass times acceleration $(m\vec{a})$ in the ϵ_r direction gives the following equation:

$$(T - D)sin\gamma - mg = m(\dot{V}sin\gamma + V\dot{\gamma}cos\gamma - \frac{V^2 cos^2\gamma}{R+H})$$

Similarly, for the ϵ_θ direction:

$$(T - D)cos\gamma = m(\dot{V}cos\gamma - V\dot{\gamma}sin\gamma + \frac{V^2 sin\gamma cos\gamma}{R+H})$$

These two equations contain two variables that need to be isolated: $\dot{V}$ and $\dot{\gamma}$. If expressions can be found that express $\dot{V}$ and $\dot{\gamma}$ in terms of the other variables, the final burnout parameters, velocity and flight path angle, will be available. The four main equations for trajectory analysis will then be in place.

To obtain an expression for $\dot{V}$, multiply the kinetic equation for ϵ_r by $sin\gamma$ and add the result to the kinetic equation for ϵ_θ multiplied by $cos\gamma$ as follows:

$$(T - D)sin^2\gamma - mgsin\gamma = m\dot{V}sin^2\gamma + mV\dot{\gamma}cos\gamma sin\gamma - \frac{mV^2cos^2\gamma sin\gamma}{R + H} +$$

$$(T - D)cos^2\gamma = m\dot{V}cos^2\gamma - mV\dot{\gamma}cos\gamma sin\gamma + \frac{mV^2cos^2\gamma sin\gamma}{R + H}$$

or

$$T - D - mgsin\gamma = m\dot{V}$$

and rearranging gives

$$\dot{V} = \frac{T - D - mgsin\gamma}{m} \tag{A.3}$$

With similar mathematical manipulation, an expression for $\dot{\gamma}$ is obtained by multiplying the ϵ_r kinetic equation by $cos\gamma$ and the ϵ_θ expression by $sin\gamma$ and then subtracting the two resulting expressions. The result is

$$mV\dot{\gamma} = m(-g + \frac{V^2}{R + H})cos\gamma$$

or

$$\dot{\gamma} = (-g + \frac{V^2}{R + H})\frac{cos\gamma}{V} \tag{A.4}$$

Equations A.1 - A.4 give the basic equations of motion that are needed to model the gravity turn trajectory. Solving these equations can be done using numerical integration techniques, and the solutions at the end of each stage can be used as initial conditions for the next stage. The stage solutions can then be combined to give a payload position, altitude, velocity and flight path angle at the end of the final booster stage burn (2 or 3). This will be discussed in more detail in the next section. First, however, the development of the equations of motion must be completed by more explicitly defining all of the variables in equations A.1 - A.4.

Equations A.3 and A.4 contain the variables T (thrust), D (drag), m (mass), and g (gravity). Thrust is a function of the solid motor grain design, and is discussed in full detail in the Appendix on

Propulsion. The thrust input for the trajectory model must capture the particular thrust "profile" as a function of time. The implementation of the thrust profile input is discussed later in this appendix.

The drag force on the missile is a function of the dynamic pressure, q, the vehicle reference area (maximum cross sectional area of the missile perpendicular to the velocity vector), S_{ref}, and the zero-lift drag coefficient, C_D0. The dynamic pressure is a function of air density, ρ, and vehicle velocity, and is defined by

$$q = \frac{\rho V^2}{2}$$

Air density is a function of altitude. Atmospheric tables are readily available, and a table look-up is easily implemented in a computer. The drag coefficient depends on the vehicle shape, Mach number, and inclination with respect to the velocity vector (angle of attack, which is zero for the ICBM gravity turn). Typical variations of C_{D0} with Mach number are available in the literature (50:p325), and the POST (79) simulation also includes a table of values that can be used for the NEMESIS application.

Mass is a function of time that depends on the burn rate of the solid booster propellant. The mass flow rate, $\dot{m}$, is an input to the trajectory simulation from the propulsion model.

Gravity is a function of altitude and the relationship is defined by

$$g = g_e \left(\frac{R_e}{R_e + H} \right)^2$$

where g_e is the force of gravity at the earth's surface (a constant 32.174 ft/sec^2), R_e is the earth radius (20,925,672.57 ft.), and H is the altitude at a particular time of interest during the flight.

With the four main equations of motion (A.1- A.4) and the supplementary expressions for thrust, drag, mass and gravity defined, attention is now given to the implementation of these equations in a mathematical model to simulate and evaluate the overall performance of a particular booster configuration.

A.3 Discussion of the Equations of Motion

An ICBM such as MM III or the proposed *NEMESIS* system is launched from a fixed vertical position. A close inspection of Equation A.4 will show that $\dot{\gamma}_i = 0$ for $\gamma = 90^0$ ($cos 90^0 = 0$) and the vehicle will continue to rise in a verticle flight path until it is (accidentally or deliberately) deflected into a different attitude. If this were to be done on or very near the launch silo, the insufficient vertical velocity would be overwhelmed by the gravity-mass force of the vehicle's weight, and the missile would crash into the ground (103:p209). However, at higher velocities, an initial deflection can be input (through a pitch program in the missile guidance software) to give the rocket a slight flight path angle off vertical. This initial deflection would have to be small to limit the transverse forces that would otherwise damage the missile's structure. After a new flight path angle is achieved, the thrust is gimballed so that the thrust vector remains in line with the velocity vector to eliminate moments on the vehicle. As the vehicle accelerates, gravity force imparts a constant $\dot{\gamma}$ until the missile has rotated to a desired final flight path angle (γ_f). The rotation is a result of forces acting through the center of mass, with no resulting torque on the rocket (see Figure A.2). The analysis of the gravity turn trajectory leads to the determination of the proper initial flight path angle input to ensure the post boost vehicle has the desired final flight path angle.

Basically, this is a boundary value problem. The required Minuteman III performance baseline establishes a known or desired final velocity, flight path angle, and altitude for a given payload weight. The first analysis needed is to determine the velocity and altitude at which to initiate a pitch angle to induce the gravity turn. At that point, the missile will be at some height above the launch silo, and will have some relatively low initial velocity. According to Wiesel (103:p104), it is best to do the initial pitchover at "low" speed since an angle of attack is induced and the vehicle structure will have to withstand the resulting moments. A review of current systems (such as MM III) can help to identify a range for V_0, H_0, and γ_0. An iterative search at various combinations of initial conditions in the identified range will then provide the correct initial γ that will be used to model the desired flight path and end point conditions. By allowing $\gamma_{initial}$ to be a variable, the effects of changing γ_i can be evaluated for various design configurations and payload weights.

After an initial pitch angle is given to the system, the equations of motion developed in the previous section will be numerically integrated in stages (corresponding to either the 3-stage baseline or the 2-stage design alternatives). At burnout of the final booster stage, the final boost

A-10
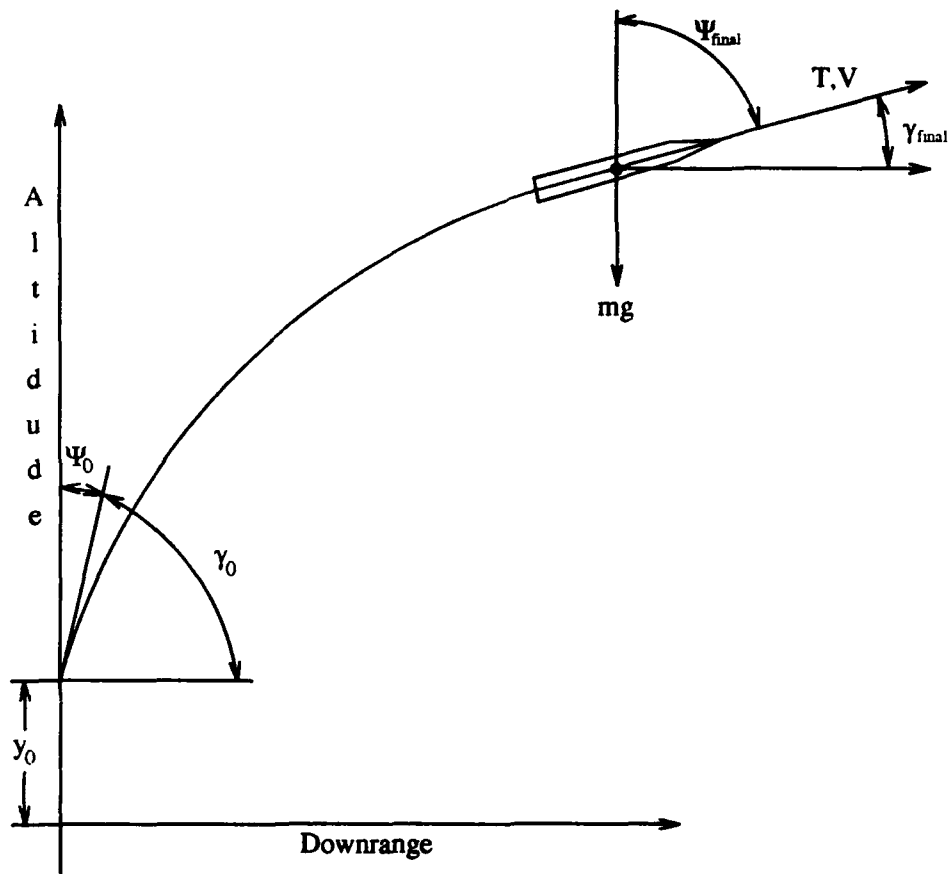
Figure A.2. Gravity Turn Trajectory

conditions (velocity, position, flight path angle) will be evaluated in terms of the total specific energy (energy per unit mass) of the post-boost vehicle. The next section details the implementation of the trajectory model using the software package $Matrix_x$.

A.4 The Trajectory/Performance Simulation

The Trajectory/Performance Simulation (TPS) was developed as a tool for defining the MM III performance requirements and for evaluating the flight vehicle performance of the various 2-stage designs. Numerous simplifying assumptions are incorporated into the TPS to provide for accurate results while maintaining an appropriate level of complexity relative to the other models used in this design study. The TPS is composed of 4 main sections: an atmosphere and gravity model, a drag model, a thrust model, and a fourth-order Runge-Kutta differential equation integration algorithm for solution of the gravity turn equations of motion. This section explains the verification and validation of the TPS, details the equations used with their underlying assumptions, outlines the implementation of the various models, and finally describes the general design philosophy used in evaluating missile performance.

A.4.1 Model Verification and Validation (V & V).

One of the most important tasks in any simulation effort is that of verifying that the model is working as intended (verification) and is accurately reflecting the physical system that is modeled (validation). This can be accomplished by comparing simulation results with actual flight test data, or by comparing it with results from another simulation that is known to produce valid results. Because actual flight test data for the MM III is unavailable, the TPS results are compared against the Phillips Lab simulation to accomplish V & V. The Phillips Lab provided maximum range, polar trajectory, MM III simulation results for payloads of 2300, 1900, 1700, and 1500 pounds.

A.4.1.1 The Phillips Lab Simulation .

The Phillips Lab simulation data was generated using the Program to Optimize Simulated Trajectories (POST). POST is a generalized point mass, discrete parameter targeting and optimization program written in FORTRAN (79:p6). POST is basically a boundary value problem solver in that given the initial and desired end conditions, it finds the optimum trajectory that passes through these endpoints, subject to any constraints placed upon the system. For the MM III POST simulation, the only constraints are that dynamic pressure

is limited to 3000 pounds per square foot, and that the the payload reentry flight path angle equal -17.5 degrees at an altitude of 300,000 feet. These constraints are chosen to force the simulation to generate the maximum range trajectory. The reentry flight path angle (-17.5 degrees) represents the shallowest angle which the warhead can re-enter the earth's atmosphere without sustaining structural damage, thus providing the maximum range trajectory, whereas the dynamic pressure constraint is based upon staging stability considerations. Further, the simulation is not restricted to pure gravity turn trajectories as is the case with the TPS. Pitch commands are simulated to initiate the gravity turn from vertical flight 3.15 seconds into the simulation. These commands generate a non-zero angle of attack for a brief period of time, which in turn, create a lift force and its associated drag penalty on the missile. This drag due to lift is not simulated by the TPS since the angle of attack is always assumed to be zero as is the case in a pure gravity turn. An additional feature of the POST simulation is that a constant thrust for each stage is assumed. This is a valid assumption for stages two and three, which operate outside of the earth's atmosphere, but for stage one, the thrust varies due to the decrease in the ambient air pressure with increasing altitude. For the MM III first stage, the thrust varies nearly linearly from approximately 190,000 pounds at launch to approximately 210,000 pounds at burnout. A constant thrust of 198,000 pounds is used for stage one in the POST simulation.

Finally, since the POST simulation provides data for the entire missile flight including the ballistic, or unpowered phase, the earth rotation effects must be included when position and velocity calculations are made. As a result, the inertial velocity term includes a component due to earth rotation that is a function of the latitude of the launch site. In this case, in order to minimize this effect, all POST trajectories are initiated at a heading of zero degrees (due north) from Grand Forks AFB, ND, which has a latitude of 48 degrees North. This heading guarantees that the earth rotation component is perpendicular to the plane of the missile's trajectory (at least initially) and makes no significant contribution to the missile's inertial velocity during the powered flight phase which lasts approximately 189 seconds. For the TPS, this effect is not simulated since only the powered portion of the flight is considered.

The basic approach for TPS V & V is to compare the missile state variables (altitude, velocity, flight path angle, and downrange position) at burnout of the first stage portion of the MM III trajectory generated by the TPS with the state at first stage burnout from the POST simulation.

A-13

Examining only first stage flight minimizes any differences due to excluding earth rotation effects and the absence of drag losses due to lift, yet it fully exercises the equations of motion and the numerical integration algorithm and interpolation routines sufficiently to ensure their proper coding and operation. The results of this comparison are presented in Table A.1

State	From POST	From TPS	% Difference
V(f/s)	5817.24	5868.30	-0.88
γ(deg)	33.083	33.595	-1.55
H(ft)	91,517.1	90,732.5	.86
X(Nm)	17.292	16.496	2.0
W(lbm)	30,161.5	30,473.29	1.0

Table A.1. MM III State Variables at Stage 1 Burnout

As can be seen, the missile states (from both simulations) compare closely. The small differences between the two simulations can be attributed to the basic differences described above. These results provide confidence that the TPS is indeed working properly and is producing valid simulation results.

A.4.2 Model Implementation (Program GTURN). This section describes the models used to build the TPS, its inputs and outputs, and the assumptions made in developing the TPS. Computer listings of the actual programs are also included.

A.4.2.1 The Atmosphere (ATMODEL) and Gravity Models. The atmospheric model used for the TPS is the ARDC Model Atmosphere developed in 1959 (10). The parameters used in the TPS atmosphere model are the speed of sound, atmospheric pressure, and atmospheric density, all functions of altitude. English units are used throughout the model.

The atmosphere model is defined for altitudes up to 400.000 feet even though the density and pressure are negligible above 150,000 feet and the speed of sound is essentially meaningless outside the earth's atmosphere. The atmosphere model is used solely for the purpose of calculating drag (a function of Mach number and density) and MM III stage 1 thrust (a function of ambient pressure). No wind or air turbulence is included in the model. The earth's gravitational attraction is modeled as described in a previous section. No oblate earth effects are included in the gravity model.

A.4.2.2 The Drag Model. The drag model is based upon a simplified version of the drag model used by the Phillips Lab simulation. Since a gravity turn trajectory is being simulated, zero angle of attack is maintained, thus modeling drag due to lift is unnecessary. The equation used for drag is:

$$D = qS_{ref}C_{D_o}$$

The drag coefficient is obtained directly from the POST simulation and includes form and skin friction drag components (22). This data was obtained (by Phillips Lab) from a combination of sources including an aerodynamic coefficient estimating computer routine called *The Aerodynamic Preliminary Analysis System (APAS)* (79:p6). The drag coefficient is determined as a function of Mach number alone.

A.4.2.3 The Thrust Model. Missile thrust calculation is handled in two different ways. First, for the MM III and Stage 1 of the 2-stage design, the thrust is calculated using the following equation:

$$T = gI_{sp}\dot{m} + (P_e - P_a)A_e$$

where I_{sp} is the stage specific impulse in seconds, $\dot{m}$ is the propellant mass flow rate in slugs/sec. P_e is the stage exit pressure in psi. P_a is the ambient atmospheric pressure in psi. and A_e is the nozzle exit area in square inches. Inherent to the use of this equation are the assumptions of constant mass flow rate, exit pressure, and specific impulse. Of these assumptions, only the first, that of constant mass flow rate, requires further discussion.

The mass flow rates are calculated by dividing the total stage propellant mass by the total stage burn time. This method of calculation implies that all of the propellant is burned and provides useful thrust. For real solid rocket boosters employed on ICBM systems, there is invariably some propellant that is not completely burned even though the stage is considered to have reached a "burnout" state. This is due to the drop in combustion chamber pressure to a point below which the combustion cannot continue. At this point, the thrust level drops off dramatically and the stage is considered to be "burned out." Assuming that the mass flow rate is constant and that all the propellant is burned causes a slight overestimation of the thrust and thus the performance of the rocket motor. However, since both the MM III and the 2-stage design first stage use this assumption, a valid comparison can still be made. Also, given that all three stages of the MM III

simulation use this assumption and that the performance measure for the 2-stage design is based upon a slightly overestimated performance, these assumptions are conservative and appropriate.

For the 2nd stage of the 2-stage design, a more accurate method for modeling thrust and mass flow rate is used. Actual time histories of the thrust and mass flow rates are generated for a particular grain design and are input directly into the simulation as thrust and mass flow rate tables. These tables are similar to the atmosphere and drag coefficient tables in that linear interpolation is used within them to generate thrust and mass flow rate levels at each integration time step. This method also eliminates the requirement to model specific impulse and exit pressure since the thrust equation for stage 1 is not used for stage 2.

A.4.2.4 Fourth Order Runge-Kutta Algorithm (Program GTURN). A fourth order *Runge-Kutta* numerical integration algorithm (57) is implemented to integrate the equations for the time derivatives of velocity, flight path angle, altitude, downrange position, and missile mass. Initial conditions obtained from the program VERT (discussed below) for each of the state variables (except for flight path angle) and time are input. The initial value for the flight path angle is guessed (initially) and iterated during subsequent runs until the target final flight path angle is obtained. The data for the drag, atmosphere, and thrust model (where appropriate) tables are then read into memory along with the values for all simulation constants. At this point, the actual integration loop is implemented.

At the beginning of each iteration of the integration, the values for the atmospheric variables (pressure, density, and speed of sound) are obtained through linear interpolation of the atmosphere model tables at the current value of altitude. The value for Mach number is then computed and a similar interpolation is performed to obtain the coefficient of drag (a function of Mach number). The local gravitational constant is then calculated. At this point, a determination as to what stage of the missile is currently burning is made. Once this is determined, the appropriate values for I_{sp}, nozzle exit area, etc. for that stage are used in the thrust equation (for the MM III simulation), or the appropriate thrust and mass flow rate tables are interpolated (for 2nd stage of the 2-stage design). The actual Runge-Kutta recursion equations are then exercised, new values for the state variables are obtained, the time is incremented, and the loop repeats. This process continues until the burnout time for the final stage is reached. At each time step, values for the state variables and several other variables are stored for plotting at the end of the simulation. The mass of the

expended stage(s) is dropped at the instant the stage burns out with a 1 second "coast" period

before ignition of the next stage. This same staging sequence is also used for the POST simulation.

A flowchart outlining this sequence of events is presented in Figure A.3.

A complete listing of the MATRIXx program GTURN follows.

```
// Program GTURN
// Runge-Kutta Equations for Trajectory Simulation
// This program integrates the gravity turn equations given the initial
// conditions from VERT.
//
        clear *
//
        dt=.2;                          // set time step in seconds
//
        mvert=73.0385;                  // propellant burned in VERT (slugs)
//
//  Thrust and Mass Flow Rate Tables
//
            exec('dataconvert')
//
            tb2=max(timedata)
//


//
// Time inputs
//
            tbo1=61.5;                  //  stage 1 burn time (sec)
//          inquire tb2 'Enter Stage 2 Burn Time (sec)' //  stage 2 burn time (sec)
//
            coast1=1;                   //  coast time between 1 & 2 (sec)
//
            s2ignit=tbo1+coast1;        //  stage 2 ignition time (sec)
//
            tbo2=tbo1+coast1+tb2;       //  stage 2 burnout time (sec)
//
//  Stage parameters
//
            pay=2300;                   //  payload weight (lbs)
            inquire pay 'Enter payload weight in pounds:'
//
            Isp1=268.60;                //  stage 1 Isp (sec)
            ae1=1641.6;                 //  stage 1 exit area (in^2)
            pe1=7.08;                   //  stage 1 exit pressure (psi)
            mp1=1425.99;                //  stage 1 propellant mass (slugs)
            inquire wp2 'Enter Stage 2 Propellant weight (lbm)'
            mp2=wp2/32.174;             //  stage 2 propellant mass (slugs)
            ms1=135.905;                //  stage 1 structural mass (slugs)
            inquire ws2 'Enter Stage 2 Structural weight (lbm)'
            ms2=ws2/32.174;             //  stage 2 structural mass (slugs)
//
            sratio2=ms2/(ms2+mp2)       //  stage 2 structural ratio
//
            mdot1=mp1/tbo1;             //  stage 1 mass flow rate (slugs/sec)
//
            sref1=23.54;                //  stage 1 reference area (ft^2)
            sref2=23.54;                //  stage 2 reference area (ft^2)
//
```
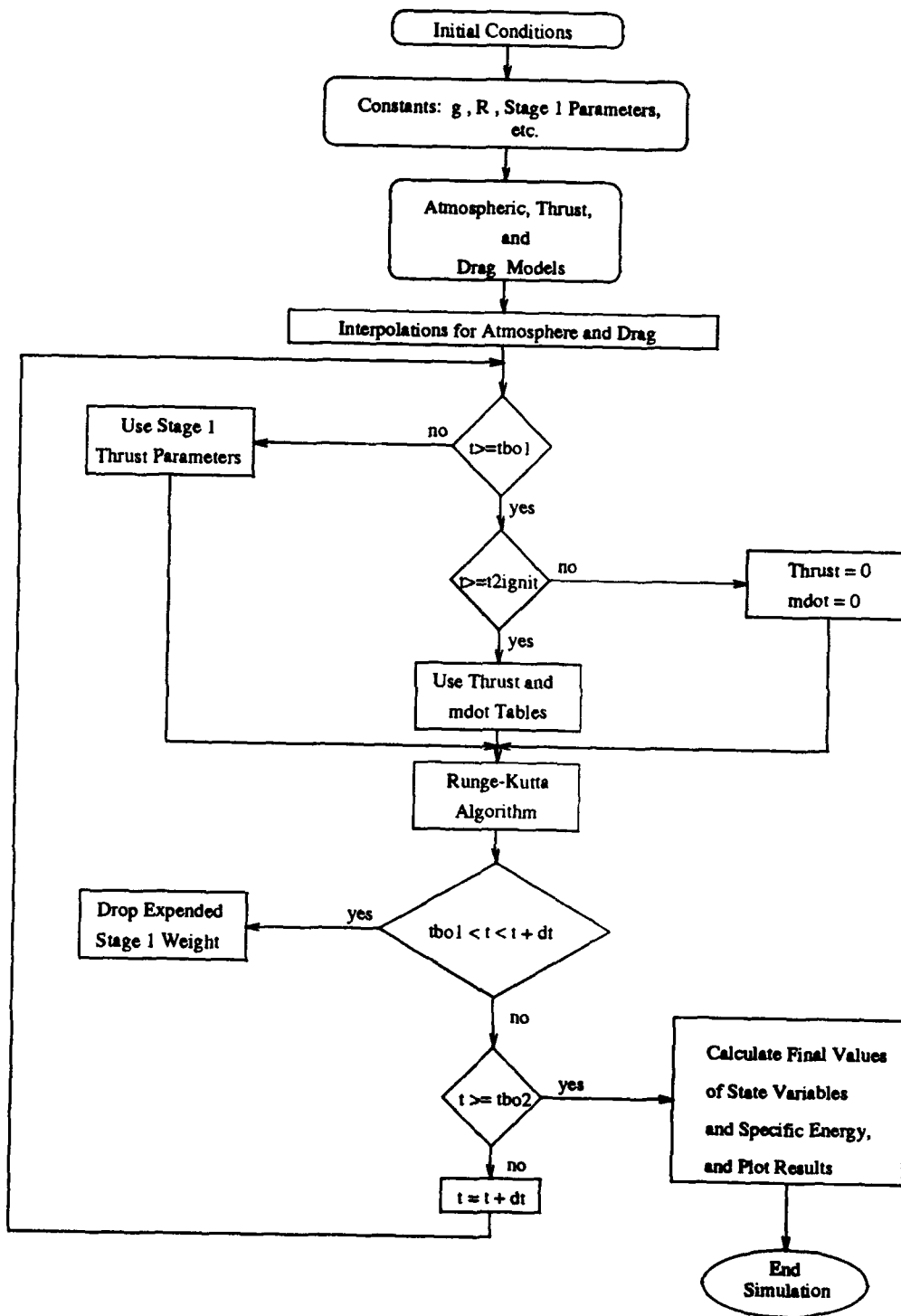
Figure A.3. Flowchart for Program GTURN

```
//    Constants
//
        ge=32.174;                          //    gravitational constant (ft/sec^2)
        re=20925672.57;                     //    earth equatorial radius (feet)
        skirt=10/ge;                        //    stages 1 & 2 skirt mass (slugs)
//
// Initial Conditions
//
        y1(1)=154.3645;                     //    initial velocity (ft/sec)
        inquire gaminit 'Enter initial flight path angle in degrees:'
        y2(1)=gaminit*pi/180;               //    initial flight path angle (radians)
        y3(1)=240.9542;                     //    initial altitude (ft)
        y4(1)=0;                            //    initial downrange (ft)
        y5(1)=(pay/ge)+mp2+ms2+skirt+ms1+mp1-mvert;   //    initial mass (slugs)
        t(1)=3.15;                          //    initial time (sec)
//
//  Atmosphere Model Table
//
        exec('atmodel')
//
        i=1;                                // initialize loop counter
//
// Begin loop
//
        while t(i)<=tbo2,...
pa(i)=spline(ht,pt,y3(i));...
        rho(i)=spline(ht,rhot,y3(i));...
sound(i)=spline(ht,at,y3(i));...
mach(i)=y1(i)/sound(i);...
        Cd(i)=spline(macht,cdt,mach(i));...
g(i)=ge*(re/(re+y3(i)))**2;...
        if t(i)<=tbo1,mdot=mdot1;sref=sref1;...
Th(i)=g(i)*Isp1*mdot+(pe1-pa(i))*ae1;end...
if t(i)>tbo1,mdot=0;sref=sref2;Th(i)=0;end...
if t(i)>=s2ignit,...
Th(i)=spline(timedata,thrustdata,t(i)-s2ignit);...
        mdot=spline(timedata,mdotvar,t(i)-s2ignit);end...
if t(i)>tbo2,mdot=0;Th(i)=0;end...
q(i)=.5*rho(i)*(y1(i)**2);...
        D(i)=q(i)*sref*Cd(i);...
    k1(1)=(Th(i)-D(i)-(y5(i)*g(i)*sin(y2(i))))/y5(i);...
    k1(2)=(1/y1(i))*cos(y2(i))*(-g(i)+((y1(i)**2)/(re+y3(i))));...
k1(3)=y1(i)*sin(y2(i));...
        k1(4)=y1(i)*cos(y2(i));...
        k1(5)=-mdot;...
z1=y1(i)+.5*dt*k1(1);...
z2=y2(i)+.5*dt*k1(2);...
z3=y3(i)+.5*dt*k1(3);...
        z5=t(i)+.5*dt;...
k2(1)=(Th(i)-(.5*rho(i)*(z1**2)*sref*Cd(i))-(y5(i))*g(i)...
            *sin(z2))/y5(i);...
k2(2)=(1/z1)*cos(z2)*(-g(i)+((z1**2)/(re+z3)));...
k2(3)=z1*sin(z2);...
k2(4)=z1*cos(z2);...
        k2(5)=-mdot;...
w1=y1(i)+.5*dt*k2(1);...
w2=y2(i)+.5*dt*k2(2);...
w3=y3(i)+.5*dt*k2(3);...
        k3(1)=(Th(i)-(.5*rho(i)*(w1**2)*sref*Cd(i))-(y5(i))*g(i)...
            *sin(w2))/y5(i);...
k3(2)=(1/w1)*cos(w2)*(-g(i)+((w1**2)/(re+w3)));...
```

```
k3(3)=w1*sin(w2);...
k3(4)=w1*cos(w2);...
        k3(5)=-mdot;...
u1=y1(i)+dt*k3(1);...
u2=y2(i)+dt*k3(2);...
u3=y3(i)+dt*k3(3);...
        u5=t(i)+dt;...
        k4(1)=(Th(i)-(.5*rho(i)*(u1**2)*sref*Cd(i))-(y5(i))*g(i)...
              *sin(u2))/y5(i);...
k4(2)=(1/u1)*cos(u2)*(-g(i)+((u1**2)/(re+u3)));...
k4(3)=u1*sin(u2);...
k4(4)=u1*cos(u2);...
        k4(5)=-mdot;...
y1(i+1)=y1(i)+(dt/6)*(k1(1)+(2*k2(1))+(2*k3(1))+k4(1));...
y2(i+1)=y2(i)+(dt/6)*(k1(2)+(2*k2(2))+(2*k3(2))+k4(2));...
        y3(i+1)=y3(i)+(dt/6)*(k1(3)+(2*k2(3))+(2*k3(3))+k4(3));...
y4(i+1)=y4(i)+(dt/6)*(k1(4)+(2*k2(4))+(2*k3(4))+k4(4));...
        y5(i+1)=y5(i)+(dt/6)*(k1(5)+(2*k2(5))+(2*k3(5))+k4(5));...
if t(i)>=tbo1,y5(i+1)=y5(i+1)-skirt-ms1;end...
        if t(i)>tbo1+dt,y5(i+1)=y5(i+1)+skirt+ms1;end...
        t(i+1)=t(i)+dt;...
        vdot(i)=(Th(i)-D(i)-(y5(i)*g(i)*sin(y2(i))))/y5(i);...
        hdot(i)=y1(i)*sin(y2(i));...
        xdot(i)=y1(i)*cos(y2(i));...
        i=i+1;...
        end
//                              end loop
        Th(i)=Th(i-1);
        D(i)=D(i-1);
        q(i)=q(i-1);
        Cd(i)=Cd(i-1);
        mach(i)=mach(i-1);
        g(i)=g(i-1);
        vdot(i)=vdot(i-1);
        hdot(i)=hdot(i-1);
        xdot(i)=xdot(i-1);
        long
    pause
        exec('plots')
        energy=.5*(y1(i)**2)+g(i)*y3(i)          // specific energy
        gammafinal=y2(i)*180/pi
        gaminitial=gaminit
        eratio=energy/287219448.4636849          // energy ratio
        maxG=max(vdot)/32.174
        sratio2
```

A.4.2.5 The Vertical Flight Phase (Program VERT) . Upon examining the TPS gravity turn equations, it is apparent that launching from rest (initial velocity equal to zero) introduces a numerical singularity (division by zero) in the equation for $\dot\gamma$. To circumvent this problem, the missile trajectory is separated into two phases. The first phase consists of purely vertical flight, with the $\dot\gamma$ equation used in GTURN set to zero, and the value of γ is held at a constant 90 degrees. This flight phase lasts 3.15 seconds (the same as the POST simulation). At the end of this phase,

the final values of the state variables are used as the initial conditions for the gravity turn flight phase simulated in GTURN. This vertical flight phase is simulated using the program VERT, a simplified version of GTURN.

A.4.3   The Performance Measure . Having developed a working missile simulation, the next task is to decide how it is to be used to evaluate the various *NEMESIS* designs. One of the most important system requirements is that the 2-stage design meet the current MM III maximum range performance capabilities. In order to determine whether the 2-stage design meets that requirement, an appropriate quantitative performance measure has to be defined. Also, since the TPS is restricted to simulation of the powered flight phase alone, the performance measure must be defined within that flight phase. Various approaches were considered in defining a proper performance measure including the total change in velocity, projecting the range from burnout using flat-earth, ballistic flight equations, and trying to match the system state at burnout with the MM III burnout state. Of these approaches, matching the burnout state was determined to provide the best measure of performance. This came to be known as the "basket in the sky" approach.

Within the constraint that the PBV remain unchanged from the current system, placing the PBV at the same altitude, velocity, downrange position, and flight path angle guarantees that the 2-stage design PBV trajectory exactly matches that of the MM III. However, realizing that the *range* is not uniqely defined by a particular combination of these variables, this definition of the missile state was abandoned. In its place, the total energy of the payload at MM III stage 3 burnout for the maximum range trajectory was adopted as the performance measure for the 2-stage design. The total energy state is defined as the sum of the kinetic energy and the potential (gravitational) energy of the PBV. This parameter is adequate as long as the PBV weights remain equal for the MM III and the 2-stage design. However, when lower 2- stage PBV weights are investigated, an inherent problem with this measure appears. Since the mass of the PBV serves as a multiplier in the total energy equation, any reduction in the PBV mass used in the 2-stage design produces a loss of energy directly proportional to the decreased mass. This problem is solved by simply dividing out the mass from the total energy equation, leaving the energy *per unit mass*, or *specific energy*, as the final performance measure. This allows direct specific energy comparisons between the various design configurations, regardless of PBV weight. Note that the specific energy requirement of the MM III is assumed to be the same for all PBV weights evaluated. This means that the energy

A-21

comparison is mission dependent. However if only small differences in payload are assumed, this comparison serves as a valid performance measure for the purposes of this study.

Another side effect of examining lowered payload weights is the question of which final flight path angle should be used to determine the maximum range of the missile for that given payload weight. This question is answered by matching the TPS-generated final flight path angles with the corresponding POST reduced-payload flight path angles. Since the only reduced-payload data available was for payload weights of 1900, 1700, and 1500 pounds, only these weights are examined. The results of these simulations are presented in Table A.2.

Payload Wt	Initial γ	Final γ(max R) (from POST)	Final γ(max R) (from TPS)
2300	80.3	21.96	22.000
1900	80.3	22.93	22.933
1700	80.3	23.43	23.427
1500	80.3	23.92	23.919

Table A.2. Reduced Payload Flight Path Angles

As can be seen, the initial flight path angle required in the TPS to match the final flight path angles for the maximum range trajectories from POST is a constant 80.3 degrees. A simple linear regression model is formulated based upon these results to allow calculation of the target flight path angle for other reduced-payload cases. This equation is:

$$\gamma_{target} = 27.504729 - 0.002397(W_{payload})$$

where $W_{payload}$ is the payload weight (in lbm). The flight path angles obtained using this equation are used in determining the payload-carrying capability of the final designs.

Appendix B. *Propulsion Performance Modeling*

B.1 Introduction

B.1.1 Purpose.
The performance of a solid propellant missile is dependent on the complex interactions of many parameters. The purpose of this appendix is to describe these interactions and how they are modeled in the development of different propulsion design options. The model takes different inputs of key parameters and yields the corresponding stage performance. Attention is given to determining which design options are feasible for the given mission. Also, the component weights of the modeled configuration are estimated for use in other performance models.

B.1.2 Relationships With Other Models.
The propulsion performance model is the starting point for estimating the performance of the given stage configuration. The choice of propellant, propulsion technologies, and physical characteristics for the propulsion model yield chamber pressure, chamber temperature, stage component weight estimates, and other outputs for the structural and thermal models. Some of the weight estimates are provided by the AIDE-II program provided by Aerojet. Thrust and mass flow time histories are generated for use by the trajectory simulation. The overall performance model interaction may be seen in Figure B.1.

B.1.3 Model Inputs and Outputs.
The propulsion model is shown schematically in Figure B.2. The choice of propulsion technology is key for determining the performance of a missile stage. Recent developments in Integrated Stage Concept (ISC) technologies make an ISC stage possible. The more conventional missile technologies are also considered. The propellant to be used is an important input, and it is linked to the choice of using ISC technologies. Boron-based propellant is necessary for ISC stages while aluminum-based propellant is suitable for conventional missile stages. Other inputs may include the nozzle throat and exit areas, stage shape, mass of propellant, and key grain design parameters. As discussed later, the feasibility of grain designs to provide the necessary thrust profile becomes the primary issue in designing a stage to meet the given mission.

Outputs of the models include the physical dimensions of the grain size and the grain design. The chamber pressure and temperature, burn time, component weight estimates, and grain pattern burn characteristics are provided to the structural and thermal models. Thrust and mass flow time
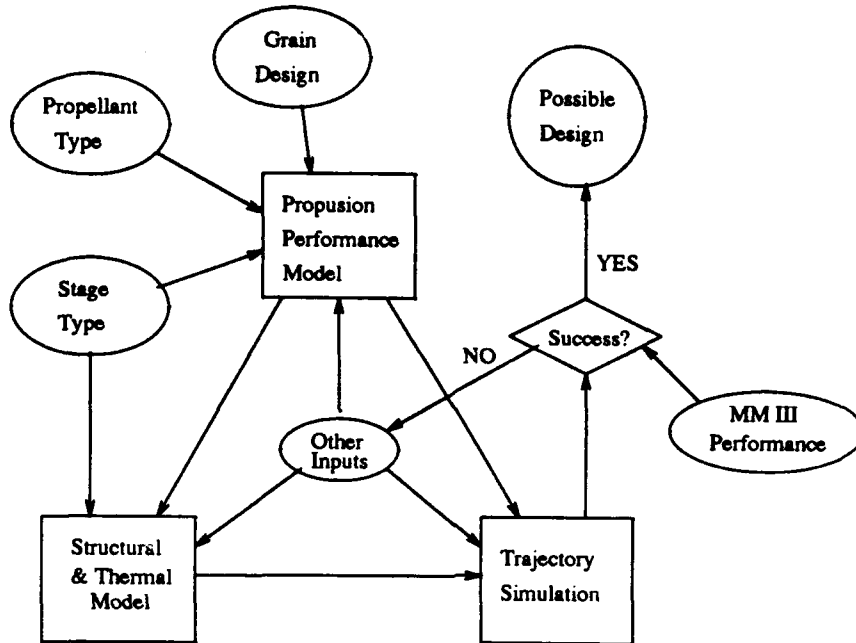
Figure B.1. Performance Model Interactions

histories are provided to the trajectory simulation. Also supplied are the nozzle exit pressure. exit velocity. and any choices and assumptions pertinent to other models.

B.1.4   Key Tasks. Several tasks are vital to the successful modeling of feasible propulsion configurations.

1. *Model Parameter Relationships* - The interactions and relationships between the chosen physical dimensions, propellant characteristics, and resulting performance are described. Assumptions are stated and equations for each relationship are listed with reference.

2. *Determine Feasible Designs* - For each proposed design. feasibility of that design to meet mission requirements is evaluated. Information provided by sample runs on the trajectory simulation is used to determine several constraints for a feasible design.

3. *Determine Specific Outputs* - For feasible designs options, the physical dimensions, performance outputs, and weight estimates are calculated.

4. *Design Optimization* - Each feasible design is optimized for maximum performance before comparing it to the performance of different designs (Chapter 5).

B-2
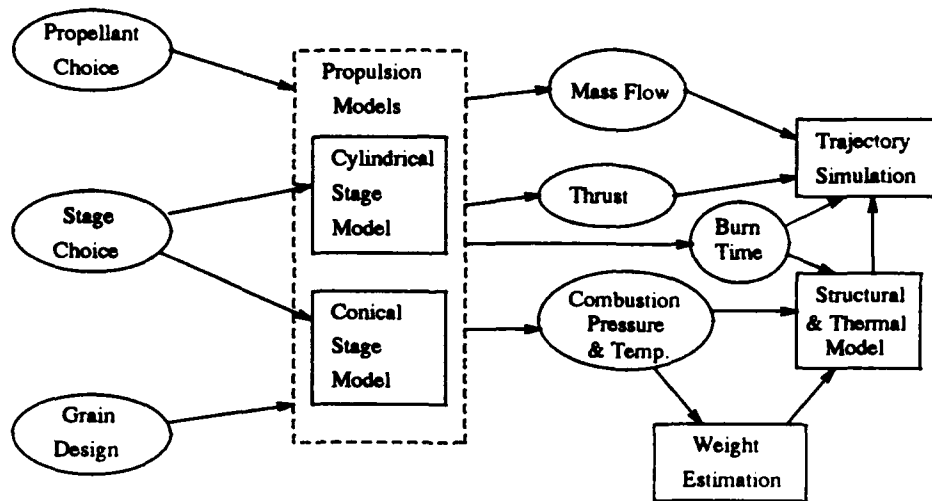
Figure B.2. Propulsion Performance Model

B.2 Solid Rocket Propulsion Concepts

B.2.1   Thrust. The thrust of a propulsion system is the net pressure integrated over its entire surface. Since this is a very difficult thing to do, a control volume approach is most commonly used. The resulting thrust equation is made up of a momentum thrust and a pressure thrust term (50:p321).

$$T = \dot{m}u_e + A_e(P_e - P_a) \tag{B.1}$$

where:

T = thrust

$\dot{m}$ = mass flow rate

u_e = nozzle exhaust velocity

A_e = nozzle exit area

P_e = nozzle exit static pressure

P_a = ambient pressure

It can be shown that for maximum thrust, a nozzle should expand the exhaust gas flow to a pressure equal to the ambient pressure. This is known as an optimally expanded nozzle. While this negates

B-3

the pressure thrust term, the corresponding increase in momentum thrust more than makes up for the loss (50:p321). Often, an equivalent exhaust velocity, u_{eq}, is defined as:

$$u_{eq} = u_e + A_e(\frac{P_e - P_a}{\dot{m}})$$ (B.2)

This combination of the pressure thrust term within the equivalent exhaust velocity enables the thrust to be expressed as (50:p321):

$$T = \dot{m}u_{eq}$$ (B.3)

B.2.2   Mass Flow Rate. The mass flow rate of a missile is dependent on several factors. First of all is the gas generation rate, or the rate at which combusted propellant is generated in the chamber. In a steady state condition, the gas generation rate is approximately equal to the mass flow rate through the nozzle throat. The difference between these two rates is the gas storage rate within the thrust chamber. In the case of a neutrally burning grain design, the gas generation rate is constant while the increase in open volume within the chamber increases linearly. Therefore, the gas storage rate is constant and the difference between the gas generation rate and the mass flow rate through the nozzle is also a constant (50:p384). (13:p304).

The mass flow rate through the nozzle is the pertinent rate for determining thrust. By using isentropic relations and a choked flow (Mach Number = 1) assumption, the mass flow rate is (50:p384):

$$\dot{m}_{noz} = \frac{A_{th}P_0}{\sqrt{RT_0}}\sqrt{\gamma}\left(\frac{2}{\gamma + 1}\right)^{\frac{\gamma+1}{2(\gamma-1)}}$$ (B.4)

where

$\dot{m}_{noz}$ = mass flow rate through nozzle

A_{th} = nozzle throat area

P_0 = chamber total pressure

T_0 = chamber total temperature

R = gas constant

γ = ratio of specific heats. $\frac{C_p}{C_v}$

B.2.3 *Combustion Pressure.* The combustion chamber pressure is one of the most important parameters in propulsion design. Higher pressures reduce dissociation in the combustion products and improve performance. However, higher pressures also require more structural weight. The pressure in the combustion chamber is a function of the gas generation rate, the throat size, temperature, and the chemical make-up of the propellant. The most dynamic of these relationships is the interaction between the chamber pressure and the gas generation rate. The gas generation rate is defined as (50:p382):

$$\dot{m}_g = \rho_p A_b r \tag{B.5}$$

where $\dot{m}_g$ is the gas generation rate, ρ_p is the propellant density. A_b is the burn surface area, and r is the propellant burn rate.

The chamber pressure can be obtained by performing a mass balance between the mass generation rate, the mass storage rate, and the mass flow rate through the nozzle throat. For constant combustion pressure, the pressure may be found from (50:p385):

$$P_0 = \left[\frac{A_b}{A_{th}} \cdot \frac{a(\rho_p - \rho_0)}{\sqrt{\frac{\gamma}{RT_0} \left(\frac{2}{\gamma+1} \right)^{\frac{\gamma+1}{\gamma-1}}}} \right]^{\frac{1}{1-n}} \tag{B.6}$$

Varying chamber pressures may occur during starting and ending burn transients or if the burn surface area is not constant. However, if the pressure does not change significantly over the time increment considered, then this equation may be used to calculate the instantaneous pressure for the instantaneous burning area (50:p385).

B.2.3.1 *Propellant Burn Rate.* The burn rate is a function of temperature and pressure. The most significant of these factors is the pressure, and the relationship is typically modelled with the following relationship (50:p383):

$$r = a P_0^n \tag{B.7}$$

where a and n are empirical values given for specific units of pressure and burn rate. Typically, burn rates given assume a reference pressure of 1000 psia. The range of pressures within which this

relationship is valid varies for the given propellant, but for the propellants to be used in this study this relationship holds from several hundred psia to several thousand (6).

B.2.4   Nozzles. The flow through a nozzle is strongly affected by the shape of the nozzle walls.   Real nozzles have divergence, rotational flow, viscosity, heat transfer, shocks, and other effects which make analysis very complex.   For this preliminary analysis the rocket nozzle flow is assumed to be isentropic and one-dimensional.
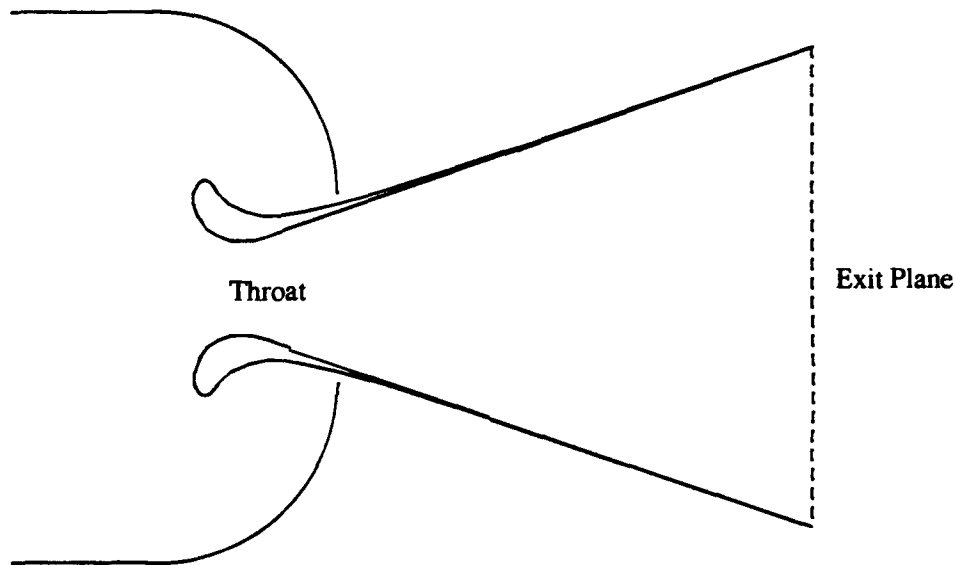
Figure B.3. Conventional Nozzle

B.2.4.1   Conventional Nozzles.   The most common nozzle is bell-shaped or conical and has a single circular throat.   Under the one-dimensional assumption, the only important geometric variable is the expansion ratio (50:p397).   With the additional assumption of isentropic flow, the Mach number can be calculated for any point in the nozzle.   With choked flow at the throat and knowledge of the nozzle expansion ratio, the nozzle exit Mach number can be calculated from (50:p49):

$$\frac{A_e}{A_{th}} = \frac{1}{M_e} \left[\frac{2}{\gamma + 1} \left(1 + \frac{\gamma - 1}{2} M_e^2 \right) \right]^{\frac{\gamma+1}{2(\gamma-1)}} \tag{B.8}$$

where M_e is the nozzle exit mach number and A_e is the nozzle exit area.

B.2.4.2   Forced-Deflection Nozzles. Conventional nozzles have the problem that for constant P_0 and γ, the expansion ratio for optimal expansion is different for varying ambient pressure. The change in ambient pressure with altitude makes a given nozzle optimum for only one instant during operation. The forced-deflection nozzle has an altitude- compensating characteristic which helps this problem and is described below.
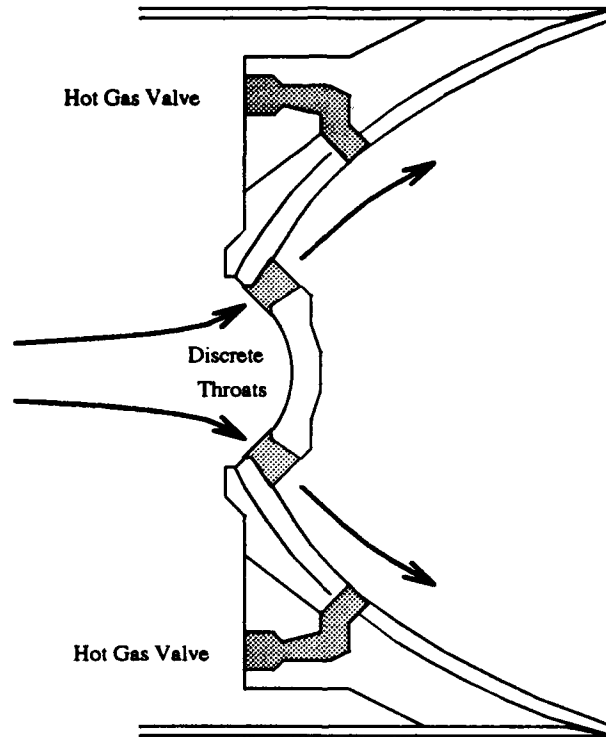
Figure B.4. Forced-Deflection Nozzle

The flow is directed from the combustion chamber through several discrete throats arranged in an circular ring. The flow is turned to be tangential to the nozzle wall. This creates a void in the middle of the nozzle flow. The effective nozzle exit area is the ring of flow at the nozzle exit. This effective area is dependent on the ambient pressure; higher ambient pressure makes the void larger and the effective exit area, and resulting expansion ratio, lower. This effect makes this nozzle self-adjusting to changes in ambient pressure. Testing of these nozzles measured the design point thrust of forced-deflection nozzles as 98% of ideal thrust (50:p414). An additional advantage of these nozzles is their short length compared to conventional nozzles (50:p404). For use in upper stages, this length advantage is the most important property of forced-deflection nozzles. The

nozzle can fit right over the top of the previous stage and minimize wasted volume and missile length.

One reason these nozzles have not been widely used is the solid particles present in the exhaust of propellants with metal aluminum as a fuel. The forced-deflection nozzle, with its smaller throats and sharp turning, can not tolerate the erosive effects of these particles. A "cleaner" burning propellant is required, such as those using boron as a fuel (7:p4).

B.2.4.3 Performance Corrections. The thrust generated from one-dimensional isentropic equations is used as the thrust for conventional nozzles. For forced-deflection nozzles, 98% of the ideal thrust is used for performance calculations. Other losses which affect the performance of real nozzles are included in the specific impulse corrections discussed later.

B.2.5 Specific Impulse. The total impulse of a missile is the area under the thrust-time curve. This is also the product of the total expended mass and the equivalent velocity.

$$I = \int T \cdot dt = M_p u_{eq}$$

where I is total impulse, t is time, and M_p is the expended mass of propellant.

Specific impulse is the impulse per unit mass which is "normalized" by dividing by the acceleration of gravity at sea-level (50:p322).

$$I_{sp} = \frac{I}{M_p g_e} = \frac{u_{eq}}{g_e} \tag{B.9}$$

where I_{sp} is the specific impulse of the motor and g_e is the standard acceleration of gravity, 32.2 ft/s^2. This definition has the advantage of always having the units of seconds. Actually, for English units specific impulse is pound-force seconds per pound-mass. Since specific impulse is directly proportional to equivalent velocity, perfect expansion will optimize the specific impulse, and therefore thrust, of a nozzle for a given ambient pressure. Often, specific impulse is given for a propellant; the value calculated for an expansion ratio of 100 and sea level operation. In general, specific impulse can be thought of as a measure of the potential energy of a particular propellant.

The specific impulse of a particular propellant is subject to several types of "real world" losses, each of which diminish the effective specific impulse from the ideal value. The percentage of theoretical specific impulse lost to these effects has been studied and documented in several sources (7:p4),(101:p18). The losses are different for solid propellants with different metal fuels. The more conventional aluminum-based propellants have a significant loss due to two phase flow. This is caused by the formation of aluminum-oxide particles in the exhaust. These solid particles do not expand and accelerate as do gases in the nozzle. The momentum flux lost due to solid particles present in the flow results in the two-phase flow loss. Alternatively, boron-based propellants have much less non-gaseous matter in the exhaust. The boron oxide remains in gaseous phase until after it is through the high turning region of the throat. The exhaust does not produce significant erosion of the nozzle wall (7:p4). Therefore, the boron-based propellant is "cleaner", with an almost entirely gaseous exhaust, and does not suffer as severe a two-phase flow loss. The other performance loss mechanisms are roughly the same for both aluminum and boron propellants. The two types of propellant experience the following losses for the same type of conventional nozzle (7:p4):

Source of I_{sp} Losses	Aluminum Propellant		Boron Propellant	
	%	seconds	%	seconds
Divergence	1	-3	<1	-3
Boundary Layer	1	-3	<1	-3
Combustion Efficiency	2	-6	<2	-6
Nozzle Submergence	1.5	-5	0	0
Two-Phase Flow	>4	-25	<3	-9
Total	11-12 %	-43	6-7%	-22

Table B.1. Comparison of I_{sp} Losses

The net result, is that while the aluminum propellant has a higher theoretical specific impulse, it also has higher losses. The delivered performance of the two types of propellants are relatively close. However, much more aging and testing data is available for the aluminum propellants, making them preferable for most risk-averse rocket designers.

B.3 Methodology

The performance of a missile stage is calculated by using an Euler integration scheme; burn parameters are assumed constant for small increments in time. This allows for variable burn surface areas and the resulting changes in combustion pressure, burn rate, mass flow, and thrust.

B-9

The propellant grain is assumed to be case-bonded to either cylindrical or conical shaped cases. Modifications to the grain to accommodate forward domes and tapered propellant aft sections are made using reasonable assumptions. Other assumptions include one-dimensional and isentropic flow, constant combustion temperature, and constant ratio of specific heats. Related to this last assumption, the propellant combustion products actually change for varying combustion pressure due to its effect on dissociation of the combustion products. This affects the exhaust molecular weight, ratio of specific heats, exhaust specific heat, and energy density. However, these values are all assumed constant for the range of pressures used in this analysis.

B.3.1 Select Inputs. The inputs required for the propulsion model include: propellant type, stage shape and diameters, mass of propellant, ambient pressure, time increment for integration, throat area, and grain geometry parameters. A summary of this data is shown in Table B.2. The decision will be made for either Integrated Stage Concept (ISC) technologies (as described in Chapter 4) or conventional missile technologies. The ISC stage includes the following technologies:

- forced-deflection nozzle

- boron-based propellant

- aft-open-ended case

- thrust vector control with hot gas valves

The selection of ISC or conventional technologies determines the use of boron or aluminum-based propellants. Characteristic propellant properties for each of these two categories were provided by Phillips Laboratory (73) or, as with the energy density. Q_R, derived from Phillips Laboratory data. These characteristics are used to define the properties of the aluminum and boron propellant used in the study. Additional information, such as the burn rate coefficients for each propellent, were provided by Aerojet Corporation (6). Table B.2 shows the properties of the two propellants used for the design study. Performance corrections for losses are broken into two factors: one for propellant type and one for nozzle type. The propellent-type correction is the reduction of specific impulse from the theoretical value to the delivered value for a conventional nozzle. The nozzle-type correction is only for the forced-deflection nozzle, reducing the delivered thrust to 98% of that for a similar conventional nozzle. The product of these two factors agrees well with the nozzle efficiencies determined from cold flow tests by Aerojet (58). Thrust is calculated from the effective specific

Parameter	Aluminum Propellant	Boron Propellant
burn rate coefficient, a	0.025238	0.021450
burn rate exponent, n	0.40	0.40
molecular weight, M	29.4	25.5
γ (constant)	1.17	1.22
density, ρ_{prop}, (lbm/in^3)	0.06413	0.06470
combustion temperature, R	6366	5637
nozzle-type correction, η_{noz}	1.0	0.98
propellant-type corr., η_{prop}	0.89	0.94
specific heat, C_p , ($ft \cdot lbf/lbm \cdot R$)	361.775	336.083
energy density, Q_R, ($ft \cdot lbf/lbm$)	2,555,560	2,023,680

Table B.2. Aluminum and Boron Propellant Parameters

impulse of the motor, so both these corrections can be applied to determining the effective specific impulse from the theoretical value for a particular nozzle and propellant.

The physical constraints of this problem determine several dimensions and factors which affect the propulsion model. The stage shape, either cylindrical or conical, affects the analysis. For the conical case the stage shape is approximated in the computer code by a series of cylinders with varying diameter. This makes the analysis a little more complex. The computer model sums the surface area and port volume for all the cylinders in a separate DO loop in the program. The cylindrical version of the model is a subset of the conical case, involving the analysis of a single cylinder. In either case, the maximum second stage diameter is equal to the first stage diameter. If a narrower stage is desired this affects the design of the interstage. The maximum stage top diameter for a conical stage is limited by the diameter of the post-boost vehicle. The existing first stage of the Minuteman III currently supports a total mass of approximately 27,000 pounds. In order to ensure at least the same structural reliability as the current system, the new design must not weigh any more than this total. For a ratio of structural weight to total weight of the stage (also called structural ratio) of 0.07 and a similar payload weight, this constraint determines that the maximum propellant weight allowed for the new stage is approximately 22,100 lbs. The propulsion model starts with this propellant weight as an input and can back down if performance requirements are exceeded.

For an ISC second stage, the nozzle exit area is approximately the circular area of the first stage diameter. For a conventional nozzle, the exit area must be chosen. The ambient pressure

for this second stage operation is assumed to be negligible. Also, the time increment for the Euler integration scheme is selected in agreement with the increment used by the trajectory simulation.

The final set of inputs are the most flexible parameters of the propulsion design. The throat area and grain design geometry parameters will be the chief means of controlling pressure, mass flow, and thrust magnitudes and time histories. The grain design parameters are different for various grain designs, so there is a similar but separate model for each separate grain design.

B.3.2 Sizing the Stage. Given the grain design parameters, the cross-sectional area of the grain port can be calculated. The combination of known mass and density of propellant determine the volume of propellant to be held by the stage. For a given stage shape (cylindrical or conical) and the top and bottom diameter of the stage, the stage height may be calculated by:

$$Volume_{stage} = Volume_{propellant} + Volume_{port}$$

where:

$$Volume_{stage} = f(\text{stage height, stage shape. grain design})$$

$$Volume_{port} = g(\text{stage height, stage shape, grain design})$$

B.3.3 Calculate Constant Values. Several important values are constant for the entire stage burn given the previously stated assumptions of constant combustion temperature and ratio of specific heats. The constant throat area and nozzle exit area mean that the nozzle exit Mach number, pressure ratio, and velocity will be constant. The Mach number is a function of expansion ratio, defined in Equation B.8.

$$\frac{A_e}{A_{th}} = \frac{1}{M_e} \left[\frac{2}{\gamma + 1} \left(1 + \frac{\gamma - 1}{2} M_e^2 \right) \right]^{\frac{\gamma+1}{2(\gamma-1)}}$$

This equation must be iterated for the given expansion ratio to solve for Mach number. A gradient search method is used to limit computing time. Once the Mach number is calculated, the

ratio of stagnation to static pressure can be calculated, assuming isentropic expansion (50:p47):

$$\frac{P_0}{P_e} = \left(1 + \frac{\gamma - 1}{2}M_e{}^2\right)^{\frac{\gamma}{\gamma-1}} \tag{B.10}$$

where P_e is the static pressure at nozzle exit and M_e is the exit Mach number.

While the combustion pressure may change during the burn, the pressure ratio will remain constant as long as the expansion ratio and ratio of specific heats remain constant. In actual nozzles, some erosion of the throat occurs, but recent improvements in throat materials and coatings make the constant throat area assumption reasonable (48:p3).

The exit velocity of the nozzle for a constant nozzle expansion ratio (non-eroding throat assumption) is also constant, and is a function of (50:p355):

- The propellant's chemical energy released during combustion

- The pressure ratio

and can be calculated by

$$u_e = \sqrt{2C_p(T_{01} + \frac{Q_R}{C_p})\left[1 - (\frac{P_e}{P_0})^{\frac{\gamma-1}{\gamma}}\right]} \tag{B.11}$$

where C_p and Q_R are the specific heat at constant pressure and the energy density of the propellant, respectively, and T_{01} is the initial propellant temperature.

The theoretical specific impulse of a motor is determined from Equation B.9. For changing propellant burn surface area the nozzle exit pressure and mass flow rate also change. However, for constant ambient pressure and the other assumptions of this study, the effects of changing nozzle exit pressure and mass flow rate cancel each other. Therefore, for a constant ambient pressure, the theoretical specific impulse is constant for the entire burn.

B.3.4   Euler Integration. The burning process is modeled by first calculating the burn surface area, combustion pressure, nozzle exit pressure, mass flow rate, and thrust, ignoring any initial transients. The burn time "clock" is still at zero. Given the combustion pressure, the initial burn rate can be calculated. The burn time "clock" is advanced one time increment, assuming that the all values are equal to their initial values for the entire time increment. At the end of the increment, the grain burn distance is equal to the product of the burn rate and time increment:

$$\Delta distance = r \cdot \Delta t$$

The grain burns perpendicular to its surface in all directions, therefore, the burn surface area at the end of the time increment can be calculated from the burn distance. The specific type of grain pattern will determine this surface area function of burn distance. From this point, the combustion pressure, mass flow rate, nozzle exit pressure, and thrust are calculated for the next time increment. The amount of propellant burned at a particular time is the sum of the expended mass for all the preceding time increments.

$$Mass_{expended} = \sum_{i=0}^{t_{burn}} \dot{m}_i \cdot \Delta t_i$$

The burning process will continue until the mass of propellent burned is equal to the initial amount present. As discussed in later sections, for some grain patterns, such as multiple-slotted grain designs, the pressure may drop off so low that termination prior to complete combustion is necessary to prevent excessively long burn times or unsatisfactory burning conditions.

B.4 Grain Design

Several types of grain design were considered and analyzed including star patterns, end-burners, modified end-burners, and slotted grain designs. A neutral burning design is the first choice, but constraints on the system make a regressive thrust profile necessary. A two-slotted grain design with a central radius provides the best performance of the designs considered. This design and others considered will be discussed.

Many possible thrust profiles are possible for a solid rocket stage, as shown in Figure B.5. Assuming constant effective exhaust velocity, thrust is directly proportional to the burn surface area. This is the case for the assumptions of this design study. There are three general classes of thrust profiles possible:

- *Neutral* - the burn surface area and thrust are constant

- *Progressive* - the burn surface area and thrust increase with time

- *Regressive* - the burn surface area and thrust decrease with time.

Grain Patterns   Thrust Profiles

Neutral

Progressive

Regressive
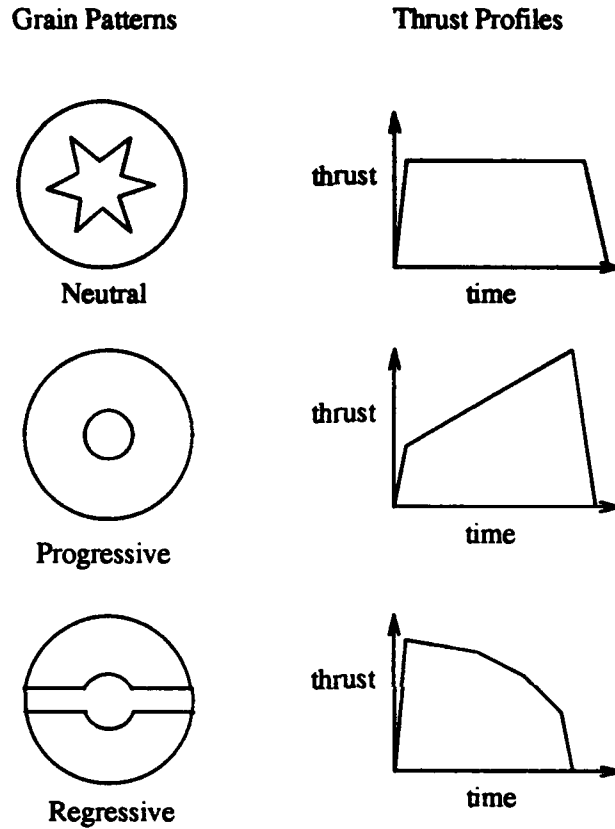
Figure B.5. Internal Burning Grain Designs With Their Thrust Profiles (50:p385)

For non-neutral profiles, the changing surface area creates changes in combustion pressure, burn rate. mass flow, and therefore thrust (50:pp382-385).

B.4.1 System Constraints on Grain Design. For most applications, a neutrally-burning grain design is desired. The constant burn area makes the combustion pressure, mass flow rate, and thrust constant for the entire burn. This makes the analysis simpler and, since the case must be designed to the maximum pressure, makes best use of structural weight. For a given total impulse, the minimum case weight should correspond to a neutral grain design. The most common neutral grain design is a case-bonded internal star pattern.

The maximum acceleration the system can tolerate is 18 times the standard acceleration of gravity, or 18 g's. For the desired payload and expected structural weight. this translates

into a maximum thrust of approximately 55,000 pounds. In order to meet the desired mission requirements, the trajectory simulation estimates the burn time required at this thrust level to be at least 115 seconds. Examination of the star pattern equations (13:p303) indicate that for a maximum case radius of 33 inches the maximum web thickness is approximately 13 inches. In order to get this length to burn in 115 seconds requires an unacceptably low burn rate. For the propellants available, the pressure would have to be extremely low for such a slow burn rate, and the resulting mass flow would not provide adequate thrust. Therefore, for the given physical and dynamic constraints on the system, a neutral star pattern will not meet the mission requirements.

A regressive thrust profile, as long as it does not exceed the acceleration limits, may deliver the necessary total impulse. A further illustration of why a regressive burn profile is promising rather than a neutral one is shown in Figure B.6. A regressive thrust profile more closely aproximates the combined second and third stage profiles of the Minuteman III.
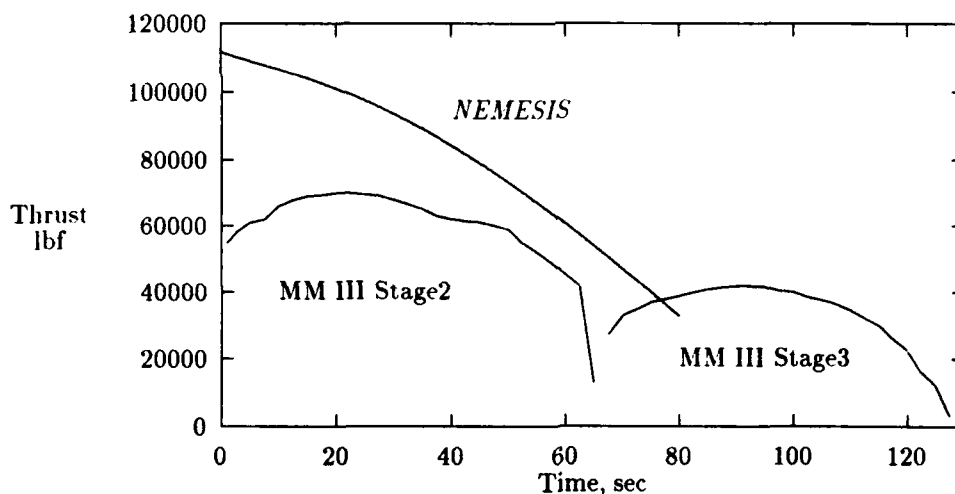
Figure B.6. One and Two Stage Thrust Comparison

B.4.2 Slotted Tube Grain Design. A regressive grain pattern is shown in Figure B.7. This cross-section shows the single slot intersecting with a central radius. The slot extends all the way to the case wall. If the slot started short of the case wall, the burn area would begin progressively till the slot reached the wall and then continue regressively. The burn proceeds perpendicular to

the propellant at all surfaces. Therefore, as the propellant burns the central tube radius increases. cutting off more and more of the slot. The slot is also increasing in thickness which in turn cuts off more of the tube arc. These two effects keep the burn regressive, which terminates when the tube radius reaches the wall. An advantage of this design over others is that none of the propellant remains unburned.
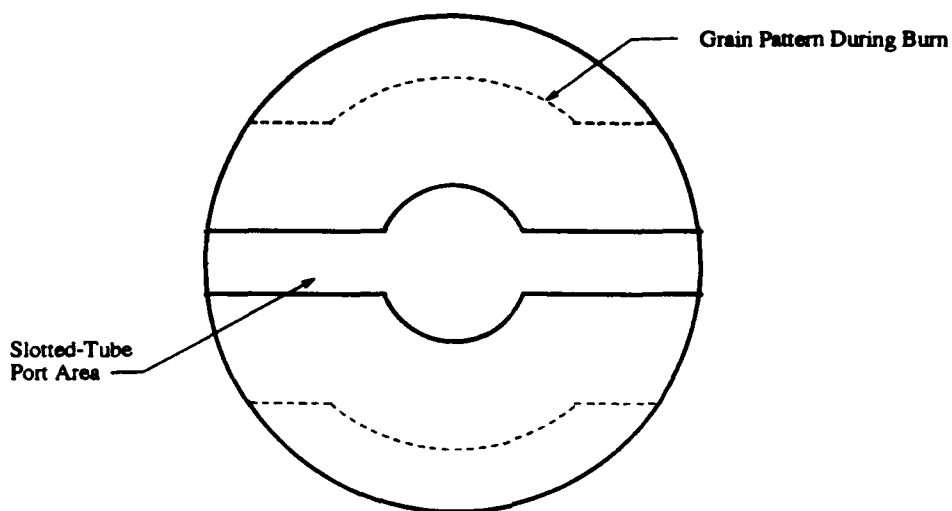
Figure B.7. Slotted Tube Grain Design

B.4.2.1   Assumptions. For either a cylindrical or conical shaped stage. the slotted tube grain design requires some assumptions to make analysis possible.

Cylindrical Case – For a cylindrical case, the slotted tube grain design has constant dimensions for the entire case length. The cross section of the grain design shown in Figure B.7 allows equations for initial port area to be calculated. Also, the perimeter is calculated in order to determine the burn surface area. These equations work well assuming that all the propellant is contained in a cylindrical case with constant cross-section. While analytically desirable, this assumption ignores the propellant contained in the forward dome and any aft tapered propellant region (see Figure B.8). A method of considering these areas is to assume that the propellant volume of the dome and tapered regions together equals that of a cylinder with the diameter of the case and height of the dome. If the tapered section's surface is covered with inhibitor, then the tapered region will burn progressively while the dome will burn regressively. The net result will be the same as if all the propellent is in a cylindrical case with the height L, as seen in Figure B.8.

Effective Cylinder for Analysis   Actual Cylindrical Grain
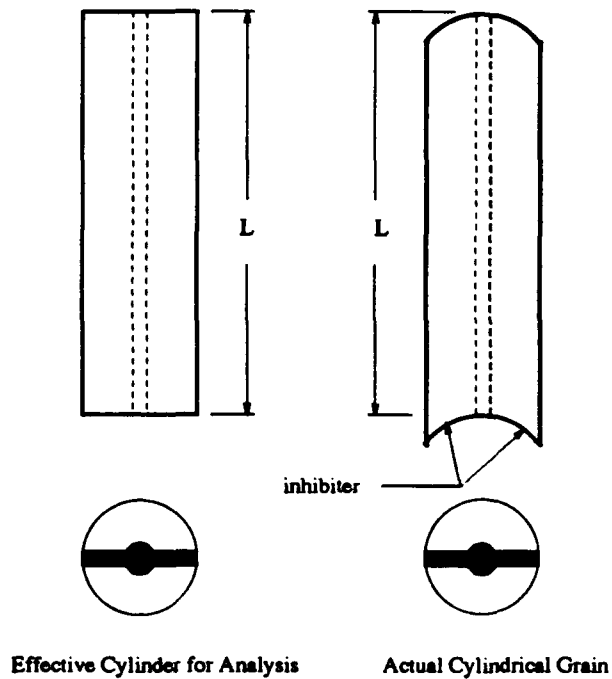
Figure B.8. Effective and Actual Cylindrical Stages

In summary, the effective cylindrical stage is assumed adequate for modeling the propulsion performance.

Conical Case – The same dome and tapered region assumption used for cylindrical stages applies to conical stages. The difference in top and bottom diameters of the cone will create a difference in the progressive and regressive sums of the two regions. However, since these two areas contain less than 10 % of the total volume, and the taper is less than 3 degrees, the difference will be considered negligible. Therefore, a cone with a flat top and bottom, as shown in Figure B.9, approximates the actual conical stage with dome and aft tapered propellant region. Also, the internal grain pattern must also be tapered along the length of the case. In order for the propellant to completely burn, the web thickness. or distance from the initial central radius to the case radius (see Figure B.7), must be the same for the entire conical case length. Therefore, the tube taper is the same as the external case taper. For analytical simplicity, the slot thickness-to-tube radius ratio is assumed constant for the entire cone length.

inhibitor

Effective Cone Used
For Analysis

Actual Conical Grain
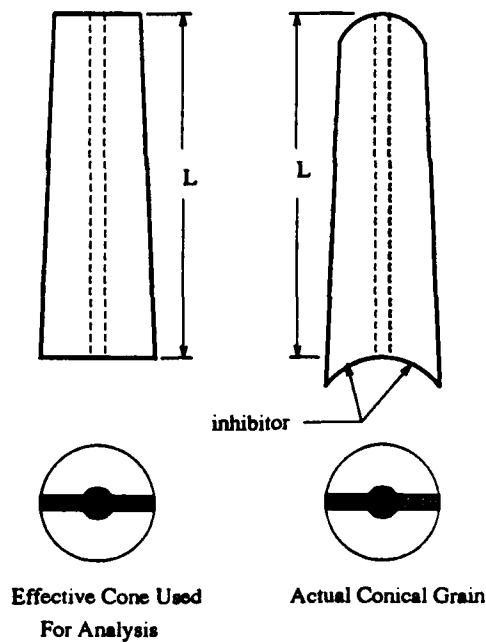
Figure B.9. Effective and Actual Conical Shapes

B.4.2.2 Slotted Tube Equations. The two key calculations are the initial port area of the slotted tube and the expression for burn surface perimeter as a function of burn distance. The symmetry of this grain design enables analysis to be done on a quarter of the cross-section and then multiply the results by four. In order to calculate either the port area or burn surface perimeter, the geometrical parameters must be defined. Figure B.10 shows the geometric variables:

- F - half the slot thickness

- R_1 - initial tube radius

- C_R - inner case radius

<u>Port Area</u> – The initial port volume is a function of port cross-section area, the port shape (cylindrical or conical), and the port length. The volume must be calculated to determine the stage size: the more empty volume the longer the stage must be to hold all the desired propellant. The port area is estimated for the cross-section and then used to calculate the initial empty volume. For a cylindrical stage, the cross-section port area is multiplied by the previously calculated cylinder height to obtain the volume. For a conical stage, the volume for each incremental cylinder is
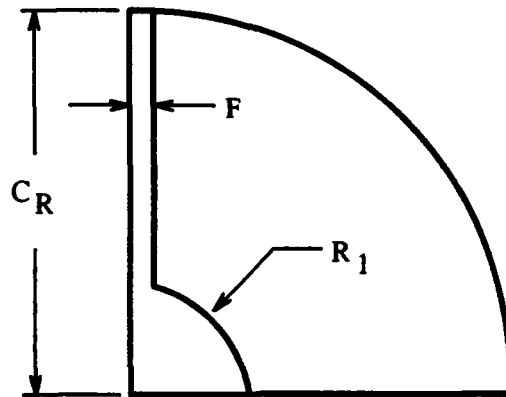
Figure B.10. Slotted Tube Quarter Section and Geometric Parameter Definitions

calculated and summed up to estimate the value for the entire cone. The port area is estimated by approximating the slot area as a rectangle with width F, and length C_R. The remaining area is calculated by taking a triangular area from the remaining wedge shape (see Figure B.11).

$$A_{section} = A_{rectangle} + A_{wedge} - A_{triangle}$$

In terms of the grain geometry parameters, Figure B.11 illustrates how these areas are calculated.
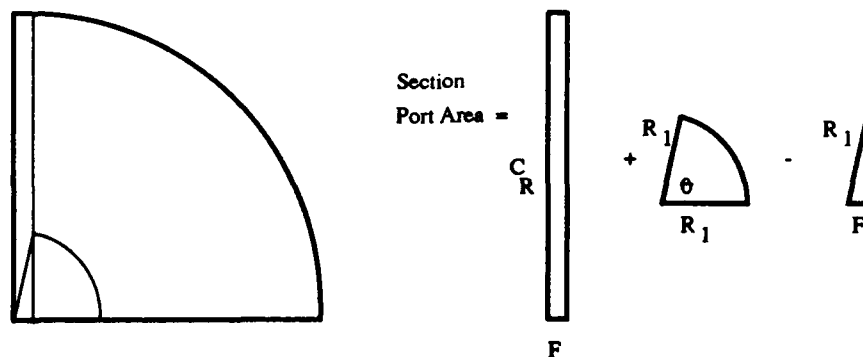
Figure B.11. Calculation of Slotted Tube Section Port Area

Wedge angle, θ:

$$\theta = cos^{-1}\left(\frac{F}{R_1}\right)$$

Area of the slot:

$$A_{rectangle} = FC_R$$

Area of the wedge:

$$A_{wedge} = \frac{\theta}{2\pi}\pi R_1^2$$

Reducing:

$$A_{wedge} = \frac{1}{2}R_1^2 cos^{-1}(\frac{F}{R_1})$$

Area of the triangle:

$$A_{triangle} = \frac{1}{2}F\sqrt{R_1^2 - F^2}$$

Quarter section area:

$$A_{section} = FC_R + \frac{1}{2}R_1^2 cos^{-1}\left(\frac{F}{R_1}\right) - \frac{1}{2}F\sqrt{R_1^2 - F^2}$$

Calculating the total port area:

$$A_{total} = 4 \cdot A_{section}$$

$$A_{total} = 4FC_R + 2R_1^2 cos^{-1}\left(\frac{F}{R_1}\right) - 2F\sqrt{R_1^2 - F^2} \qquad (B.12)$$

Burn Surface Equation – The burn surface area is calculated by determining the instantaneous perimeter of a cylinder cross-section. For a cylindrical stage, the burn surface area is calculated by multiplying the cylinder height and the burn perimeter. For a conical stage the same calculation is made for each incremental cylinder and summed up to approximate the burn surface area. The burn perimeter is calculated in terms of the parameters defined in Figures B.10 and B.12. The perimeter for a section is:

$$S_{section} = L_{slot} + L_{arc}$$

where S is perimeter and L is length. Figure B.12 illustrates how these lengths are calculated. The wedge angle, θ, is the same as before:

$$\theta = cos^{-1}\left(\frac{F}{R_1}\right)$$
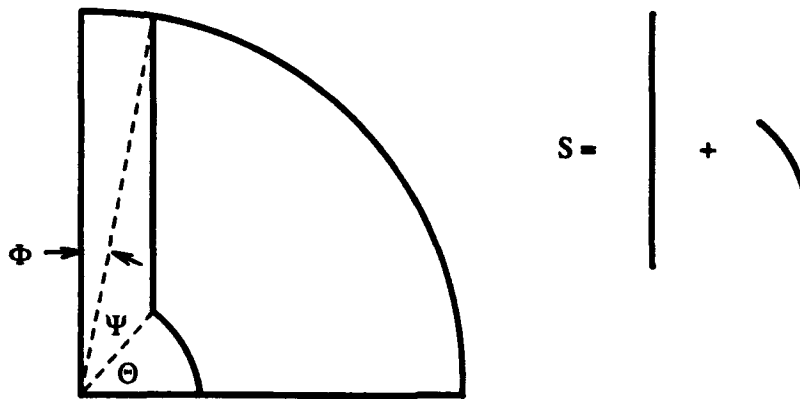
Figure B.12. Calculation of Slotted Tube Section Perimeter

The complement of the wedge angle, ψ, is:

$$\psi = sin^{-1}\left(\frac{F}{R_1}\right)$$

The slot angle, ϕ, is defined as:

$$\phi = sin^{-1}\left(\frac{F}{C_R}\right)$$

The slot edge length formed by the truncation of the slot by the case and tube is:

$$L_{slot} = C_R cos(\phi) - R_1 cos(\psi)$$

Substituting:

$$L_{slot} = C_R cos\left(sin^{-1}\left(\frac{F}{C_R}\right)\right) - R_1 cos\left(sin^{-1}\left(\frac{F}{R_1}\right)\right)$$

The arc length is:

$$L_{arc} = R_1 \theta$$

Substituting:

$$L_{arc} = R_1 cos^{-1}\left(\frac{F}{R_1}\right)$$

The total section perimeter is therefore:

$$S_{section} = C_R cos\left(sin^{-1}\left(\frac{F}{C_R}\right)\right) - R_1 cos\left(sin^{-1}\left(\frac{F}{R_1}\right)\right) + R_1 cos^{-1}\left(\frac{F}{R_1}\right)$$

Calculating the total perimeter:

$$S_{total} = 4 \cdot S_{section}$$

Substituting:

$$S_{total} = 4\left[C_R cos\left(sin^{-1}\left(\frac{F}{C_R}\right)\right) - R_1 cos\left(sin^{-1}\left(\frac{F}{R_1}\right)\right) + R_1 cos^{-1}\left(\frac{F}{R_1}\right)\right] \qquad (B.13)$$

The burn surface perimeter is recalculated during the performance model for each time increment. The values for F and R_1 are increased by the burn distance for the preceding time increment:

$$\Delta d = r \cdot \Delta t$$

Where Δd = burn distance in Δt and r = burn rate, assumed constant for Δt.

Therefore:

$$F_{new} = F_{old} + \Delta d$$

and

$$R_{1_{new}} = R_{1_{old}} + \Delta d$$

In this manner, the varying burn surface area is calculated as the burn progresses.

B.4.2.3 Performance Characteristics. The slotted tube grain design provides a regressive burn profile. An example of how the burn surface area changes with time is shown in Figure B.13.

The corresponding thrust profile is similar, and is shown in Figure B.14.
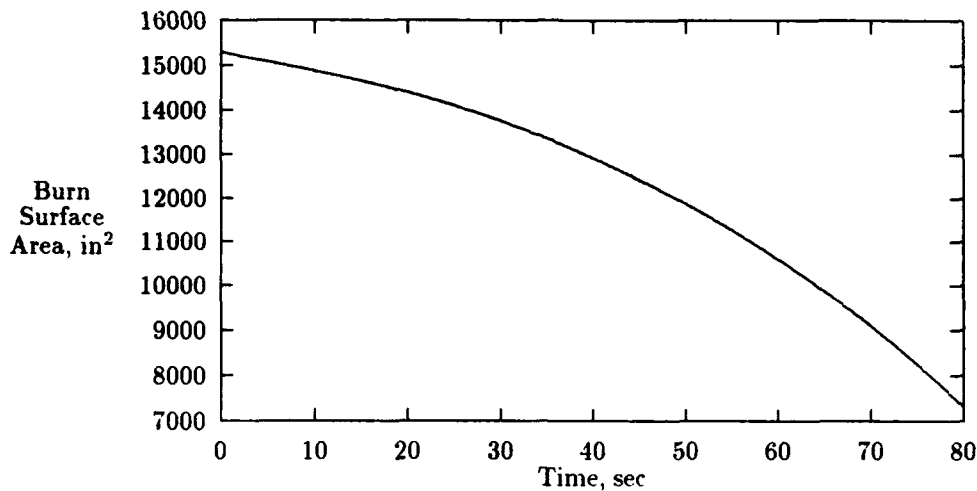
Figure B.13. Typical Slotted Tube Burn Surface Time History

A key feature of this grain design's regressive thrust profile is that the curve is convex instead of concave, like an exponential function. The burn tapers off at a reasonable rate, rather than quickly diminishing asymptotically to zero thrust. This results in a burn profile which terminates while still providing a significant level of thrust. As will be illustrated later, this is a major advantage of the slotted tube over other regressive grain designs.

B.4.3   Multiple-Slotted Regressive Grain Designs. Another regressive grain design considered is a slotted pattern with more than two slots. This pattern, illustrated in Figure B.15, consists of slots with semi-circular ends radiating from the center of the case cross-section. If the slot length is equal to the case radius, then the triangular regions between the slots burn away in a regressive manner. If the slots do not initially extend to the case wall, then the burn profile will start off progressive until the slots reach the wall and then continue regressively.

A circular central radius may be included, but will disappear as the slot edges intersect during the burn. Since they do not add much to the design, they were left out of the analysis.

B.4.3.1   Burn Equations. As with all central-burning grain designs, the initial port area and burn perimeter function must be calculated. It is convenient to divide the grain into $2 \cdot N$

B-24
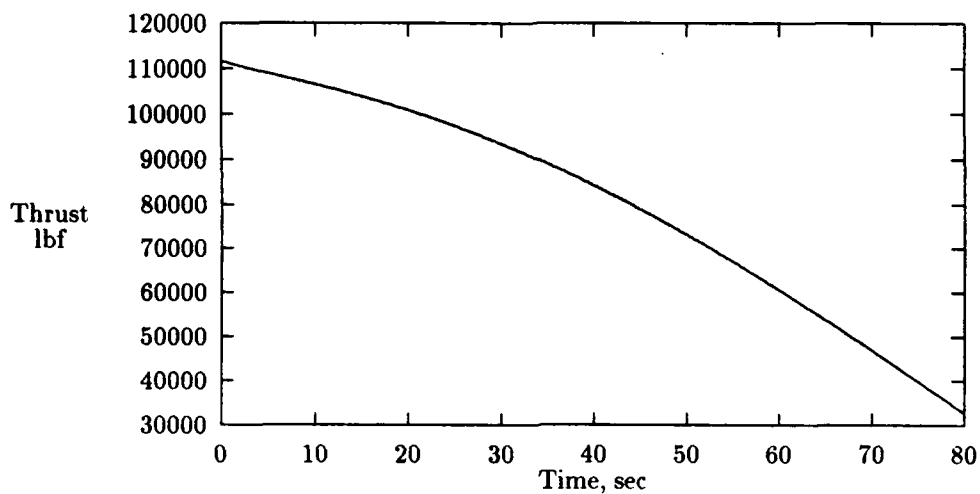
Figure B.14. Typical Slotted Tube Thrust Profile

equal wedges, where N is the number of slots. Figure B.16 shows a sectional element for a three-slot grain design. The port area easily calculated by:

$$2N\left(\frac{\pi f^2}{4} + f(l - \frac{f}{tan\theta}) + \frac{f^2}{2}tan\theta)\right) \tag{B.14}$$

The burn surface area is calculated as a function of f, half the slot thickness. As this distance grows the grain transitions through three burn regions labeled in Figure B.16.

Burn Region 1: Valid for $f \leq (C_R - l)$

Burn perimeter for region 1:

$$S_{region1} = 2N(\frac{\pi f}{2} + (l - \frac{f}{tan\theta})) \tag{B.15}$$

Burn Region 2: Valid for $(C_R - l) \leq f \leq \sqrt{C_R^2 - l^2}$

B-25
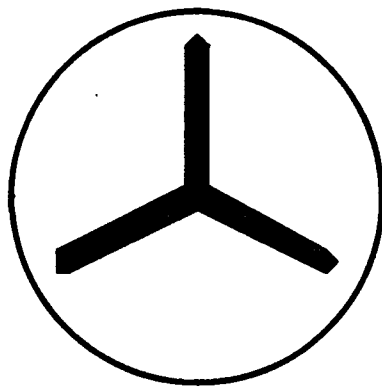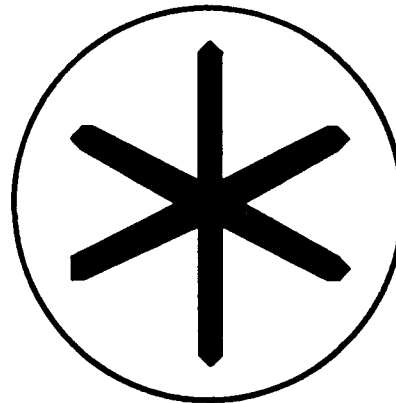
<center>3-Slotted Grain Design   6-Slotted Grain Design</center>

<center>Figure B.15. Multiple-Slotted Grain Designs</center>

Burn perimeter for region 2, using orthogonal projections to calculate the angles necessary to calculate the arc length (37:p251):

$$S_{region2} = 2N \left[l - \frac{f}{tan\theta} + f \left(\frac{\pi}{2} - cos^{-1} \left(\frac{f^2 + C_R^2 - l^2}{2C_R f} \right) - cos^{-1} \left(\frac{l^2 + C_R^2 - f^2}{2C_R l} \right) \right) \right] \quad (B.16)$$

Burn Region 3: Valid for $f \geq \sqrt{C_R^2 - l^2}$

Burn perimeter for region 3:

$$S_{region3} = 2N \left(l - \frac{f}{tan\theta} - (f - \sqrt{C_R^2 - l^2}) \right) \quad (B.17)$$

These burn equations are implemented in the propulsion model. The current half slot thickness determines which burn region the grain is currently in, and the model uses the appropriate perimeter equation.

> *B.4.3.2 Performance Characteristics.* There are many possible different combinations of the burn parameters: slot thickness, slot length, and number of slots. Several different combinations of these parameters yield approximately the same total impulse. However, several drawbacks to this grain pattern make it only marginally successful.

<center>B-26</center>
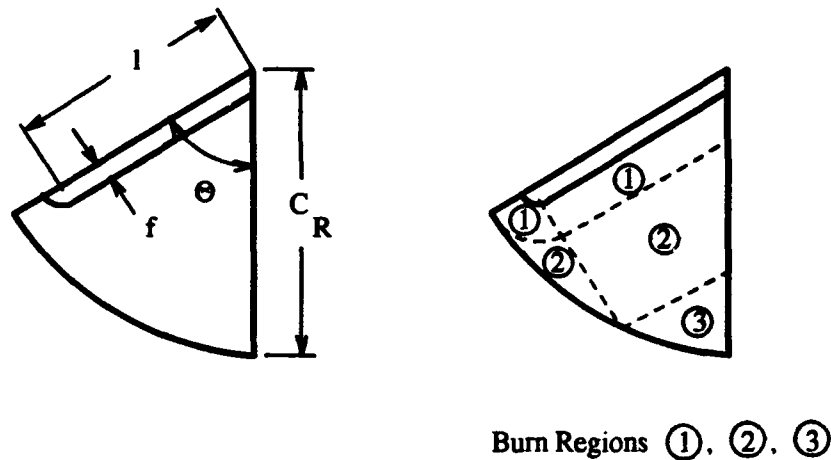
Burn Regions ①. ②. ③

Figure B.16. Multi-Slot Grain Pattern Section and Burn Regions

Once the burn becomes regressive, as it must to prevent excessive accelerations at the end of the burn, the thrust level drops off quickly. The thrust decreases almost exponentially, and becomes asymptotic to zero thrust. Figure B.17 illustrates this rapid decline in thrust once the slot burns to the case.

Operating at such a low thrust level while experiencing the effects of a gravity field does not provide much additional performance. Therefore, the thrust probably should be terminated prior to complete combustion. This of course wastes some of the propellant and leaves the total impulse short of the required value. This aspect of the slotted grain design makes the slotted tube a more attractive grain design selection.

B.4.4 Endburning Grain Designs. Endburning grain designs were originally considered in an attempt to get a neutral burn with a longer burn time than the star pattern. The burn surface area on an end burner remains constant: the cross-sectional area of the grain. Of course, this is only true for a cylindrical stage. Conical endburners will have the thrust drop off regressively as the burn progresses up to the thinner portion of the grain. Unfortunately, the endburning stages are limited in the surface area available to burn. The cross-sectional area of a cylindrical stage with diameter of 64 inches is about 3200 in^2. The resulting low mass generation rate makes for low thrust values, as seen in Figure B.18. In order to get the required total impulse out of the stage, burn times of several hundred seconds are necessary. For orbital maneuvers this burn time may
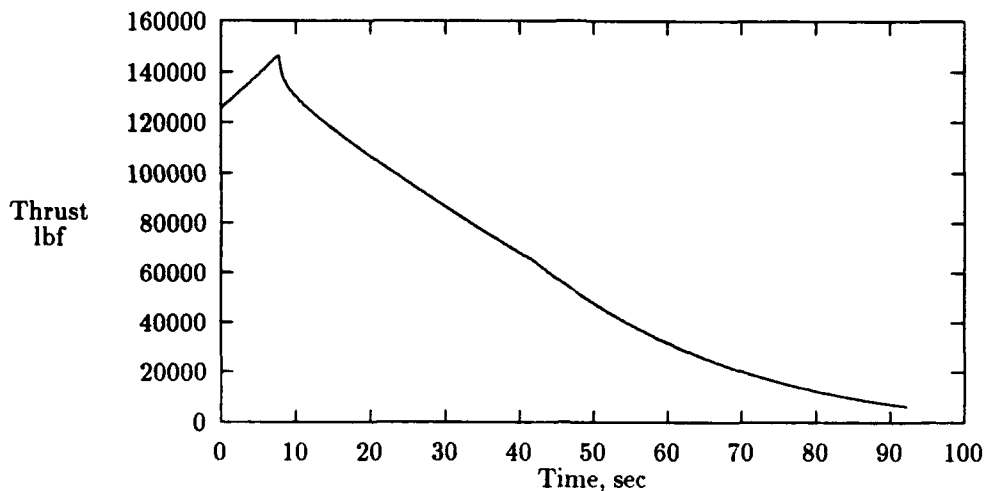
Figure B.17. Typical Multi-Slot Thrust Profile

be acceptable, but for an ICBM stage, the long burn is unacceptable. The effect of gravity during the burn as well as thrust vector control system limitations make a long burn time infeasible for an ICBM stage.

B.4.4.1   Modified Endburners. In an attempt to provide more thrust from endburning designs, modifications to the initial end shape were investigated. Instead of a flat bottom to the grain, parabaloids, ellipsoids, and even star-pattern tubes of varying height were analyzed. The resulting burn patterns are regressive. As the grain burns upward, the curvature to the grain-end becomes less and less, until the area approaches the circular cross-sectional area. This provides a regressive burn, but unfortunately, the thrust drops off too quickly and the burn time is still too long (see Figure B.19).

B.4.5   Programs. The propulsion performance calculations are performed in two separate computer models: one each for a cylindrical and conical stage. Either ISC or conventional technologies are used in either program. The different propellant parameters and system efficiencies are defined according to the selection of which type of technology. This decision is made by the user when prompted by the program. Each program is written in FORTRAN-77.
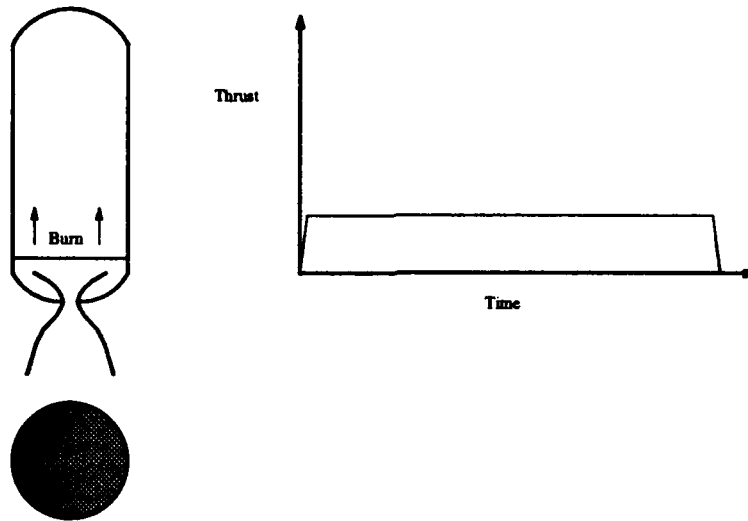
Figure B.18. Endburner Grain Design and a Typical Thrust Profile

There are several of each type of program, one for each different grain type considered and analyzed:

- slotted tube

- multi-slot

- endburner

- modified endburner (various modifications)

The version for the slotted tube grain design with a cylindrical stage is called SLOT. The version for the slotted tube grain design with a conical stage is SLOTCONE. SLOT is a subset of SLOTCONE in that the latter includes an extra loop to sum up the surface area and volume of a series of cylinders used to approximate the conical-shaped stage. The following is a listing of SLOTCONE.

```
        PROGRAM SLOTCONE
*
****************************************************************
*       This program will calculate the mass flow, pressure,
*       and thrust time histories for a conical missile stage.
*       The cone's base and top diameters, mass of propellant,
*       propellant parameters and nozzle throat area are
*       requred.  A regressive single slot design with a
*       central radius will be used, otherwise known as a
*       slotted tube.
****************************************************************
        REAL MP,ME,M,MDOT,MBAR,K,N,ISP,MPAY,MSTR,LCONE,D(500)
```
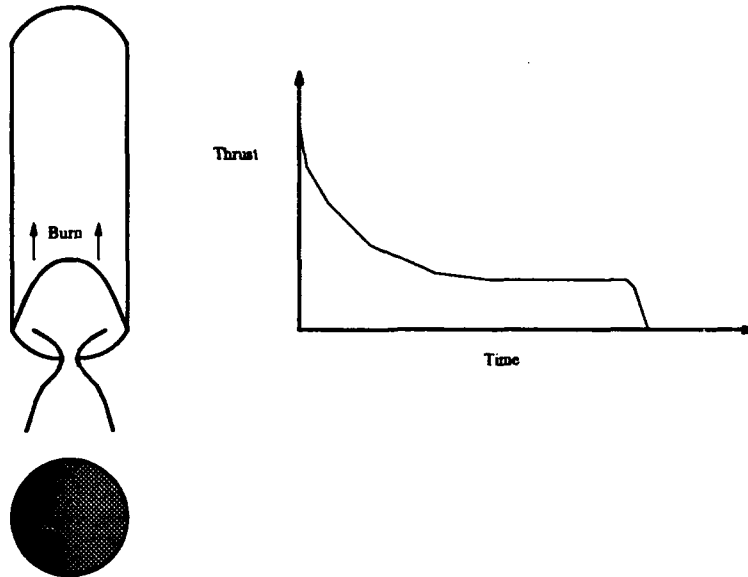
Figure B.19. Modified Endburner Grain Design and a Typical Thrust Profile

```
REAL F(500),R1(500),APORT(500)
INTEGER ANSWER
OPEN(UNIT=8,FILE='pchamber',STATUS='UNKNOWN')
OPEN(UNIT=9,FILE='burnarea',STATUS='UNKNOWN')
OPEN(UNIT=10,FILE='dougdata',STATUS='UNKNOWN')
OPEN(UNIT=11,FILE='accel',STATUS='UNKNOWN')
OPEN(UNIT=12,FILE='dvector')
OPEN(UNIT=13,FILE='f')
OPEN(UNIT=14,FILE='r1')
OPEN(UNIT=16,FILE='aport')
OPEN(UNIT=15,FILE='massprop',STATUS='UNKNOWN')
OPEN(UNIT=17,FILE='output',STATUS='UNKNOWN')
*
*    Input the mass of Propellant
*
PRINT*,'ENTER THE MASS OF PROPELLANT IN LBM'
READ*,MP
*
*    Input mass of payload for acceleration calculation
*
PRINT*,'ENTER THE MASS OF PAYLOAD IN LBM'
READ*,MPAY
*
*    Input structural ratio for acceleration calculation
*
PRINT*,'ENTER THE STRUCTURAL RATIO'
READ*,EPSILON
*
*    Calculate structural mass
*
MSTR=EPSILON*MP/(1-EPSILON)
*
*    Input grain cylinder diameters, base and top
*
```

```
      PRINT*,'ENTER THE GRAIN CONE BASE DIAMETER, INCHES'
      READ*,DBASE
*
      PRINT*,'ENTER THE GRAIN CONE TOP DIAMETER, INCHES'
      READ*,DTOP
*
*     Calculate the inner case radius
*
      CR=DBASE/2
*
*     Input nozzle throat area
*
      PRINT*,'ENTER THE NOZZLE THROAT AREA IN SQ. INCHES'
      READ*,AT
*
*     Input the slot half thickness
*
      PRINT*,'ENTER HALF THE SLOT THICKNESS (CONE BASE)'
      READ*,FBASE
      F0=FBASE
*
*     Input the central radius
*
      PRINT*,'ENTER THE CENTRAL RADIUS (CONE BASE)'
      READ*,R1BASE
      R10=R1BASE
*
*     Input the ambient pressure, assumed low and constant
*     for 2nd stage
*
      PRINT*,'ENTER THE AMBIENT PRESSURE IN PSIA, (< 2)'
      READ*,PA
*
*     Input the time increment
*
      PRINT*,'ENTER THE TIME INCREMENT IN SECONDS'
      READ*,DT
*
*****************************************************************
*     This part of the program will define initial parameters
*     depending on the choice of integrated stage concept or
*     conventional technologies
*****************************************************************
*
*     Choose ISC or Conventional missile technologies
*
      ANSWER=1
      RBAR=1545.43
      PI=3.14159
      PRINT*,'ENTER 1 FOR ISC, 0 FOR CONVENTIONAL'
      READ*,ANSWER
*
*****************************************************************
*     If this is an ISC stage then define the propellant
*     parameters, efficiencies, and temperatures
*     corresponding to Boron based propellant and ISC
*     technologies
*****************************************************************
*
*     Boron Propellant and Forced-Deflection Nozzle Numbers
*
```

```
        IF(ANSWER.EQ.1)THEN
                A=.02145
                N=.4
                MBAR=25.5
                K=1.22
                RHOP=.0647
                T2=5637
                ETANOZ=.98
                ETAPROP=.94
                CP=336.083
                QR=2023680
*
*       Calculate the nozzle exit area for reverse dome FD
*       nozzle
*
                AE=PI*DBASE**2/4
        ELSE
                A=.025238
                N=.4
                MBAR=29.4
                K=1.17
                RHOP=.064131
                T2=6366
                ETANOZ=1.0
                ETAPROP=.89
                CP=361.775
                QR=2555560
                PRINT*,'ENTER THE NOZZLE EXIT AREA, IN^2'
                READ*,AE
        ENDIF
*
********************************************************
*       Sizing the Stage:  Calculate the cone height based on
*       the known propellant volume and cone base & top
*       diameters. The cone will be approximated by
*       J number of cylinders with diameters varying from
*       DBASE to DTOP.
********************************************************
*       Fill the arrays for diamters (D), half slot
*       thickness (F), and central radius (R1).
*
        PRINT*,'ENTER # OF CYLINDERS TO APPROX. THE CONE, <500'
        READ*,J
*
*       Web thickness must be constant for each cylinder,
*       so it must be calculated at the cone base and used
*       to determine each cylinders central radius.  The F:R1
*       ratio will be the same for each cylinder.
*
        WEB=DBASE/2-R1BASE
*
        DO 15 I=1,J
                D(I)=DBASE-(I-1)*(DBASE-DTOP)/J
                R1(I)=D(I)/2-WEB
                F(I)=R1(I)*FBASE/R1BASE
 15     CONTINUE
*
*       Calculate the height of the cone by equating the volume
*       of propellant to the total volume of each cylinder minus
*       each cylinder's port volume.
*
```

```
*       Calculate the volume of propellant
*
        VP=MP/RHOP
*
*       Assuming that 100% of the propellant is in the cone
*       then calculate the cone height.
*
        DENOM=0
        DO 20 I=1,J
                APORT(I)=4*F(I)*D(I)/2+2*ACOS(F(I)/R1(I))*
     +                   R1(I)**2-2*F(I)*SQRT(R1(I)**2-
     +                   F(I)**2)
                DENOM=DENOM+D(I)**2*PI/4-APORT(I)
  20    CONTINUE
*
*       Calculate cylinder's height
*
        H=VP/DENOM
*
*       Cone height:
*
        LCONE=H*J
*
*       Calculate gas constant
*
        RGAS=RBAR/MBAR
*
*
*       Define the initial propellant temperature
*
        T1=527
*
********************************************************************
*       Iterate to find the nozzle exit Mach number.
*       First calculate the expansion ratio, then use a
*       gradient search to iterate on the expansion ratio /
*       Mach number equation to find Mach number.
********************************************************************
*
        E=AE/AT
*
*       Initial guess for exit mach number
*
        ME=2
*
*       Set up continue loop structure to iterate
*
  50    CONTINUE
        VALUE=(2/(K+1)*(1+(K-1)/2*ME**2))**((K+1)/(2*(K-1)))/ME
        DIFF=E-VALUE
*
*       Calculate the derivative of the Mach number equation
*
        DM=2*((K+1)/(2*(K-1)))*(2/(K+1)*(1+(K-1)/2*ME**2))**
     +  ((3-K)/(2*(K-1)))-(2/(K+1)*(1+(K-1)/2*ME**2))**((K+1)/
     +  (2*(K-1)))/ME**2
        DIFF2=DIFF**2
        IF(DIFF2.LE.0.001)GO TO 55
        ME=ME+DIFF/DM
        GO TO 50
  55    CONTINUE
```

```
*
******************************************************************
*        This section will be a large IF-WHILE loop which will
*        start with initial geometry and step through the burn
*        process with delta-time increments.
******************************************************************
*
*        Set initial parameters
*
         T=0
         M=0
         TI=0
         AB=0
         ACMAX=0
*
*        Calculate initial burn surface area
*
         DO 25 I=1,J
                 CR=D(I)/2
                 AB=AB+4*H*(CR*COS(ASIN(F(I)/CR))-
     +               R1(I)*COS(ASIN(F(I)/R1(I)))+
     +               R1(I)*ACOS(F(I)/R1(I)))
   25    CONTINUE
*
                 WRITE(9,*)T,AB
*
*        Calculate inital chamber pressure
*
         WRITE(8,40)
         G=32.174
         PC=((AB*A*RHOP)/(AT*G*((K*(2/(K+1))**((K+1)/(K-1)))/
     +      (RGAS*T2*G))**.5))**(1/(1-N))
         WRITE(8,*)T,PC
         PCMAX=PC
*
*        Calculate inital mdot
*
         MDOT=AT*PC*G*SQRT(K)*(2/(K+1))**((K+1)/(2*(K-1)))/
     +    SQRT(RGAS*T2*G)
*
*        Calculate nozzle exit pressure
*
         PE=PC/(1+((K-1)/2)*ME**2)**(K/(K-1))
*
*        Calculate nozzle exit velocity
*
         UE=(CP*2*G*(T1+QR/CP)*(1-(PE/PC)**((K-1)/K)))**.5
         UE=UE*ETANOZ*ETAPROP
*
*        Calculate motor ISP
*
         ISP=(UE+(PE-PA)*AE/MDOT)/G
*
*        Calculate the inital thrust
*
         THRUST=MDOT*ISP
         WRITE(10,40)
   40    FORMAT('data = [')
         WRITE(10,*)T,THRUST,MDOT
*
******************************************************************
```

```
*          Start the incremenal burning process; will continue
*          as long as the total burned mass is less than the
*          specified mass of propellant
****************************************************************
*
  60      IF(M.LE.MP)THEN
*
*          increment time by DT
*
              T=T+DT
*
*          Calculate burn rate, R
*
              R=A*PC**N
*
*          Calculate the burn distance during delta-t
*
              DD=R*DT
*
*          Perform loop to calculate the burn surface area
*
          AB=0
          DO 30 I=1,J
*
*              Calculate the new slot half thickness
*
              F(I)=F(I)+DD
*
*              Calculate the new central radius
*
              R1(I)=R1(I)+DD
*
              CR=D(I)/2
*
*          Calculate the new burn surface area
*
          IF(R1(I).LE.CR)THEN
*
              AB=AB+4*H*(CR*COS(ASIN(F(I)/CR))-
     +             R1(I)*COS(ASIN(F(I)/R1(I)))+
     +             R1(I)*ACOS(F(I)/R1(I)))
          ELSE
              GO TO 65
          ENDIF
*
  30      CONTINUE
*
              WRITE(9,*)T,AB
*
*          Calculate the new chamber pressure for this increment
*
          PC=((AB*A*RHOP)/(AT*G*((K*(2/(K+1))**((K+1)/(K-1)))/
     +      (RGAS*T2*G))**.5))**(1/(1-N))
*
*          is this the maximum pressure?
*
              IF(PC.GT.PCMAX)THEN
                  PCMAX=PC
              ENDIF
*
              WRITE(8,*)T,PC
```

```
*
*         Calculate new mdot for this increment
*
          MDOT=AT*PC*G*SQRT(K)*(2/(K+1))**((K+1)/(2*(K-1)))/
     +    SQRT(RGAS*T2*G)
*
*         Calculate new nozzle exit pressure for this increment
*
                PE=PC/(1+((K-1)/2)*ME**2)**(K/(K-1))
*
*         Calculate nozzle exit velocity for this increment
*         (should be same for entire burn)
*
          UE=(CP*2*G*(T1+QR/CP)*(1-(PE/PC)**(((K-1)/K))))**.5
          UE=UE*ETANOZ*ETAPROP
*
*         Calculate motor ISP for this increment (should be same)
*
          ISP=(UE+(PE-PA)*AE/MDOT)/G
*
*         Calculate the new thrust for this increment
*
                THRUST=MDOT*ISP
*
                WRITE(10,*)T,THRUST,MDOT
*
*         Calculate the mass burned up to this time increment
*
                M=M+MDOT*DT
*
                WRITE(15,*)T,M
*
*         Calculate total impulse up to this time increment
*
                TI=TI+THRUST*DT
*
*         Calculate the acceleration in g's;
*         is this the max acceleration?
*
                ACCEL=THRUST/(MP-M+MPAY+MSTR)
                IF(ACCEL.GT.ACMAX)THEN
                        ACMAX=ACCEL
                ENDIF
*
                WRITE(11,*)T,ACCEL
*
*         Loop back and check if M < Mp
*
                GO TO 60
          ENDIF
   65     CONTINUE
*
*         Calculate average diameter, final radius, and
*         central radius
*
          DAVG=(DBASE+DTOP)/2
          FAVG=(F(1)+F(J))/2
          R1AVG=(R1(1)+R1(J))/2
*
          WRITE(10,68)
          WRITE(8,68)
```

```
   68    FORMAT('];')
*
***************************************************
*       Write output to file
***************************************************
*
        WRITE(17,70)
   70   FORMAT('RESULTS')
        WRITE(17,80)M,TI,LCONE,T,UE,ISP,PCMAX,ACMAX,
     +              FO,R10,DAVG,FAVG,R1AVG
   80   FORMAT('MASS OF PROP. =',2X,F9.2,2X,'LBM'
     +  /'TOTAL IMPULSE =',2X,E13.6,2X,'LBF-SEC'
     +  /'LENGTH OF CYLINDER =',2X,F10.2,2X,'INCHES'
     +  /'BURN TIME =',2X,F6.2,2X,'SECONDS'
     +  /'EXIT VELOCITY =',2X,F8.2,2X,'FT/S'
     +  /'ISP =',2X,F6.2,2X,'LBF-SEC/LBM'
     +  /'MAXIMUM PRESSURE =',2X,F8.2
     +  /'MAXIMUM ACCELERATION = '2X,F6.2,2X,'G'S'
     +  /'INITIAL SLOT HALF THICKNESS, BASE =',2X,F8.2,2X,'IN.'
     +  /'INITIAL CENTRAL RADIUS, BASE =',2X,F8.2,2X,'IN.'
     +  /'AVERAGE CONE RADIUS =',2X,F8.2,2X,'IN.'
     +  /'AVERAGE FINAL HALF SLOT =',2X,F8.2,2X,'IN.'
     +  /'AVERAGE FINAL CENTRAL RADIUS =',2X,F8.2,2X,'IN.')
*
*       terminate program
*
        STOP
        END
```

Appendix C. *Structural, Thermal, and Materials Design*

C.1 *Introduction*

The four subsystems in the *NEMESIS* Structural, Thermal, and Material (STM) design are the external protective material (EPM), case, internal insulation, and liner. Figure C.1 shows a cross sectional view and Figure C.2 shows the linear relationship of the four subsystems to each other.
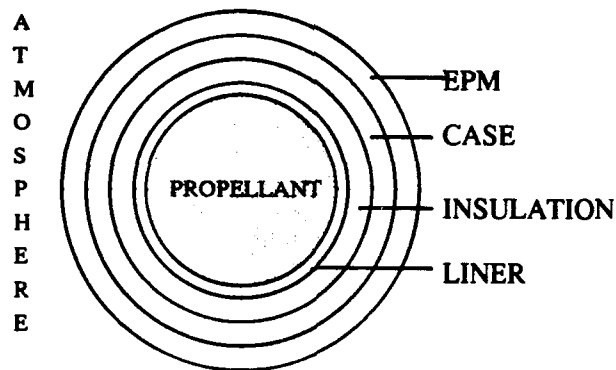
Figure C.1. STM Cross Sectional Interfaces

Basic functions of each subsystem include the EPM protecting the case from atmospheric debris impact and aerodynamic heating effects while the case provides the missile's basic structural properties needed to withstand the extreme in-flight loading conditions. Internal insulation protects the case from the high temperature combustion of the propellant. Finally. the liner provides the bond between propellant and insulation, and prevents age-limiting chemical reactions. Each subsystem performs a function in maintaining the structural integrity of the missile. If one of these subsystems fails to perform its task, a complete mission failure results.

C.2 *Scope*

This appendix covers the research, analysis, simplified models, and preliminary designs of the four subsystems required for structural and thermal integrity of *NEMESIS*. The outcome of the research effort was a realization of key attributes that required modeling and potential approaches to modeling. The underlying purpose for the analysis and models was to allow for preliminary design determination. As a result, many simplifying assumptions were made, and they will be

```
A                                        I                      P
T                                        N                      R
M                   E          C          S          L          O
O                   P          A          U          I          P
S                   M          S          L          N          E
P                              E          A          E          L
H                                         T          R          L
E                                         I                     A
R                                         O                     N
E                                         N                     T
```
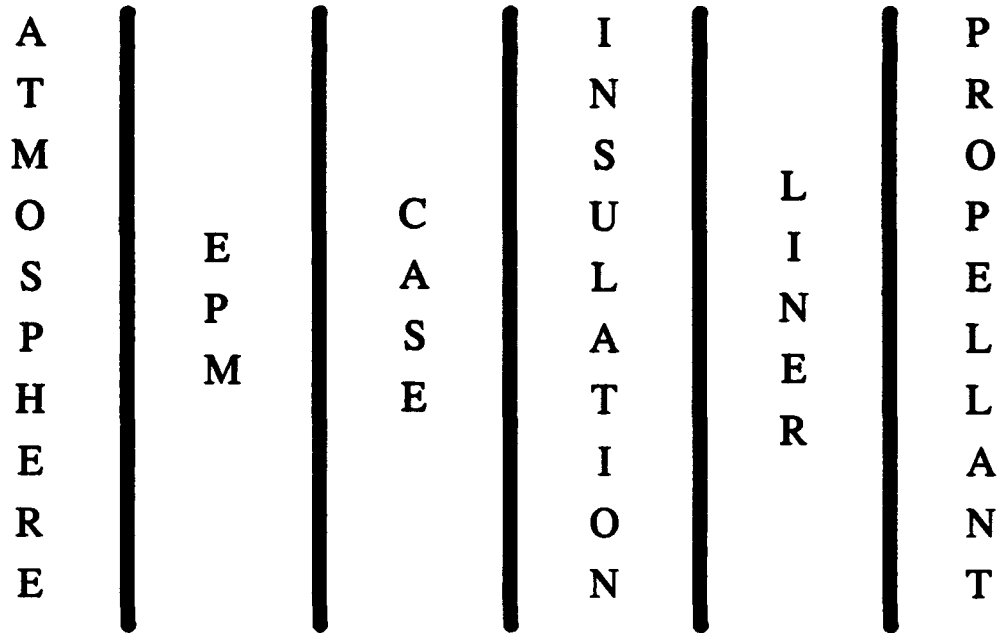
Figure C.2. STM Interfaces

introduced where appropriate. The simplified models allowed for exploration of the *NEMESIS* design space, and ultimately the definition of four *optimal* missile designs.

The availability and cost aspects of the *NEMESIS* STM design are addressed from a qualitative standpoint. The detailed availability and cost analysis are covered in other portions of this document. In addition to being cost-effective and reliable, the *NEMESIS* STM design must be producible using conventional processing techniques. This appendix addresses the STM design manufacturing process and the cost and reliability benefits associated with the approach. The first stage of *NEMESIS* is constrained to be the current MM III first stage. To prevent exceeding the structural capability of the MM III first stage, the *NEMESIS* second stage and payload weight is limited to the current 27,000 pound limit of the MM III second and third stages and payload.

C.3   Feasibility Study and Results

The first task of the design group was to determine the feasibility of the project based on preliminary analysis and prior studies. Thus, a feasibility study was initiated to determine if

Table C.1. Structural Ratios of Various Systems

Document	Diameter (inches)	Stage	SR
AFRPL-TM-82-25 (Dec 82) *	26	1	0.08
	26	2	0.128
SAWE Paper No. 1838 (May 88) **	92	1	0.06
	92	2	0.091
	92	3	0.1
	46	1	0.073
	46	2	0.089
Philips Lab (Mar 91) ***	46	1	0.077
	46	2	0.11
	46	3	0.123
	46	1	0.068
	46	2	0.076
	51.7	1	0.065
	51.7	2	0.073
Philips Lab (Jul 91) ****	50.3	1	0.065
	50.3	2	0.073

- * (34)
- ** (97)
- *** (83)
- **** (25)

previous design studies had been able to achieve structural ratios commensurate with those required. Structural ratio (SR) of a stage is defined as follows:

Define the following parameters:

- m_s - structural mass of the stage
- m_p - propellant mass of the stage

$$SR = \frac{m_s}{m_s + m_p}$$

Based on a preliminary trajectory analysis, using the ideal rocket equations and MM III data, a structural ratio of approximately 0.07 is required (see Chapter 1). Table C.1 shows representative structural ratios calculated from the designs presented in four reports that were reviewed.

All of these designs incorporated integrated stage technologies and some were able to achieve structural ratios below 0.07 for first stages. An initial concern was that 0.07 might not be possible on a second stage, because second stages in Table C.1 carry a higher structural ratio. However,

to meet performance requirements, the designed second stage had to be as large as some of the reported first stages, leading to the belief that the structural ratio required for the project was indeed feasible.

C.4 Case Design and Structural Model

This section documents the literature review and research performed to support the development of a case design for an integrated second stage booster. Questions that will be asked and answered range from "What is filament winding?" to "How can filament winding be used to produce a viable second stage?"

C.4.1 Background.

From early on in the design process, the selection of composites over metals was made for reasons ranging from weight savings to producibility. The method of manufacturing a rocket motor case focused on a technique known as *filament winding*. Filament winding is a technology often associated with composites but sometimes rarely understood despite its usage for numerous years. Numerous journals, magazines, and nearly every book dealing with composites outline the basic principles of filament winding. Filament winding was chosen as the primary method to design the integrated second stage as it is especially suited for the fabrication of rocket motor cases where internal operating pressure dictates the design and fabrication of the case. P.R. Evans explains filament winding by stating the process as one whereby "...alternating layers of *helix* or *polar* wraps with 90^0 or hoop wraps [are placed] onto a mandrel shaped to form the desired case interi. r profile." (38:p4A-3) The mandrel, the determiner of shape, permits a variety of designs, from spherical to conical to geodesic. (63:p449) A filament wound case is used in pressure vessel applications because of its ability to carry loads. Principally, the helical layers carry the axial loading whereas the hoop layers carry the internally generated hoop stress loads forming a sound vessel. Filament winding is accomplished by physically winding composite fiber in a "continuous band consisting of several tows or rovings" from one end of the mandrel to the other. Figure C.3 shows the general process of how composite cases are wound. (38:pp 4A-3 - 4A-10) In addition, a conventional rocket motor case is shown in Figure C.4. Shape is determined via the mandrel and openings at one or both ends are determined using *bosses*. In the rocket motor case, skirt attachments, the portions extending beyond the pressure vessel itself for interstage connections, can either be wound or laid as composite laminate.
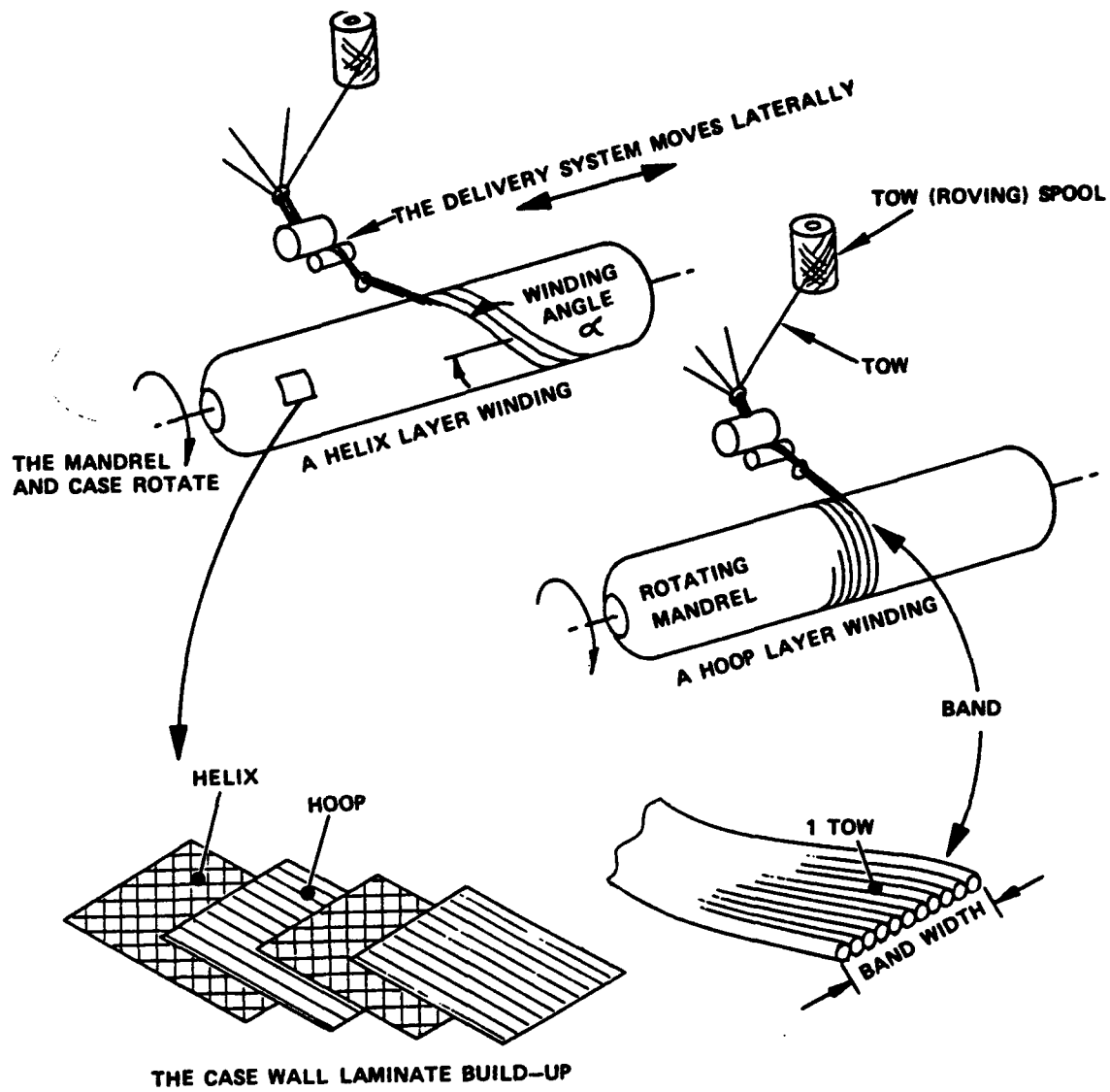
Figure C.3. Filament Winding Mandrel
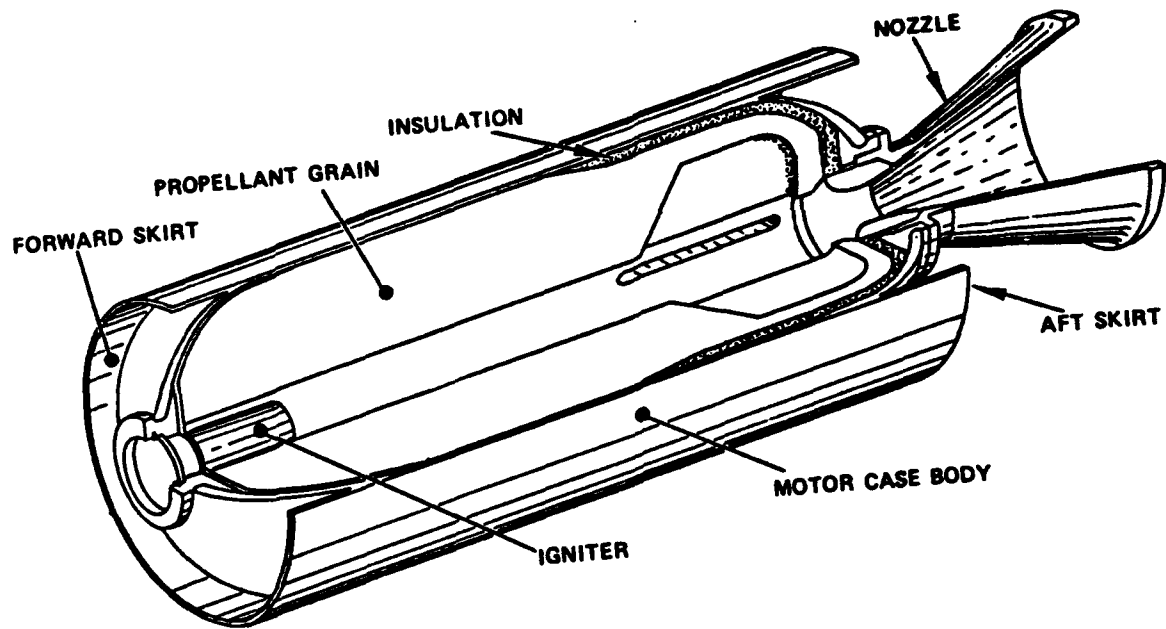
Figure C.4. A Conventional Rocket Motor Case

Filament winding can be accomplished in many ways. One way is for a spool of dry fiber to be passed through a resin bath as it is wound onto the mandrel. Secondly, the composite may already be immersed in the resin, a condition known as *preimpregnated*, and directly wound from the spool onto the mandrel. Lastly, and the most questionable method, is to wind the fiber dry onto the mandrel and soak it with resin primarily through vacuum pressure techniques. All of these methods must be evaluated prior to actually building a rocket motor case. After the case has been wound, a *curing* cycle occurs where the case forms a rigid vessel and the mandrel is removed.

Success with filament winding lies in understanding the anisotropic behavior of composites. Composites are "very strong and stiff in the direction of the fiber but [are] comparatively weak in other directions where only the resin matrix is available to resist loads." (38:p. 4A-2) A wide range of materials and properties exist and will be discussed in greater detail later in this appendix. However, the primary materials used in filament winding are graphites and carbons for fibers, with epoxies, polyesters, polyimides, and silicones used for resins. (93:p.449)

Filament winding exploits the unidirectional strength of composites by creating numerous load paths due to the helical and hoop layering process. Loading of the rocket motor case is not restricted to a single direction. Axial loads arise primarily in thrust and pressure and coexist with bending and internal pressure loads. The alternating layer process allows for a filament wind design to handle these varying loading conditions. However, "...in general, space motors and ballistic motors are dominated by internal pressure loads." (70:p.10) This key factor forms the basis for developing equations, shown later, to design a viable rocket motor case. Knowing the maximum expected operating pressure (MEOP), the designer, with material properties known, creates a filament wound design of sufficient thickness to withstand this load.

As mentioned earlier, filament winding has been used extensively for rocket motor cases for over two decades. J.P. Denost, in charge of the France's Aerospatiale Filament Winding Program, details the design and usage of filament wound rocket motor cases for the past 25 years. (30:p. 5-2) Here in the United States, filament winding has made its way onto space structures ranging from the Space Shuttle to the developmental Small ICBM and Peacekeeper missiles. In each instance, the advantages of composites over metals warranted design, development, and usage of filament wound structures to meet operational needs. The principal advantage is, of course, a weight savings.
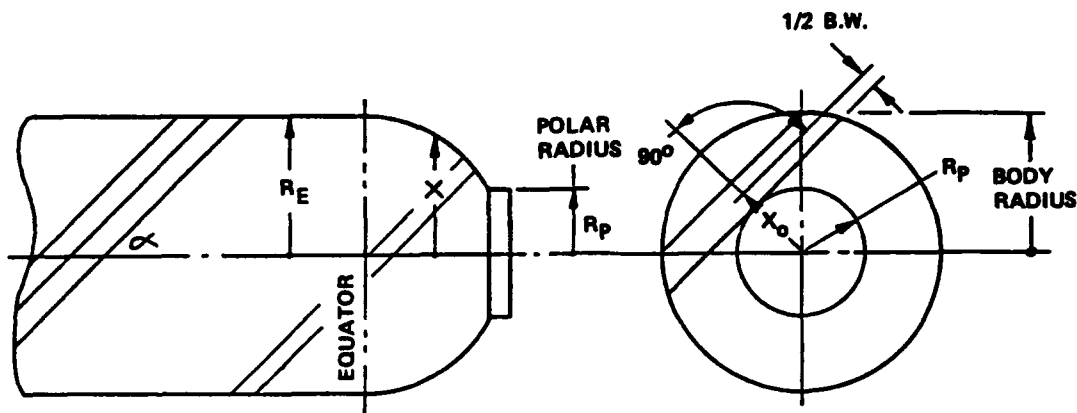
Figure C.5. Winding Angle is Crucial to Proper Case Builup

Composites are comparatively less dense than metals and coupled with design in loading paths, filament wound vessels are able to achieve a significant weight reduction for equally capable cases.

Nevertheless, there are numerous problems encountered with filament winding. First, determining the winding angle presents a challenge. The winding angle, or α, is the angle at which composite fiber is laid on the mandrel in the helical direction. With regards to a rocket motor case where an opening exists at the forward end to accommodate an igniter, the angle must be determined that will allow for a complete wrap of the vessel without overstressing the opening (see Figure C.5).

Secondly, determining material properties and actual delivered strength of the pressure vessel is an iterative process. Exact composite material properties may vary from batch to batch and are usually the result of existing microscopic flaws or environmental factors such as moisture and humidity. (93:p. 451) Stephen Swanson of the University of Utah examined this point in depth in his paper, *Strength Design Criteria for Carbon/Epoxy Pressure Vessels*. (100) His basic premise is well known: namely, the failure mode for composite structures lacks consistency in failure compared to

metals. The inconsistencies, he states, originate with micromechanical defects in individual fibers, variations in composite production, and/or differences in the bonding resin. (100:pp. 522-526) The basic conclusion compares predicted pressure vessel failure with actual failure. For the majority of design work, prediction failure based on normal stresses in the fibers is sufficient for analyzing the strength of pressure vessels. (100:p.526) A third problem that arises during the filament winding process is the difficulty of keeping uniform tension on the fibers. Finally, preventing fiber damage and making sure the fibers have sufficient shelf life during winding must be taken into consideration. These problems can be overcome for design and development of a viable rocket motor case.

Understanding how filament winding was used in the past is critical to understanding how to employ it in this design application. As mentioned earlier, the Small ICBM (SICBM) used filament winding techniques for production of its rocket motor case. The SICBM was originally a 30,000 pound ICBM upgraded to a 37,000 pound capability with a single warhead payload. Development of a filament wound pressure vessel was crucial to its successful operation. The SICBM first stage motor case is a filament wound carbon epoxy primary structure utilizing Amoco's T-40(810)/8P preimpregnated material system. The pressure vessel utilizes a variable angle helical (16.9^0 at the fwd datum and $29.5^0/32^0$ at aft datum) and 90^0 hoop plies, while the skirts incorporate unidirectional tape in 0^0 and plus/minus 45^0 orientations along with 90^0 filament wound hoop plies." (45:p. 13) The case used interspersed hoop and helical plies in order to *debulk* the case as it was fabricated resulting in a low void, high performance composite. (45:p. 13) Figure C.6 outlines the filament wound configuration of the 256 inch long SICBM case.

Filament winding has also seen application in the design and production of the Peacekeeper ICBM. Typical Stage I properties were a MEOP of 2385 psi and a cylinder length of 204 inches. Again, the design loads were withstood using a carbon epoxy filament wound pressure vessel. Because of the success with these designs in the past, i.e. the proven technology of filament winding, the *NEMESIS* second stage case design uses proven principles and tested concepts in developing a viable rocket motor case.

The method used to determine a minimum composite thickness for the integrated second stage is called *netting analysis*. The Handbook of Composites defines netting analysis as "...a simplified procedure used mainly to estimate fiber stress in a cylindrical vessel subject to internal pressure. This method is based on the assumptions that only the reinforcing fibers have a load
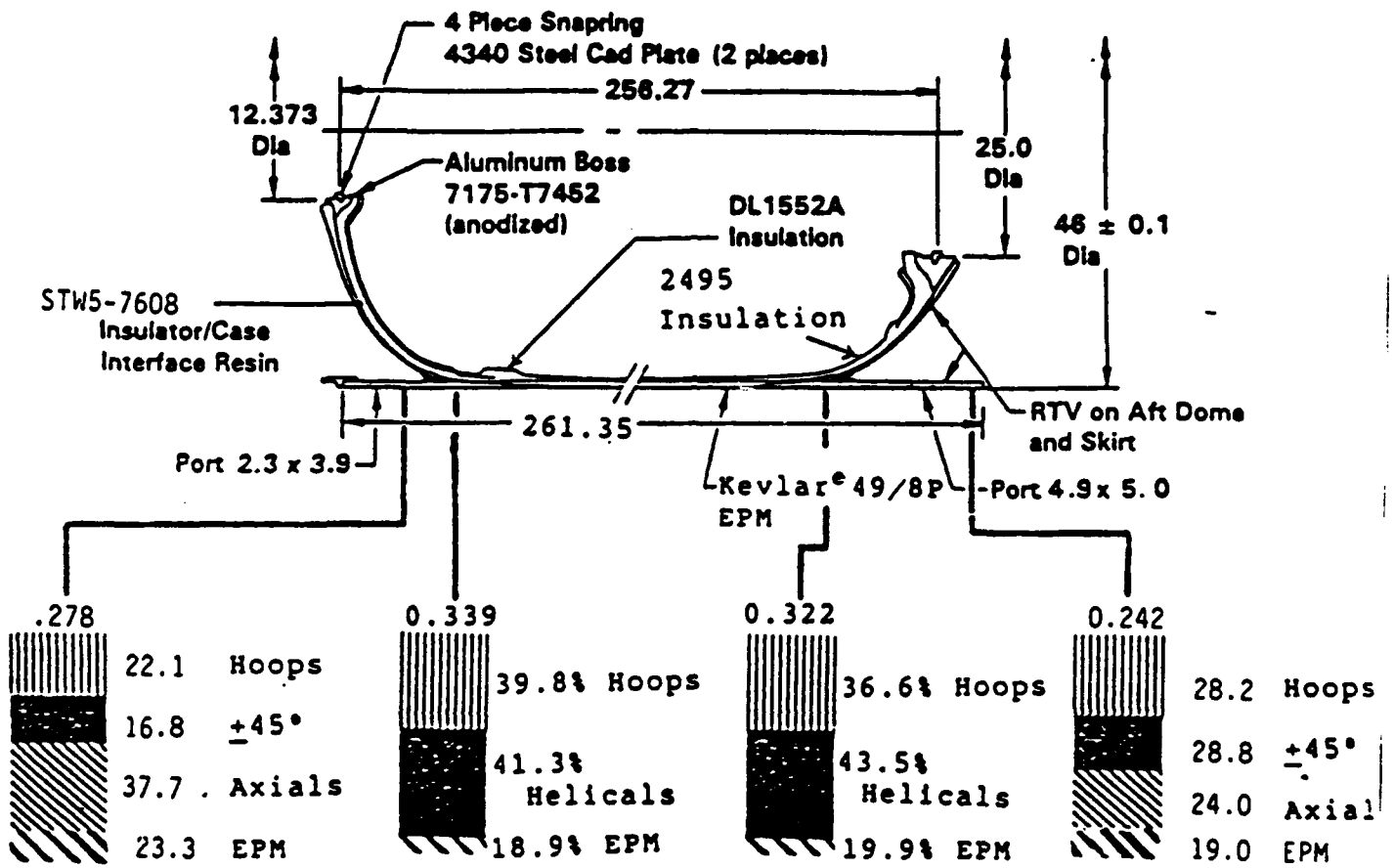
Figure C.6. The SICBM Composite Case Layup

carrying capability and that all fibers are uniformly stressed in tension." (93:p. 468) Though not quite as advanced as a finite element analysis, netting analysis does allow the designer some insights into the workings of a filament wound pressure vessel. The netting analysis procedure adapted for this study first determines a minimum thickness, divided into hoop and helical plies, to withstand internal pressure loads. Figure C.7 outlines the netting analysis procedure. (104:p. 6-12) With knowledge of shape, each step builds upon the other to design a filament wound pressure vessel using netting analysis. Next, an examination of buckling criteria ensues along with the defining of some geometric properties. Finally, a weight is estimated based on thickness, length, and density of the case.

The following equations were developed by P.R. Evans and are presented in several papers including his *Composite Motor Case Design*. (38:p. 4A) Given the radius of the pressure vessel and the MEOP, axial and hoop line loads are calculated and converted into minimum thicknesses based strictly on fiber properties, i.e. contributions from the resin are ignored.

Define the following parameters:

- t_α - helix fiber thickness (in)
- t_{90} - hoop fiber thickness (in)
- σ_α - helix fiber tensile strength (psi)
- σ_{90} - hoop fiber tensile strength (psi)
- N_ϕ - axial line load (lb/in)
- N_θ - hoop line load (lb/in)
- P - internal pressure (psig)
- R - radius (in)
- α - helix winding angle (^{o})
- t - total thickness (in)
- E - Young's Modulus (psi)
- ν - Poisson's Ratio (dimensionless)

$$N_\phi = \frac{PR}{2} \qquad N_\theta = PR$$

$$t_\alpha = \frac{N_\phi}{\sigma_\alpha(\cos(\alpha))^2} \qquad t_{90} = \frac{N_\theta - [N_\phi(\tan(\alpha))^2]}{\sigma_{90}}$$

Geometric | Shape

```
               │
               ▼
┌─────────────────────────────────┐
│ Calculate winding angle at Aft  │
│ major diameter  α_A  and Fwd    │
│ tangent line  α_F               │
└─────────────────────────────────┘
       α_A   │   α_F
             ▼
┌─────────────────────────────────┐
│ Calculate number of Helical     │
│ layers (N_α) required at point  │
│ of max tension load (usually    │
│ at max diam)                    │
└─────────────────────────────────┘
        N_α  │  t_α
             ▼
┌─────────────────────────────────┐
│ Calculate Helical buildup along │
│ conical/cylindrical section     │
│                                 │
└─────────────────────────────────┘
        N_α  │
             ▼
┌─────────────────────────────────┐
│ Compute number of Hoop layers   │
│ (N_90) required at stations     │
│ along conical/cylindrical length│
│                                 │
└─────────────────────────────────┘
        N_α  │  N_90
             ▼
┌─────────────────────────────────┐
│ Compute composite thickness at  │
│ Aft major diameter and Fwd Tan  │
│ for Helicals (t_α) and Hoops    │
│ (t_90)                          │
└─────────────────────────────────┘
        t_α  │
             ▼
┌─────────────────────────────────┐
│ Design dome shapes              │
│                                 │
│                                 │
└─────────────────────────────────┘
```

Figure C.7. Netting Analysis Flow Diagram

$$t = t_\alpha + t_{90}$$

Buckling equations are examined to ensure that the pressure vessel does not collapse under a given load or the increased load seen during flight. Buckling is a condition whereby compressive loads, whether static or dynamic, result in a columar failure of the rocket motor case. This failure can occur at stress levels significantly below the composite strength values. Other instances of buckling are termed *localized* buckling and can occur in highly stressed regions or areas of local discontinuity. This type of buckling is often best handled via FEA type programs. The following calculation predicts a columar buckling stress for the given vessel that will cause failure. (3:p. 4) To ensure that the vessel does not fail, actual stress must be below this buckling stress. A simplifying assumption of an orthotropic Young's Modulus is adopted for the equation using the concepts of netting analysis that stress is carried in the fiber direction.

$$\sigma_{buck} = \frac{1}{\sqrt{3}} \frac{E}{\sqrt{1 - \nu^2}} \frac{t}{R}$$

$$\nu = 0.3 \implies \sigma_{buck} = 0.6 E \frac{t}{R}$$

Other principal normal stresses are calculated (via the following equations) to ensure vessel integrity. (42:p. 311) The normal stresses should be below fiber strength to prevent rupture.

$$\sigma_1 = \frac{PR}{t}$$
$$\sigma_2 = \frac{PR}{2t}$$
$$\sigma_3 = -P$$

Finally, weight and volume calculations are made based on both geometric and material properties. (37)

Define the following parameters:

- ρ_c - density of composite
- V_f - fiber volume (as a percentage)
- ρ_f - fiber density
- V_r - resin volume
- ρ_r - resin density

$$\rho_c = V_f \rho_f + V_r \rho_r$$

$$W = \pi D t \rho_c$$

$$W_{case} = W L$$

$$V_{case} = \pi R^2 L$$

Similar type calculations are used for a conical pressure vessel. The majority of these equations come from the report, *Design of Filament Wound Rocket Cases*, by Alex Wozchieechowicz. Whereas Evans uses a single wind angle, Wozchieechowicz optimizes a wind angle for each of the three sections of the conical body: aft dome, barrel, and forward dome. (see Figure C.7) An optimal wind angle ensures the entire vessel is covered adequately with composite material in sufficient quantity to provide strength. Further, optimized wind angles prevent band (composite fiber) slippage and allow for a stable winding path. (104:p. 6-6) From here, minimum thicknesses for each section are calculated. Finally, buckling analyses and geometric properties are developed for conical sections.

For a conically shaped rocket motor, it must be understood that the winding angle for a filament wound case must transverse three curved surfaces: (1) the forward dome (subscript f), (2) the barrel (the length of the pressure vessel, subscript b), and (3) the aft dome (subscript a). The three sections are wound integrally via machine. Since no one wrapping angle uniquely maximizes

the wrap, a series of winding angles must be calculated. When unequal polar openings occur for a case, a geodesic wrap angle is impossible (104:p. 6-6). A series of three equations are calculated using the following parameters:

- $r_{f,b}$ - radius of the forward dome (in)
- bw - bandwidth of the fiber (in)
- $x_{of,b}$ - radius of the filament band meanline (in)
- α_f - helical winding angle of forward dome (^{0})
- α_b - helical winding angle overr barrel (^{0})
- α_a - helical winding angle of aft dome (^{0})
- $t_{f,b,a}$ - thickness of composite for section (in)
- $r_{\epsilon f,b,a}$ - radius of conical section before dome (in)
- Other parameters as definded earlier

$$x_{of,a} = r_{f,a} + \frac{bw}{2}$$

$$\sigma_{f,a} = \arcsin \frac{x_{of,a}}{r_{ef,a}} \qquad \sigma_b = \frac{1}{3}[2\sigma_a + \sigma_f]$$

$$N_{\phi f,a,b} = \frac{P r_{ef,a,b}}{2} \qquad N_{\theta f,a,b} = P r_{f,a,b}$$

$$t_{\alpha f,a,b} = \frac{N_{\phi f,a,b}}{\sigma_\alpha [\cos(\alpha_{f,a,b})^2]} \qquad t_{90f,a,b} = \frac{N_{\theta f,a,b} - [N_{\phi f,a,b}\tan(\alpha_{f,a,b})^2]}{\sigma_{90}}$$

$$r_b = \frac{r_{ef} + r_{ea}}{2}$$

- Total forward dome thickness: $t_f = t_{\alpha f} + t_{90f}$
- Total aft dome thickness: $t_a = t_{\alpha a} + t_{90a}$
- Total thickness of the barrel: $t_b = t_{\alpha b} + t_{90b}$

C.4.2 Operating Conditions and Requirements . For the integrated second stage motor case, the MEOP multiplied by a factor of safety of 1.25 forms the basis for a filament wound design. A typical loading scheme for a rocket motor case is shown in Figure C.8.
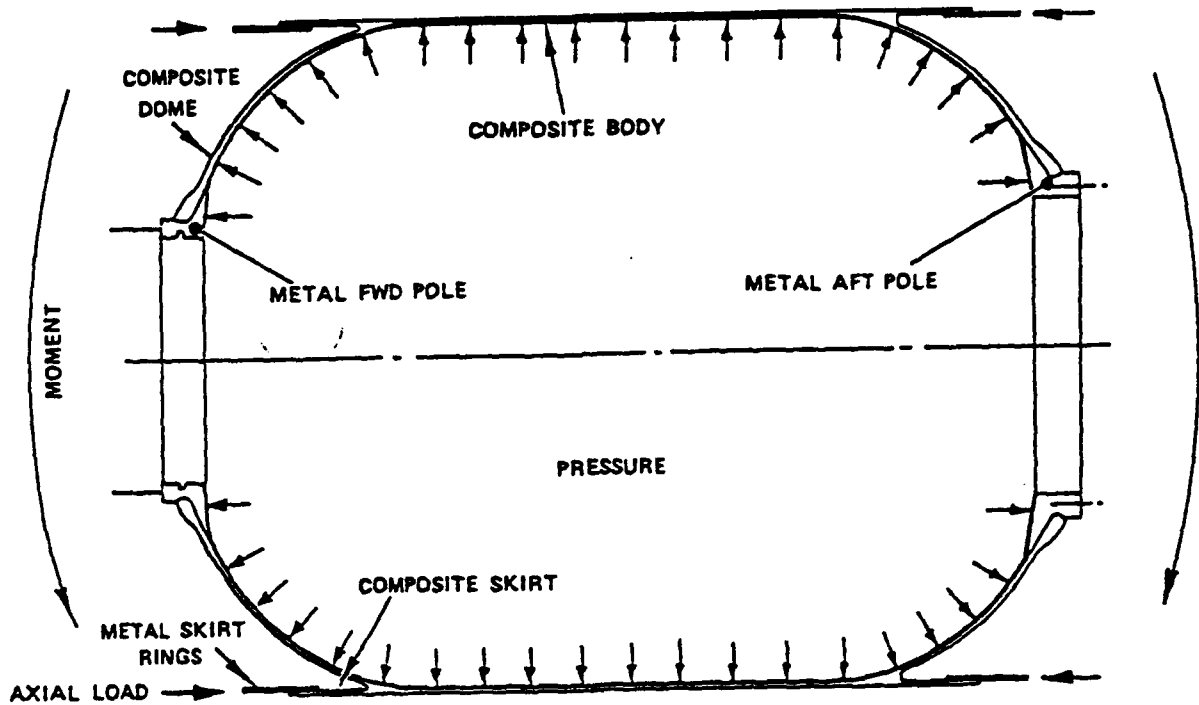
Figure C.8. Typical Rocket Motor Case Loading Scheme

Besides MEOP, other driving design requirements are temperature and external loading. With regards to temperature, the case experiences heat from two sources: aeroheating due to friction and internal combustion temperature. In each instance, the case must be designed to withstand these temperatures and remain operational for the duration of flight. For aeroheating, external protective material (EPM) serves a dual purpose in keeping the baseline case cool and preventing fragmentation damage. Internal insulation helps maintain a desired temperature within the combustion chamber. Tension, compression, and bending form the external loading scheme

that must be withstood. With loading conditions analyzed, development of a viable rocket motor case can be undertaken.

C.4.3 Structural Model Development . Because the success of the entire second stage design is so closely tied to overall vehicle strength and weight, it is crucial to design a lightweight, structurally sound vessel to integrate with the other portions of the design. To do this job, it was critical that the STM model receive information from the propulsion model to produce a viable design that could in turn be used by the trajectory model for evaluation of performance. Hence, a structural model of inputs and outputs was needed that would take into consideration those factors necessary to integrate with the other models. Figure C.9 is an outline of the STM model. As an illustration, with an input of MEOP from the propulsion model. the STM model would develop a rocket motor case of sufficient size and strength for the mission. The weight of this vessel would be submitted to the trajectory group for analysis in the area of performance. As the process was dynamic and iterative, many variations in design parameters allowed for a constantly evolving design. Nevertheless, Figure C.9 served a key role in developing an integrated second stage.
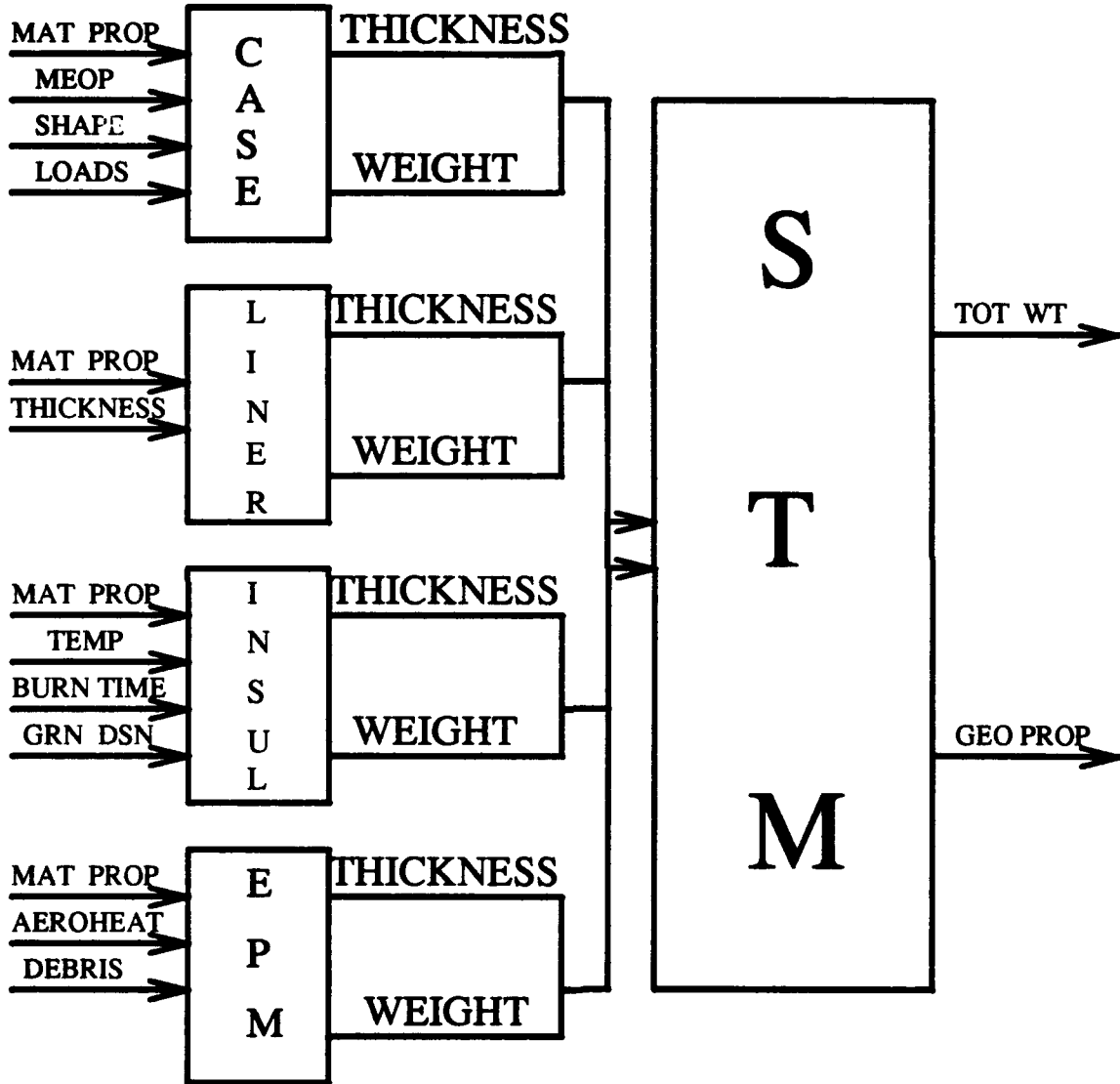
Figure C.9. STM Input/Output Model

The next step within model development used two techniques: Response Surface Methodology (RSM) and Optimization. RSM is typically a technique employed when the underlying equations are not explicitly known. However, RSM did help provide an understanding of the factors which were significant for the design. From the netting analysis equations developed previously, it can be seen that many parameters help determine the design of a filament wound pressure vessel. But, there is only intuitive, not definitive, knowledge of which factors predominate in design. Therefore, a basic RSM study was undertaken.

There are numerous ways to approach RSM, but one of the easiest and quickest is to examine a small number of factors at two levels. Factors are merely the variables themselves and levels are distinct values that the variables may range between. For example, the length of the pressure vessel is in a known range. However, its exact length changes to fit design requirements. By looking at length between a given range, e.g. 120 inches up to 200 inches, the relative significance of length on overall weight can be estimated. For a more in depth look at RSM, several excellent texts exist. (19)

The following four studies, Tables C.2- C.3- C.4- C.5, look at some of the key variables influencing the structural part of this project. The variables (labeled factors) are given followed by the two levels the variable was set at in calculating weight. The charts show the variables tested in all possible combinations, with a minus sign (or -1) corresponding to the low setting of that variable and a plus sign (or +1) corresponding to the high setting. The numbers at the bottom of each column are called *effects* and give a relative significance of how that variable influences the response (weight). For example, a *-10* in fiber strength indicates that as fiber strength goes from its low setting (300 ksi) to a high setting (600 ksi) the overall effect would be to decrease weight. This makes both intuitive and mathematical sense when examined closely. It can be expected that case weight would decrease as the composite gets stronger and less material is required. The columns corresponding to two or three digits are interaction columns. They merely show the relative influence of one variable on another variable in the overall weight estimation. The cubical graphs that follow, Figure C.10, are three dimension representations for each of the three variable cases. They can be interpreted by visualizing a 3-D axis system where the origin corresponds to a (-1, -1, -1) level for each factor extending out and up to a +1 level for each factor

Case 1:

Factors:
1. Fiber Strength   Low=300 ksi   High=600 ksi
2. Pressure   Low=1250 psi   High=2000 psi
3. Radius   Low=26 in   High=32 in

Table C.2. Compariosn Between Fiber Strength, Pressure, and Radius

Run	I	1	2	3	12	13	23	123	Weight(lbs)
1	+	-	-	-	+	+	+	-	282.985
2	+	+	-	-	-	-	+	+	141.493
3	+	-	+	-	-	+	-	+	452.774
4	+	+	+	-	+	-	-	-	226.388
5	+	-	-	+	+	-	-	+	428.664
6	+	+	-	+	-	+	-	-	214.332
7	+	-	+	+	-	-	+	-	685.862
8	+	+	+	+	+	+	+	+	342.931
	347	-231	160	142	-53	-47	32	-11	

Case 2:
Factors
1. Fiber Strength   Low=300 ksi   High=600 ksi
2. Density   Low=.052 pci   High=.065 pci
3. Length   Low=180 in   High=230 in

Table C.3. Comparison Between Fiber Strength, Density, and Length

Run	I	1	2	3	12	13	23	123	Weight(lbs)
1	+	-	-	-	+	+	+	-	270.646
2	+	+	-	-	-	-	+	+	135.323
3	+	-	+	-	-	+	-	+	315.372
4	+	+	+	-	+	-	-	-	157.686
5	+	-	-	+	+	-	-	+	345.826
6	+	+	-	+	-	+	-	-	172.913
7	+	-	+	+	-	-	+	-	398.579
8	+	+	+	+	+	+	+	+	199.290
	249	-166	36	59	-12	-19	3	-1	
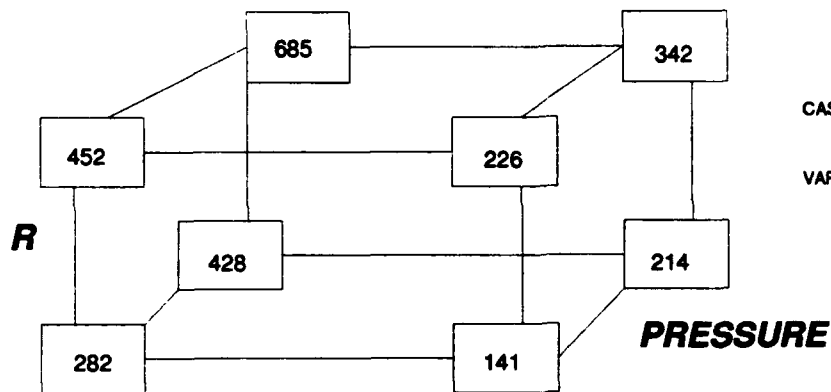
CASE WEIGHT IN LBS BASED ON

VARYING 3 FACTORS AT 2 LEVELS

MATERIALS

EFFECTS

1	FIBER STRENGTH	LOW=300 KSI	HIGH=600 KSI
2	PRESSURE	LOW=1250 PSI	HIGH=2000 PSI
3	RADIUS	LOW=26 IN	HIGH=32 IN
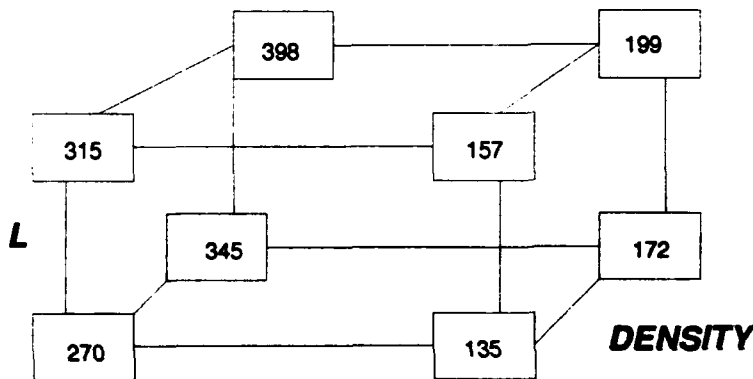
CASE WEIGHT IN LBS BASED ON

VARYING 3 FACTORS AT 2 LEVELS

MATERIALS

EFFECTS

1	FIBER STRENGTH	LOW=300 KSI	HIGH=600 KSI
2	DENSITY	LOW=.052 LB/IN^3	HIGH=.065 LB/IN^3
3	LENGTH	LOW=180 IN	HIGH=230 IN

Figure C.10. RSM Study for Cases 1 and 2

Case 3:

Factors

1.	Density	Low=.052 pci	High=.065 pci
2.	Pressure	Low=1250 psi	High=2000 psi
3.	Radius	Low=26 in	High=32 in
4.	Fiber Strength	Low=350 ksi	High=600 ksi

Table C.4. Comparison between Density, Pressure, Radius and Fiber Strength

Run	I	1	2	3	4	12	13	14	1234	Weight(lbs)
1	+	-	-	-	-	+	+	+	+	242.559
2	+	+	-	-	-	-	-	-	-	303.198
3	+	-	+	-	-	-	+	+	-	388.094
4	+	+	+	-	-	+	-	-	+	485.118
5	+	-	-	+	-	+	-	+	-	367.426
6	+	+	-	+	-	-	+	-	+	459.283
7	+	-	+	+	-	-	-	+	+	587.882
8	+	+	+	+	-	+	+	-	-	734.853
9	+	-	-	-	+	+	+	-	-	141.493
10	+	+	-	-	+	-	-	+	+	176.866
11	+	-	+	-	+	-	+	-	+	226.388
12	+	+	+	-	+	+	-	+	-	282.985
13	+	-	-	+	+	+	-	-	+	214.332
14	+	+	-	+	+	-	+	+	-	267.915
15	+	-	+	+	+	-	-	-	-	342.931
16	+	+	+	+	+	+	+	+	+	428.664
	353	157	326	289	-371	-41	-85	-170	-2	

Case 4:
Factors:

Pressure	Low=1250 psi	High=2000 psi
Radius	Low=26 in	High=32 in
Helical	Low=450 ksi	High=650 ksi
Hoop	Low=500 ksi	High=700 ksi
Length	Low=150 in	High=180 in
Density	Low=.052 pci	High=.065 pci

Table C.5. A Fractionated Design Comparing 6 Factors at 2 Levels

Run	I	1	2	3	4	5	6	Weight(lbs)
1	+	-	-	-	-	-	-	129.839
2	+	+	-	-	-	+	-	263.141
3	+	-	+	-	-	+	+	311.410
4	+	+	+	-	-	-	+	393.359
5	+	-	-	+	-	+	+	178.288
6	+	+	-	+	-	-	+	225.205
7	+	-	+	+	-	-	-	170.570
8	+	+	+	+	-	+	-	345.688
9	+	-	-	-	+	-	+	135.935
10	+	+	-	-	+	+	+	275.495
11	+	-	+	-	+	+	-	208.659
12	+	+	+	-	+	-	-	263.569
13	+	-	-	+	+	+	-	115.914
14	+	+	-	+	+	-	-	146.418
15	+	-	+	+	+	-	+	173.276
16	+	+	+	+	+	+	+	351.172
	230	210	186	-68	-86	102	100	

Finally, the fourth case used a software program called SAS (Statistical Analysis System) to examine the interaction of six variables: pressure, radius, helical fiber strength, hoop fiber strength, length, and density. A full combinatorial run of six factors would have amounted to running 128 cases, however, using Box's technique of fractionating, the effects of just the main variables can be achieved in only 16 runs.

The overall conclusions of the RSM brought some interesting observations to light. Yes, pressure does play an integral part in determining weight of the pressure vessel, but other factors are also key. Intuitively, composite strength determines a great deal of the overall weight. As strength increases, weight of the case decreases. As length and radius increase, so does the weight of the filament wound structure. By conducting RSM, it was possible to see how varying one of the variables could influence the others as well as overall structural weight.

To further refine the idea of minimizing case weight, an optimization program called GINO (General Interactive Nonlinear Optimizer) was employed. (62) GINO employs a variation of the simplex method whereby variables are manipulated to find a feasible solution and then maximized or minimized according to the objective funstion. Inputting the combined thicknesses equation developed from Evans as the objective equation and placing a range on each variable, GINO determined the mix to minimize weight. The conclusion of using GINO is, not surprisingly, where each variable is optimized, i.e. when fiber strength is highest and overall length is lowest, etc., weight is minimal. The results (inputs and respective output) are shown below and in Table C.6 where the *optimal* minimal weight is reported as Objective Function Value.

```
MODEL:
1) MIN=6.283*R*L*H*((P*R)/(2*S1*(COS(57.297*A
   ))^2) + ((P*R - ((P*R/2*((TAN(57.297*A))^2
   ))))/S2));
2) R=32.5;            (R=radius)
3) A>10;              (A=Alpha, helix wind angle)
4) A<25;
5) L>150;             (L=length)
6) L<180;
7) H>.052;            (H=density of composite)
8) H<.065;
9) P>1250;            (P=MEOP)
10) P<2000;
11) S1>500000;        (S1=helix fiber tnesile strength)
12) S1<650000;
13) S2>550000;        (S2=hoop fiber tensile strength)
14) S2<700000;
END
```

OBJECTIVE FUNCTION VALUE = 142.280840

Table C.6. GINO Output for Minimum Weight Objective Function

VARIABLE	VALUE	REDUCED COST
R	32.50	0.0
L	150.00	0.0
H	0.52	0.0
P	1250.00	0.0
S1	650000	0.0
A	25	0.0
S2	700000	0.0

C.4.4 Material Selection/Comparison . Because material strength played such an integral role in case development, extensive effort was expended to research typical composite properties. Solicitation of all major manufacturers (DuPont, Hercules, BASF, Fiberite, etc.) resulted in receiving data sheets on material specifically suited for filament winding a pressure vessel. In addition, typical resins and cure cycles were examined. The intent of material selection was not to identify a single *best* material combined with a single *best* resin. Rather, an overall examination of materials along with tradeoffs became the central focus. Finally, representative material properties would be used for analysis and design of a filament wound rocket motor case.

The majority of this portion examined a report from Morton-Thiokol, Inc. to the Rocket Propulsion Laboratory entitled: *Advanced Composite Case Materials Evaluation* (ACCME). authored by Neal Mumford. The intent of the report was to identify materials for possible future development in a pressure vessel application. Figure C.11 outlines design and driving requirements for various missiles.(70:p. 13) The emphasis for *NEMESIS* is the ballistic motor category with a driving requirement of internal operating pressure.

Fibers that the structural group examined fell into the carbon/graphite category, which demonstrate high fiber strength and an intermediate modulus. This type of material becomes well suited for filament winding. Within the ACCME, the importance of interrelationships between heat, compaction, winding tension. cure and prepreg rheology is outlined. (70:p. 8) Additionally, the benefits of interspersing hoop and helical wound layers are expounded. Finally, Mumford points out that the design variables showing the greatest effects on case strength are: (1) stress ratio (a ratio of helix fiber stress to hoop fiber stress). (2) interspersment of helical and hoop layers, and (3) dome reinforcements. (70:p. 12) Surprisingly, "...wrap angle, wrap pattern and polar openings and skirts have no known material dependent effect on the performance of properly designed cases." (70:p. 12) From these types of studies, an idea of how to develop a viable motor case becomes evident.

It is important to keep in mind that MEOP is the primary design driver with external structural loads being secondary drivers for design of cases. Therefore, those materials that provide the greatest resistance to internal pressure loads become primary candidates. The fibers that most often meet these specifications are carbon fibers. "Carbon fibers have a high specific strength with very good fatigue properties, are nonhygroscopic (i.e. non water absorbing) and form high modulus.

DESIGN REQUIREMENT	SPACE MOTORS	BALLISTIC MOTORS	OTHER (TACTICAL,ETC)
MEOP (PSIG)	1,000	700 TO 2,000	700 TO 3,600
TEMPERATURE (F)	20 TO 100	25 TO 110	UP TO -65 TO 145
EXT LOADS (LB/IN)	1,000	1,500 TO 5,000	UP TO 7,000
AEROHEAT (F)	NONE	TO 350	300 TO 1,400
OTHER	LOW OUTGASSING	LOCAL SUPPORT LOADS	VERY HIGH ACCELER

DRIVING REQUIREMENT	MEOP	MEOP/TEMP/LOADS	EXT LOAD/AEROHEAT
MAT REQUIREMENTS			
FIBER STRENGTH	HIGH	HIGH	NOT A DRIVER
STIFFNESS	NOT IMPORTANT	MODERATE - HIGH	HIGH
COMPRESSIVE STRGT	NOT IMPORTANT	MODERATE - HIGH	HIGH
SHEAR STRENGTH	NOT IMPORTANT	MODERATE - HIGH	HIGH
TEMPERATURE EFFECT	LOW WITHIN 30 TO 100	LOW WITHIN 30 TO 100	LOW WITHIN -65 TO 145. SHORT AEROHEAT
RESIN TOUGHNESS	NOT REQUIRED		HIGH IMPACT RESIST
CANDIDATE MATERIAL RESIN	KEVLAR, GRAPHITE EPOXY, LOW DENSITY	KEVLAR, GRAPHITE RIGID EPOXY	GRAPHITE HIGH TEMP RESIN

Figure C.11. Missile Loading Scheme Design Drivers

high shear strength composites." (70:p. 19) Table C.7 is a typical list of fibers and some of their associated properties collected from representative composite manufacturers.

Table C.7. Typical Fiber Properties

FIBER	DENSITY (pci)	STRENGTH (ksi)	MODULUS (msi)
Kevlar 49	.0520	538	20.1
T-700	.0652	646	41.0
T-40(810)	.0645	763	40.2
IM-6	.0615	684	44.3
T-650	.064	700	42.0
T-40 (12K)	.065	820	42.0
IM-7	.064	770	40.0

From this list. selected material properties were chosen for the design and analysis of a filament wound case. With respect to resins. the most important factor considered was the glass transition temperature, Tg. Tg is important due to aeroheating and internal operating temperatures. To ensure the composite maintains its integrity, the temperature seen by the composite must not exceed the Tg of the resin. Examination of resins looks primarily at the epoxy family. Mumford points out other considerations with regards to resins such as safety (toxicity), pot life, cure temperature, modulus, damage sensitivity, etc. The majority of resin candidates were those developed by Fiberite, Inc. and Thiokol, Inc. Table C.8 lists typical resin properties from these companies.

Table C.8. Typical Resin Properties

RESIN	TYPE	Tg^0C	DENSITY (g/cc)	STRENGTH (ksi)	MODULUS (msi)
930	Epoxy	180	1.36	12	0.66
934	Epoxy	190	1.3	4.0	0.6
974	Epoxy	180	1.27	17	0.6
977-3	Epoxy	200	1.25	20	0.7
UF-3299	Epoxy	52	1.26	2.4	0.33
UFX-83-19	Epoxy	228	1.26	11.2	3.88

Netting analysis was outlined earlier – this analysis relies strictly on fiber strength, ignoring the effects of the matrix. Today's fibers have demonstrated strengths in excess of 1000 ksi, however, such high strength is not the only consideration in rocket motor cases. The interrelationships can not be forgotten, and as will be seen later. a thinner case generally implies thicker insulation. Therefore, a balance must be struck between material properties and other needs. Finally, thought

must also be given towards the handling, manufacturing, producability, and cost of the composite case.

C.4.5 Design of the Integrated Second Stage. Based on the equations presented earlier in this appendix, along with typical material properties, a candidate rocket motor cases were designed. The following are the equations and solutions generated on Mathcad in development of a representative filament wound rocket motor case. The equations originate from Evans, Wozchieechowicz, and Roark and Young.

This portion of the design will help determine case wall thickness using a process called Netting Analysis.

Definitions:
  (1) $t\alpha$=helix fiber thickness (in)
  (2) t90=hoop fiber thickness (in)
  (3) $\sigma\alpha$=helix fiber tensile strength (psi)
  (4) $\sigma90$=hoop fiber tensile strength (psi)
  (5) Nϕ=axial line load (lb/in)
  (6) Nθ=hoop line load (lb/in)
  (7) P=max pressure to design to (psig)
  (8) R=radius of cylinder (in)
  (9) α=helix winding angle (in degrees)
  (10) E=Young's Modulus (psi)
  (11) μ=Poisson's Ratio (dimensionless)

The first portion of this program deals with cylindrical sections:
The series of equations come from P.R. Evans' article, 'Composite Motor Case Design'. (see Bibliography for full citation)

Let's put in some numbers based upon our proposed design:

P := 1246.69·1.25   psi $\sigma\alpha$:= 500000   lb/in^2   L := 157.72 + 28
R := 33   in $\sigma90$:= 600000   lb/in^2

$\alpha := 25 \cdot \left[\dfrac{\pi}{180} \right]$ first number in degrees converted to radians for MCAD

$$D := 2 \cdot R \qquad D = 66 \qquad \text{diameter}$$
$$P = 1558.3625 \qquad \text{psi}$$

$$N\phi := \frac{P \cdot R}{2}$$

$$N\phi = 2.5713 \cdot 10^{4} \qquad \text{lb/in}$$

$$N\theta := P \cdot R$$

$$N\theta = 5.1426 \cdot 10^{4} \qquad \text{lb/in}$$

$$t\alpha := \frac{N\phi}{\sigma\alpha \cdot (\cos(\alpha))^{2}}$$

$$t\alpha = 0.0626 \qquad \text{in}$$

$$t90 := \frac{N\theta - \left[N\phi \cdot (\tan(\alpha))^2\right]}{\sigma 90}$$

$$t90 = 0.0764 \quad \text{in}$$

Total thickness = $t\alpha$ + t90

t := $t\alpha$ + t90

$$t = 0.139 \quad \text{in}$$

Determining the weight per unit length of material
        (1) ρc = density of composite
        (2) Vf = fiber volume
        (3) ρf = fiber density
        (4) Vr = resin volume
        (5) ρr = resin density

Vf := .6 ρf := .0625 lb/in^3   Vr := .4 ρr := .043

ρc := Vf·ρf + Vr·ρr

$$\rho c = 0.0547 \quad \text{lb/in}^3$$

W := $\pi \cdot D \cdot t \cdot \rho c$

$$W = 1.5765 \quad \text{lb/in}$$

Moving on to calculating loads

Based on the thickness we just calculated, we come up with:

Axial stress

$$\sigma_\phi := \frac{P \cdot R}{2 \cdot t}$$

$$\sigma_\phi = 1.8499 \cdot 10^5 \quad \text{lb/in\textasciicircum 2}$$

Hoop stress

$$\sigma_\theta := \frac{P \cdot R}{t}$$

$$\sigma_\theta = 3.6997 \cdot 10^5 \quad \text{lb/in\textasciicircum 2}$$

We need to define a few more variables for the material:

Young's Modulus   (based on IM-7 in 977-3 resin) $E := 23500000$ lb/in^2
Poisson's Ratio $\mu := 0.3$

The resulting equations can now be used: (See Roark and Young)

Radial displacement of a circumference

$$\delta R := \frac{P \cdot R^2}{E \cdot t} \cdot \left[1 - \left[\frac{\mu}{2} \right] \right]$$

$$\delta R = 0.4416 \quad \text{inches}$$

Change in height dimension

$$\delta L := \frac{P \cdot R \cdot L}{E \cdot t} \cdot (0.5 - \mu)$$

$$\delta L = 0.5848 \quad \text{inches}$$

Buckling stress is perhaps the greatest concern for axially loaded
cylindrical bodies. The following formula predicts a critical buckling
load; however, most tests show that actual structures fail at between
40 - 60 % of the predicted value. This is due in part to imperfections
in the material, manufacturing, etc. (see Roark and Young, 'Formulas for
Stress and Strain', pp. 449, 557)

Buckling stress

$$\sigma_{buck} := \left[\frac{1}{\sqrt{3}}\right] \cdot \left[\frac{E}{\sqrt{1 - \mu^2}}\right] \cdot \left[\frac{t}{R}\right]$$

$$\sigma_{buck} = 5.9908 \cdot 10^4 \quad lb/in^2$$

This value is how much the given design can withstand - to ensure the
missile will not fail due to buckling, the axial stress must be lower
than this value.

Use classical formula: stress = load/area

Load = total weight above Stage I $Load := 27000$ lbs
Area of a very thin annulus (p.66 formu) $Area := 2 \cdot \pi \cdot R \cdot t$

$$Area = 28.8209 \quad lb/in^2$$

Then, our stress is:

$$stress := \frac{Load}{Area}$$

$$stress = 936.8205 \quad lb/in^2$$

Finally, the case weight and volume equations are as follows:

$$W_{case} := W \cdot L \qquad W_{case} = 292.7881 \quad lbs$$

$$V_{case} := \pi \cdot R^2 \cdot L \qquad V_{case} = 6.3538 \cdot 10^5 \quad in^3$$

Let's look at some of the stresses in a conical section: ·
(see Roark and Young, p.557)

The Principal Normal Stresses are:
Let the angle of taper $=\beta$

$$\beta := 1 \cdot \left[\frac{\pi}{180} \right] \qquad \text{in degrees converted to radians}$$

For right, truncated cone there are two radiuses,
the first was our big R, the coning part is r.

R := 33

Uniform internal pressure with tangential edge support

r := 26

$$\sigma_1 := \frac{P \cdot r}{2 \cdot t \cdot (\cos(\beta))}$$

$$\sigma_1 = 1.4577 \cdot 10^5 \quad \text{psi}$$

$$\sigma_2 := \frac{P \cdot r}{t \cdot (\cos(\beta))}$$

$$\sigma_2 = 2.9154 \cdot 10^5 \quad \text{psi}$$

Examining some buckling cases

Define the following parameters:

(1) $E := 23500000$ psi

(2) $\mu := 0.3$

Case 1: Thin truncated conical shell under axial loading

$$load_{buckl} := \frac{2 \cdot \pi \cdot E \cdot t^2 \cdot \left[(\cos(\beta))^2 \right]}{\sqrt{3 \cdot \left[1 - \mu^2 \right]}}$$

$$load_{buckl} = 1.7261 \cdot 10^6 \quad lbs$$

Actual buckling strength is from 40-60%, or:

(Roark and Young) $load_{bucklact} := 0.3 \cdot \left[2 \cdot \pi \cdot E \cdot t^2 \cdot \left[(\cos(\beta))^2 \right] \right]$

$$load_{bucklact} = 8.5559 \cdot 10^5 \quad lbs$$

Case 2: Same shell under combined axial load and internal pressure

$$load_{buck2} := \left[\frac{P}{E} \cdot \left[\frac{r}{t \cdot \cos(\beta)}\right]^2\right] \cdot 2 \cdot \pi \cdot E \cdot t^2 \cdot \left[(\cos(\beta))^2\right]$$

$$load_{buck2} = 6.619 \cdot 10^6 \quad lbs$$

Some geometric properties of a right truncated conical section:
(see Eshbach)

(1)
$$V := \left[\pi \cdot \frac{L}{3}\right] \cdot \left[R^2 + r^2 + (R \cdot r)\right]$$

$$V = 5.1014 \cdot 10^5 \quad in^3$$

(2)
$$CG := \frac{L \cdot \left[R^2 + (2 \cdot R \cdot r) + \left[3 \cdot r^2\right]\right]}{4 \cdot \left[R^2 + R \cdot r + r^2\right]}$$

$$CG = 85.5494 \quad in \ from \ base$$

(3)   Let m=W/g $g := 32.2$ $m := \frac{W \cdot L}{g}$

$$I_c := 3 \cdot m \cdot \frac{R^5 - r^5}{10 \cdot \left[R^3 - r^3\right]}$$

$$I_c = 4049.0481$$

(4)
$$k_c := \sqrt{3 \cdot \frac{R^5 - r^5}{10 \cdot \left[R^3 - r^3\right]}}$$

$$k_c = 21.1022$$

The following information is based on the report 'Design of Filament
Wound Rocket Cases' by Alex Wozchieechowicz, prepared for Hercules, Inc.
on 1 December 1968.

For a conically shaped rocket motor, it must be understood that the winding
angle for a filament wound case must transverse three curved surfaces: (1)
the forward dome, (2) the barrel (the length of the pressure vessel) , and
(3) the aft dome. No one wrapping angle uniquely maximizes the wrap.
Therefore, a series of winding angles must be calculated.

When unequal polar openings occur for a case, a geodesic wrap angle is
impossible. The reasons are outlined in section 6.3.3, p 6-6 of the
report.

Therefore, a series of three equations are used:

Calculating the optimal winding angle of the forward dome:

Define the following parameters:
  (1) rf=radius of the forward dome
  (2) bw=bandwidth of the fiber
  (3) xof=radius of the filament band meanline
  (4) αf=helical winding angle of forward dome
  (5) ref=radius of conical section before dome

Let:

$$r_f := 16 \quad \text{inches} \qquad r_{ef} := 26 \text{ inches}$$

$$bw := .1 \quad \text{inches}$$

$$x_{of} := r_f + \left[\frac{bw}{2}\right] \qquad x_{of} = 16.05 \quad \text{inches}$$

$$\alpha_f := \text{asin}\left[\left[\frac{x_{of}}{r_{ef}}\right]\right] \cdot \left[\frac{180}{\pi}\right]$$

$$\alpha_f = 38.1198 \quad \text{degrees}$$

Calculating the optimal winding angle of the aft dome:

Define the following parameters:
  (1) ra=radius of the aft dome
  (2) bw=bandwidth of the fiber
  (3) xoa=radius of the filament band meanline
  (4) αa=helical winding angle of forward dome
  (5) rea=radius of conical section before dome

Let:

$$r_a := 16 \quad \text{inches} \qquad r_{ea} := 33 \quad \text{inches}$$

$$bw = 0.1 \quad \text{inches}$$

$$x_{oa} := r_a + \left[\frac{bw}{2}\right]$$

$$x_{oa} = 16.05 \quad \text{inches}$$

$$\alpha_a := \text{asin}\left[\left[\frac{x_{oa}}{r_{ea}}\right]\right] \cdot \left[\frac{180}{\pi}\right]$$

$$\alpha_a = 29.1019 \quad \text{degrees}$$

Calculating the optimum winding angle over the barrel portion:

Define:

(1) αb=helical winding angle over barrel.

Let:

$$\alpha_b := \left[\frac{1}{3}\right] \cdot \left[2 \cdot \alpha_a + \alpha_f\right]$$

$$\alpha_b = 32.1078 \quad \text{degrees}$$

Calculating the required thickness for each of the three sections:

Define the following parameters:

P=internal pressure in psi
R=radius in inches
A=tensile loading in lbs
M=bending moment in in-lbs
$t\alpha$=helical layer thickness in inches
t90=hoop layer thickness in inches
$\sigma\alpha$=ultimate helical fiber stress in psi
σ90=ultimate hoop fiber stress in psi
α=winding angle (in degrees converted to rads for MathCad
$N\phi$=meridional tensile load in lbs/in
$N\theta$=hoop membrane tensile load in lbs/in

Calculating the thickness for the forward dome:

Let:

$$P := 1933 \cdot 1.25 \qquad \sigma_\alpha := 500000 \qquad \sigma_{90} := 600000$$
$$P = 2416.25$$

$$N_{\phi f} := \frac{P \cdot r_{ef}}{2}$$

$$N_{\phi f} = 3.1411 \cdot 10^4 \ \text{lbs/in}$$

$$N_{\theta f} := P \cdot r_{ef}$$

$$N_{\theta f} = 6.2823 \cdot 10^4 \ \text{lbs/in}$$

$$t_{\alpha f} := \frac{N_{\phi f}}{\sigma_{\alpha} \cdot \left[\cos\left[\alpha_f \cdot \left[\frac{\pi}{180}\right]\right]\right]^2}$$

$$t_{\alpha f} = 0.1015 \quad \text{inches}$$

$$t_{90f} := \frac{N_{\theta f} - \left[N_{\phi f} \cdot \left[\left[\tan\left[\alpha_f \cdot \left[\frac{\pi}{180}\right]\right]\right]^2\right]\right]}{\sigma_{90}}$$

$$t_{90f} = 0.0725 \quad \text{inches}$$

TOTAL FORWARD DOME THICKNESS:

$$t_f := t_{\alpha f} + t_{90f}$$

$$t_f = 0.174 \quad \text{inches}$$

Calculating the thickness for the aft dome:

$$N_{\phi a} := \frac{P \cdot r_{ea}}{2}$$

$$N_{\phi a} = 3.9868 \cdot 10^{4} \ \text{lbs/in}$$

$$N_{\theta a} := P \cdot r_{ea}$$

$$N_{\theta a} = 7.9736 \cdot 10^{4} \ \text{lbs/in}$$

$$t_{\alpha a} := \frac{N_{\phi a}}{\sigma_{\alpha} \cdot \left[\cos\left[\alpha_{a} \cdot \left[\frac{\pi}{180}\right]\right]\right]^{2}}$$

$$t_{\alpha a} = 0.1044 \quad \text{in}$$

$$t_{90a} := \frac{N_{\theta a} - \left[N_{\phi a} \cdot \left[\left[\tan\left[\alpha_{a} \cdot \left[\frac{\pi}{180}\right]\right]\right]^{2}\right]\right]}{\sigma_{90}}$$

$$t_{90a} = 0.1123 \quad \text{inches}$$

TOTAL AFT DOME THICKNESS:

$$t_{a} := t_{\alpha a} + t_{90a}$$

$$t_{a} = 0.2167 \quad \text{inches}$$

Calculating the thickness for the cylindrical section:

Define the following parameters:

$$r_b := \frac{r_{ef} + r_{ea}}{2} \qquad r_b = 29.5 \quad \text{inches}$$

$$N_{\phi b} := \frac{P \cdot r_b}{2}$$

$$N_{\phi b} = 3.564 \cdot 10^4 \quad \text{lbs/in}$$

$$N_{\theta b} := P \cdot r_b$$

$$N_{\theta b} = 7.1279 \cdot 10^4 \quad \text{lbs/in}$$

$$t_{\alpha b} := \frac{N_{\phi b}}{\sigma_\alpha \cdot \left[\cos\left[\alpha_b \cdot \left[\frac{\pi}{180} \right] \right] \right]^2}$$

$$t_{\alpha b} = 0.0993 \quad \text{inches}$$

$$t_{90b} := \frac{N_{\theta b} - \left[N_{\phi b} \cdot \left[\left[\tan\left[\alpha_b \cdot \left[\frac{\pi}{180} \right] \right] \right]^2 \right] \right]}{\sigma_{90}}$$

$$t_{90b} = 0.0954 \quad \text{inches}$$

TOTAL THICKNESS OF THE BARREL:

$$t_b := t_{\alpha b} + t_{90b}$$

$$t_b = 0.1948 \quad \text{inches}$$

C.5 Internal Insulation Design, EPM Design and Thermal Model

Without protective materials, the case cannot withstand the extreme thermal and atmospheric debris impact environments. Therefore, compatible protective materials were selected and a thermal model constructed to determine protective material thicknesses required.

C.5.1 Internal Insulation Design . Internal insulation protects the inside of the case from the high temperature combustion that occurs during missile flight. The case must remain at a relatively low temperature, compared to the propellant burn temperature, to maintain its structural properties. The insulation is designed such that it sufficiently inhibits conductive heat transfer to keep the case wall temperature below a preset limit. This preset limit is driven by the resin case composite resin, because the case composite fibers can withstand a much higher temperature before their structural properties degrade. The insulation must also have chemical compatibility with the materials it interfaces with (case and the liner) so that long term aging is not an issue. However, the material selection is primarily driven by insulation properties.

C.5.1.1 Background .   Asbestos-based insulators have been the material of choice for missile insulation for many years. The ban on asbestos-based insulators has led to extensive research and development of asbestos-free rubbers for use as missile insulators. A rubber based insulator. Kevlar filled Ethylene Propylene Diene Monomer (EPDM), has thermal properties similar to or better than its asbestos counterpart. Atlantic Research Corporation completed a study (106) in 1986 that characterized Kevlar/EPDM thermally, structurally and chemically. The thermal characterization obtained thermal properties of Kevlar/EPDM as a function of temperature and heating rate (see Table C.11). The structural characterization showed Kevlar/EPDM's ability to withstand the high speed flow environments within the combustion chamber. As long as local Mach numbers were kept below 0.09, mechanical removal of the insulation material is not a concern. The chemical characterization showed that Kevlar/EPDM provided excellent bonds with many different conventional propellants.

C.5.1.2 Operating Conditions and Requirements . Due to the two propellants (aluminum and boron) considered for this study, there are two thermal environments that the internal insulation must withstand. First, integrated stage technology uses boron-based propellant with a burn temperature of $2859^{\circ}C$. Second, conventional technology uses aluminum-based propellant

with a burn temperature of 3264^OC. The required internal insulation thickness at each point depends on exposure time and temperature. The exposure time is a function of second stage burn time and propellant grain configuration. The exposure temperature is a constant for a particular propellant. These parameters are obtained from the propulsion design. In order for structural integrity to be maintained, the case wall temperature must be kept below 135^OC through the completion of second stage burn. 135^OC was chosen as the limiting temperature because it is slightly below the typical glass transition temperature for the resins used in missile composite case material. (54)

C.5.1.3 Material Selection . The selection of Kevlar/rubber (EPDM) is based on its thermal, structural and chemical properties. Rubber is used because of its excellent insulation properties. Kevlar fibers are used because of their structural and erosion resistant properties. Another important consideration in material selection, is its ability to conform to the surface shape. Kevlar/rubber can be molded, laid-up or filament wound over the mandrel. (101:p. 9) Filament winding is chosen so that only one manufacturing technique is needed for the EPM. case, and internal insulation. This is a significant producibility advantage and a potential area of cost savings.

C.5.1.4 Further Study for Detailed Design . Several areas for further study have been identified. First, charring of the insulation at the propellant/insulation interface was not taken into account. Charring occurs when Kevlar undergoes decomposition at approximately 450^OC and forms a char layer. The char layer resists erosion much better than the underlying virgin material, but has different thermal and structural properties than the virgin region. (106:p. 2) Second, the thermal properties of the insulation vary with temperature. Since worst case values were used in the thermal model, accounting for varying thermal properties will decrease insulation thickness, and therefore weight. Third, insulation erosion occurs if the velocity of the propellant gases being expelled exceeds a Mach number of approximately 0.09. (106:p. 3) Erosion occurs when the propellant is expelled at high enough velocities to shear off the insulation char layer. Fourth, the parameter driving insulation thickness is the case's ability to withstand heat while maintaining its structural properties. The *NEMESIS* design does not allow the case temperature to exceed 135^OC. Although the composite fibers can withstand a temperature well above 135^OC, the requirement is derived from the glass transition temperature of the composite resin. In a study performed by

Morton-Thiokol on high temperature composites, several commercially available fibers were used along with high temperature resin to filament wind test pressure vessels. Test results showed that high temperature composites were effective up to $315^{o}C$, a significant improvement over the *NEMESIS* design. (70:p. 30) Based on results from the thermal and weight models, internal insulation weight would be reduced by approximately one-third for each design (up to 70 pounds).

C.5.2 External Protective Material (EPM) Design . The purpose of the EPM is to prevent degradation of the case's structural properties from aerodynamic heating or collision with atmospheric debris. The case must remain at a relatively low temperature, compared to the exterior missile wall temperature, to maintain its structural properties. The location of the EPM between the case and the atmosphere, allows it to act as a heat sink for aerodynamic heating and as a deflector/absorber for atmospheric debris. The EPM is designed such that it absorbs enough heat to keep the case wall temperature below a preset limit. The EPM must also have material compatibility with the case. However, the material selection is primarily driven by insulation properties and an ability to withstand debris impact.

C.5.2.1 Background . The determination of the heat transfer to the missile body, due to aerodynamic heating, is a complex problem involving many variables. Atmospheric temperature, density, thermal conductivity, specific heat, and viscocity, to name a few, vary as the missile gains altitude. Actual heat transfer depends on the missiles aerodynamic characteristics and whether the boundary layer flow is laminar or turbulent. Heat transfer also varies with the missile's velocity, material properties, and flight path angle. The Small ICBM had a requirement for an EPM design and extensive tests were performed (28) to determine the best design approach. Twenty-four EPM designs were constructed from various materials and each design was subjected to three tests, based on pebble mass, pebble velocity and impact angle. The selected design used layers of Kevlar 49/Epoxy Resin filament wound over the graphite/epoxy pressure vessel. Although the design was driven by the atmospheric debris requirement, this design met all aerodynamic heating, producibility, and thermal flash requirements for the Small ICBM. Morton-Thiokol determined that the minimum EPM thickness for debris impact was 0.064 inches. This thickness is based on two hoop plies wrapped over the case (0.018 inches), followed by two plies at minus 10^{0} (0.023 inches) and two plies at plus 10^{0} (0.023 inches). In the *NEMESIS* design, the actual thickness may be higher for aerodynamic heating mitigation as determined by the thermal model.

C.5.2.2 Operating Conditions and Requirements . The need for EPM is driven by:

(1) *NEMESIS* must fly through and survive post-nuclear blast debris. This environment originates when a nuclear blast occurs in the vicinity of the missile silo prior to launch. Debris from the nuclear blast is spread throughout the immediate area and the ICBM must pass through these particles at very high velocities. The specific requirements, shown in Table C.9, are based on Morton-Thiokol testing. (28:p. 97)

(2) As an ICBM flies through the atmosphere, it is heated by aerodynamic friction. *NEMESIS* must withstand aerodynamic heating effects that raise the external skin temperature to 260^0C (98). Even though the atmospheric temperature and density decrease as the ICBM's altitude increases, the velocities achieved by the ICBM are large enough that the external temperature increases drastically. The Minuteman III Stage 2 specification (98) states a maximum temperature of 260^0C at the outside motor wall. This occurs at about 73 seconds after first stage ignition. Because *NEMESIS* uses the MM III first stage and has similar above first stage weight, the assumption is made that *NEMESIS* has the same maximum external wall temperature. Therefore, the EPM thickness must be a minimum of 0.064 inches for debris impact and sufficient to prevent the case wall temperature from rising above 135^0C.

Table C.9. Debris Requirements

	1	2	3
Pebble Mass	.91	.883	.977
Pebble Velocity (fps)	317.0	382.2	218.0
Panel Angle (deg)	21.2	15.4	34.0

C.5.2.3 Aerodynamic Heating Model . Given the MM III requirement of 260^OC at 73 seconds, identification of the aeroheating profile prior to and after 73 seconds from first stage ignition is required. Rather than arbitrarily assuming a profile, the adiabatic wall equations (61:pp. 271-291) below are used to calculate the basic shape (not the actual temperatures) of the aerodynamic heating curve up to 73 seconds after launch. The altitude, time and velocity are obtained from the trajectory model for a simulated MM III flight. The physical properties of the air are determined at the reference temperature (T_R). Table C.10 shows the results.

Define the following parameters:

- T_{AW} - Adiabatic Wall Temperature (^oK)

Table C.10. Calculated Air Properties

TIME (s)	NEW T_{AW}	ALT (ft)	V_∞^2	T_∞	T_W	T_{AW}	T_R	PRANDTL	C_p
0	288.2	0K	0	288.2	288.2	288.2	288.2	0.707	1007
20	322.2	10K	129139	268.2	288.2	288.2	282.6	0.707	1007
28	368.6	20K	287776.5	248.5	322.2	322.2	301.5	0.707	1007
35	434.0	30K	495310.8	228.7	368.6	368.6	329.4	0.7	1009
40	508.5	40K	712835.7	216.5	434.0	434.0	373.1	0.69	1014
44	616.5	50K	986125.3	216.5	508.5	508.5	426.8	0.686	1021
48	746.4	60K	1319721	216.5	616.5	616.5	504.5	0.684	1030
52	879.1	70K	1682803	216.5	746.4	746.4	598.0	0.685	1051
55	1033.8	80K	2107614	216.5	879.1	879.1	693.6	0.695	1075
58	1216.4	90K	2591951	223.5	1033.8	1033.8	806.9	0.709	1099
61	1404.7	100K	3139284	232.5	1216.4	1216.4	940.9	0.726	1141
63	1466.9	110K	3328920	241.6	1404.7	1404.7	1079.0	0.728	1159
66	1540.7	120K	3504690	250.6	1466.9	1466.9	1126.4	0.728	1159
68	1594.6	130K	3676794	259.7	1540.7	1540.7	1181.9	0.728	1175
71	1676.3	140K	3876993	268.7	1594.6	1594.6	1223.4	0.728	1175
73	1729.9	150K	4072650	277.7	1676.3	1676.3	1284.7	0.719	1189

- T_∞ - Free Stream Temperature (^oK)

- T_W - Wall Temperature (^oK)

- T_R - Reference Temperature (^oK)

- V_∞ - Missile Velocity ($\frac{m}{s}$)

- C_p - Specific Heat ($\frac{kJ}{kg-^oK}$)

- μ - Coefficient of Viscosity ($\frac{N-s}{m^2}$)

- k - Thermal Conductivity ($\frac{W}{m-^oK}$)

- Prandtl - (unitless)

$$T_{AW} = T_\infty + \sqrt{Prandtl}\frac{V_\infty^2}{2C_p}$$

$$Prandtl = \frac{C_p\mu}{k}$$

$$T_R = T_\infty + 0.5[T_W - T_\infty] + 0.22[T_{AW} - T_\infty]$$

The temperature values for the adiabatic wall ($15^O - 1457^OC$) are linearly transformed to the temperature range actually experienced by the external missile wall ($26.7^O - 260^OC$). Using polynomial curve fitting, as shown below, the approximate temperature at the external wall is

estimated from launch to 73 seconds. After 73 seconds, the external wall temperature is assumed to stay at the peak temperature of $260^{O}C$. This profile is used in the thermal model (Node 1 temperature) for EPM thickness determination.

This MATHCAD program shows how a quadratic function
was fit to the missile's external wall temperature.
The quadratic function was then used in the thermal
model to estimate the time dependent temperature at
node 1 of the missile structure.

First, the data is read in:

$j := 0 .. 15$ Index for temperature samples

$i := 0 .. 14$ Index for temperature differences

t - Time in seconds at which temperature was calculated

AW - Adiabatic wall temperature in Celsius

EW - Estimated temperature change at exterior missile wall
     in Celsius

$$
t := \begin{bmatrix} 0 \\ 20 \\ 28 \\ 35 \\ 40 \\ 44 \\ 48 \\ 52 \\ 55 \\ 58 \\ 61 \\ 63 \\ 66 \\ 68 \\ 71 \\ 73 \end{bmatrix}
\qquad
AW := \begin{bmatrix} 15 \\ 49 \\ 96 \\ 161 \\ 236 \\ 344 \\ 473 \\ 606 \\ 761 \\ 943 \\ 1131 \\ 1194 \\ 1268 \\ 1322 \\ 1403 \\ 1457 \end{bmatrix}
$$

The following equation shows the ratio of the actual
external wall temperature range to the adiabatic wall
temperature range. This ratio is used to transform
the AW-vector into the EW-vector.

$$
r := \frac{260 - 26.7}{AW_{15} - AW_0} \qquad r = 0.162
$$

The following vector shows the temperature differences
in the adiabatic wall at the succesive time increments

$$AW_{i+1} - AW_i$$

34
47
65
75
108
129
133
155
182
188
63
74
54
81
54

The following vectors transform the adiabatic
wall temperature differences into the external
wall temperature differences.

$$\left[AW_{i+1} - AW_i \right] \cdot r$$

5.501
7.604
10.516
12.134
17.473
20.871
21.518
25.077
29.446
30.416
10.193
11.972
8.737
13.105
8.737

$$EW := \begin{bmatrix} 26.7 \\ 32.2 \\ 39.8 \\ 50.3 \\ 62.4 \\ 79.9 \\ 100.8 \\ 122.3 \\ 147.4 \\ 176.8 \\ 207.2 \\ 217.4 \\ 229.4 \\ 238.1 \\ 251.2 \\ 260 \end{bmatrix}$$

$$EW_{i+1} - EW_i$$

5.5
7.6
10.5
12.1
17.5
20.9
21.5
25.1
29.4
30.4
10.2
12
8.7
13.1
8.8

The following is the quadratic fit of the external
wall temperature as a function of time using
matrix operations.

Create second variable: t squared $\qquad$ $t2 := \overrightarrow{\begin{bmatrix} t^2 \end{bmatrix}}$

Create T matrix:

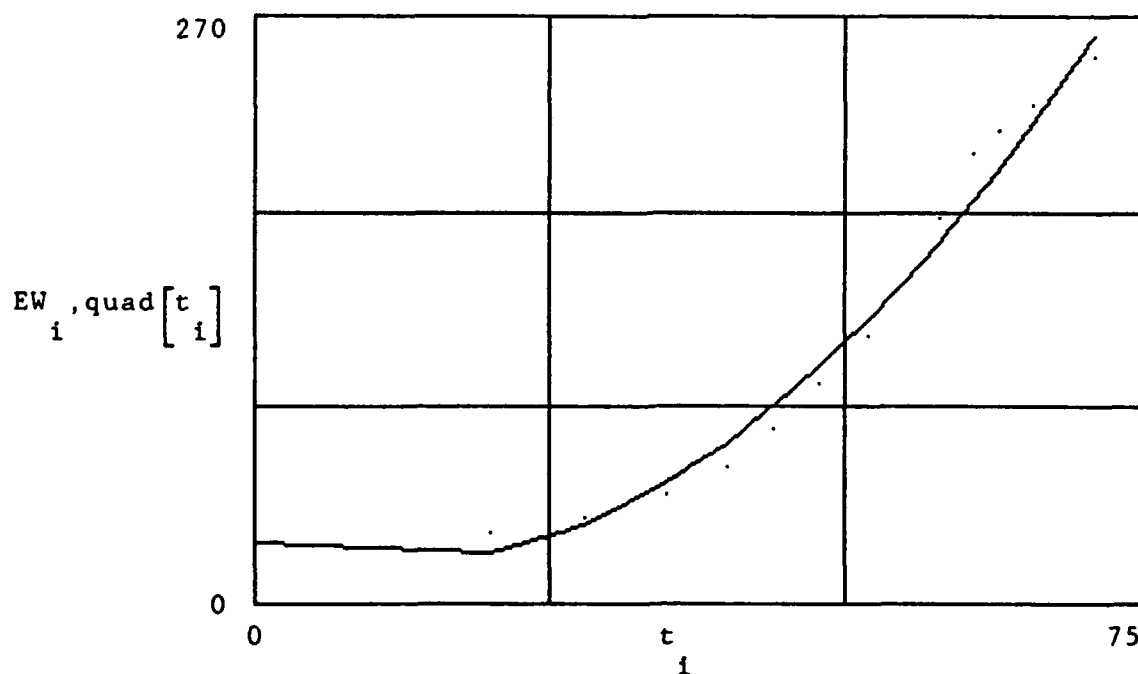$$T_{j,0} := 1 \qquad T^{<1>} := t \qquad T^{<2>} := t2$$

$$b := (T^T \cdot T)^{-1} \cdot (T^T \cdot EW)$$

$$b = \begin{bmatrix} 27.595 \\ -1.628 \\ 0.069 \end{bmatrix} \qquad \text{Parameters for polynomial curve fit}$$

Fitted curve:

$$\text{quad}(t) := b_0 + b_1 \cdot t + b_2 \cdot t^2$$

The following graph shows the external wall temperature
vs time, and the quadratic curve used in the thermal model.

C.5.2.4 Material Selection .   The selection of Kevlar/epoxy as the EPM material is based on the extensive debris impact testing done on the SICBM program. (28) For the debris impact requirement, Kevlar fiber is superior to carbon fiber. The composite resin chosen for the *NEMESIS* EPM and case designs will be the same so that the two subsystems have material compatibility. As with the case resin, the EPM resin's temperature must remain below 135°C for the composite to retain its resistance to bending. However, the EPM is not required to provide bending resistance. Therefore, *NEMESIS* is not designed to limit the EPM temperature. Also, the use of Kevlar/epoxy allows for a common manufacturing technique for the EPM, case and internal insulation.

C.5.2.5 Further Study .   As mentioned previously, the particle impact requirement drives EPM design. If this requirement becomes unnecessary and high temperature composite materials are used for the case wall, then the EPM system can be deleted altogether. High temperature composites can withstand $315^O C$, (70:p. 30) which is more than sufficient for the $260^O C$ aeroheating requirement. The resulting weight savings (up to 185 pounds) could be used for increased performance.

C.5.3 Thermal Model .   A thermal model is required to determine EPM and internal insulation thicknesses required to protect the composite case from high temperatures for each proposed design. The following sections cover the thermal model development and use. Figure C.12 shows the EPM, case, and internal insulation physical relationships established for the thermal model.

C.5.3.1 Derivation .   Define the following parameters:

- k - thermal conductivity
- ρ - density
- c - specific heat
- Δt - time increment
- t - time
- Δr - spatial increment
- r - horizontal distance
- T - temperature
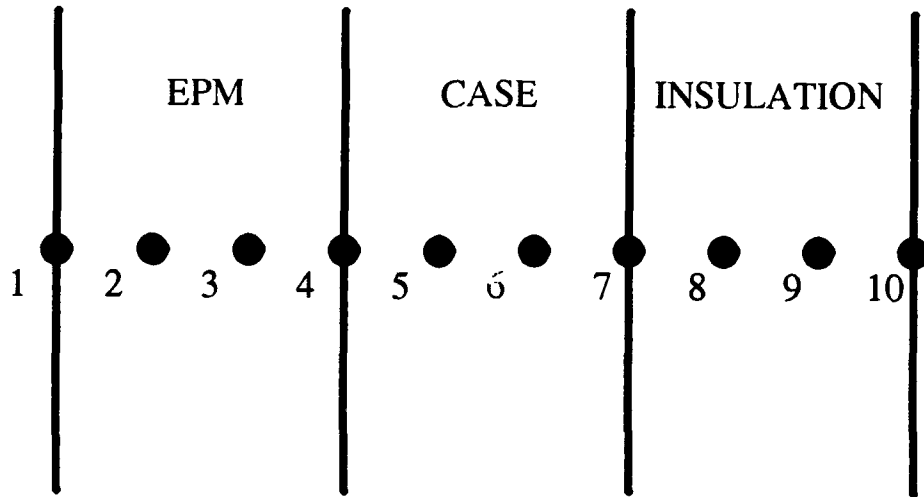
Figure C.12. Thermal Model

Conductive heat transfer occurs because of temperature differences. Prior to launch, each of the STM subsystems are at ambient temperature. From launch to second stage ignition, the external surface temperature (Node 1) of NEMESIS increases according to the aerodynamic heating profile. After second stage ignition. not only does the external temperature continue to rise, but the internal surface temperature (Node 10) increases drastically when it becomes exposed to the propellant burn temperature. Therefore, heat transfer occurs in both horizontal directions after launch.

In order to determine case temperatures, knowledge of the temperature distibution throughout the cross section of the STM design, versus time. is required. Solving the following one-dimensional general heat diffusion equation at each location and time is ideal, but difficult.

$$\frac{\partial T}{\alpha \partial t} = \frac{\partial^2 T}{\partial x^2}$$

$$\alpha = \frac{k}{\rho c}$$

A finite difference approximation of the general heat diffusion equations provides a simpler approach. With a computer model of the finite difference approach. the temperature at several discrete points within each material and at the material interfaces, is tracked versus time. As

the number of nodal points increases, the approximation more closely represents the general heat diffusion equation.

To discretize the heat diffusion equation in time and space, the following approximations (55:ch. 5) are used to determine the node temperatures within a particular material. Conservation of energy concepts are also used to develop the node temperatures at the material interfaces (Nodes 4 and 7).

$$\frac{\partial^2 T}{\partial x^2} = \frac{[T_{i+1}^t - 2T_i^t + T_{i-1}^t]}{(\Delta x)^2}$$

$$\frac{\partial T}{\partial t} = \frac{T_i^{t+1} - T_i^t}{\Delta t}$$

The (t) superscript denotes the time dependence of (T), where (t+1) is the new temperature and (t) is the previous temperature. Thus, each nodal temperature is updated based on the last temperature at that node. The calculations are performed at successive times separated by (Δt). Likewise, the (i) subscript denotes the spatial dependence of (T), where (i+1), (i), and (i-1) are successive nodes separated by (Δx). Thus, each nodal temperature is updated based on the last temperature at the nodes on either side of it.

Using the finite difference equations shown below, and known initial (ambient temperature) and boundary (Nodes 1 and 10 temperatues for all time) conditions, the temperature at discrete nodes is tracked over time. However, the finite difference is not unconditionally stable. To maintain stability, the following stability criteria must be met.

$$\frac{\alpha \Delta t}{(\Delta x)^2} < \frac{1}{2}$$

Finite Difference Equations for Node Temperatures (^0C)

- Node 1: $T_1 = 27.595 - [(1.626)(t)] + [(0.69)(t^2)]$ when $0 < t < 73$ and $T_1 = 260$ when $t > 73$
- Nodes 2,3: $T_i^{t+1} = T_i^t + \frac{\alpha_1 \Delta t}{(\Delta r_1)^2}[T_{i+1}^t - 2T_i^t + T_{i-1}^t]$ where $\alpha_1 = \frac{k_1}{\rho_1 c_1}$
- Node 4: $T_4^{t+1} = T_4^t + \frac{\Delta t}{\rho_1 c_1 \frac{\Delta r_1}{2} + \rho_2 c_2 \frac{\Delta r_2}{2}}[k_2 \frac{T_5^t - T_4^t}{\Delta r_2} - k_1 \frac{T_4^t - T_3^t}{\Delta r_1}]$
- Nodes 5,6: $T_i^{t+1} = T_i^t + \frac{\Delta t}{(\Delta r_2)^2}[T_{i+1}^t - 2T_i^t + T_{i-1}^t]$ where $\alpha_2 = \frac{k_2}{\rho_2 c_2}$

C-53

- Node 7: $T_7^{t+1} = T_7^t + \frac{\Delta t}{(\rho_2 c_2 \frac{\Delta r_2}{2} + \rho_3 c_3 \frac{\Delta r_3}{2})}[k_3 \frac{T_8^t - T_7^t}{\Delta r_3} - k_2 \frac{T_7^t - T_6^t}{\Delta r_2}]$

- Nodes 8,9: $T_i^{t+1} = T_i^t + \frac{\alpha_3 \Delta t}{(\Delta r_3)^2}[T_{i+1}^t - 2T_i^t + T_{i-1}^t]$ where $\alpha_3 = \frac{k_3}{\rho_3 c_3}$

- Node 10: $T_{10} = 2859^\circ C$ for Integrated Stage and $T_{10} = 3264^\circ C$ for Conventional Stage (applied at the appropriate time)

C.5.3.2 Model Inputs / Outputs . The model inputs are:

(1) Thermal conductivity (k), specific heat (c), and density (ρ) of the EPM, case and internal insulation materials (see Table C.11). Since thermal conductivity and specific heat are not varied with temperature, worst case values are chosen for all designs.

(2) Number of nodes (x, y, and z) and thicknesses (TH1, TH2, and TH3) of the EPM. case and internal insulation. There are four nodes per material, but because two of the nodes lie at material interfaces (Nodes 4 and 7), there are a total of 10 nodes (not 12). The case thickness is defined by the structural model. so only the EPM and insulation thickness is varied with each successive computer run.

(3) Second stage burn time (TCRIT) for internal heating determination and total missile burn time (TBURN) for aerodynamic heating determination. Both burn times are defined by the propellant model.

Table C.11. Material Properties

STM SUBSYSTEM	T ($^\circ C$)	DENSITY ($\frac{kg}{m^3}$)	SPECIFIC HEAT ($\frac{kcal}{kg-^\circ C}$)	THERMAL CONDUCTIVITY ($\frac{kcal}{m-s-^\circ C}$)	α ($\frac{m^2}{s}$)
EPM *	38	1350	0.323	4.30E-05	9.86E-08
INSULATION **	37.8	1145	0.325	4.15E-05	1.11E-07
CASE ***	50	1514	0.263	1.79E-04	4.49E-07

- * (46)

- ** (106)

- *** (91)

Since selection of material properties, thicknesses and number of nodes have already been made, only Δt remains as a variable to satisfy the stability condition. Within the FORTRAN program, Δt is selected such that the stability criteria is met for all three materials.

The model outputs are the temperatures at selected nodes at each time increment. The temperatures of concern are the inner (node 7) and outer edge (node 4) of the case wall. After each iteration. the Node 4 and 7 temperatures at second stage burnout are compared to the 135°C

criteria. If the temperature at either node is above $135°C$ than the appropriate material thickness is increased. If the temperature at either node is below $135°C$ than the appropriate material thickness is decreased. The EPM and internal insulation thicknesses are varied until the nodes 4 and 7 temperatures are $135°C$. Note: This model does not account for any thermal benefit the 50 mil liner might contribute.

        C.5.3.3 Data . Table C.12 (in the STM design section) shows the insulation and EPM thicknesses required to meet the specified burn times and propellant grain designs for each of the 33 designs. Below, the FORTRAN model for the integrated stage design is shown. The only difference between the integrated stage and conventional models is the propellant burn temperature.

```
PROGRAM HEATISC
C
C THIS PROGRAM WILL COMPUTE THE TEMPERATURE OF THE INTEGRATED
C STAGE MISSILE STRUCTURE (EPM/CASE/INSULATION) THROUGHOUT
C THE TRAJECTORY OF FLIGHT
C
C INPUT THE VALUES OF THERMAL CONDUCTIVITY (KCAL/M-S-C),
C        SPECIFIC HEAT (KCAL/KG-C), DENSITY (KG/M3), THICKNESS (M)
C AND NUMBER OF NODES FOR THE EPM, CASE AND INSULATION
C
C DIMENSIONALIZE THE OLD AND NEW NODE ARRAY
DIMENSION TE(40), TEN(40)
C
C EPM VALUES
TC1=.00004301
SH1=.323
P1=1350
WRITE(*,*)'ENTER EPM THICKNESS (M)'
READ(*,*)TH1
A1=(TC1)/(P1*SH1)
X=4
DX=TH1/(X-1)
B1=P1*SH1*DX/2
NODEX=X
C
WRITE(*,*)'EPM A1,DX,B1',A1,DX,B1
C
C CASE VALUES
TC2=.0001791
SH2=.263
P2=1514
WRITE(*,*)'ENTER CASE THICKNESS (M)'
READ(*,*)TH2
```

```
A2=(TC2)/(P2*SH2)
Y=4
DY=TH2/(Y-1)
B2=P2*SH2*DY/2
NODEY=X+Y-1
C
WRITE(*,*)'CASE A2,DY,B2',A2,DY,B2
C
C INSULATION VALUES
TC3=.00004145
SH3=.325
P3=1145
WRITE(*,*)'ENTER INSULATION THICKNESS (M)'
READ(*,*)TH3
A3=(TC3)/(P3*SH3)
Z=4
DZ=TH3/(Z-1)
B3=P3*SH3*DZ/2
NODEZ=X+Y+Z-2
C
WRITE(*,*)'INSULATION A3,DZ,B3',A3,DZ,B3
C
C TOTAL MISSILE BURN TIME (FIRST AND SECOND STAGE)
WRITE(*,*)'ENTER THE TOTAL MISSILE BURN TIME'
READ(*,*)TBURN
C
C CALCULATE NUMBER OF NODES
NNODES=X+Y+Z-2
C
C ENTER TIME WHICH DRIVES INSULATION THICKNESS (SECOND STAGE)
WRITE(*,*)'ENTER TIME INSULATION IS EXPOSED TO BURN TEMPERATURE'
READ(*,*)TEXP
TCRIT=TBURN-TEXP
C
C INITIALIZE ALL NODES TO AMBIENT TEMPERATURE
DO 10,I=1,NNODES
          TE(I)=26.7
 10       CONTINUE
C
C CHECK FOR STABILITY CONDITION (A*DT/DX**2)<.5
C
DT1=(.25*DX**2)/A1
DT2=(.25*DY**2)/A2
DT3=(.25*DZ**2)/A3
WRITE(*,*)'3 DELTA TIMES,LOOK FOR LOWEST',DT1,DT2,DT3
C
IF(DT1.LE.DT2)THEN
          DT=DT1
ELSE
  DT=DT2
ENDIF
```

```
      IF(DT3.LE.DT)THEN
        DT=DT3
      ENDIF
C
C CALCULATE NUMBER OF TIME STEPS
NTIMES=TBURN/DT
C
C INITIALIZE AT TIME=0
T=0
C
C OUTER LOOP THAT INCREMENTS TIME
 70    CONTINUE
      IF(T.LE.TBURN) THEN
        T=T+DT
C
C TEMPERATURE AT NODE 1
        IF(T.LE.73)THEN
        TE(1)=27.595-(1.626*T)+(.069*T**2)
      ELSE
        TE(1)=260
      ENDIF
C
C TEMPERATURE AT NODE Z
      IF(T.GT.TCRIT)THEN
        TE(NODEZ)=2859
      ENDIF
C
C TEMPERATURE BETWEEN NODE 1 AND X
      DO 30,I=2,X-1
        TEN(I)=TE(I)+(A1*DT/DX**2)*(TE(I+1)-2*TE(I)+TE(I-1))
 30        CONTINUE
C
C TEMPERATURE AT NODE X
TEN(X)=TE(X)+(DT/(B1+B2))*((TC2*(TE(X+1)-TE(X))/DY)-
      +          (TC1*(TE(X)-TE(X-1))/DX))

C TEMPERATURE BETWEEN NODE X AND Y
      DO 40,J=X+1,NODEY-1
        TEN(J)=TE(J)+(A2*DT/DY**2)*(TE(J+1)-2*TE(J)+TE(J-1))
 40        CONTINUE
C
C TEMPERATURE AT NODE Y
TEN(NODEY)=TE(NODEY)+(DT/(B2+B3))*((TC3*(TE(NODEY+1)-
      +            TE(NODEY))/DZ)-(TC2*(TE(NODEY)-TE(NODEY-1))/DY))
C
C TEMPERATURE BETWEEN NODE Y AND Z
      DO 50,K=NODEY+1,NODEZ-1
        TEN(K)-TE(K)+(A3*DT/DZ**2)*(TE(K+1)-2*TE(K)+TE(K-1))
 50        CONTINUE
C
      DO 60, L=2,NNODES-1
```

```
            TE(L)=TEN(L)
  60    CONTINUE
C
WRITE(*,*) T,(TE(4),TE(7))
C
        GO TO 70
ENDIF
C
STOP
END
```

C.6 Internal Liner

In solid rocket motors, the primary liner function is providing a bonding surface for the propellant on one side and the insulation on the other. The secondary liner function is preventing chemical migration to the insulation from the propellant and vice versa. As the solid rocket motor ages, it is critical that the liner preserve the desired propellant/liner/insulation interface. Liner design is primarily concerned with long term material compatibility. (20)

C.6.1 Background .

During the Minuteman Long Range Service Life Analysis (LRSLA) program, degradation of the Minuteman III Stage 2 liner was determined to be the primary life limiting factor. After testing more than 100 samples from full-scale motors, liner degradation was determined to be critical 14 to 17 years after manufacture. Therefore, a remanufacture program was initiated in 1978 to replace the propellant/liner/insulation system of each stage as they approach 17 years of age. (2) The primary failure mechanism is reduced bond strength due to a degraded liner. The degraded liner is caused by high humidity in the MM III silos and the liner's propensity to absorb water which leads to chemical decomposition of the propellant/liner/insulation bondline system. In extreme cases, complete debonding occurs between the propellant and liner. (2)

Currently, the following techniques are used to further assess liner aging: 1) Full-scale motor firings show actual missile performance, 2) Examination of laboratory samples made concurrently with the full-scale motors, 3) Dissection of full-scale motors from operational silos, 4) Examination of excised samples from operational motors (no damage to motor), and 5) Nondestructive test methods. (102) These techniques are the result of over 30 years of trial and error.

C.6.2 Operating Conditions and Requirements . The liner must maintain the propellant-to-insulation bond in the *NEMESIS* which will be placed in MM III silos that experience temperature and humidity variations.

C.6.3 Material Selection . The conventional *NEMESIS* design uses a new liner being developed for the MM III remanufacture. (84) Development of this 35 year service life liner is under Air Force contract. The integrated stage *NEMESIS* design uses a new liner developed by Aerojet. Due to funding cuts, there are no plans to further develop this liner.

C.6.4 Further Study for Detailed Design . Of the four STM subsystems. the liner requires the most research and development prior to implementation. For both the conventional and integrated stage designs. liner aging information is scarce. The area of greatest concern is long-term compatibility with conventional and integrated stage propellants.

C.7 Other Structural Attachments

The interstage used in the *NEMESIS* design is the MM III interstage for the conventional design and the Aerojet integrated stage interstage for the integrated stage design.

C.8 STM Model Integration

Figure C.9 shows the relationship between the structural, thermal and weight estimating models. The inputs to the structural and thermal models are derived by the propulsion model. The material thicknesses from the structural and thermal models are the inputs to the weight models (separate models for integrated stage and conventional). The weight models and associated Mathcad ouput are shown below and use common geometric relationships (37) and material properites to calculate STM weights. Additional *NEMESIS* weights are calculated by the propulsion model as required.

The following MATHCAD model calculates the EPM, case internal insulation and liner weights for the conventional stage missile designs. Additional weights are calculated by the propulsion group. All weights are in pounds and all lengths are in inches.

$l := 184.16 + 28$ Missile length for case weight calculation (12 inches for propellant clearance and 16 inches for lower dome)

$l_1 := l$ Missile length for EPM weight calculation

$l_2 := l - 32$ Missile length for liner and insulation weight calculation (subtract 16 inches for the lower skirt and 16 inches for the upper skirt)

$r_c := 5$ Nozzle throat radius in lower dome

$r_{dome} := 33$ Radius of lower dome

$r_{udome} := 33$ Radius of upper dome

$h_{dome} := 16$ Height of upper and lower dome

$r_1 := 33$ Missile radius at the bottom

$r_u := 33$ Missile radius at the top

$t_{epm} := .07874$ Thickness of the EPM

$t_{case} := .1654$ Thickness of the case

$f := 21.54$ Final slot half thickness of propellant grain, as defined by the propellant group

$cr := 25.04$ Final central radius of propellant grain, as defined by the propellant group

$$\theta := \operatorname{asin}\left[\frac{f}{cr}\right] \qquad \theta = 1.036$$

Angle in radians that represents the portion of 1/4 of the cylinder exposed to the propellant burning at stage burnout

$$P := \frac{4 \cdot \theta}{2 \cdot \pi} \qquad P = 0.659$$

Percent of cylinder covered with more than minimum insulation thickness

$$t_{adins} := .3268$$ Lower dome insulation thickness

$$t_{insmax} := t_{adins}$$ Maximum insulation thickness

$$t_{insmin} := .02$$ Minimum insulation thickness

The following equation calculates the uniform insulation thickness to be used for the weight calculation

$$t_{ins} := \left[t_{insmin} \right] + \left[\left[t_{insmax} - t_{insmin} \right] \cdot .55 \cdot P \right]$$

$$t_{ins} = 0.131$$

$$t_{liner} := .05$$ Constant liner thickness for all designs

$$t_{epm} + t_{case} + t_{ins} + t_{liner} = 0.425$$ Combined thickness

$$\rho_{epm} := .04877$$ Density of EPM

$$\rho_{case} := .0547$$ Density of case

$$\rho_{ins} := .04137$$ Density of insulation

$$\rho_{liner} := .066$$ Density of liner

Top and bottom radiuses for EPM

$$r_{uepm} := r_u - t_{epm} \qquad r_{lepm} := r_l - t_{epm}$$

Top and bottom radiuses for case

$$r_{ucase} := r_u - t_{epm} - t_{case} \qquad r_{lcase} := r_l - t_{epm} - t_{case}$$

Top and bottom radiuses for insulation

$$r_{uins} := r_u - t_{epm} - t_{case} - t_{ins}$$

$$r_{lins} := r_l - t_{epm} - t_{case} - t_{ins}$$

Top and bottom radiuses for liner

$$r_{uliner} := r_u - t_{epm} - t_{case} - t_{ins} - t_{liner}$$

$$r_{lliner} := r_l - t_{epm} - t_{case} - t_{ins} - t_{liner}$$

Upper and lower dome heights and radiuses for case

$$h_{dcase} := h_{dome} - t_{case} \qquad r_{dcase} := r_{dome} - t_{case}$$

$$r_{udcase} := r_{udome} - t_{case}$$

Upper and lower dome heights and radiuses for insulation

$$h_{dins} := h_{dome} - t_{case} - t_{insmax}$$

$$h_{udins} := h_{dome} - t_{case} - t_{ins}$$

$$r_{dins} := r_{dome} - t_{case} - t_{insmax}$$

$$r_{udins} := r_{udome} - t_{case} - t_{ins}$$

Upper and lower dome heights and radiuses for liner

$$h_{dliner} := h_{dome} - t_{case} - t_{insmax} - t_{liner}$$

$$h_{udliner} := h_{dome} - t_{case} - t_{ins} - t_{liner}$$

$$r_{dliner} := r_{dome} - t_{case} - t_{insmax} - t_{liner}$$

$$r_{udliner} := r_{udome} - t_{case} - t_{ins} - t_{liner}$$

$$W_{epm} := \pi \cdot \left[1_1^2 + \left[r_{lepm} - r_{uepm}\right]^2\right]^{.5} \cdot \left[r_{lepm} + r_{uepm}\right] \cdot t_{epm} \cdot \rho_{epm}$$

$W_{epm} = 168.526$ Total weight of EPM

$$W_{case} := \pi \cdot \left[1_1^2 + \left[r_{lcase} - r_{ucase}\right]^2\right]^{.5} \cdot \left[r_{lcase} + r_{ucase}\right] \cdot t_{case} \cdot \rho_{case}$$

$W_{case} = 395.053$ Cylinder portion of case weight

$$W_{ins} := \pi \cdot \left[1_2^2 + \left[r_{lins} - r_{uins}\right]^2\right]^{.5} \cdot \left[r_{lins} + r_{uins}\right] \cdot t_{ins} \cdot \rho_{ins}$$

$W_{ins} = 200.539$ Cylinder portion of insulation weight

$$a := t_{liner} \cdot \rho_{liner}$$

$$W_{liner} := \pi \cdot \left[1_2^2 + \left[r_{lliner} - r_{uliner}\right]^2\right]^{.5} \cdot \left[r_{lliner} + r_{uliner}\right] \cdot a$$

$W_{liner} = 121.683$ Cylinder portion of liner weight

Lower dome weight calculations

$$e_1 := \frac{\sqrt{r_{dcase}^2 - h_{dcase}^2}}{r_{dcase}} \qquad e_1 = 0.876$$

$$b := .5 \cdot t_{case} \cdot \rho_{case}$$

$$W_{dcase} := \left[\left[\left[2 \cdot \pi \cdot h_{dcase}^2 + \left[2 \cdot \pi \cdot r_{dcase} \cdot h_{dcase} \cdot \left[\frac{asin\left[e_1\right]}{e_1}\right]\right]\right]\right] - \left[\pi \cdot r_c^2\right]\right] \cdot b$$

$W_{dcase} = 24.78$

C-63

$$e_2 := \frac{\sqrt{r_{dins}^2 - h_{dins}^2}}{r_{dins}} \qquad e_2 = 0.879$$

$$c := .5 \cdot t_{adins} \cdot \rho_{ins}$$

$$W_{adins} := \left[\left[\left[2 \cdot \pi \cdot h_{dins}^2\right] + \left[2 \cdot \pi \cdot r_{dins} \cdot h_{dins} \cdot \left[\frac{asin\left[e_2\right]}{e_2}\right]\right]\right] - \left[\pi \cdot r_c^2\right]\right] \cdot c$$

$$W_{adins} = 35.837$$

$$e_3 := \frac{\sqrt{r_{dliner}^2 - h_{dliner}^2}}{r_{dliner}} \qquad e_3 = 0.879$$

$$d := \pi \cdot r_c^2 \qquad e := .5 \cdot t_{liner} \cdot \rho_{liner}$$

$$W_{dliner} := \left[\left[\left[2 \cdot \pi \cdot h_{dliner}^2\right] + \left[2 \cdot \pi \cdot r_{dliner} \cdot h_{dliner} \cdot \left[\frac{asin\left[e_3\right]}{e_3}\right]\right]\right] - (d)\right] \cdot e$$

$$W_{dliner} = 8.703$$

Upper dome weight calculations

$$e_1 := \frac{\sqrt{r_{udcase}^2 - h_{dcase}^2}}{r_{udcase}} \qquad e_1 = 0.876$$

$$f := .5 \cdot t_{case} \cdot \rho_{case}$$

C-64

$$W_{udcase} := \left[2 \cdot \pi \cdot h_{dcase}^2 + \left[2 \cdot \pi \cdot r_{udcase} \cdot h_{dcase} \cdot \left[\frac{asin\left[e_1 \right]}{e_1} \right] \right] \right] \cdot f$$

$$W_{udcase} = 25.136$$

$$e_2 := \frac{\sqrt{r_{udins}^2 - h_{dins}^2}}{r_{udins}} \qquad e_2 = 0.88$$

$$e_3 := \frac{\sqrt{r_{udliner}^2 - h_{dliner}^2}}{r_{udliner}} \qquad e_3 = 0.881$$

$$W_{udins} := \left[2 \cdot \pi \cdot h_{dins}^2 + \left[2 \cdot \pi \cdot r_{udins} \cdot h_{dins} \cdot \left[\frac{asin\left[e_2 \right]}{e_2} \right] \right] \right] \cdot .5 \cdot t_{ins} \cdot \rho_{ins}$$

$$W_{udins} = 14.684$$

$$g := .5 \cdot t_{liner} \cdot \rho_{liner}$$

$$W_{udliner} := \left[2 \cdot \pi \cdot h_{dliner}^2 + \left[2 \cdot \pi \cdot r_{udliner} \cdot h_{dliner} \cdot \left[\frac{asin\left[e_3 \right]}{e_3} \right] \right] \right] \cdot g$$

$$W_{udliner} = 8.879$$

EPM weight $\qquad W_{epm} = 168.526$

Case weight $\qquad W_{casetot} := W_{case} + W_{dcase} + W_{udcase}$

$\qquad\qquad\qquad W_{casetot} = 444.969$

Insulation weight $\qquad W_{instot} := W_{ins} + W_{udins} + W_{adins}$.

$$W_{instot} = 251.06$$

Liner weight $\qquad W_{linertot} := W_{liner} + W_{dliner} + W_{udliner}$

$$W_{linertot} = 139.266$$

Total STM weight

$$W_{TOT} := W_{epm} + W_{casetot} + W_{instot} + W_{linertot}$$

$$W_{TOT} = 1003.821$$

The following MATHCAD model calculates the EPM, case, internal insulation and liner weights for the integrated stage missile designs. Additional weights are calculated by the propulsion group using the Aerojet model and other estimates. All weights are in pounds and all lengths are in inches.

$l := 195.57$ — Length of missile without Aerojet model length for case weight calculation

$l_1 := l + 43$ — Total missile length including Aerojet model length for EPM calculation

$l_2 := l - 16$ — Length of missile without Aerojet model lenght minus upper skirt length for liner and insulation calculation

$r_{dome} := 26$ — Radius of the upper dome

$h_{dome} := 16$ — Height of the upper dome

$r_1 := 33$ — Missile radius at the bottom

$r_u := 26$ — Missile radius at the top

$t_{epm} := .1181$ — Thickness of the EPM

$t_{case} := .095$ — Thickness of the case

$f := 25.55$ — Final slot half thickness of propellant grain, as defined by the propellant group

$cr := 28.48$ — Final central radius of propellant grain, as defined by the propellant group

$\theta := \text{asin}\left[\dfrac{f}{cr}\right]$ $\theta - 1.113$ — Angle in radians that represents the portion of 1/4 of the cylinder exposed to the propellant burning at stage burnout

$P := \dfrac{4 \cdot \theta}{2 \cdot \pi}$ $P - 0.709$ — Percent of cylinder covered with more than minimum insulation thickness

$t_{insmax} := .3937$ Maximum insulation thickness

$t_{insmin} := .02$ Minimum insulation thickness

The following equation calculates the uniform insulation thickness
to be used for the weight calculation

$$t_{ins} := \left[t_{insmin} \right] + \left[\left[t_{insmax} - t_{insmin} \right] \cdot .55 \cdot P \right]$$

$t_{ins} = 0.166$

$t_{liner} := .05$ Constant liner thickness for all designs

$t_{epm} + t_{case} + t_{ins} + t_{liner} = 0.429$ Combined thickness

$\rho_{epm} := .04877$ Density of EPM

$\rho_{case} := .0547$ Density of case

$\rho_{ins} := .04137$ Density of insulation

$\rho_{liner} := .066$ Density of liner

Top and bottom radiuses for EPM

$r_{uepm} := r_u - t_{epm}$ $r_{lepm} := r_l - t_{epm}$

Top and bottom radiuses for case

$r_{ucase} := r_u - t_{epm} - t_{case}$ $r_{lcase} := r_l - t_{epm} - t_{case}$

Top amd bottom radiuses for insulation

$r_{uins} := r_u - t_{epm} - t_{case} - t_{ins}$

$r_{lins} := r_l - t_{epm} - t_{case} - t_{ins}$

Top and bottom radiuses for liner

$r_{uliner} := r_u - t_{epm} - t_{case} - t_{ins} - t_{liner}$

$$r_{lliner} := r_l - t_{epm} - t_{case} - t_{ins} - t_{liner}$$

Upper dome height and radius for case

$$h_{dcase} := h_{dome} - t_{case} \qquad r_{dcase} := r_{dome} - t_{case}$$

Upper dome height and radius for insulation

$$h_{dins} := h_{dome} - t_{case} - t_{ins}$$

$$r_{dins} := r_{dome} - t_{case} - t_{ins}$$

Upper dome height and radius for liner

$$h_{dliner} := h_{dome} - t_{case} - t_{ins} - t_{liner}$$

$$r_{dliner} := r_{dome} - t_{case} - t_{ins} - t_{liner}$$

$$W_{epm} := \pi \cdot \left[l_1^2 + \left[r_{lepm} - r_{uepm} \right]^2 \right]^{.5} \cdot \left[r_{lepm} + r_{uepm} \right] \cdot t_{epm} \cdot \rho_{epm}$$

$W_{epm} = 253.785$ Total weight of EPM

$$W_{case} := \pi \cdot \left[l_1^2 + \left[r_{lcase} - r_{ucase} \right]^2 \right]^{.5} \cdot \left[r_{lcase} + r_{ucase} \right] \cdot t_{case} \cdot \rho_{case}$$

$W_{case} = 187.13$ Cylinder portion of case weight

$$W_{ins} := \pi \cdot \left[l_2^2 + \left[r_{lins} - r_{uins} \right]^2 \right]^{.5} \cdot \left[r_{lins} + r_{uins} \right] \cdot t_{ins} \cdot \rho_{ins}$$

$W_{ins} = 225.35$ Cylinder portion of insulation weight

$$a := t_{liner} \cdot \rho_{liner}$$

$$W_{liner} := \pi \cdot \left[l_2^2 + \left[r_{lliner} - r_{uliner} \right]^2 \right]^{.5} \cdot \left[r_{lliner} + r_{uliner} \right] \cdot a$$

$W_{liner} = 108.323$ Cylinder portion of liner weight

$$e_1 := \frac{\sqrt{r_{dcase}^2 - h_{dcase}^2}}{r_{dcase}} \qquad e_1 = 0.789$$

$$b := .5 \cdot t_{case} \cdot \rho_{case}$$

$$W_{dcase} := \left[2 \cdot \pi \cdot h_{dcase}^2 + \left[2 \cdot \pi \cdot r_{dcase} \cdot h_{dcase} \cdot \left[\frac{asin\left[e_1\right]}{e_1}\right]\right]\right] \cdot b$$

$$W_{dcase} = 11.882 \qquad \text{Dome portion of case weight}$$

$$e_2 := \frac{\sqrt{r_{dins}^2 - h_{dins}^2}}{r_{dins}} \qquad e_2 = 0.791$$

$$W_{dins} := \left[2 \cdot \pi \cdot h_{dins}^2 + \left[2 \cdot \pi \cdot r_{dins} \cdot h_{dins} \cdot \left[\frac{asin\left[e_2\right]}{e_2}\right]\right]\right] \cdot .5 \cdot t_{ins} \cdot \rho_{ins}$$

$$W_{dins} = 15.397 \qquad \text{Dome portion of insulation weight}$$

$$e_3 := \frac{\sqrt{r_{dliner}^2 - h_{dliner}^2}}{r_{dliner}} \qquad e_3 = 0.792$$

$$c := .5 \cdot t_{liner} \cdot \rho_{liner}$$

$$W_{dliner} := \left[2 \cdot \pi \cdot h_{dliner}^2 + \left[2 \cdot \pi \cdot r_{dliner} \cdot h_{dliner} \cdot \left[\frac{asin\left[e_3\right]}{e_3}\right]\right]\right] \cdot c$$

$$W_{dliner} = 7.374 \qquad \text{Dome portion of liner weight}$$

EPM weight
$$W_{epm} = 253.785$$

Case weight
$$W_{casetot} := W_{case} + W_{dcase}$$

$$W_{casetot} = 199.012$$

Insulation weight
$$W_{instot} := W_{ins} + W_{dins}$$

$$W_{instot} = 240.747$$

Liner weight
$$W_{linertot} := W_{liner} + W_{dliner}$$

$$W_{linertot} = 115.697$$

Total STM weight

$$W_{TOT} := W_{epm} + W_{casetot} + W_{instot} + W_{linertot}$$

$$W_{TOT} = 809.241$$

C.9 STM Integrated Design

In the completed *NEMESIS* STM design, the four subsystems are integrated in a cost effective and reliable manner. The materials and processes used are currently available (except for the liner) and should not introduce new failure modes into the system. The first step is to filament wind the Kevlar/EPDM internal insulation over the mandrel. Second, the case is filament wound over the insulation. Third, the EPM is filament wound over the case. At this point the entire assembly is cured. Lastly, the mandrel is removed and the liner is applied to the inside surface of the insulation by slinging, spraying or brush painting.

The integrated stage case has a fully open diameter at the aft end. The primary issue with the fully open diameter is the capabilty of the cut composite and the stage connection joint device to withstand the greatest forces. Aerojet test results (66) show that the lap-shear joint withstands the required loads. Based on these results, ISC cases are now considered a low risk technology and are a cost effective way to decrease the LCC of future missile programs.

C.10 STM Availability/Reliability

The availability of the current MM III STM design is quite good. The goal is to achieve at least the same availability performance in the *NEMESIS* STM design. Since liner aging is the primary cause of STM failure in the MM III, analysis concentrates on liner aging. Refer to Appendix D for a complete analysis.

C.11 STM Cost

Due to the selection of fibers in the EPM, case and internal insulation, all three subsystems can be manufactured using the filament winding process. Significant cost savings will result from less manufacturing equipment, and fewer manufacturing processes. Also, filament winding allows for automation, thus reducing manpower requirements and providing more reproducible quality.

In addition, there are additional cost advantages of the integrated stage filament wound case. The use of ISC case technology reduces manufacturing cost drastically over conventional case technology. The major difference in the two cases is that the aft end of the ISC case has a fully open diameter. Therefore, two cases can be manufactured back to back using a single mandrel and

a single winding. This is possible because each case is symmetric with the other. When filament winding is completed, the assembly is cut in half and the mandrel is removed. The result is two identical filament wound cases. Actual costs on an experimental program show that manufacturing one conventional case is twice as expensive as two ISC cases. Additional savings are achieved because fewer tools with less complexity are needed. (66)

C.12 STM Producibility/Manufacturing

Part of the effort was selecting state-of-the-art materials that are (1) well characterized and qualified, (2) suitable without further modifications, and (3) manufacturable using conventional processing techniques. All the materials (except for the liner) are existing and well understood. In addition, all the materials can be manufactured using existing techniques. One area that requires further development is filament winding of the Kevlar/EPDM internal insulation. Although preliminary development has been accomplished, this technique has yet to be used on an ICBM program. In addition, obtaining variable thickness in the internal insulation design is possible with filament winding, but has not been done on an ICBM program. (53)

C.12.1 STM Design Options .

Table C.12 outlines the generated designs in terms of the STM model. Included are the EPM, case, insulation and liner thicknesses (in inches), MEOP (in psia), and burn time (in seconds). A total of 33 designs were generated. These designs are conservative for the following reasons: 1) the case thickness is designed using a 1.25 burst pressure safety factor, 2) worst case thermal properties for the EPM, case, and internal insulation are used to determine EPM and insulation thickness. 3) the filament wound EPM and insulation fibers add extra strength to *NEMESIS*.

Table C.12. Design Matrix

DESIGN NO.	EPM(in)	CASE(in)	INSULATION(in)	LINER(in)	PRESSURE(psia)	BURN TIME (s)
1	0.122	0.1472	0.425	0.05	1319.9	82.4
2	0.1575	0.0912	0.4724	0.05	817.14	99.8
3	0.122	0.171	0.433	0.05	1536.1	89.2
4	0.1614	0.106	0.4921	0.05	951.04	108
5	0.0787	0.2163	0.2992	0.05	1939.9	49.2
6	0.1501	0.134	0.3512	0.05	1201	59.6
7	0.787	0.2288	0.2992	0.05	2051	49.4
8	0.1035	0.1416	0.3512	0.05	1269.8	59.8
9	0.1204	0.1548	0.3583	0.05	1547.2	62.6
10	0.1343	0.707	0.4803	0.05	706.9	85.8
11	0.984	0.1782	0.3622	0.05	1780.4	65
12	0.1378	0.0814	0.4724	0.05	1813.4	88.4
13	0.0827	0.1862	0.3971	0.05	1861	48.6
14	0.1299	0.0851	0.3858	0.05	850.23	66.6
15	0.0787	0.2079	0.2992	0.05	2077.8	49
16	0.1181	0.095	0.3937	0.05	949.28	67
17	0.0945	0.1945	0.3622	0.05	1744.4	62.6
18	0.122	0.1054	0.4567	0.05	945.1	80
19	0.0945	0.2264	0.374	0.05	2030.3	67.8
20	0.1339	0.1226	0.4528	0.05	1100	86.6
21	0.709	0.2368	0.2992	0.05	2124.2	47.4
22	0.1063	0.1283	0.37	0.05	1150.9	60.6
23	0.0709	0.2566	0.2992	0.05	2301.1	47.8
24	0.1024	0.139	0.37	0.05	1246.7	61.2
25	0.0906	0.152	0.3465	0.05	1509.1	53.8
26	0.122	0.0941	0.3937	0.05	934.27	65.2
27	0.0906	0.175	0.3465	0.05	1736.5	55.8
28	0.120	0.1083	0.3976	0.05	1075.1	67.6
29	0.0709	0.1829	0.2953	0.05	1815	41.8
30	0.0945	0.1132	0.3504	0.05	1123.7	50.6
31	0.0709	0.2042	0.2913	0.05	2026.5	42.2
32	0.0945	0.1264	0.3465	0.05	1254.6	51
33	0.07874	0.1654	0.3268	0.05	1882.6	47

Appendix D. *SYSTEM READINESS*

D.1 Introduction

In recent years, the United States military establishment has been shifting its priorities in systems development. A past emphasis on operational performance has now been broadened to include higher levels of equipment reliability and supportability (5:p1). Evidence for a growing concensus that reliability merits increased attention and resources is abundant, starting at the top levels of Department of Defense (DoD) policy, working down into specifications for new systems and even being reflected in the attention given by publications such as *Aviation Week and Space Technology* to emphasis on design and engineering that will result in reliable equipment (35).

The *Reliability and Maintainability Action Plan R&M 2000* defines the Air Force policy that Reliability and Maintainability will be considered coequal with cost, schedule and performance during acquisition (or major modification) of new systems(94:p3). The five R&M goals established by this policy are

- increase combat capability

- decrease vulnerability of combat support structure

- decrease mobility requirements per unit

- decrease manpower requirements per unit output

- decrease costs.

Due to ICBM-unique requirements, these goals are viewed differently by the acquistion, logistics and operating agencies in the ICBM community (94:p4). "Increase combat capability" is viewed as maintaining or slightly increasing the already high (75) alert rate of current ICBM systems. "Decrease vulnerability of combat support structure" is interpreted as maintaining or increasing the R&M of missile support equipment. "Decrease mobility requirements per unit" addresses the maintenance requirements of the system. Improved R&M means that fewer maintenance personnel and less equipment are needed when a team is dispatched to a silo to perform repairs or general maintenance. With increased reliability, the frequency of maintenance dispatches should decrease. Similarly, "decrease manpower requirements per unit output" means that fewer personnel are required to perform repairs and that requirements for depot level repair should decrease.

Finally, "decrease costs" is viewed as the challenge to most effectively use available dollars. Any modification should decrease the expected life cycle cost of the system (94:p4).

Lieutenant General James McCarthy, 8thAF (SAC) Commander in 1987, discussed the force multiplier effects of R&M from an operating command perspective in his paper entitled "R&M 2000-The Strategic Air Command Perspective" (64). This paper leaves no doubt that specific attention must be given to the areas of reliability, maintainability and supportability of any proposed ICBM modification. LtGen McCarthy makes the following key points:

- To maintain a credible deterrent force "demands" that only systems with the highest possible reliability and maintainability are fielded.

- All weapon systems must be able to encounter and survive difficult operating environments.

- Investment in better reliability and maintainability can directly improve readiness and combat capability.

- R&M becomes a force multiplier–increased combat capability using fewer resources at little or no additional cost.

- Proper R&M planning throughout the design, test, and production phases will help insure that weapon systems delivered in the future are mature and supportable.

- The proliferation of special tools and support equipment for new systems must cease–new systems must use existing tools and support equipment.

- Designing new weapon systems, or modifying older ones, with R&M in mind means that, upon system delivery, missiles can be put on alert with confidence the system will work or, if it fails, that downtime will be minimized.

The *SAC Perspective on ICBM Programs* (11) brings LtGen McCarthy's guidance into the context of the changes in the international and domestic environment that have been witnessed in the last few years. Mounting budget deficits and perceptions of a declining strategic threat have led to reductions in fiscal resources, personnel and United States force structures. These realities have caused the strategic community to make some difficult decisions to preserve the capability of the current ICBM force, and one of these decisions is to view Minuteman III as the centerpiece of the ICBM force well into the next century (11:p2). Key factors that led to this decision included the following:

- high future costs to maintain Peacekeeper

- guidance repair on Peacekeeper is considerably more expensive and manpower intensive than for other ICBMs

- the need to replace Peacekeeper-unique suport equipment by the year 2003

- upgrades to MM III have the potential to reduce maintenance, security and manpower costs (11:p2,3).

Therefore, Air Force policy (as defined by the goals of the *R&M 2000 Action Plan*), and the operating command's view of the importance of R&M (as reflected in LtGen McCarthy's remarks and the *SAC Perspective* memo) provide a clear framework for the systems engineer who wants to propose a major modification to the Minuteman III weapon system. Since each missile is located in an unmanned, remote silo and must be maintained continuously on alert, the missile and its supporting equipment must remain highly reliable and maintainable. These factors become critical in the weapon system design.

D.2 Scope

It is difficult to quantify direct impacts to programs in terms of the goals discussed in the introduction to this appendix. To improve the already high alert rate of the Minuteman III system will be difficult. Any new design candidate may improve the reliability of one subsystem, which in turn decreases the frequency of maintenance dispatches due to failures in that subsystem. However, another subsystem may continue to drive maintenance dispatches. Another complicating factor is the fact that many of the failures that occur in ICBM motors are not detected at the time of failure. In fact, they are not detected at all unless the missile is returned to depot for another (possibly unrelated) failure or if the system is chosen for test firing. Of all the equipment associated directly with the MM III airborne vehicle, only the NS-20 Guidance System (MGS) and the vehicle's payload equipment are monitored continuously. Other checks done on a monthly basis include tests of flight control equipment (electronics, thrust vector contfol valves), command signal decoder, and raceway electrical continuity. Because of the location of the MGS and payload at the top of the missile, if a failure occurs, the offending item can be pulled and replaced in the silo. However, if a downstage, detectable failure occurs, the entire missile must be pulled and returned to depot for repair (29:p7).

If it has been more than a year since a particular missile has been at depot, additional tests are run and additional failed states may then be identified. For example, during planned recycle of Stage 2 motors (driven by age surveillance of propellant and propellant-liner bonds), cracks were observed in silicon rubber motor nozzle entrance caps (75:p).

The only other mechanisms available to detect motor failure tendancies are static firings and operational flight tests. If a motor is chosen for one of these tests and the test results in a failure, two pieces of information are available:

- the age of the particular missile motor

- the failure mode and potentially the cause of failure

However, if the cause of failure was present in the failed motor before the test occurred, the exact time that the failure occurred is not known. For example, suppose propellant/liner/insulation debonds occur over time in a Stage 2 motor while it stands alert in the silo. If such a motor is fired, there is a good possibility that chunks of propellant can break off and cause damage to the nozzle (and ultimately a failed mission test) (75). The time of failure is recorded as the time of the firing, however, the actual failure (the debond) occurred at some unknown time prior to the test firing. Other specific examples can be found in the Weapon System Effectiveness Reports (74, 75).

If the alert rate impacts are difficult to pin down, the impact of design changes on mobility and manpower is even more difficult to quantify early in the design phase. Therefore, it is important to make an assessment of the scope of the work in the areas of Reliability, Maintainability, Availability and Supportability that is appropriate for this project.

First, a full blown Integrated Logistics Support (ILS) Analysis is not intended. Such an analysis would include (21)

1. field maintenance manhours

2. depot maintenance manhours

3. field maintenance skills

4. number of different containers

5. number of different pieces of field support equipment

6. number of different pieces of depot support equipment

7. number of training courses

8. number of depot overhauls per year

9. component inspection frequency

10. volume of containers

11. failure rate of equipment

12. replacement rate

13. number of parts

14. number of spares

15. average field skill level

16. Tech Order page count

17. number of Tech Orders

18. number of different pieces of training equipment

19. square feet of field maintenance/repair facilities

20. square feet of depot maintenance/repair facilities

For the purpose of this study, the focus will be specifically on those areas where there is a chance to show some impacts on the R&M policy goals in a quantifiable way. In the remaining ILS elements, there will be an attempt made to assess design impacts at a top-level, qualitative level only. Specifically, the goal of "maintaining or slightly improving the high alert rate of ICBM's",which corresponds to ILS elements 1,2,8,9,11,12 and 13, will be addressed with a Markov Process model of system availability. A definition of availability that is appropriate for an ICBM will be presented, failure modes and model components will be explained, and alert status Markov models for the 3-stage baseline and the 2-stage design configurations will be derived. Results from these models will be used to evaluate the performance of various 2-stage *NEMESIS* design options with respect to the performance of the baseline (MM III) system. An in-flight reliability allocation will also be done, based on a three stage baseline system reliability.

The goal of "maintaining or increasing the R&M of missile support equipment" will not be quantitatively addressed in this report. However, Reference(94) describes several programs planned to upgrade the R&M of existing support and test equipment. With this goal in mind, the design(s) coming out of this effort will be evaluated to insure compatibility with the existing (and upgraded) support and test equipment. Consideration will be given to eliminating the need for specific pieces of equipment if at all possible. This level of effort covers ILS elements 4,5,6,10 and 18.

Changes to the current MM III maintenance policy are beyond the scope of this work, and so the only anticipated change in the area of "addressing the maintenance requirements of the system" will be to try to design a system that fails less often and requires fewer maintenance dispatches. Modifications such as Peacekeeper's drawer-insertable missile guidance set (64) are not possible as nothing downstage lends itself to "remove and replace" in the silo without modifying the silo maintenance equipment as well. Since all downstage failures are returned to depot for repair (77) and since (regardless of failure mode) the missile typically spends between six and eight days(77) at depot for various checks even after repair is completed, it will be difficult to justify a significant, quantitative improvement in time to repair. Therefore, in the availability model, a constant repair rate will be assumed for all downstage failure modes.

It is expected that the number of personnel required to support/repair a new design will not increase. Therefore, a level of support manpower (ILS elements 3 ,7,15) similar to the baseline system will be assumed.

Finally, the goal to "decrease expected life cycle cost of the system" will be discussed and quantified in the cost section of the report. ILS elements 14,16,17,19 and 20 will be reflected in the total costs, but will not be specifically addressed in the reliability/availability/supportability analysis.

D.3 Definitions

In previous sections, the need to design systems that are reliable, available and supportable has been presented. The scope of the work in these areas has also been discussed. Two important tasks remain:

- to establish a set of clear definitions to describe the basis of a mathematical model for quantitative analysis

- to define criteria upon which to base qualitative assessments of system performance

These two tasks are the focus of this section.

Minuteman is stored in Air Force inventory on years-long alert to defend the nation. The basic Minuteman maintenance philosophy is to obtain maximum missile operational time. This means not only a great emphasis on basic *reliability* of the equipment, but also on the time required to isolate a malfunction and repair it (29:p15).

Various measures of system "goodness" or "effectiveness" are available in the literature. Kapur and Lamberson define seven descriptors to measure the "goodness" of a system from a customer's viewpoint (60:p224):

- *reliability* - the probability that, when operating under stated environmental conditions. the system will perform its intended function adequately for a specified interval of time.

- *serviceability* - the ease with which a system can be repaired.

- *maintainability* - the probability that a failed system can be made operable in a specified interval of downtime.

- *repairability* - the probability that a failed system will be restored to a satisfactory operating condition in a specified interval of active repair time.

- *operational readiness* - the probability that either a system is operating or can operate satisfactorily when the system is used under stated conditions.

- *availability* - the probability that a system is operating satisfactorily at any point in time and considers only operating time and downtime, thus excluding idle time. *Operating satisfactorily* implies operating under the stated environmental and load conditions just as in the definition of reliability.

- *intrinsic availability* - the probability that a system is operating in a satisfactory manner at any point in time when used under stated conditions. It is a more restrictive measure than *availability* in that administrative and logistics time connected with the repair cycle (included

in the *availability* measure) are left out. For example, unavailability of spare parts decreases the availability of a system, but does not impact the *intrinsic availability*.

Sandler (90) defines three measures of availability and also discusses *probability of survival,mean time to failure*, and *duration of single downtime* as measures of system reliability effectiveness. His definition of *instantaneous availability* as the "probability that the system will be available at any random time t seems particularly relevant to the current design work. Sandler says the instantaneous availability measure is applicable to systems which are "required to perform a function at any random time and then remain idle for a length of time"(90:p13).

The Air Force Operational Test and Evaluation Center (AFOTEC) defines availability as "the parameter that translates the reliability, maintainability and logistics supportability characteristics of the system into a measure of interest to the user. It is generally considered synonymous with *operational readiness* (AFR 80-14)"(51:p). AFOTEC further breaks *availability* into categories of "real" and "apparent" availability. This distinction is especially important to this study because ICBMs spend a vast majority of their useful life in storage or in a dormant state. Failures in a silo may not be discovered for long periods of time and other failures may occur that are undetectable until a firing event is actually attempted. These situations or states – where an item is failed (and consequently *unavailable*) but undetected for long periods of time – give rise to the definitional terms "apparent" and "real" availability.

Apparent availability is defined as the percentage of total assets thought to be operable or perceived as ready for immediate use. *Real availability* is the percentage of total assets that would actually operate as intended if the user began a mission execution (51:p9-3). AFOTEC generally uses the following basic mathematical definition of availability

$$A = \frac{t_{up}}{t_{up} + t_{down}}$$

where t_{up} and t_{down} are the uptime and downtime respectively. What is included in uptime and downtime depends on the particular application of the availability measure (ranging from judging the availability of the asset under test to considering the entire procurement, phased in over time, to produce a global, force-wide view of availability). For the purpose of this study, a measure is needed that describes combined reliability and maintainability characteristics of the system or

defines one in terms of the other without worrying about such things as standby or delay times associated with preventive maintenance, administrative and logistics downtime, no-defect maintenance, maintenance due to induced failures, etc. For early conceptual phases of a design when, generally, these terms cannot be defined individually, AFOTEC recommends defining system availability only with respect to operating time and corrective maintenance. Availability defined in this manner, under the ideal conditions already described, is referred to as "Inherent Availability" (51:p9-6) and is defined (in the steady state limit) as

$$A_i = \frac{MTBF}{MTBF + MTTR}$$

where MTBF is the mean time between failures and MTTR is the mean time to repair.

The search for system effectiveness measures for this project would not be complete without consulting the AFIT System Reliability and Maintainability Textbook. Here, reliability is defined as the "probability that an item will perform its intended function for a specified period under stated conditions"(4:p4). Maintainability is the "probability that an item will conform to specified conditions within a given period of time when maintenance action is performed in accordance with prescribed procedures and resources"(4:p5).

Finally, since the current design work will be compared to the Minuteman baseline, there is a need to understand the measures of effectiveness that are currently used by the operating and support agencies to describe the "goodness" of the Minuteman III system. A review of Weapon System Effectiveness Reports (WSER)(75, 74) produced two relevant measures :

- Strategic Alert Reliability (SA_r)–the probability that a deployed missile is capable of reacting to a valid launch execution order

$$SA_r = \frac{MHMC}{TMHA}$$

where *Missile Hours Mission Capable*, MHMC, is defined as the available missile hours (TMHA) minus hours down for *unscheduled* reasons (UM):

$$MHMC = TMHA - UM$$

Total Missile Hours Available, TMHA, is defined as the total number of hours the missiles are possessed by the operating command (TP) minus the sum of the hours missiles are in alert preparation (IP), phasedown (PD), special test (ST), and other *scheduled* downtime (SD):

$$TMHA = TP - (IP + PD + ST + SD)$$

.

- In-Flight Reliability (IF_r) covers the period from Stage 1 Ignition through reentry vehicle deployment and is defined as the probability that a launched missile will place the reentry vehicle in the correct ballistic trajectory to impact in the target area:

$$IF_r = B_r \cdot PB_r$$

where Boost Reliability (B_r) is defined as

$$B_r = PR_1 \cdot PR_2 \cdot PR_3 \cdot FCR_1 \cdot FCR_2 \cdot FCR_3 \cdot GSR \cdot SRR$$

and PR_i is the stage motor reliability. FCR_i is the stage flight control system reliability. GSR is the Guidance System reliability, and SRR is the shroud removal reliability. Post-Boost reliability (PB_r) is

$$PB_r = SM_r \cdot PBV_r$$

where SM_r is the Propulsion System Rocket Engine *steadying maneuver* reliability and PBV_r is the reliability of the entire post boost vehicle.

What is noteworthy with the WSER definitions is that insufficient fidelity is manifest in areas such as stage motor reliability and stage flight control reliability (one number to represent a variety of equipment), and many components are included that are not a part of the current design effort (guidance system, shroud removal, post-boost propulsion system and vehicle). While this suits the level of analysis done in the WSER, some modification of these definitions will be needed to capture the similarities and differences between the current system and the two-stage alternative.

For the purpose of this study, the following approach will be taken:

1. The definition of availability will be what Kapur and Lamberson (60) refer to as "intrinsic availability"

$$A_i = \frac{OperatingTime}{OperatingTime + ActiveRepairTime}$$

This definition is consistent with the concept development or preliminary design phase into which this project fits, and it focuses only on those areas that are within the controllable scope of the project. This definition also seems to capture the essence of AFOTEC's *inherent availability* and Sandler's *instantaneous availability* in focusing only on those factors that are inherent to the design and not dependent on the support structure associated with a given system. As previously stated, this project will deal with the support structure only at a qualitative level and thus support factors are properly excluded from the design availability model. Finally, the WSER definitions of both *alert reliability* and *in-flight reliability* can be broken down to the basics of how often things fail and how quickly they can be put back into service. If an intrinsic availability is calculated for each relevant design component, the resulting component availabilities can be combined in a series fashion to provide a measure of availability for the system

$$A_{isystem} = \prod_{j=1}^{n} A_{ij}$$

where the index j covers all relevant components of the (2 or 3 stage) system design.

2. Reliability will be defined from Stage 1 ignition through reentry vehicle deployment

3. Mathematical models of system alert availability will be constructed using a Markovian (16, 39, 86, 96) approach for describing stochastic behavior under a variety of failure and repair conditions. The details of these models will be described in the next section.

4. In-flight reliability will be assessed by allocating component reliabilities based on a system reliability requirment derived from a systems analysis of the baseline.

5. In areas where there is no reliability or availability history associated with a given component (e.g. Boron propellants or hot gas valves associated with an integrated stage design), an allocation will be made to determine the required performance if the system design is to meet the baseline requirement.

6. Availability and Reliability of various two-stage design options will be calculated and compared to the availability/reliability of the baseline 3-stage system. Results will be given equal weight with performance and cost criteria in making judgements about final candidate designs.

7. ILS factors that are specifically excluded from the models will be discussed qualitatively, and recommendations for follow-on efforts will be addressed.

D.4   Model Description

D.4.1   Purpose . The purpose of developing a mathematical model is to aid in the decision process. Early in the conceptual design phase, models can provide a timely means of emphasizing potential reliability and maintainability problems and guiding design tradeoffs. A primary objective of this study is to compare alternative designs and to choose the one which best achieves system operational requirements. In order to model the reliability or availability of a given system, it is necessary to specify

- the equipment failure process

- the system configuration which describes how the equipment is connected and the rules of operation

- the state in which the system is to be defined as failed

- the repair mechanism

The equipment failure process describes the probability law governing failures. From a mathematical viewpoint, an easy assumption to make is that equipment fails in accordance with a negative exponential distribution. This is a good assumption in many cases. However, other distributions may prove more appropriate to model some ICBM failure mechanisms. The *Weibull* distribution, for example, has application in modeling failures induced by aging phenomena(1:p1). Both exponential and Weibull formulations allow a Markovian approach to modeling system reliability or availability.

The system configuration defines the manner in which the system reliability function will behave(90:p66). For example, two pieces of equipment may be connected in parallel (and the

D-12

system operates as long as one works), or the equipment may be connected in series such that if one fails, the system fails. An ICBM is configured as a series connection of elements, each of which must work for the system to perform.

The third consideration in developing the reliability or availability function for a maintained system is to define the conditions for system failure. Again, for this project, the system fails if any of its series components fails.

Finally, the repair mechanism must be considered. If a piece of equipment is designed so that items expected to fail frequently have a relatively short repair time compared with those items that fail less frequently, an exponential distribution of repair times would be expected. For the great majority of cases, this is a good assumption(90:p110).

In the system design or development environment, information regarding the reliability and maintainability of various alternatives is likely to be imperfect. Therefore, a simulation model is needed so that different values can be included without difficulty, and sensitivity analysis can be performed to determine how parameter changes impact simulated system performance.

D.4.2 Markov Processes . When measures of system worth such as reliability and availability are computed by Markov techniques, they are based on Markovian failure and repair models of the system. Availability, as a function of time, $A(t)$, includes the probability that the system does not fail in the interval $t_o - t$, which is the reliability, $R(t)$. It also includes the probability that if the system does fail prior to t, it will be returned to a satisfactory operating condition by t. System availability, then, can be calculated from the combined Markovian failure and repair models of a system and is expressed as

$$A(t)_{system} = \sum_{i=1}^{n} P_i(t)$$

where i represents the set of unfailed system states and $P(t)$ is the probability of being in the ith "up" state. The specific expression of system availability is a function of the configuration of the system as discussed previously.

A Markov process may be defined as a special type of stochastic process, wherein the probabilistic outcome of any event depends only upon the outcome of the directly preceding event.

Mathematically, a stochastic process, $X(t)$, is a Markov process if

$$P[X(t) = j | X(t - \Delta t) = i, ..., X(0) = a] = P[X(t) = j | X(t - \Delta t) = i]$$

where $a...i$ and $j...n$ represent values assumed by the process at time points $0, ..., t - \Delta t, t, ..., t_n$ (39:p5).

The time parameter of a Markov process may be discrete or continuous, and likewise the state space may also be discrete or continuous. Most engineering applications, including this study, involve a definable (discrete) number of states, so discrete state space Markov processes are appropriate. The figure of merit, availability, will be employed to determine the probability that the system is in an acceptable ("up") state at any time t given that the system was fully operational at t=0.(90:p109).

For simplicity of explanation, consider a system with constant failure and repair rates (*exponential*). For some small time interval, Δt, the probability that the system fails in Δt, P_f, is

$$P_f = \lambda \cdot \Delta t$$

and the probability that the system is repaired in Δt, P_r, is

$$P_r = \mu \cdot \Delta t$$

where λ and μ are the failure and repair rates, respectively. If the availability, $A(t)$, is defined as previously discussed,

$$A(t + \Delta t) = A(t) \cdot (1 - \lambda \cdot \Delta t) + (1 - A(t)) \cdot \mu \cdot \Delta t$$

$$A(t + \Delta t) = A(t) - \lambda \cdot A(t) \cdot \Delta t - \mu \cdot A(t) \cdot \Delta t + \mu \cdot \Delta t$$

Rearranging gives

$$\frac{A(t + \Delta t) - A(t)}{\Delta t} = -(\lambda + \mu) \cdot A(t) + \mu$$

and taking the limit as Δt goes to zero, gives

$$\dot{A}(t) = -(\lambda + \mu) \cdot A(t) + \mu$$

which is a linear homogeneous differential equation with constant coefficients that can be easily solved. In the multidimensional case, the "availabilities" take the form of state variables, and state transition matrices can be found to solve for the probability of being in each state at a particular time.

From a Markov process point of view, let $X(t)$ represent the system state at time t where

$$X(t) = \begin{cases} 1, & \text{if system up at time } t; \\ 0, & \text{if system down at } t. \end{cases}$$

$\lambda(t)\Delta t$ represents the probability of making a transition from the *up* state to the *down* state in the small time increment Δt, and $\mu(t)\Delta t$ represents the corresponding probability of transitioning from *down* to *up*. If the assumption is made that no more than one transition can occur in Δt and that the transition rate depends only on the length of the interval of interest (t) and not where in the time history of the system the transition occurs, the system failure and repair process can be modeled as a homogeneous Poisson process. This simplifies analysis considerably, as the solution reduces to the same set of homogeneous differential equations described previously(86:p2). More realistically, failure and repair density functions of systems can involve classes of functions such as Weibull, lognormal, Rayleigh, etc. Singh and Billinton have shown a Markovian method of representing these non-exponential states by combinations of "stages", each of which is exponentially distributed (96:p179-185).

D.4.3 Failure Mode Data . With the preceeding discussion of failure and repair modeling as a background, it is appropriate to discuss the application of Markov process modeling to ICBM systems and to the current design project in particular. As previously mentioned, there are really two types of availability to evaluate with an ICBM:

- strategic alert availability

- in-flight reliability

As a missile stands alert in a silo for years at a time, there are certain components that fail due to stress or environmental conditions (guidance electronics, flight control electronics, batteries, payload components, case coatings), while other components fail due simply to aging (propellants, ordnance, liners). On the other hand, when the system is called upon to perform its mission, the stresses it must withstand and the environment in which it operates are totally different. In addition, there is no way to repair an ICBM once it is launched. Therefore, an "availability" model must capture and evaluate performance under alert conditions, while a "flight reliability" model must capture mission reliability.

The system readiness "model" for this project, then, is really four distinct models:

- a 3-stage baseline alert availability model

- a 3-stage baseline in-flight reliability model

- a 2-stage alert availability model

- a 2-stage in-flight reliability model

Each model treats the system measure of merit (availability or reliability) as a series combination of subsystems. A series configuration was chosen because all equipment must function for the system to be considered available (alert status) or for the system to adequately perform its mission (flight reliability). Though the basic model is simple enough, extensive research was required to adequately define system failure modes in terms of probability distributions.

The main sources of information in this area for the current Minuteman III system were

- The Silo-Based ICBM Long Range Planning Logistics Program Management Plan(94)

- The Minuteman III Life Extension Founding Father's Review(67)

- Weapon System Effectiveness Reports for the Minuteman System(75, 74)

- Interviews with system experts

Failure and repair data obtained from the documents and interviews is based on 21 years of Minuteman III flight testing and static motor firing, 18 years of simulated electronic launch and environmental testing, more than 20 years of aging surveillance and more than 20 years of failure reporting on fielded systems.

D-16

Information for the two-stage design alternatives comes from research on the Peacekeeper weapon system, work done to support the Small ICBM development program, and extensive personal and telephone interviews with government system experts and corporate (Aerojet, Thiokol, Hercules, etc.) engineers who are actively working on Minuteman upgrade programs.

A review of the available data produces several general observations:

- the Minuteman III system has proven to be a very reliable system over the years

- the system has exceeded its design service life

- the percentage of in-flight system failures is very small

- many of the failures that have occurred can be traced to one-shot process or manufacturing anomalies that were identified and fixed

- programs are planned (and in some cases in progress) to deal with those items known to be maintenance drivers

Minuteman, as a baseline for this project, has been an extremely reliable system and continues to meet alert and flight performance requirements even though it has exceeded its service life goal by ten years(94:p1). This is not to say there are no problems. However, the problems are well characterized and programs are in place to address the known problems(94). So, as a goal, if this design project can simply meet current requirements, the design will be a success from an availability or reliability point of view.

Over the years, the following ICBM failure modes have been identified:

- age-related service life limitations of liners, propellant, igniter ordnance, nozzle entrance caps, o-ring seals, batteries, flight control ordnance, stage separation and skirt jettison ordnance, and post-boost vehicle liquid propellants

- guidance system and payload failures on fielded systems (maintenance driver on current system)

- field downstage failures in flight control equipment, command signal decoder and raceway cables

- random flight or static fire failures of motors, flight control equipment, ordnance, guidance set, post-boost vehicle and reentry systems

D-17

- random personnel-induced handling failures

The scope of this design project is focused on a single stage motor replacement for the current Minuteman stages 2 and 3. Therefore, no re-design is intended in Stage 1, the missile guidance set or the post-boost vehicle. For modeling purposes, any failure and repair of these components will be the same for both the baseline and the 2-stage design. In the case of the stage igniters and ordnance and the interstage ordnance, no design change is planned other than to remove the need for an entire set of this equipment (no stage 3 ingnition needed and no stage 2-stage 3 separation required). The differences between the predicted reliability or availability, then, will come from

- removal of potential failure mechanisms due to reduction in number of stages

- any specific reliability improvements in the project's stage 2 motor design (conventional or integrated stage)

To account for differences due to both stage reduction and fundamental design change, these elements will be included in the series system models:

- Stage 1

- Post-Boost Vehicle and Payload

- Missile Guidance Set

- Command Signal Decoder

- Upper stage - PBV Separation Ordnance

- $Stage_i$ Flight Control Subsystem

- $Stage_i$ Propulsion Subsystem (propellant, propellant-liner bonding, nozzle components)

- $Stage_i$ Igniter Ordnance

- $Stage_i$ Flight Control Subsystem Ordnance

- Stage 1-2 Separation Ordnance

- Stage 2-3 Separation Ordnance (3-stage model only)

The first four elements listed will be constant (unchanged) for all designs. Differences due to ordnance will be due only to reduction in numbers of stages. not to any fundamental changes in

the design of these elements. Differences due to flight control and propulsion subsystems will be impacted by both reduction in number of stages and fundamental changes in design, so fidelity is required in these two components, but nowhere else. In the next sections, the actual failure models for each model element are presented.

D.4.4 Model Element Distributions . The failure and repair mechanisms associated with each model element presented in the previous section must be modeled mathematically using appropriate stochastic distributions. Age-related failure phenomena will be modeled using Weibull distributions. Random field or flight failures will be handled with exponential models. Only guidance and reentry system failures are detected at time of failure. For elements that are monitored monthly, a stage representing failure "discovery" must be included in the model with a transition rate into the stage of 12 per year (constant). For elements such as liner degradation. ordnance aging and propellant cracking that are not monitored unless the missile is returned to depot for some other failure, the transition out of the "discovered" stage is the average rate at which missiles are returned to depot: 12 out of the fleet of 500 per year ($\lambda = 0.024$). Repair times will be modeled as a constant 100 hours for guidance and 75 hours for reentry system elements and as a constant 7 days for all downstage equipment, based on past Minuteman III experience (77, 26).

For the Weibull failure density function, two parameters are needed (60:p292)(the location parameter or minimum life parameter. δ, is assumed to be zero)

- β, the shape parameter or Weibull slope
- θ, the scale parameter or characteristic life

Both the characteristic life parameter, θ, and the shape parameter, β, associated with each Minuteman III (baseline) element modeled with a Weibull distribution are taken from aging surveillance data presented in the Minuteman Weapon System Effectiveness Reports. For each element of the model that fails due to aging phenomena, θ corresponds to the service life estimate (SLE) for that element and β is chosen to match the variance of the SLE data. Table D.1 summarizes the model parameters associated with the 3-stage "aging" failure modes.

The "method of stages"(96) will be used to approximate the Weibull failure distribution elements with a series combination of exponential stages. A "discovery" stage will be included as discussed previously. An exponential repair rate of one every seven days will be assumed for

ELEMENT	β	θ(yrs)
S2 Liner	4	17
S3 Liner	4	17
S2 Igniter	6	29
S3 Igniter	4	26
S2 FC Ordnance	4	30
S3 FC Ordnance	4	24
S1-S2 Sep Ordnance	4	26
S2-S3 Sep Ordnance	4	26
Upper Stage Sep Ord	4	26
S2 Propellant	8	18.5
S3 Propellant	8	18.5

Table D.1. 3-Stage Baseline Aging Failures - Weibull Parameters

downstage failures (77), and a repair rate of one in 100 hours will be assumed for guidance set and 75 hours for payload repairs (26).

Flight and static firing failures, field recycles and simulated test failures will be modeled using exponential (constant failure rate) distributions. The baseline failure rate parameters. λ_i, again are estimated from data found in the Minuteman Weapon System Effectiveness Reports (75, 74) and in the Founding Fathers report (67). Table D.2 summarizes the model parameters associated with the 3-stage baseline random failures.

ELEMENT	$\lambda(peryr)$
Guidance	0.796
Stage 1	0.01
S2 FCE	0.006
S3 FCE	0.006
Cmd Signal Decoder	0.002
Reentry System	0.4645

Table D.2. 3-Stage Baseline Random Failures - Exponential Parameter

For the two-stage design, engineering estimates will be made of deltas from the baseline parameters. Test results will be used where they are available, similarity to existing equipment will be relied on where necessary, and "engineering judgement" based on conversations with system experts will be used to fill in any remaining holes. Tables of parameters for all candidate designs will be generated and presented in the next section.

D.4.5 Derivation of Markov Element Models

D.4.5.1 3-Stage Element Models . In the last section, Weibull distributions were postulated for nine model elements: stage 2 and stage 3 propulsion, stage 2 and 3 ignition, stage 2 and 3 flight control ordnance, and stage separation ordnance (1-2, 2-3 and upper stage-PBV) (Table D.1). Singh and Billinton (96) have shown that Weibull distributions with $\beta \geq 1$ can be modeled as a series of stages or phases (Figure D.1). The time to failure (TTF) is a random variable with an Erlang probability density function (pdf)

$$f(t) = \sum_{i=1}^{n} P_i(0)\tau_i \exp(-\tau_i t)$$

where $P_i(0)$ is the probability of transitioning to stage i from the "down" or non-operating state, and the $\tau_i's$ are constant transition rates that may be different.

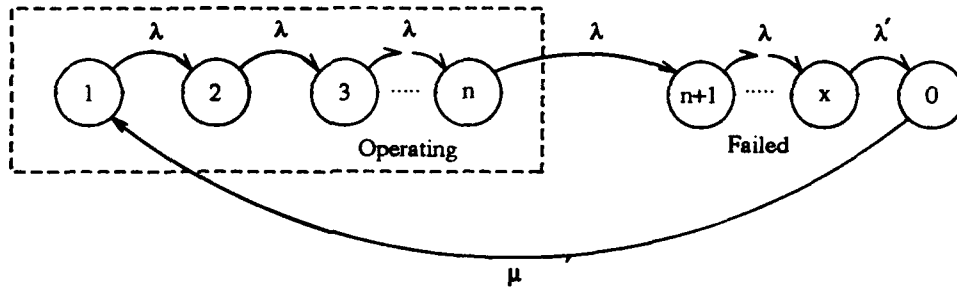

Figure D.1. Weibull Stages

Let

$$P_1(0) = 1$$

and

$$P_2(0) = P_3(0) = ... = P_n(0) = 0$$

where

$$\tau_i = \tau$$

That is, the transition will always be to stage 1 from the "down" state and all $\tau's$ are the same. Next, an estimate is needed for τ and n to approximate the given Weibull pdf for TTF. When all stages are

identically distributed with parameter τ, the corresponding pdf is the Special Erlangian(96:p183)

$$f(t) = \frac{\tau(\tau t)^{n-1}\exp(-\tau t)}{(\tau - 1)!}$$

To approximate the TTF density function with f(t), the two parameters, τ and n, must be estimated. The simplest approach (86:p26) is to use the method of moments. The rth moment of f(t) (for integer n) is given by

$$m_r = \frac{1}{\tau_r}\prod_{k=1}^{r}(n + k - 1)$$

Solving for the first two moments:

$$M_1 = \frac{n}{\tau}$$

and

$$M_2 = \frac{n(n + 1)}{\tau^2}$$

Solving for n and τ gives

$$n = \frac{M_1^2}{(M_2 - M_1^2)} \tag{D.1}$$

and

$$\tau = \frac{M_1}{(M_2 - M_1^2)} \tag{D.2}$$

For the Weibull pdf.

$$f(t) = \frac{(\beta t)^{\beta-1}}{\theta^\beta)} \cdot \exp[-(t/\theta)^\beta]$$

, the first and second moments in terms of the parameters are

$$M_1 = \theta\Gamma(\frac{1}{\beta + 1}) \tag{D.3}$$

and

$$M_2 = \theta^2\Gamma(\frac{2}{\beta + 1}). \tag{D.4}$$

Since β will have a value of 4,6 or 8 for all elements of this model(Figure D.1), the arguements for the Gamma function will not be integer values and thus the function

$$\Gamma(x) = \int_0^\infty t^{x-1} \exp(-t)dx$$

must be evaluated to get values for $\Gamma(\frac{1}{\beta+1})$ and $\Gamma(\frac{2}{\beta+1})$. For $\beta = 4$,

$$\Gamma(1.25) = 0.9064$$

and

$$\Gamma(1.5) = 0.8862$$

(15:p429) If the first two moments of the true (Weibull) TTF (Equations D.3 and D.4) are substituted for M_1 and M_2 in Equations D.1 and D.2, (equating moments), the required number of stages, n, and the transition rate, τ, needed to approximate the given Weibull distributions with exponential stages can be determined. Using these relationships and substituting the appropriate values for θ and β from Table D.1, the Markov state transition diagrams and state transition matrices can be derived for each element of the 3-stage model. The following is a sample calculation done for the Stage 2 (3) Liner element ($\beta = 4, \theta = 17$).

Using Equation D.3,
$$M_1 = 17(.9064) = 15.4088$$

Using Equation D.4,
$$M_2 = 17^2(.8862) = 256.1118$$

and

$$M_2 - (M_1)^2 = 18.68$$

Using Equation D.1, the number of stages is calculated as

$$n = \frac{15.4088^2}{18.68} = 12.7 \approx 13$$

and τ is calculated using Equation D.2:

$$\tau = \frac{15.4088}{18.68} = 0.82488.$$

An alternative approach uses the SLE from the Weapon System Effectiveness Report as the *expected value* or *mean* life of the element under consideration. The first moment, M_1 is then simply the SLE, and the second moment, M_2, is calculated from

$$M_2 = E(X^2) = \sigma^2 + [E(X)]^2$$

where σ is determined from the data and $E(X)$ is the SLE from the data. Equations D.1 and D.2 are again used to calculate n and τ. The choice of method was made based on the better fit to the available data.

In the example of the Stage 2 Propulsion element, the "SLE $= M_1$" approach produced results that best approximated the data. The resulting Markov state transition diagram is shown in Figure D.2
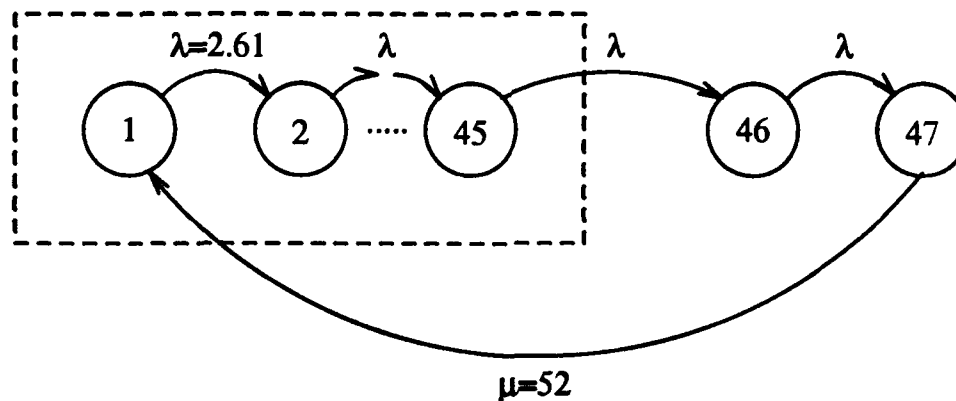

Figure D.2. State Transition Diagram for St 2 Propulsion Element

Calculations were done for all the elements in Table D.1, and the results are shown in Table D.3.

For the 3-stage model elements of Table D.2, the method of stages is not required. Here, the model is a simple two stage failure-repair Markov model if the element is monitored continuously.

ELEMENT	NUM OF STAGES,n	TRANSITION RATE, τ
S2 Propellant	45	2.61
S3 Propellant	45	2.61
S2 Ign Ord	34	1.16
S3 Ign Ord	13	0.54
S2 LITVC Ord	25	0.833
S3 LITVC Ord	16	0.67
S1-S2 Sep Ord	19	0.722
S2-S3 Sep Ord	19	0.722
S3-PBV Sep Ord	19	0.722
S2 Liner	33	1.89
S3 Liner	33	1.89

Table D.3. 3-Stage Markov Parameters for Weibull Approximation

If the element is monitored monthly or not monitored at all, a third "discovery" state is included. State 0 is the "up" state, State 1 is the "down" state for the continuously monitored elements and the "discovery" state for the rest. A State 2 is added as the failed state for those element models that include the discovery state. Transitions are made from up to down with the rates given in Table D.2 and from down to up with the rates appropriate for upper stage (guidance or payload) or downstage repairs. Transitions out of the discovery state are 12 per year for monthly monitoring and .024 per year otherwise.

D.4.5.2   2-Stage Element Models .   As discussed previously, interstage ordnance, flight control ordnance and stage igniter elements are not candidates for design change with the two stage alternative, but are included because there is a reduction of an entire stage with this design (and a corresponding reduction in the numbers of these equipments). In the two-stage system model, only one set of igniter and flight control ordnance is required versus two sets for the 3-stage alternative. Similarly, two sets of interstage ordnance (1-2 and 2-Post Boost) are needed against three for the current configuration. The Markov models for these elements will be exactly the same for the two-stage design as they were for the three-stage design, but there will be fewer elements included in the model.

Markov models for Stage 1, missile guidance set, payload/post-boost vehicle, and command signal decoder are also transferred (without any modification) directly to the two-stage model.

The elements that do change for the two-stage model are the following:

- liner aging properties

- propellant aging properties

- flight control system equipment

Some discussion of the expected design changes is presented first, and then the corresponding Markov element models are derived using the same equations developed in the previous section. Liner properties are discussed first, followed by propellant and thrust vector control elements.

Liner Properties

In solid rocket motors, the primary liner function is to provide a bonding surface for the propellant (on one side) and the insulation (on the other). The secondary function is to prevent chemical migration between propellant and insulation due to the close proximity of two materials with very different chemical properties. As the solid rocket motor ages, it is critical that the liner acts to preserve the tight interface bond needed for reliable motor performance. Therefore, liner design is primarily a material compatibility exercise.

One of the primary failure mechanisms discussed previously was a propellant-liner "debonding". A better description of this phenomenon really would address reduced bond strength resulting from a degraded liner. High humidity in silos combined with the liner material's propensity to absorb water cause chemical decomposition of the propellant/liner/insulation bondline system. Liner degradation is a function of moisture content, and in extreme cases, complete debonding occurs between propellant and liner.

Since the liner debond problem is a primary driver in Minuteman Stage 2 and Stage 3 motor service life estimates, a new liner is being developed for the stage remanufacture programs. Development of this new liner, expected to double (to 35 years) the current service life estimate, is currently under Air Force contract (84). According to project engineers at Aerojet corporation, the new liner is "fairly well characterized with the current Minuteman III propellant and insulation", but very little life testing has been done. Because of the lack of data, the uncertainty associated with the 35 year service life liner is much higher than that associated with the current system's 17 year service life. For the boron propellants associated with an Integrated Stage design, Aerojet developed a liner, but it has not been fully characterized or age tested with the new propellants. Due to funding cuts, there are no plans to do any further work to fully develop this liner. System

experts feel there is no technical reason that a 35 year liner could not be developed for integrated stage, given funding and "sufficient development time". However, confidence in such an assumption would have to be considered very low at this point in time.

Another consideration in estimating a service life for the two-stage design liner is the size of the design stage motor. Bondline stress is not a function of length, but it is a function of both missile diameter and bore (propellant center "hole") diameter. Since the *NEMESIS* second stage has different dimensions than current MM III second or third stages, the following relationship will be used to scale the service life estimate for the AFIT design:

$$SLE_{AFIT} = SLE_{35} \cdot [\frac{1 - (T_1/T_2)}{2} + \frac{T_1}{T_2}]$$

where T_1 is the difference between outer and inner propellant diameters for MM III and T_2 is the corresponding difference for the new Stage 2 design. Using this scaling factor gives a new service life estimate of 31.5 years for a cylindrical second stage design (outer stage diameter of 64 inches, bore diameter of 5 inches).

Using 31.5 years as the characteristic life parameter for the Weibull distribution, and assuming a β of 2.75 (reflecting the degree of uncertainty associated with the characteristic life parameter), the Markov stages and transition rates can be calculated as previously done for the three stage model. Results for an integrated stage design: $n = 7$ and $\tau = 0.231$. Using a mean life of 29 years and a standard deviation of 8 years yields $n = 13$ and $\tau = 0.453$.

Propellant Properties

The aging of solid propellants often causes cracks to form. The complex chemistry of the propellants makes precise prediction of aging effects very difficult. Most failure information is based on experimental results and aging surveillance data. The most serious impact of cracks is the subsequent increase in surface area exposed to the hot combustion gases within the motor chamber.

Burning solid rocket propellants produce exhaust gases proportional to the amount of surface area exposed to the hot gases of the combustion chamber. The design point of solid rockets corresponds to a balance of the mass generation rate of the burning surface, the mass storage rate in the chamber, and the mass flow rate through the nozzle throat.

By increasing the burn surface area, more hot gases are produced and the pressure in the chamber increases. Cracks in solid propellants cause the internal burn pressure to increase, and if the total of all cracks is large enough, the pressure can exceed the burst limit for the motor case, causing a very obvious system failure!

The probability of significant cracking in solid propellants increases as a function of time. Since the failure rate increases with an increasing rate, a Weibull probability distribution ($\beta \geq 1$) can be used to model propellant cracking failures. For propellants with aluminum fuels, aging surveillance data is abundant and has shown that significant cracks develop with a mean between 17 and 20 years, with a 3σ lower limit of 13 years (2). The parameters to be used for calculation of Weibull stages are $\theta = 18.5$ years and $\beta = 8$, which results in $n = 45$ and $\tau = 2.61$.

For boron-based propellants (used with Integrated Stage design), very little aging data is available. Early estimates (68) put the life of boron propellants at only about half that of the aluminums, but more recent work (72) with improving boron propellants indicates that their design life is as long as the aluminum propellants. However, since these estimates were obtained from accelerated life testing rather than from actual aging surveillance, much more uncertainty is involved. For the purpose of this project, $M_1 = 18.5$ years and $\sigma = 4$ years is assumed, giving $n = 22$ and $\tau = 1.16$ for boron propellants.

Thrust Vector Control

Secondary injection of hot combustion chamber gases into a nozzle exit cone for thrust vector control was investigated extensively in the early 1960's (69). Various tests determined that nozzle flow could be diverted to provide the small corrections needed to steer large rocket booster stages. At the time, however, "hot gas" valve designs were large and heavy, and could not compete with more conventional systems (gimballed nozzles, liquid injection systems, etc.). With the advent of the integrated stage concept and advances in material technology that made lighter valves (that could still stand up to high temperatures and flow rates) possible, the hot gas valve can be put to optimum use.

Aerojet Corporation has studied and tested several valve configurations in conjunction with the U.S. Army's MIST program. The valves have performed "satisfactorily" (9) towards a design storage life goal of 20 years. The materials used for the valves are inert ceramics, so there is no real concern about corrosion or breakdown in the silo. There is an electrical solenoid that is needed for

operation, and the electrical continuity of this element can be monitored as part of the monthly monitoring of the TVC subsystem.

The major design risk for hot gas valves in the current project lies in the relatively long operating time required for potential second stage design motor burns of between 60 and 90 seconds. Current testing has been limited to a maximum motor operating time of 40 seconds. Though hard data is not available above this 40 second limit, valve experts (36, 80) see no reason why the valves will not perform for longer duty cycles and still achieve design lives of 25 years or longer, and in fact United Technologies Chemical System Division proposed a valve for the Navy's *Trident* program that had a required design life of 25 years with a 50 year goal (36).

Since the risk in hot gas valve technology lies in the development and testing of valves that meet in-flight performance for required mission lengths in the 60-90 second range, this issue will be addressed in the in-flight model. For silo availability, the materials are no longer new and exotic, and designs are not complicated to manufacture. To reflect some risk in the projected design life, a characteristic life parameter of $\theta = 22$ years was chosen with $\beta = 7$. This results in a Markov stage model with $n = 35.421 \approx 36$ and $\tau = 1.721$.

D.5 Calculation of System Availability

In previous sections, justification was given for using Markov processes to model the availability of maintained systems. The number of stages and the transition rates for each of the Markov element models were also derived and state transition diagrams were formed. The following steps remain:

1. form state transition matrices from the state transition diagrams of each model element

2. solve each state transition matrix by finding the probability of being in each state and summing the probabilities of being in "available" states

3. find the "system availability" as the product of all individual element availabilities (series model)

D.5.1 STEP 1: Form State Transition Matrices . The state transition matrix is formed directly from the state transition diagram. Examples are given for a continuously monitored element

D-29

(e.g. guidance), an element tested monthly (flight control electronics), and for an element whose failures go undetected unless returned to depot for another failure (liner/propellant debonding). Note that the *transpose* of each original state transition matrix is presented because it is the transpose that is used by the solver program.

```
-0.796   0.796
 87.6   -87.6
```

Missile Guidance Set

```
-.006    .006    0.
 0.     -12.    12.
 52.      0.   -52.
```

Stage 2/3 Flight Control Equipment

```
-52. 52. 0. 0. 0. 0. 0. 0. 0. 0. 0. 0. 0. 0. 0.
 0. -.825 .825 0. 0. 0. 0. 0. 0. 0. 0. 0. 0. 0. 0.
 0. 0. -.825 .825 0. 0. 0. 0. 0. 0. 0. 0. 0. 0. 0.
 0. 0. 0. -.825 .825 0. 0. 0. 0. 0. 0. 0. 0. 0. 0.
 0. 0. 0. 0. -.825 .825 0. 0. 0. 0. 0. 0. 0. 0. 0.
 0. 0. 0. 0. 0. -.825 .825 0. 0. 0. 0. 0. 0. 0. 0.
 0. 0. 0. 0. 0. 0. -.825 .825 0. 0. 0. 0. 0. 0. 0.
 0. 0. 0. 0. 0. 0. 0. -.825 .825 0. 0. 0. 0. 0. 0.
 0. 0. 0. 0. 0. 0. 0. 0. -.825 .825 0. 0. 0. 0. 0.
 0. 0. 0. 0. 0. 0. 0. 0. 0. -.825 .825 0. 0. 0. 0.
 0. 0. 0. 0. 0  0. 0. 0. 0. 0. -.825 .825 0. 0. 0.
 0. 0. 0. 0. 0. 0. 0. 0. 0. 0. 0. -.825 .825 0. 0.
 0. 0. 0. 0. 0. 0. 0. 0. 0. 0. 0. 0. -.825 .825 0.
 0. 0. 0. 0. 0. 0. 0. 0. 0. 0. 0. 0. 0. -.825 .825
.024 0. 0. 0. 0. 0. 0. 0. 0. 0. 0. 0. 0. 0. -.024
```

Stage 2/3 Liner/Propellant Debond
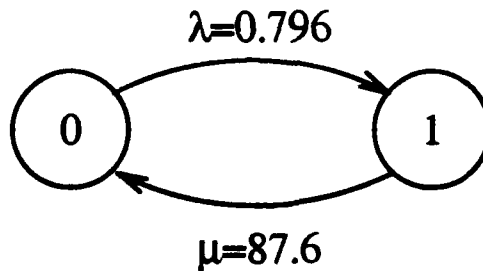

$\lambda = 0.796$

$\mu = 87.6$

Figure D.3. State Transition Diagram for Guidance Set

All state transition matrices will be presented in the thesis for both the 3-stage baseline model and for all 2-stage *NEMESIS* design alternatives.
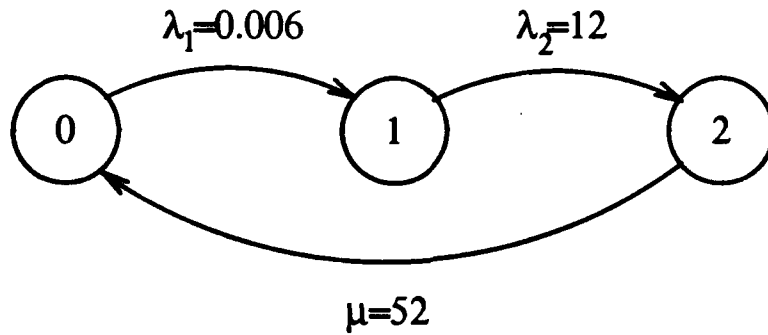
Figure D.4. State Transition Diagram for Stage 2/3 FCE
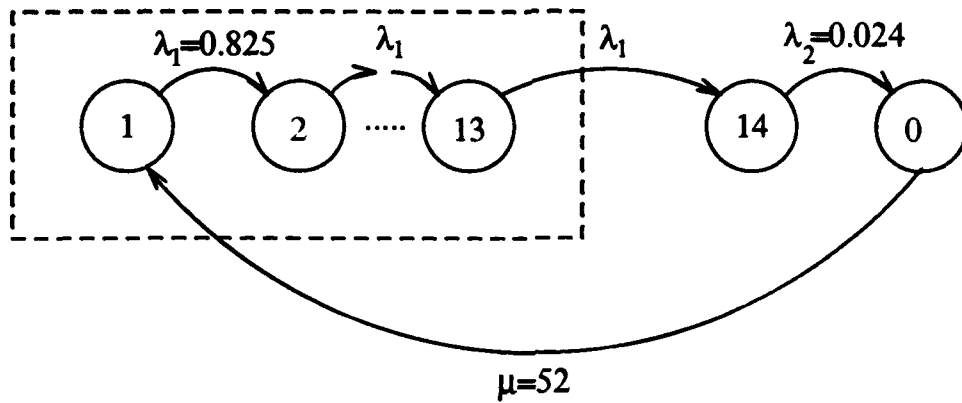
Figure D.5. State Transition Diagram for Stage 2/3 Liner Debond

D.5.2 *STEP 2: Solve the Element Matrices* . A FORTRAN program called "pdf" written by Maj David Robinson (86) to support an ASD/ENS linear system model of preventive maintenance was modified and used to solve each of the element state transition matrices. This program

- reads in the size of the **A** (state transition) matrix, the order of the Taylor Series approximation for $\exp^{A\delta}$, the time increment, δ, the number of time steps, a normalizing factor (timek), the vector of initial state probabilities, and the transpose of **A**

- calculates $\exp^{A\delta} = \Phi(\delta) = I + A\delta + \frac{A^2\delta^2}{2!} + ...$ using subroutine "eat" which computes $\Phi(\delta)$ by

$$\frac{A\delta\left[[A\delta(A\delta + 3)] + 6\right]}{6} + I = \Phi(\delta)$$

(using subroutine "matmul" to implement all matrix multiplication)

D-31

- calculates the probability of being in each state at each time increment (δ) by

$$P(\delta) = \Phi(\delta)P(0)$$

$$P(n\delta) = \Phi^n(\delta)P(0)$$

- writes the probability of being available at each time increment. Note that this definition of *availability* changes depending on the state transition diagram and the initial probability vector. For the exponential models, Availability = P[being in state 0]. For the Weibull stage models, if a detection state is used,

$$Availability = 1 - \left[P(being\,in\,detection\,state) + P(being\,in\,failed\,state)\right]$$

Otherwise, Availability = 1 - P(being in failed state).

The main program and the subroutines are given below. Note that some of the original program is commented out and only the code needed for this project is executed.

```
        program pdf
c
c 6 Sep 1992 - update
c written in support of ASD/ENS
c linear system model of preventive maintenance
c
c modified for use in GSE-92D thesis
c
c m    = number of rows/columns in transition matrix
c k    = order of approx of Taylor series for exp(At)
c delta= delta time step
c n    = number of time steps
c p0   = array of initial probabilities
c
c a(i,j)= array of transition rates
c timek= maximum entry in a(ij) matrix
c disclamer : this is a crude program and is meant to be used for first
c             order results. For more accurate results care should be
c             taken in the double precision routines and parameters
c             and checks should be accomplished in input accuracy and
c             compatibility. To be safe, various combinations of k, delta, timek
c             should be run. If the results agree to the accuracy required
c             you can feel confident in your answers.
c***********************************************************************
        double precision a(50,50),delta
        double precision phi(50,50),p0(50),p(2500,50),rel
        integer m,k,nsteps
```

```fortran
        open (10,file='csd.dat')
        open (11,file='out.dat')
c
c read in data
 c
          read (10,*) m,k,delta,nsteps,timek
          read (10,*) (p0(j),j=1,m)
        do 1 i=1,m
          read (10,*) (a(i,j),j=1,m)
 1        continue
c
c rescale with 1/max(a(i,j)) for better approximation
c
        timek=1/timek
        do 20 i=1,m
         do 20 j=1,m
 20       a(i,j)=timek*a(i,j)
        call eat (phi,a,delta,m,k)
c
c reguratate some input & output for future reference
c
c        write(11,*) delta,m,k
c        do 2 i=1,m
c         write(11,*) (phi(i,j),j=1,m)
c2        continue
c
        do 10 j=1,m
 10       p(1,j)=p0(j)
c
        do 5 i=2,nsteps
           do 40 j=1,m
            sum=0
            do 30 k=1,m
 30           sum=sum+phi(k,j)*p(i-1,k)
            p(i,j)=sum
 40          continue

c    rel =0.
c    do 99 ii=1,m
c 99     rel = rel + p(i,ii)
c     rel = 1. - rel
c
   k =i-1
c           write(11,*) k,delta, timek, k*delta*timek,1.-p(i,1)
            write(11,*) p(i,1)

   5      continue
          end
c
c*****************************************************************
c
        subroutine eat(b,a,h,m,k)
c
c function: calculates the matrix exp(ah); returning the result
c          in matix b.
c          k - order of Taylor series expansion
c          m - dimension of a
c external functions required: matmul (matrix multiplication)
c
        double precision b(50,50),h
        double precision a(50,50)
```

```fortran
      integer m,k,n,kntr
      n=k
      do 1 i=1,m
        do 2 j=1,m
            a(i,j)=a(i,j)*h
            b(i,j)=a(i,j)
2         continue
1     continue
      do 30 kntr=1,k-1
        do 20 i=1,m
            b(i,i)=b(i,i)+n
20        continue
        call matmul(b,a,m)
        n=n*(k-kntr)
30    continue
      do 70 i=1,m
        do 60 j=1,m
          b(i,j)=b(i,j)/n
60        continue
      b(i,i)=b(i,i)+1.
70    continue
      return
      end
c
c*************************************************************************
c
      subroutine matmul(x,y,n)
c
c function: performs matrix multiplication XY
c           result is stored in X
c           n - dimension of X and Y
c
      double precision x(50,50),y(50,50),z(50,50),sum
      integer n
      do 120 i=1,n
        do 110 j=1,n
            sum=0.0
            do 100 k=1,n
              sum=sum+x(i,k)*y(k,j)
100         continue
            z(i,j)=sum
110       continue
120   continue
      do 140 i=1,n
        do 130 j=1,n
            x(i,j)=z(i,j)
130       continue
140   continue
      return
      end
c
c*************************************************************************
```

Output from this program is in the form of a column vector representing predicted element availabilities in years 1-20. The program is run for each element in the system model, and the

resulting collection of element availabilities is stored in data files that are used in the next step to calculate overall system availability.

D.5.3 STEP 3: Calculate System Availability . Another short FORTRAN program was written to collect all the element output data files from runs of "pdf" and to combine the data in a series model of System Availability. Program "sysavail"

- reads in element availability files generated by "pdf"

- implements the series availability model for either the 3-stage baseline or the 2-stage *NEME-SIS* design

- writes the resulting system availability as a function of time for years 0-20

For the 3-stage baseline, system availability is the product of 17 element availabilities:

- reentry system

- stage separation systems (3 needed)

- missile guidance set

- stage 3 liner, propellant, flight control equipment, igniter and TVC ordnance

- stage 2 liner, propellant, flight control equipment, igniter and TVC ordnance

- command signal decoder

- stage 1

For the 2-stage design, the number of system elements is reduced to 11 (for a conventional design) or to 10 (for an integrated stage design). A summary of two-stage system elements is now presented. For the integrated stage design:

- reentry system, missile guidance, command signal decoder and stage 1 same as above

- two sets of stage separation equipment

- second stage liner, boron propellant, igniter, and hot gas valves

and for the conventional design:

- reentry system, missile guidance, command signal decoder, stage 1

- two sets of stage separation equipment

- liner, aluminum propellant, igniter, actuators, flight control equipment

The code for the 3-stage baseline is presented below. Note that the differences for the 2-stage version would be in the input data files read and in the equation to calculate system availability.

```
        program sys3avail
c
c  9 Sep 92
c
c  Written to Support GSE-92D ICBM Project Thesis Chapter on Readiness
c
c  This program reads data files generated by program eat.f (subsystem
c  availabilities in years 1-20) and computes the overall system availability
c  according to a series model.  "SUBI's" are vectors of subsystem "I"
c  availability.
c
c  THIS VERSION USES SLE=M1 TO CALCULATE N AND TAU FOR A 3-STAGE MARKOV MODEL
c
        double precision sys1(1000),sys2(1000),sys(1000),sub1(1000)
        double precision sub2(1000),sub3(1000),sub4(1000),sub5(1000)
        double precision sub6(1000),sub7(1000),sub8(1000),sub9(1000)
double precision sub10(1000), sub11(1000), sub12(1000)

c
c
        open (10,file='reens.dat')
open (11,file='mgss.dat')
open (12,file='stgoxs.dat')
open (13,file='s3ixs.dat')
open (14,file='linxs.dat')
open (15,file='alums.dat')
open (16,file='s3tvoxs.dat')
open (17,file='s23fcs.dat')
open (18,file='s2ixs.dat')
open (19,file='s2tvoxs.dat')
open (20,file='csds.dat')
open (21,file='s1s.dat')
open (30,file='out.dat')
c
c
do 1 i=1,1000
read(10,*) sub1(i)
read(11,*) sub2(i)
read(12,*) sub3(i)
read(13,*) sub4(i)
read(14,*) sub5(i)
read(15,*) sub6(i)
read(16,*) sub7(i)
read(17,*) sub8(i)
read(18,*) sub9(i)
read(19,*) sub10(i)
read(20,*) sub11(i)
read(21,*) sub12(i)
```

```
c
c
sys1(i)=sub1(i)*sub2(i)*sub3(i)*sub3(i)**2*sub4(i)
sys2(i)=sys1(i)*sub5(i)**2*sub6(i)**2*sub7(i)*sub8(i)**2
sys(i)=sys2(i)*sub9(i)*sub10(i)*sub11(i)*sub12(i)
c
write(30,*) i/50., ' ', sys(i)
c
  1 continue
end
```

D.6   Results of Availability Analysis .

The calculated system "real" availabilities are now presented for the 3-stage baseline, one Integrated Stage *NEMESIS* design option, and one conventional option. It is again important to note that though the parameters for the 3-stage design were based on Minuteman III data, the model of availability used in this report was not intended to match reported System Availability in the Weapon System Effectiveness Reports. Rather, the intent was to baseline an availability yardstick for 2-stage design evaluation. Therefore, these model numbers, which do not account for all logistics elements involved in a true system availability analysis, should not be construed as reflecting the actual reported Minuteman Availability. In fact, a true comparison would need to be classified, and that problem was intentionally avoided for this study.

The calculated system "real" availabilities over a period of twenty years are given below. Recall that "real" system availability was defined in Section 3 as *the percentage of time that an asset would actually operate as intended if the user began a mission execution.* The fact that a missile could sit failed and therefore "unavailable" in the silo for a period of time before the failure is detected is accounted for in these calculations.

```
        3-STAGE "REAL" AVAILABILITY
        (USING M1 = SLE FOR ELEMENT CALCULATIONS)

        YEAR        SYSTEM AVAILABILITY

        0.50000     0.98076643779529
        1.00000     0.97595973106006
        2.00000     0.96658887461609
        3.00000     0.95753150396677
        4.00000     0.94877620415692
        5.00000     0.94031275947876
        6.00000     0.93212316954753
        7.00000     0.92415610480403
        8.00000     0.91620720942807
```

```
9.00000      0.90741715621602
10.00000     0.89460360984377
11.0000      0.86853779207278
12.0000      0.81007298715534
13.0000      0.69517707988211
14.0000      0.51838739732669
15.0000      0.31691701860479
16.0000      0.15201077072682
17.0000      5.6206251992312D-02
18.0000      1.6342271926321D-02
19.0000      4.0175482736661D-03
20.0000      9.6104333067406D-04
```

2-STAGE (INTEGRATED STAGE)
"REAL" AVAILABILITY
(USING WEIBULL PARAMETERS AND M1 = SLE
AS APPROPRIATE)

YEAR	SYSTEM AVAILABILITY
0.50000	0.98197049887035
1.00000	0.97716045534430
2.00000	0.96777806991798
3.00000	0.95870955574999
4.00000	0.94994349764175
5.00000	0.94146992770754
6.00000	0.93327200805903
7.00000	0.92529903319264
8.00000	0.91735961955578
9.00000	0.90885708120251
10.00000	0.89834735205013
11.0000	0.88304899097819
12.0000	0.85858919467338
13.0000	0.81931820161137
14.0000	0.75953227726334
15.0000	0.67578778382137
16.0000	0.56974298095295
17.0000	0.44978303648227
18.0000	0.32949343356189
19.0000	0.22295734208270
20.0000	0.13955675058805

2-STAGE (CONVENTIONAL STAGE)
"REAL AVAILABILITY"
(USING WEIBULL PARAMETERS AND M1 = SLE
AS APPROPRIATE)

```
0.500000     0.98136828367189
1.00000      0.97655990865375
2.00000      0.96718328553644
3.00000      0.95812018592779
4.00000      0.94935763216118
5.00000      0.94087806707175
```

```
 6.00000      0.93264393724348
 7.00000      0.92457832166004
 8.00000      0.91652568507258
 9.00000      0.90811840958917
10.00000      0.89822423724963
11.0000       0.88331204640022
12.0000       0.85476190145032
13.0000       0.79805088336619
14.0000       0.69907623621054
15.0000       0.55748982267722
16.0000       0.39495143781742
17.0000       0.24553434291005
18.0000       0.13470007392556
19.0000       6.7251769785559D-02
20.0000       3.2583529688547D-02
```

As can be seen in the results, the two-stage alternative designs track the high availability of the baseline very well for the first ten years of operation. The risk associated with the boron propellants, the new liners and the hot gas valves (in the integrated stage designs) appears to be offset by the gains due to the reduction of an entire set of equipment associated with the extra stage. After year 10, a fairly dramatic improvement can be seen in the availability of the two-stage design. Fewer failures can be expected as the years go on with this design, hence availability falls at a much slower rate than is seen with the 3-stage vehicle. These observations should be tempered by the fact that several design life improvements are already on contract for Minuteman III. and gains made by these potential improvements are not reflected in the baseline calculations presented here.

D.7 In-Flight Reliability Analysis

D.7.1 Approach . In-flight failures of an ICBM can be traced to several general failure mode categories:

- failures in rocket motor components (propellant cracks, insulation/liner/propellant debonds, nozzle seal cracking, etc.) that were never detected as the missile stood in the silo

- staging failures

- guidance hardware/software failures or related flight control electronics failures

- failures in post-boost flight path correction or payload deployment

- human error (preparation, handling or execution)

The occurrence of an in-flight failure is not something that can be predicted with certainty, and thus it can be treated as a random event that can be modeled with appropriate probability distributions. In previous sections, Markov process models were developed and used to predict alert availability. In this section, a "reliability allocation" approach is taken to model in-flight reliability of the 2-stage *NEMESIS* design alternatives. The reason an allocation approach is taken to in-flight reliability (rather than the Markov approach taken in the availability analysis) is that data needed to support the assignment of failure rates in a flight environment is not available for the technologies associated with the design alternatives. Rather than guess at what those failure rates would be, the design group decided to find out what they would have to be in order to meet the baseline system requirement.

The process of assigning reliability requirements to individual components to attain a specified system reliability is called *reliability allocation* (60:p405). The allocation approach involves (basically) two key steps:

1. Calculation of a baseline system reliability, R^*_{sys}

2. Assignment of reliability requirements, R_i, to all second stage design components such that the overall system reliability matches the baseline.

   The allocation problem is complicated by several factors:

- the role a component plays in the function of the system

- the interaction of components within the overall system design

- the complexity of a particular component or set of components

- the lack of detailed information on many of these factors early in the system design phase.

Despite these problems, implementation of a reliability allocation program early in the design phase has some inherent advantages that make it a worthwhile thing to do:

- forces the designer to understand and develop the relationship between component, subsystem and system reliabilities, which leads to an understanding of the basic reliability problems inherent in the design

- the designer is obliged to consider reliability equally with other system parameters such as weight, cost and performance

- setting reliability goals usually leads to improved design, manufacturing methods and testing procedures (60:p406).

Most of the basic reliability allocation methods are based on the assumptions that

1. component failures are independent

2. failure of any component results in system failure

3. failure rates of the components are constant

These assumptions are valid for the ICBM case, and they lead to the following equation, which is required to allocate a baseline system reliability, R^*_{sys}, to the component reliabilities, R_i:

$$\prod_{i=1}^{n} R_i(t) \geq R^*_{sys}(t) \qquad (D.5)$$

which says that the product of all the component reliabilities must be equal to or exceed the required overall system reliability.

If constant failure rates are assumed, an exponential model can be used for the individual failure rates:

$$R(t) = \exp(-\lambda t)$$

and equation D.5 becomes

$$\prod_{i=1}^{n} \exp(-\lambda_i t) = \exp(-\lambda^* t)$$

where the λ_i's are individual component failure rates and λ^* is the required system failure rate. Thus, the reliabilty allocation in terms of R^* or λ^* can be performed by similar approaches.

A slight modification of this approach will be used for this study. Failure rates imply a knowledge of time (failures per unit time). The data on the in-flight performance of the Minuteman system is given (67) in terms of numbers of failures/successes in a total number of tests. This type of success/failure data lends itself more to a binomial model of system/component reliability.

Computation of system or component reliability by a binomial method in this case comes very close to an exponential prediction, as demonstrated in the following example.

Suppose data shows 2 failures of a particular motor component in 100 flight tests and 50 static firings. The failure rate (per test) is then 2/150 or 0.01333. If the time of each test is assumed to be about 60 seconds (approximate motor burn time), then, in terms of failures per second, $\lambda_2 = 2/(150)(60) = 0.000222$. λ_2 could now be used to compute the component reliability:

$$R_i(t) = \exp(-\lambda_2 t)$$

If the reliability at the end of motor burn ($t = 60sec$) is desired:

$$R_i(t) = \exp[-(.000222)(60)] = 0.986755$$

Using a binomial success/failure approach:

$$R_i = \frac{148 successes}{150 tests} = 0.9867$$

which is essentially the same result.

In the sections that follow, a system baseline for a 3-stage system will be calculated using failure rate data from the Minuteman Founding Fathers Review (67). This system baseline will then be used as the required system reliability in a *reliability allocation* model for a 2-stage *NEMESIS* design.

D.7.2 3-Stage Baseline, R^*_{sys} .   The Minuteman III Life Extension Founding Fathers' Review (67) presents data on the results of over 20 years of Minuteman system testing. Based on this data, a summary table (Table D.4 was prepared. Since these numbers are classified SECRET, they are replaced by the letters A-Z in this report. The actual numbers can be found in References (67, 74, 75), or in an unclassified addendum that becomes classified when attached to this report.

Using this data and the binomial approach described previously, the component reliabilities were calculated, and the results are shown in Table D.5.

Component No.	Component	No.Tests	No.Failures
1	S2Motor	378	B
2	S3Motor	198	C
3	S2LITVC	226	D
4	S3LITVC	226	E
5	Stage1	244	F
6	IntOrd	244	G
7	Raceway	244	H
8	Batteries	244	I
9	CSD	244	J
10	PSRE	244	K
11	REEV	244	L
12	MGS	244	M

Table D.4. Baseline System Test Results by Component

Component No.	Component	R_i
1	S2Motor	N
2	S3Motor	O
3	S2LITVC	P
4	S3LITVC	Q
5	Stage1	R
6	IntOrd	S
7	Raceway	T
8	Batteries	U
9	CSD	V
10	PSRE	W
11	REEV	X
12	MGS	Y

Table D.5. Baseline Component In-Flight Reliabilities

The baseline system reliability was then calculated using Equation D.5:

$$R^*_{sys} = \prod_{i=1}^{12} R_i = A$$

Therefore, for the 2-Stage *NEMESIS* design to meet or exceed this system goal, the product of all the *NEMESIS* component reliabilities must be $\geq A$.

D.7.3 2-Stage System Reliability Allocation .   Some components of the baseline model are transferred to the 2-stage design without change (Stage 1, interstage ordnance, raceway, batteries. CSD, PSRE, REEV, MGS). Therefore, the reliability of all those components is assumed to be

unchanged in the 2-stage calculations. Of these components, four (Stage 1, raceway, batteries, CSD) have a reliability of 1.0, and hence will not change the calculated system reliability. The remaining four components (interstage ordnance (R4), PSRE (R3), REEV (R2) and MGS (R1)) and the second stage motor (R5) and TVC (R6) are the components that must be included in a 2-stage system in-flight reliability calculation. As previously stated, very little (or no) testing has been done of new liners, boron propellants, and hot gas valves in an operational environment. Therefore, any estimate of the in-flight failure rate associated with these components would have little meaning at this point. Instead, an allocation procedure is used to assess the reliability required of the Stage 2 motor and the TVC components in order to meet the overall system baseline (A) requirement.

Using an *effort minimization* algorithm presented in Kapur and Lamberson (60:p411). the problem breaks down to finding R_i^*'s (optimal component reliabilities) to minimize the effort required to achieve the target system reliability (R_{sys}^*). If the effort required to improve the reliabilities of all system components is assumed to be equal (and there was no data available to support any other approach), and the components are ordered such that $R_1 \leq R_2 \leq ... \leq R_n$, the solution to the problem is

$$R_i^* = \begin{cases} R_0^*, & \text{for } i \leq k_0; \\ R_i, & \text{for } i \ \raise1pt{\text{\scriptsize$\dot{c}$}}\ k_0. \end{cases} \tag{D.6}$$

where k_0 is the maximum value of j such that

$$R_j < [\frac{R_{sys}^*}{\prod_{j=k_0+1}^{n+1} R_j}]^{1/j}, (R_{n+1} = 1.0)$$

or

$$R_0^* = [\frac{R^*}{\prod_{l=j+1}^{n+1} R_j}]^{1/k_0} \tag{D.7}$$

where R_0^* is the minimum allocated reliability for components if the system reliability requirement is to be met.

To show how this method works, consider the 2-stage model shown in Figure D.6, where $R_1 - R_4$ are known from the baseline model. If equal allocation is considered as a starting point,

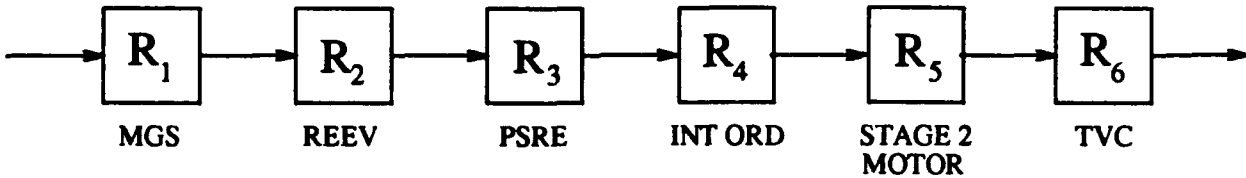$$R_{equal}^* = (R_{sys}^*)^{1/n} = (A)^{1/6} = Z$$

Figure D.6. 2-Stage In-Flight Model for Reliability Allocation

which means that to achieve a system reliability of A, all components must have a reliability of at least Z. From previous calculations (Figure D.5, three components already have higher reliabilities:

$$R_2 = X$$

$$R_3 = W$$

$$R_4 = S$$

By Equation D.6 these components are not changed. and $R_2^* = R_2$, $R_3^* = R_3$, and $R_4^* = R_4$. For the remaining components, Equation D.7 is applied:

$$R_0^* = [\frac{A}{(X)(W)(S)}]^{1/3} = 0.968898 \approx 0.97$$

If R_0^* is allocated equally to R_1, R_5 and R_6, the resulting system reliability is

$$R_{sys}^* = (X)(W)(S)(0.97)^3 = A$$

which is the desired result.

D.7.4   Results of In-Flight Reliability Analysis.   To summarize the results:

Assuming equal effort is required to achieve component reliabilities of 0.97, and assuming that all three components (MGS, Stage 2 motor subsystem, stage 2 TVC subsystem) can be designed to meet a 0.97 operational reliability allocation, the 2-stage *NEMESIS* system can meet the baseline reliability requirement.

Efforts are already underway (94) to improve the reliability of the Minuteman III Missile Guidance Set, and there is good reason to believe that the goal is achievable (12) for that component. With a conventional second stage, the fact that aluminum propellants and flex-seal actuators are well- tested and proven technology means that the risk of achieving 0.97 for either TVC or motor reliability is very small. Indeed, the current MM III Stage 2 motor already exceeds that target number (Figure D.5, Reference (67)). With integrated stage technologies (boron propellant, hot gas valves), the risk is higher, but seems reasonable in light of the development work done to date (56, 85, 94).

D.8 Integrated Logistics Support Impacts: A Qualitative Discussion .

Availability and reliability capture an important facet of the *NEMESIS* design. However, a system design study would be incomplete without some assessment of design impacts in some other key logistics support areas. This section takes a top level. qualitative look at how the 2-stage designs compare with the 3-stage baseline in terms of:

- level of required manpower support and skills.

- shipping container size and volume,

- field and depot test and support equipment needed.

- required training equipment, and

- field/depot maintenance and repair facility space requirements.

Manpower Support and Skill Level Requirements — With increased availability and reliability. the level of manpower support for maintenance and repair is expected to decrease (though not very much for the level of improvement shown in the previous sections). Additional benefit would be expected by a reduction in the sparing requirement and from a reduced parts count from the reduction of an entire stage. Less manpower should be required to maintain the reduced number of spare parts. Skill levels of the maintainers are not expected to change with either the ISC or the conventional design approach.

Shipping Containers — Four of the five *NEMESIS* designs are smaller than the current system. and the fifth is only about three inches taller overall. Therefore, with minor modifications.

existing shipping containers for the system should still be useful. However, if a container is required for the second stage motor alone, a new container is necessary. All *NEMESIS* Stage 2 designs are bigger than either of the existing stage designs. One possible approach to avoid an entirely new container would be to modify an existing Stage 1 container.

Field/Depot Support and Test Equipment — Since *NEMESIS* alternatives were designed to fit existing silo requirements and to stay within size and weight constraints driven by Stage 1 capability, existing handling equipment (transporter winches, missile transporters, motor transporters, transporter erector actuators, etc.) should be adequate for the new designs. With respect to test equipment (TE), much of the existing equipment is becoming obsolete and upgrades are planned (94:pp60-116). The 2-stage design, whether ISC or conventional, should be compatible with planned upgrades to automatic test equipment, shop replaceable unit test sets, shock/vibration flight simulation equipment, electrodynamic vibration equipment, hardness TE, servo test stands, cable test sets, etc. Non-destructive inspection equipment (for motor chambers and ordnance), whether current or planned (computed tomography) is big enough to handle any *NEMESIS* configuration.

Training Equipment — Most of the training equipment used with Minuteman III focuses on lanch communications, power systems, pre-flight procedures, ground control monitoring, and computer programming. None of these equipments or procedures changes with the designs presented in this study.

Facility Space — If anything, less space is needed with the 2-stage alternative. Fewer spare stages and fewer parts within those stages (in the case of ISC at least) should reduce the overall facility space devoted to storage and repair.

Though a full Integrated Logistics Support analysis should really be done to quantify and verify these conclusions, a top level, qualitative look at some key factors does not seem to highlight any particular problems with the 2-stage approach. On the contrary, with the possible exception of the shipping containers, a 2-stage approach would seem to have inherent benefits, especially in the areas of manpower and facility savings. Operations and Support cost analysis in Chapter 6 shows that these two factors have a significant impact on overall system life cycle cost.

D.9 Conclusions

The models developed for this project gave results that "made sense" in terms of expected and documented performance of the baseline system. Because of this consistency, the Markov chain model is used as a vehicle for assessing the "availability" of all 2-stage system design options generated in the ICBM group thesis work. The results indicate good potential for a 2-stage design (either conventional or integrated stage) to exceed the already excellent alert availability performance of the baseline system. In-flight reliability is calculated using an allocation method, and these results are also presented for the three stage baseline and for conventional and integrated stage 2-stage designs. Results indicate that the in-flight reliability of the baseline can be matched with realistic allocation of component reliability to the designs for the second stage motor and thrust vector control subsystems. The availability and reliability assessments, together with the qualitative assessment of other Ingegrated Logistic Support (ILS) factors. are given equal consideration with system cost and mission performance to identify the best overall system design (Chapter 7).

Bibliography

1. Aero Propulsion Laboratory, AF Wright Aeronautical Laboratories, AF Systems Command, WPAFB, Ohio 45433. *Weibull Analysis Handbook* (Afwal-tr-83-2079 Edition), November 1983.

2. Aerojet Strategic Propulsion Company. *Aging and Surveillance Program Minuteman II/III Stage II Program Progress*, 15 March-31 August 1985. No. 0162-06-SAAS-35, DTIC No. AD-A162 884.

3. Aeronautics, National and Space Administration, "Buckling of Thin-Walled Circular Cylinders," August 1968. SP-8007.

4. Air Force Institute of Technology, School of Systems and Logistics, AFIT, WPAFB, Ohio. *System Reliability and Maintainability Textbook*.

5. Alexander, A.J. *The Cost and Benefits of Reliability in Military Equipment*. Technical Report, Rand Corporation, December 1988. DTIC No. AD-A207344.

6. Alexander, Richard V., Jun-Sep 1992. Senior Engineering Specialist, GenCorp, Aerojet Propulsion Division, Telephone Interview.

7. Andrews, W.G. "Integrating the Integrated Stage." *AIAA Paper 81-145, Colorado Springs, CO* (July 1981).

8. Arora, Jasbir S. *Introduction to Optimum Design*. New York: McGraw Hill Book Company, 1989.

9. Asoo, C., 9 September 1992. Design Engineer, GenCorp, Aerojet Propulsion Division, Sacramento, California, Telephone interview.

10. Atlas, D. *Handbook of Geophysics*. New York: The Macmillan Company, 1960.

11. Bailey, LTC S.D. "The SAC Perspective on ICBM Programs." Draft Memo from HQ SAC/XRQX, 2 December 1991.

12. Ballistic Missile Organization (MYEG), Norton AFB, CA. *Technical Requirements Document for the Advanced Inertial Measurement System* (Bmo-89-22c Edition), 15 March 1991.

13. Barrere, Marcel. *Rocket Propulsion*. New York: Elsevier Publishing Company, 1960.

14. Bennett, David R., June 1992. Project Manager, GenCorp, Aerojet Propulsion Division, Telephone interview.

15. Beyer, W. H., editor. *CRC Handbook of Mathematical Sciences* (Sixth edition Edition). Boca Raton, Florida: CRC Press Inc., 1987.

16. Blakney, Capt K.L. and Capt F.L. Dietrich. *Applications of Markov Processes to Reliability and Maintainability Engineering*. MS thesis, AFIT School of Engineering, WPAFB, Ohio, December 1966. GRE/MATH/66-3/4.

17. Blanchard, B.S. and W.J. Fabrycky. *Systems Engineering and Analysis*. Englewood Cliffs, NJ: Prentice Hall, 1981.

18. Booz-Allen & Hamilton, Bethesda, MD. *Solid Technology Assessment and Cost Evaluation Model* (Volumes 1,2, version 2.3 Edition).

19. Box, George E.P. and Norman R. Draper. *Empirical Model-Building and Response Surfaces*. New York: John Wiley and Sons, 1987.

20. Brashers. H.C. *Liner Barrier Technology Program*. Technical Report, Sacramento. CA: Aerojet Solid Propulsion Co., May 1984.

21. Byard, Capt K.F. *Design of an Air-to-Air Missile Incorporating LCP*. MS thesis. AFIT School of Engineering, WPAFB, Ohio, December 1991. AFIT/GSE/ENY/91D-1.

22. Castro, Lt Paul, 24 June 1992. Project Engineer, Propulsion Directorate, Phillips Lab, Edwards AFB, CA. Telephone interview.

23. Chase, C. A. *Low Cost Solid Propulsion Study*. Technical Report, UTC, Chemical Systems Division, Mar 1990.

24. Chase, W.P. *Management of Systems Engineering*. New York: John Wiley, 1982.

25. Chew, J.S.B. and others. *Advanced ICBM Technologies*. Technical Report, Edwards AFB, CA: Rocket Propulsion Laboratory, July 1991.

26. Clemons. Maj G.L. and Capt C.A. Schell. *Impact of External Environmental Factors on MM III Inertial Guidance System (NS-20) Failures*. MS thesis. AFIT School of Systems and Logistics. WPAFB. Ohio. August 1975. SLSR 27-75B DTIC No. ADA016392.

27. Culler. G.J. and B.D. Fried. "Universal Gravity Turn Trajectories." *Journal of Applied Physics, Vol. 28. No. 6* (June 1957).

28. Darius. Marcus A. *Evaluation of Various External Protective System Designs for SICBM*. Technical Report. Brigham City. UT: Morton-Thiokol, May 1988.

29. DeArmond, F.B. and A.R.Lombardo. *Minuteman II Weapon System Self-Test and Operational Status Display Techniques*. Technical Report. North American Aviation. Inc. (Autonetics Division). 14 July 1966. DTIC No. AD 906056.

30. Denost. J.P. "Design of Filament-Wound Rocket Cases." *AGARD LS-150* (1988).

31. Department of the Air Force. HQ USAF, Washington. D.C. *Cost Analysis* (Afr 173-13 Edition). September 1986.

32. Devlin. J., editor. *The New Universities Webster Dictionary*. New York: World Syndicate Publishing Co.. 1938.

33. Dragoo. R.A. "Small ICBM HML Operating and Support Cost Estimate." Report to BMO Cost Analysis Personnel. June 1991.

34. Ductor. David C. *Range Improvement for a Missile with an Integrated Stage*. Technical Report, Edwards AFB. CA: AFRPL. December 1982.

35. Editorial. "Military Stresses Maintainability. Reliability." *Aviation Week and Space Technology*, 42-43 (6 October 1980).

36. Ellis, R.. 10 September 1992. Valve Engineer, United Technologies, Chemical Systems Division. Telephone interview.

37. Eshbach. Ovid W., editor. *Handbook of Engineering Fundamentals* (Third edition Edition). New York: John Wiley and Sons, 1975.

38. Evans, P.R. "Composite Motor Case Design," *Advisory Group for Aerospace Research and Development* (March 1987). LS-150.

39. Fullerton, Maj R.A. *Further Applications of Markov Processes to Reliability and Maintainability Engineering*. MS thesis, AFIT School of Engineering. WPAFB. Ohio. December 1969. GRE/MATH/69-2.

40. GenCorp. Aerojet Propulsion Division, "Missile Integrated Stage Technology." 1989. Ongoing Program for the US Army.

41. GenCorp, Aerojet Propulsion Division, "AIDE II, Software Program to Generate Weights for Integrated Stage Designs," 1992.

42. Gere, James M. and Stephen P. Timoshenko. *Mechanics of Materials, Second Edition*. Boston, MA: PWS Engineering, 1984.

43. Hall, A.D. "Three-Dimensional Morphology of Systems Engineering." *IEEE Transactions on Systems, Science and Cybernetics SSC-5, No. 2*. April 1969.

44. Hall, Capt C. "Basic Equations of Motion for a Single Stage Rocket." Lecture Notes from MECH 423, 'Dynamics'. AFIT School of Engineering, WPAFB, OH, January 1992.

45. Halling, K.R., "CDRL 323A2, Stage Design Data Book," September 1990. TWR-90536.

46. Hess, Kelly. Phone call on EPM.

47. Hicks, Charles R. *Fundamental Concepts in Design of Experiments*. New York: Holt, Rinehart, and Winston, 1982.

48. Hildreth, J.H. "Advances in Solid Rocket Nozzle Design and Analysis in the United States Since 1970," *Advisory Group for Aerospace Research and Development (AGARD Lecture Series No. 150* (April 1988).

49. Hill, J.D. and J.N. Warfield. "Unified Program Planning." *IEEE Transactions on Systems. Man, and Cybernetics SMC-2, No. 5*. November 1972.

50. Hill, P.G. and C.R. Peterson. *Mechanics and Thermodynamics of Propulsion*. Reading. MA: Addison-Wesley Publishing Company, 1965.

51. HQ Air Force Operational Test and Evaluation Center, HQ AFOTEC. Kirtland AFB. New Mexico 87117-7001. *Operational Suitability Test and Evaluation*, May 1991. AFOTECP 400-1.

52. HQ SAC/XR. *SAC 001-92 Draft Mission Need Statement for Prompt Strategic Strike Capability for 2010*, 10 January 1992.

53. Humphrey, Don. 10 November 1992. Project Engineer, Brunswick Corporation. Defense Division, Lincoln, NE. Telephone interview.

54. ICI Fiberite, Inc., Tempe, AZ. *ICI Fiberite Materials Handbook*, March 1989.

55. Incropera. Frank P. and David P. Dewitt. *Introduction to Heat Transfer*. New York: John Wiley and Sons. 1990.

56. Jackson, R.E. and T.K. McKinley. *A New Approach to High Performance ICBM Design*. Technical Report, Kaman Sciences Corporation, Feb 1990.

57. James, M.L. *Applied Numerical Methods for Digital Computation with FORTRAN and CSMP*. New York: Harper and Row, 1977.

58. J.D. Mockenhaupt, G.J. Felix. "Cold Flow Tests of Forced Deflection Nozzles for Integrated Stage Application," *AIAA Paper 81-1420, Colorado Springs, CO* (July 1981).

59. Joyce, Lieutenant Brian and Capt Pat Poppert. *Life Cycle Cost of Alternative ICBM, Second Stage Designs*. MS thesis, AFIT School of Systems and Logisitics, WPAFB, Ohio, Sep 1992. AFIT/GCA/LSG/92S-5.

60. Kapur, K.C. and L.R. Lamberson. *Reliability in Engineering Design*. New York: John Wiley and Sons, 1977.

61. Kays, W.M. *Convective Heat and Mass Transfer*. New York: McGraw-Hill, 1966.

62. Lasdon. Leon and Allen Warren. *GINO*. Palo Alto, CA: The Scientific Press, 1985.

63. Lubin, George, editor. *Handbook of Composites*. New York: Van Nostrandt Company, 1982.

64. McCarthy, LtGen J.P. "R&M 2000: The Strategic Air Command Perspective." *IEEE Transactions on Reliability Vol. R-36, No. 3*. August 1987.

65. McParland, G.C. "Integrated Stage Concept and Study Results," *AIAA/ASME/ASEE 22nd Joint Propulsion Conference* (1986). AIAA-86-1581.

66. Meyer, D.H. and P.E. Poweel-Croy. "The Integrated Stage Chamber Development Program," *AIAA/ASME/ASEE 25th Joint Propulsion Conference* (1989).

67. Minuteman III Integration Life Extension Office, Ogden Air Logistics Center, Hill AFB, Utah. *Minuteman III Life Extension–Founding Fathers' Review*, 10-11 December 1991. Briefing Charts.

68. Mittermaier, N., 10 July 1992. Program Manager, GenCorp, Aerojet Propulsion Division, Sacramento, CA.. Personal interview.

69. Mockenhanpt. J.D. "Cold Flow Tests With Chamber-Bleed Gas Injection Thurst Vector Control," *AIAA Journal* (1988). AIAA-88-3334.

70. Mumford, Neal A. *Advanced Composite Case Materials Evaluation, Volume 1*. Technical Report, Morton-Thiokol, Inc., May 1986. DTIC AD-B102 167.

71. Murphy, Dr. R.L. "Defense Cost Modeling." Class Lecture, QMGT 671, October 1991.

72. Napier, J., 7 September 1992. MIST Program Manager. GenCorp, Aerojet Propulsion Division, Sacramento, CA., Telephone interview.

73. Nguyen, Hugh, 8 June 1992. Project Engineer, Propulsion Directorate. Phillips Lab. Edwards AFB, CA. Telephone interview.

74. Ogden Air Logistics Center MMGR, Ogden Air Logistics Center, Hill AFB, Utah 84056. *Minuteman Weapon System Effectiveness Semiannual Report*, November 1985. TR-WSE-1.0-24. ICBM System Program Management Division. Document Classified SECRET/Formerly Restricted Data.

75. Ogden Air Logistics Center MMGR, Ogden Air Logistics Center, Hill AFB, Utah 84056. *Minuteman Weapon System Effectiveness Semiannual Report*, May 1989. TR-WSE-1.0-30, ICBM System Program Management Division. Document Classified SECRET/Formerly Restricted Data.

76. Patterson, Joel E. and James D. Erikson. "Development of a High Performance Carbon/Epoxy Motor Case for the First Stage Small ICBM." *The JANNAF Composite Motor Case Subcommittee Meeting* (May 1988).

77. Peterson, G., 16 July 1992. Flight Control System Engineer, TRW, Ogden, Utah. Telephone interview.

78. Phillips Laboratory, RKSA, "AICBM SRG Review, Briefing Charts, One for Two Stage," 21 November 1991. RKSA, Edwards AFB, CA.

79. Phillips Laboratory, RKSA. *Advanced ICBM Technical Integration Study*. 20 March 1991. Computer Program Documentation.

80. Polosio, F. Valve Engineer, Aerojet Corporation, Sacramento, CA. Telephone interview.

81. Remen, John, June - August 1992. Project Engineer, Phillips Laboratory, Telephone Interview.

82. Rickman. D.K. *Development of a Graphnol N3M Hot Gas Valve*. Technical Report. GenCorp Aerojet: Propulsion Division, 1987.

83. RKSA, "Study Based on Data Supplied by AICBM Group," March 1991.

84. Robinson, K., 16 July 1992. Program Manager, Propellant Technology. Gencorp, Aerojet Propulsion Division, Sacramento, CA. Telephone interview.

85. Robinson, K.P. "Technology Innovation for MM Insertion." GenCorp Aerojet Propulsion Division, Briefing to Phillips Laboratory, Edwards AFB, CA, 22 May 1992.

86. Robinson, Maj David G. "Markov Processes." Assistant Professor of Aerospace and Systems Engineering - Lecture Notes from SENG 685, 'Reliability in Systems Engineering'. AFIT School of Engineering, WPAFB, Ohio, July 8 1992.

87. R.R. Bate, D.D. Mueller, J.E. White. *Fundamentals of Astrodynamics*. New York: Dover Publications, Inc., 1971.

88. Sage, A.P. "A Case for a Standard for Systems Engineering Methodology." *IEEE Transactions on Systems, Man and Cybernetics SMC-7, No. 7*. July 1977.

89. Sage, A.P. *Methodology for Large Scale Systems*. New York: McGraw-Hill Book Co., 1977.

90. Sandler, G.E. *System Reliability Engineering*. Englewood Cliffs, New Jersey: Prentice-Hall Inc., 1963.

91. Scott, Elaine P. and James V. Beck. "Estimation of Thermal Properties in Epoxy Matrix/Carbon Fiber Composite Materials," *Journal of Composite Materials* (1992). Volume 26, No.1.

92. Seldon, M. Robert, editor. *Life Cycle Costing: A Better Method of Government Procurement*. Boulder, Co: Westview Press, Inc., 1979.

93. Shibley, A.M. *Handbook of Composites*, chapter Filament Winding. New York: Van Nostrandt Company, 1982.

94. Silo-Based ICBM System Program Office, Ogden Air Logistics Center, Hill AFB, Utah 84056-5990. *Silo-Based ICBM Long Range Planning Logistics Program Management Plan*, April 1992.

95. Sinard, L.D. and D.R. Bennett. "Integrated Stage Concept, A New Concept For Ballistic Missiles." Draft paper for presentation to Society of Allied Weight Engineering, 23 May 1988.

96. Singh, C. and R. Billinton. *System Reliability Modeling and Evaluation*. London: Hutchinson & Company Ltd., 1977.

97. Slivard, Lewis D. and David R. Bennett. "Integrated Stage Concept: A New Concept for Ballistic Missiles," *SAWE Paper No. 1838* (May 1988).

98. Solid Propulsion Information Agency, Hill AFB, UT. *SPIA/M1, 62-KS-63*, October 1965.

99. Sutton, George P. *Rocket Propulsion Elements: An Intoduction to the Engineering of Rockets* (Fifth Edition). New York: John Wiley and Sons, 1986.

100. Swanson, Stephen R. "Strength Design Criteria for Carbon/Epoxy Pressure Vessels," *Journal of Spacecraft and Rockets* (September-October 1990).

101. Truchot, A., "Design and Analyses of Soild Rocket Motor Internal Insulation."

102. Veit, P.W. "Evolution of an Aging Program for Minutemena Stage II Solid Rocket Motor," *JANNAF Propulsion Meeting, Volume I* (1990). pp. 45-54, W91-24273.

103. Wiesel, William E. *Spacecraft Dynamics*. New York: McGraw-Hill, 1989.

104. Wozchieechowicz, Alexander. *Design of Filament Wound Rocket Motor Cases*. Technical Report, Hercules, Inc., 1968.

105. Wuerth, J.M. *The Evolution of Minuteman Guidance and Control.* Technical Report, Anaheim, CA: Rockwell International Autonetics Group, 11 June 1975. DTIC ADB018836.

106. Yezzi, Catherine A. and Barry B. Moore. *Characterizations of KEVLAR/EPDM Rubbers for Use As Rocket Motor Case Insulators.* Technical Report, Gainesvill, VA: Atlantic Research Company, June 1986.

107. Zarchan, P. *Tactical and Strategic Missile Guidance.* AIAA, 1990.

Vitae

Capt David P. Blanks was born on 13 August 1965 in Roxboro, North Carolina. He graduated from Person Senior High School in Roxboro in 1983 and accepted an appointment to the United States Air Force Academy. He graduated from the Academy in 1987 with a Bachelor of Science degree in Engineering Mechanics and was commissioned a 2nd Lieutenant in the Regular USAF. His first assignment was to Hill Air Force Base in Ogden, Utah where he began his tour in the F-4 System Program Management Division. His tasks centered around technology and safety modifications to the aircraft with primary responsibility for development and implementation of the One-Piece windscreen replacement program. In 1990, he was transfered to the F-16 SPM where he worked on programs ranging from side stick controller interference modifications to main fuel shut-off valve safety problems. From 1989-1991 he attended the University of Phoenix and in May 1991 received his Masters of Business Administration degree. He was selected to attend the School of Engineering, Air Force Institute of Technology, beginning in May 1991. Captain Blanks is married to the former Pamalyn Sue Belnap from Ogden, Utah.

<p style="text-align:center">Permanent Address: 1138 Wimbledon Drive
Roxboro, NC 27573</p>

Capt Douglas M. Bruce was born on 12 November 1961 in Bellefonte, Pennsylvania. He graduated from Prattville High School in Prattville, Alabama in 1979. He enrolled at The Pennsylvania State University in 1982, and graduated with a Bachelor of Science degree in Aerospace Engineering in May, 1986. While at Penn State, he was offered and accepted a 2-year Air Force Reserve Officer's Training Corps scholarship and was commissioned upon graduation. He entered into active duty on 1 October 1986 and was assigned to the Directorate of Flight Systems Engineering, Deputy for Engineering, Aeronautical Systems Division at Wright-Patterson AFB, Ohio. There he served as a Flight Stability and Control Engineer in support of the F-15E, F-16, C-17A, and B-1B programs, primarily working with engineering simulations for aircraft flying qualities analysis. In January 1989, he was reassigned to the Directorate of Fighters, Systems Program Office and worked as the Lead Flight Controls Engineer for the YA-7F, Peace Pearl, and both the USAF and Royal Australian Air Force F-111 Digital Flight Control System programs. He was selected to attend the School of Engineering, Air Force Institute of Technology, beginning in May, 1991. Captain Bruce is married to the former Nadene Linda Dunmire, of Apollo, Pennsylvania, and the couple have three children, Natalie, age 9, Stephanie, age 6, and Tyler, age 2.

Permanent Address: 396 Echo Ridge Road
Apollo, PA 15613

Capt Anthony M. Logue was born on 9 July 1963 in Auburn, New York. He graduated from Auburn High School in 1981 and attended the Georgia Institute of Technology, graduating with a Bachelor of Aerospace Engineering in June 1985. He obtained his reserve commission from Air Force ROTC upon graduation. He entered active duty on 5 October 1985 and served his first assignment at Det 44/AFCMD AFPRO Fairchild Republic Company, Farmingdale, New York. He was a project engineer on the T-46A Next Generation Trainer, responsible for all contractor test activities at the plant. He was reassigned to Det 49/AFCMD Eaton AIL Corporation, Deer Park, New York in April 1987. There he served as the test and evaluation focal point for the B-1B ALQ-161 Defensive Avionics and as the on-site assistant program manager. In January 1989, he was reassigned to the Special Projects Office, ASD/VJ, a multiservice special access program. Initial duties were as a configuration specialist for all hardware items. He was moved into the position of lead flight control engineer in February of 1990, responsible for development and qualification of the flight control system and government analyst for all flight test data. He received a regular commission in August 1989. He was selected to attend the School of Engineering, Air Force Institute of Technology, beginning in May 1991. Captain Logue is married to the former Jean Marie Cassese of Massapequa, New York.

Permanent Address: 315 Genesee Gardens 9A
Auburn, NY 13021

First Lieutenant Ralph A. Sandfry was born on 27 December 1965 in Rochester, Minnesota. He graduated from Hickman High School in Columbia, Missouri in 1984 and attended The University of Kansas, graduating with a Bachelor of Science degree in Aerospace Engineering in January 1989. He obtained his reserve commission in the USAF through the Air Force ROTC program in January 1989 and served his first tour of duty at Space Systems Division, Los Angeles AFB, California. He began at the Systems Engineering Directorate of the Global Positioning System (GPS) Joint Program Office where he served as test director for a critical system-level test. In February 1990 he was reassigned to the Space and Control Directorate of the GPS Joint Program Office where he supported GPS satellite launch processing, integration with the Delta II launch vehicle, as well as launch and early-orbit operations. He was selected to attend the School of Engineering, Air Force Institue of Technology, beginning in May 1991. Lieutenant Sandfry is married to the former Marilyn Gregory of Emporia, Kansas.

Permanent Address: 2209 Rose Drive
Columbia, MO 65202

Capt Stephen J. Skotte was born on 28 January 1964 in Pasadena, California. He graduated from Hilltop High School in Chula Vista, California in 1982 and attended the U.S. Air Force Academy, graduating with a Bachelor of Science in Electrical Engineering in May 1986. Upon graduation, he received a regular commission in the USAF and served his first tour of duty at Los Angeles AFB, California. He began as the Satellite Integration and Test Manager at the Spacecraft and Satellite Integration Division of the Milstar Joint Program Office where he directed the design and development of the test facility to integrate and test the Milstar satellite hardware and software. In August 1987 he was reassigned within the Spacecraft and Satellite Integration Division as Milstar Data Processing Subsystem Manager where he was responsible for the design, development and test of the $150 million Data Processing Subsystem. In June 1989 he was reassigned to the Advanced Technology Division of the Milstar Joint Program Office as Milstar Advanced Space Communications Manager. There he directed the successful integration and test of the first Milstar crosslink payload, and fabrication of the units necessary for the second crosslink payload. He was selected to attend the School of Engineering, Air Force Institute of Technology, beginning in May 1991. Captain Skotte is married to the former Jane Suzanne Wright from Providence, Rhode Island.

Permanent Address: 259 MiraMar Avenue
Long Beach, CA 90230

Capt Michael L. Zywien was born on 11 September, 1953 in Whitinsville, Massachusetts. He graduated from Northbridge High School in Northbridge, Massachusetts in 1971 and attended Holy Cross College where he was named Co-Captain of the football team and received a Bachelor of Arts degree in 1975. After teaching and coaching track and field at Blackstone-Millville (Massachusetts) High School for seven years, he obtained his reserve commission in the USAF through Officer Training School, where he was named a distinguished graduate. After obtaining a Bachelor of Science in Electrical Engineering degree through an AFIT/CI program at the University of New Mexico, he was assigned to the Joint Surveillance Target Attack Radar (JSTARS) System Program Office at Hanscom AFB, Massachusetts, as a Radar Project Engineer. After completing Squadron Officer School, he was reassigned to the Foreign Technology Division at Wright-Patterson AFB as a Surface-to-Air Missile (SAM) System Analyst. During Operations Desert Shield and Desert Storm, he served in the Joint Intelligence Center (NMIC - Pentagon) as one of three joint service scientific and technical intelligence analysts. He was selected to attend the School of Engineering, Air Force Institute of Technology in May, 1991. He has been awarded two Air Force Achievement Medals, the Air Force Commendation Medal and the Meritorious Service Medal. Capt Zywien is married to the former Shirley Marie Carlee, and has two children (Joshua and Jarrod) and two step-children (Tom Kenney and Michelle Kenney).

        Permanent Address: 58 Emond St.
                           Northbridge, MA 01534

December 1992   Master's Thesis

A Two-Stage Intercontinental Ballistic Missile (ICBM)
Design Optimization Study and Life Cycle Cost Analysis

David P. Blanks, Capt; Douglas M. Bruce, Capt; Anthony M. Logue, Capt;
Ralph A. Sandfry, 1Lt; Stephen J. Skotte, Capt; Michael L. Zywien, Capt

Realities of recent changes in the fiscal environment and the international domestic security structure have caused the strategic community to make some difficult decisions to preserve the capability of the current ICBM force. One of these decisions is to view Minuteman III as the centerpiece of the strategic force well into the next century. Extending the life of the 24-year-old Minuteman III system requires system solutions that provide required performance at an affordable life cycle cost. The intent of this study is to demonstrate the feasibility of designing a 2-stage ICBM to perform the Minuteman III mission. The main area of research is to take advantage of recent developments in missile technology and materials, including "Integrated Stage Concept" and more conventional technologies. It is believed that such a system could prove more affordable to build, maintain and support while providing the required system performance. Five final missile designs are developed and presented. A recommendation is made to pursue an Integrated Stage second stage design based on mission performance, system readiness and cost decision criteria.

370

ICBM, Integrated Stage Concept, Two-Stage Boosters Systems Engineering,
Optimization, Life Cycle Cost Analysis, Trajectory Analysis, Readiness

Unclassified   Unclassified   Unclassified   SAR

Public reporting burden for this collection of information is estimated to average 1 hour per response, including the time for reviewing instructions, searching existing data sources, gathering and maintaining the data needed, and completing and reviewing the collection of information. Send comments regarding this burden estimate or any other aspect of this collection of information, including suggestions for reducing this burden, to Washington Headquarters Services, Directorate for Information Operations and Reports, 1215 Jefferson Davis Highway, Suite 1204, Arlington, VA 22202-4302, and to the Office of Management and Budget, Paperwork Reduction Project (0704-0188), Washington, DC 20503.

1. AGENCY USE ONLY (Leave blank)	2. REPORT DATE	3. REPORT TYPE AND DATES COVERED
	December 1992	Master's Thesis

4. TITLE AND SUBTITLE

A Two-Stage Intercontinental Ballistic Missile (ICBM)
Design Optimization Study and Life Cycle Cost Analysis

5. FUNDING NUMBERS

6. AUTHOR(S)

David P. Blanks, Capt; Douglas M. Bruce, Capt; Anthony M. Logue, Capt;
Ralph A. Sandfry, 1Lt; Stephen J. Skotte, Capt; Michael L. Zywien, Capt

7. PERFORMING ORGANIZATION NAME(S) AND ADDRESS(ES)

Air Force Institute of Technology, WPAFB OH 45433-6583

8. PERFORMING ORGANIZATION REPORT NUMBER

AFIT/GSE/ENY/92D-1

9. SPONSORING/MONITORING AGENCY NAME(S) AND ADDRESS(ES)

Phillips Laboratory
PL/RKSA
Edwards AFB, CA 93523-5000

10. SPONSORING/MONITORING AGENCY REPORT NUMBER

11. SUPPLEMENTARY NOTES

12a. DISTRIBUTION/AVAILABILITY STATEMENT

APPROVED FOR PUBLIC RELEASE; DISTRIBUTION UNLIMITED

12b. DISTRIBUTION CODE

13. ABSTRACT (Maximum 200 words)

Realities of recent changes in the fiscal environment and the international domestic security structure have caused the strategic community to make some difficult decisions to preserve the capability of the current ICBM force. One of these decisions is to view Minuteman III as the centerpiece of the strategic force well into the next century. Extending the life of the 24-year-old Minuteman III system requires system solutions that provide required performance at an affordable life cycle cost. The intent of this study is to demonstrate the feasibility of designing a 2-stage ICBM to perform the Minuteman III mission. The main area of research is to take advantage of recent developments in missile technology and materials, including "Integrated Stage Concept" and more conventional technologies. It is believed that such a system could prove more affordable to build, maintain and support while providing the required system performance. Five final missile designs are developed and presented. A recommendation is made to pursue an Integrated Stage second stage design based on mission performance, system readiness and cost decision criteria.

14. SUBJECT TERMS

ICBM, Integrated Stage Concept, Two-Stage Boosters Systems Engineering,
Optimization, Life Cycle Cost Analysis, Trajectory Analysis, Readiness

15. NUMBER OF PAGES

370

16. PRICE CODE

17. SECURITY CLASSIFICATION OF REPORT	18. SECURITY CLASSIFICATION OF THIS PAGE	19. SECURITY CLASSIFICATION OF ABSTRACT	20. LIMITATION OF ABSTRACT
Unclassified	Unclassified	Unclassified	SAR